

3 COMPARATIVE STUDY OF THRUST-VECTOR-CONTROL
SYSTEMS FOR LARGE, SOLID-FUELED LAUNCH VEHICLES, 2F

△ VOLUME II TECHNICAL REPORT 6

9 NOVEMBER 1967 10CV

6 By G.D. BUDRIS 9

Distribution of this report is provided in the
interest of information exchange. Responsibility
for the contents resides with the author
or organization that prepared it.

25
27A CV
Prepared under Contract No. NAS 1-7109

by Douglas Aircraft Company

2 Missile and Space Systems Division 3

Huntington Beach, California 2

for

NATIONAL AERONAUTICS AND SPACE ADMINISTRATION

PREFACE

This document is the final report on NASA Contract No. NAS1-7109. It presents the results of Tasks I, II, and III. There are two companion documents: Volume I--Summary, and Volume III--Appendixes.

The work was performed under the direction of J. W. Wilkey and J. M. Riebe, Langley Research Center (LRC).

At Douglas, R. J. Gunkel, Director of Advance Spacecraft and Launch Systems and W. H. Siefried, Program Manager of Launch Systems provided technical direction, and G. D. Budris acted as Study Manager. Douglas personnel who participated in the investigation described in this report include I. M. Sarlat, O. F. Lippoldt, J. J. Kelley, J. M. Vandewalle, E. M. Pollack, C. H. Goldthorpe, J. R. Quartucy, R. L. Buchanan, R. E. Schenbeck, D. E. Goldberg, A. T. West, Jr., J. P. Mikulicich, D. L. Crosby, and D. Pickering.

CONTENTS

	LIST OF FIGURES	vii
	LIST OF TABLES	xi
Section 1	INTRODUCTION	1-1
Section 2	DESIGN AND CRITERIA DATA	2-1
	2.1 Baseline Mission	2-1
	2.2 Basic Launch Vehicle and Payload	2-1
	2.3 Thrust Histories	2-4
	2.4 Trajectory Data	2-4
	2.5 Wind Profile	2-4
	2.6 Motor Details	2-8
	2.7 Basic Nozzle Design	2-8
	2.8 TVC System Concepts	2-14
Section 3	LAUNCH VEHICLE SYSTEM COMPARISONS	3-1
	3.1 Structural Design Criteria	3-1
	3.2 Structural Design	3-8
	3.3 Integration of TVC Designs	3-10
	3.4 Stage Weight Breakdowns	3-16
	3.5 Vehicle Performance	3-16
	3.6 Stability and Control Analysis	3-23
Section 4	TVC SYSTEMS COMPARISON	4-1
	4.1 Lockseal Design Requirements	4-1
	4.2 Gas Injection TVC Design Data	4-2
	4.3 Lockseal Actuator Design	4-13
	4.4 Lockseal Hydraulic Power Systems	4-20
	4.5 Thiokol Hot Gas TVC Actuator Design	4-25
	4.6 Thiokol Hot Gas Valve Power Systems	4-27
	4.7 Vickers Warm Gas Pneumatic Valve	4-30
	4.8 TVC System Weight	4-31
	4.9 Electronic Design	4-34
	4.10 First- and Second-Stage TVC Systems Reliability Analysis	4-49
	4.11 Reliability Comparison	4-55
	4.12 Degree of Development	4-55

Section 5	ROLL CONTROL SYSTEM	5-1
5.1	Independent Roll Control System	5-1
5.2	Dependent Roll Control System	5-6
5.3	Roll Control Reliability Analysis	5-9
Section 6	LAUNCH OPERATIONS	6-1
6.1	Gimbal Nozzle System	6-1
6.2	Warm Gas System	6-3
6.3	Hot Gas Systems	6-4
Section 7	GENERAL COMPARISONS	7-1
7.1	Vehicle Configurations	7-1
7.2	TVC Comparison Chart	7-5
7.3	Payload Capability	7-5
7.4	Launch Vehicle Weight Matrix	7-8
7.5	Vehicle Reliability Versus Configuration	7-8
7.6	Launch Operations-- Total Vehicle System	7-8
Section 8	BIBLIOGRAPHY	8-1

FIGURES

2-1	Mission Profile	2-2
2-2	Basic Launch Vehicle and Payloads (Extracted from Phase II HES Study)	2-3
2-3	Thrust Profiles	2-4
2-4	First-Stage Trajectory Parameters	2-5
2-5	First-Stage Trajectory Parameters	2-5
2-6	Second-Stage Trajectory Parameters	2-6
2-7	Second-Stage Trajectory Parameters	2-6
2-8	95% Wind Profile	2-7
2-9	First-Stage 260-in. - Diam SRM	2-9
2-10	Second-Stage 156-in. - Diam SRM	2-10
2-11	Nozzle Assembly: First-Stage 260-in. - Diam SRM	2-15
2-12	Gimbal Nozzle TVC (Lockheed)	2-17
2-13	Warm Gas TVC (Vickers)	2-18
2-14	Hot Gas TVC (Thiokol) - Modulated	2-19
2-15	Hot Gas TVC (ABL) - Basic On-Off Design	2-20
3-1	SRM TVC System Configurations	3-2
3-2	Preliminary Loads--Configuration 1A	3-4
3-3	Ground Wind Loads	3-5
3-4	Mass Distribution--Configuration 1A	3-5
3-5	Axial-Force Coefficient--Configuration 1A	3-6
3-6	Normal-Force Coefficient Gradient Max $q\alpha$ Condition--Configuration 1A	3-6
3-7	Normal-Force Coefficient Gradient Burnout Condition--Configuration 1A	3-6
3-8	Shear Diagram, Max $q\alpha$ Condition	3-6
3-9	Bending-Moment and Axial-Load Diagram, Max $q\alpha$ Condition	3-7
3-10	Flight Loads--Burnout Condition	3-7
3-11	Aft-Skirt Structural Details	3-9

3-12	Forward-Skirt Interstage Structural Details	3-11
3-13	EI Distribution	3-12
3-14	Layout--Solid Motor TVC System Configuration	3-13
3-15	Payload Sensitivity to First-Stage Weight	3-20
3-16	Payload Sensitivity to First-Stage Specific Impulse	3-20
3-17	Payload Sensitivity to First-Stage Propellant Weight	3-21
3-18	Payload Sensitivity to Second-Stage Weight	3-21
3-19	Payload Sensitivity to Second-Stage Specific Impulse	3-22
3-20	Payload Sensitivity to Second-Stage Propellant Weight	3-22
3-21	Sources of Disturbing Moments and their Uncertainty Levels	3-24
3-22	First-Stage Duty Cycle--Ballos Payload	3-26
3-23	First-Stage Duty Cycle--Winged Payload	3-27
3-24	Second-Stage Duty Cycle--Ballos Payload	3-28
3-25	Second-Stage Duty Cycle--Winged Payload	3-29
3-26	Yaw Attitude--Gimbal Nozzle Vehicle	3-32
3-27	Yaw Thrust-Vector Deflection--Gimbal Nozzle Vehicle	3-32
3-28	Second-Stage Control System Stability Boundaries--Configuration II	3-34
3-29	Second-Stage Thrust-Vector Deflection Angle Transient	3-36
3-30	Attitude Angle Transient Following Separation: Configuration II--Ballos Payload	3-36
3-31	Thrust-Vector Deflection Angle Transient Following Separation: Configuration IIA HL ₇ -10 Payload	3-37
3-32	Attitude Angle Transient Following Separation: Configuration IIA--HL-10 Payload	3-37
3-33	First-Stage Duty Cycle--Optimum Fins and Winged Payload	3-39
3-34	Fin Performance	3-41
3-35	Body Bending Modes for Configuration IA	3-42
3-36	Peak Bending Moment as a Function of Control Frequency	3-44
3-37	Peak Angle-of-Attack as a Function of Control Frequency	3-44

3-38	Peak Thrust-Vector Deflection as a Function of Control Frequency	3-45
4-1	Effect of Injector Nozzle Location and Mach Number on Side-Force Performance	4-3
4-2	Effect of Injector Angle and Number of Valves Per Quadrant on Side Force Performance	4-3
4-3	Effect of Injector Location on Hot Gas Performance Parameter	4-4
4-4	260-in. -diameter Hot Gas TVC Gain Performance	4-5
4-5	260-in. Diameter Hot Gas Performance Factors	4-6
4-6	156-in. Diameter Hot Gas TVC Gain Performance	4-6
4-7	156-in. -Diam Hot Gas TVC Performance Factors	4-6
4-8	Effect of Nozzle Location on Warm Gas TVC Performance	4-7
4-9	260-in. Diameter Warm Gas TVC Gain Performance	4-8
4-10	156-in. -Diameter Warm Gas TVC Gain Performance	4-8
4-11	260-in. Diameter Warm Gas TVC Performance Factors	4-9
4-12	156-in. -Diameter Warm Gas Performance Factors	4-9
4-13	Schematic of Hydraulic Servo-Actuator Assembly	4-15
4-14	Hydraulic Flow Requirements for Lockseal Gimbal Design--260-in. -diam SRM First Stage	4-21
4-15	Hydraulic Flow Requirements for Lockseal Gimbal Design--156-in. -diam Second Stage	4-22
4-16	First-Stage Hydraulic Power System Schematic	4-24
4-17	Second-Stage Hydraulic Power System Schematic	4-26
4-18	Hydraulic Servo-Actuator Hot-Gas Pintle Assembly	4-27
4-19	Hydraulic Flow Requirements for Thiokol Hot Gas Design--260-in. -diam SRM First Stage	4-29
4-20	Hydraulic Flow Requirements for Thiokol Hot Gas Design 156-in. -diam SRM Second Stage	4-29
4-21	Warm Gas Ducting for the 260-in. -diam SRM First Stage	4-31
4-22	Warm Gas Ducting for the 156-in. -diam SRM Second Stage	4-32
4-23	Lockseal Control System--260-in. -diam SRM	4-37
4-24	Lockseal Control System--156-in. -diam SRM	4-39

4-25	Hot Gas Control System--260-in. -diam SRM	4-40
4-26	Warm Gas Control System--260-in. -diam SRM	4-42
4-27	Warm Gas Control System--156-in. -diam SRM	4-43
5-1	Roll Control System Schematic	5-3
5-2	S-IVB Auxiliary Propulsion System	5-5
5-3	Saturn IB/S-IVB Auxiliary Propulsion System Module (Mockup)	5-5
5-4	Roll Control System Using Warm Gas TVC Bypass	5-7
5-5	Roll Control System Using Hot Gas TVC Bypass	5-8
7-1	Study Launch Vehicle Comparisons	7-2
7-2	Phase II HES Study Launch Vehicle Data	7-3
7-3	TVC System Comparisons	7-6

TABLES

2-1	Basic SRM Parameters	2-8
2-2	Motor Weight Breakdown (lb)	2-11
2-3	Nozzle Mass Characteristics	2-12
2-4	260-in. -diam SRM Lockseal Nozzle Weight Summary (lb)	2-14
3-1	Frame Dimensions	3-12
3-2	Vehicle Weight Comparison (lb)	3-17
3-3	Equipment and Instrumentation Weight Breakdown (lb)	3-19
3-4	Nominal Stage Weight, Propellant Weight, and I_{sp}	3-23
3-5	Comparison of Control-System Duty Cycles	3-30
3-6	Minimum Acceptable Second-Stage TVC System Design Requirements	3-35
3-7	Duty-Cycle Area Breakdown	3-40
3-8	Body-Bending Frequencies (cps)	3-42
4-1	Gimbal Nozzle TVC System Design Requirements	4-1
4-1A	TVC Design Summary	4-11
4-2	Warm Gas and Hot Gas Valve Design Data	4-12
4-3	Lockseal Actuator and Servo-Valve Design Data	4-19
4-4	Maximum Flow Rates Required	4-22
4-5	Thiokol Hot Gas TVC Servo-Actuator Design Data	4-28
4-6	Maximum Flow Rates Required	4-30
4-7	Hot Gas TVC System Weight Summary (lb)	4-32
4-8	Warm Gas TVC System Weight Summary (lb)	4-33
4-9	Lockseal TVC System Weight Summary (lb)	4-33
4-10	Critical Measurements for Lockseal TVC System	4-45
4-11	Critical Measurements for Warm Gas TVC System	4-46

4-12	Critical Measurements for Hot Gas TVC System	4-47
4-13	Electronic Comparison	4-48
4-14	TVC System Reliability Comparisons	4-55
4-15	Flex-Bearing Firing History	4-56
4-16	Thiokol Hot-Gas Valve Test Summary	4-57
4-17	Vickers Warm-Gas Static Test Summary	4-58
5-1	Design Features of Roll Control Systems	5-4
5-2	First-Stage Roll Control System Weight Breakdown	5-6
5-3	Second-Stage Roll Control System Weight Breakdown	5-7
5-4	Dependent Roll Control System Data	5-9
5-5	Reliability Comparison of Roll Control Systems	5-10
7-1	Variation in Cargo Weight--260-nmi Orbit Compared to Configuration V (LITVC)	7-7
7-2	Launch Vehicle Weight Matrix--Hot Gas First Stage (lb)	7-9
7-3	Launch Vehicle Weight Matrix--Warm Gas First Stage (lb)	7-10
7-4	Launch Vehicle Weight Matrix--Gimbal Nozzle First Stage (lb)	7-11
7-5	Weight Above the Second Stage (lb)	7-12
7-6	Reliability Comparison of Potential Launch Vehicle Configurations	7-13

Section 1

INTRODUCTION

The National Aeronautics and Space Administration (NASA) awarded the Douglas Aircraft Company a 6-month contract (NAS1-7109) to perform comparative analyses of 4 advanced thrust-vector-control (TVC) system designs as applied to a large, solid-fueled launch vehicle. The technical effort started 28 February 1967 and terminated 6 September 1967. The objective of this study was to summarize TVC design and performance data in a comparative format which will enable the NASA to judge the merits of each TVC concept for future application in research and development efforts.

The four TVC systems include as their principal components the Lockheed Lockseal, Thiokol hot-gas pintle valve, Vickers warm-gas valve, and Allegany Ballistics Laboratory (ABL) chamber bleed zero leak hot gas valve. Each of these systems deflect the thrust vector in a different manner, but only two basic principles are involved: nozzle gimbaling and secondary gas injection into the nozzle. Two ABL secondary injection hot-gas valve designs were investigated during the first 9 week period for thrust vector control of large solid rocket motors. One injects hot gas in a pulsating or cyclic mode, full on or off; the other is fully modulated. The on-off concept was not studied in detail (see Appendix A.5 for a discussion), because TVC requirements are met efficiently by a fully-modulating propellant gas valve which uses a balance plug to reduce actuation loads. The general valve design can be used either as a submerged valve, usually with a submerged nozzle, or an external valve with associated ducting. The submerged-valve design is best because of weight saving (see Appendix A.5), and mounting the valves to provide accessibility, ease of maintenance, etc. makes this TVC concept generally identical to that of the Thiokol hot-gas TVC system. Detail design and materials used differ in the ABL and Thiokol hot gas valves, but the primary interest of this study is to compare operation characteristics, requirements, and conditions rather than provide a detailed description of

component parts. The Thiokol hot-gas TVC system was selected to represent this TVC technique, because performance predictions of this system are supported by large scale valve (115 lb/sec flow rate) test data. Therefore, the general comparative data in this report pertaining to the Thiokol hot-gas valve applies to the ABL modulated valve design TVC concept.

The Lockheed Lockseal allows omniaxial nozzle deflection while providing an effective static seal of main-motor gases. Two gas injection systems are represented in the Thiokol and ABL hot-gas injection and the Vickers warm-gas injection TVC methods. The Thiokol hot-gas valve and the ABL modulated valve uses the solid rocket motor (SRM) combustion chamber gas at 5,800°F. The pintle of these hot-gas valves can be extended or retracted to any required length to provide the flow of hot gas necessary to meet thrust vector requirements. A gas generator, designed to operate with the Vickers warm-gas valve, supplies injection gas at 2,000°F for this TVC technique. Each of these three TVC concepts were expanded into workable control systems for a two-stage SRM launch vehicle. This task was initiated after Douglas personnel visited each of these companies and ABL. The cooperation and response to our request for information was excellent.

To obtain compatible comparison data, basic information was taken from a previous study of vehicles using various control techniques--the Phase II Head-End Steering (HES) Study. Design criteria such as the mission, launch vehicle, natural environment, vehicle geometric and aerodynamic uncertainties, maneuvering requirements, and steering analysis were obtained from this study, and data supplied by the TVC system manufacturers were used in this study's design and analytical tasks, resulting in consistent comparative data on TVC and vehicle systems as well as allowing general comparisons to be made with results of the Phase II HES Study. It should be noted that only general vehicle comparisons can be made between the two studies, because advances in solid rocket motor technology have been incorporated in this study resulting in changes in nozzle location and design. In addition, two of the three Phase II HES study launch vehicles have different first and second stage propellant loadings as a result of normalizing launch vehicles to specific payload in 260-nmi orbit. Fins for aerodynamic stabilization of the launch vehicles studied were not added (as applied in the Phase II HES study) to allow a more direct comparison of the candidate TVC techniques.

Two payload shapes were included to allow the effect of vehicle stability on control system response to be evaluated. The primary payload is the ballistic Ballo spacecraft with maneuvering engines and cargo module. The secondary payload, used only in stability and control analyses, is a modified HL-10.

The study was structured into three tasks: Task I, Initial Design and Analysis; Task II, System and Mission Refinements; and Task III, Comparative Analysis. Task I terminated with a review of the first 9 weeks of technical effort, presenting basic data relative to the candidate TVC and vehicle systems. During Task I design criteria was established, TVC system data were obtained from reports and consultation, data and analytical techniques were substantiated, initial concepts for TVC and launch vehicle system integration were made and the approach to completing the remainder of the study and obtaining meaningful comparisons was developed. This approach, implemented in Task II, refined the vehicle structural and configuration design relative to the installation of each TVC concept. To obtain TVC requirements and design systems to meet them, vehicle geometry, stiffness, and weight data are calculated and input into the stability and control analyses. In addition to the resulting TVC requirements, this vehicle design effort provides comparative data relative to dimensions, stage weights, reliability, and payload weight. Task II includes the following vehicle-oriented studies:

1. Development of a family of launch vehicle configurations that show the effects of each of the three TVC systems.
2. Integration of the TVC and roll-control systems into the basic launch vehicle.
3. Preparation of weight statements for the vehicle, stages, TVC systems, and ancillary subsystems.
4. Development of vehicle-payload trade factors.
5. Determination of stability and control comparison data and requirements used to design TVC and roll-control systems.

TVC and roll control system design integration, sizing, and performance data were developed by the following:

1. Investigation of the gas injection TVC systems to determine significant parameters in selecting injector location.
2. Placement of injector nozzle location and determining the number and size of valves.

3. Sizing the gas generator and ducting used in the warm gas TVC system.
4. Determination of roll control propellant requirements and system placement.
5. Design of actuators, power systems, and electronic subsystems required to operate the complete TVC system.
6. Determination of SRM I_{sp} losses resulting from TVC.

Reliability analyses were performed for all TVC and launch vehicle systems. Figures of merit were calculated for the TVC systems, roll-control systems, stages, and vehicles. A final matrix of all possible combinations of these is presented in this report.

During Task III, the technical data were put into comparative format.

Comparisons are shown for the following:

1. Vehicle size, stability, and payload capability.
2. TVC/vehicle system design integration.
3. TVC requirements and control system response as a function of payload shape, fins, and control system.
4. Actuator and electronic system designs.
5. Reliability and weights for stage, vehicle, TVC, and roll-control systems.
6. Launch operation consideration.

Section 2

DESIGN AND CRITERIA DATA

This section contains general information describing the mission, natural and induced environment, basic launch vehicle, and the four TVC system concepts. These data provide the basic design criteria for this study and were obtained from the Phase II HES Study reports and unpublished data, from reports by Lockheed, Thiokol, Vickers, and ABL, and their response to Douglas's request for further information during the course of the study.

2.1 BASELINE MISSION

For purposes of this study, the launch vehicle's mission was to rendezvous with the Large Orbital Research Laboratory (LORL) at 260-nmi circular orbit, employing a Hohmann transfer from a 105-nmi parking orbit (Figure 2-1). First- and second-stage flight trajectory is ballistic with a ΔV at second-stage apogee of 25,360 fps. The propulsion system of the Ballos payload must provide a ΔV of 201 fps for circularization in the 105-nmi orbit, a ΔV of 272 fps for the Hohmann transfer to a 260-nmi orbit, and a ΔV of 269 fps for circularization in the 260-nmi orbit.

2.2 BASIC LAUNCH VEHICLE AND PAYLOAD

Configuration V from the Phase II HES Study was used as the basic launch vehicle (Figure 2-2). It is a two-stage SRM launch vehicle. The first stage uses a 260-in. -diam SRM, and the second stage uses a 156-in. -diam SRM. The primary payload is the Ballos spacecraft with cargo module and maneuvering engine. An alternate or secondary winged payload is a modified HL-10 spacecraft. Each of the candidate TVC systems was incorporated in both stages of this vehicle.

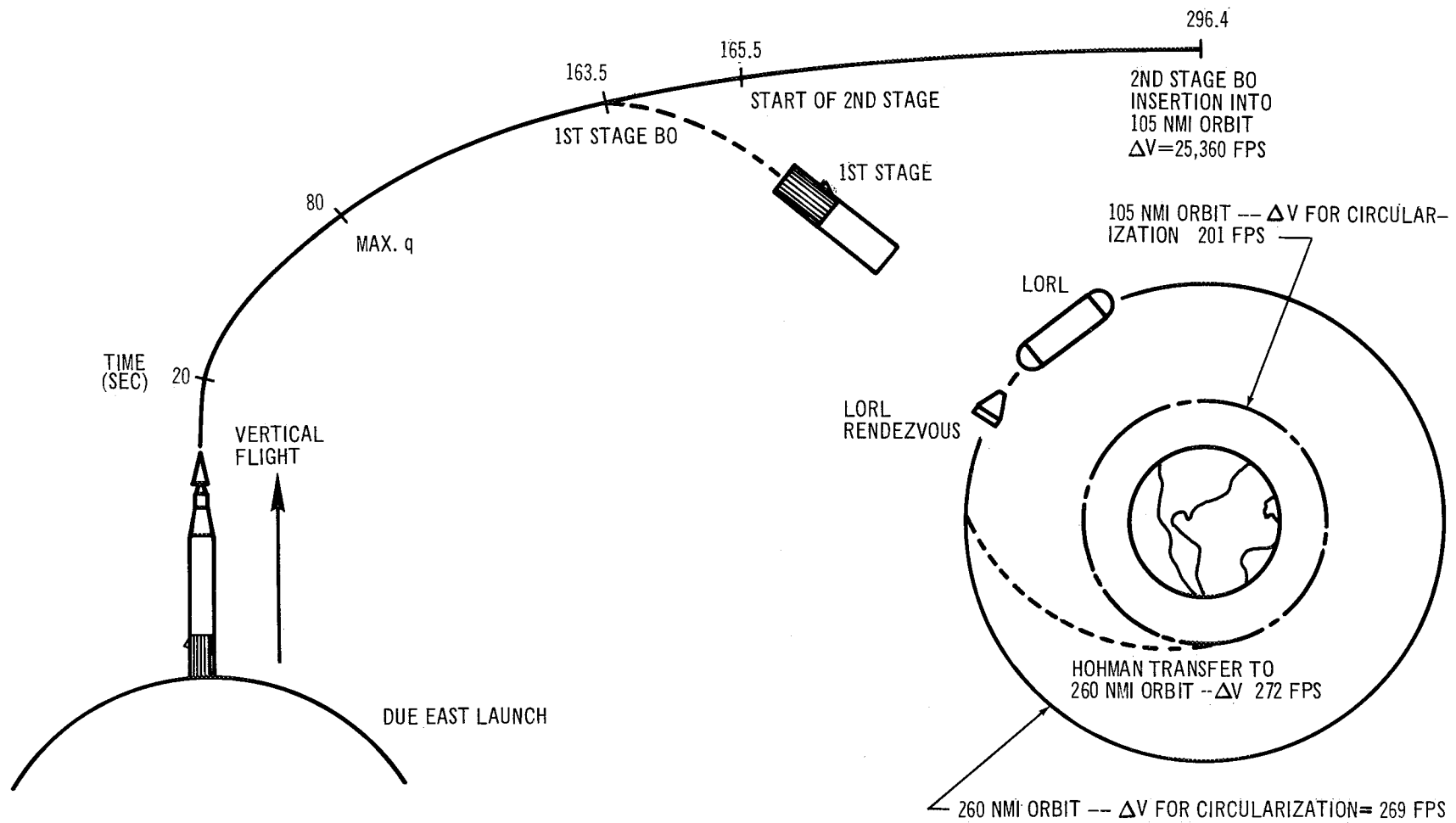


Figure 2-1 Mission Profile

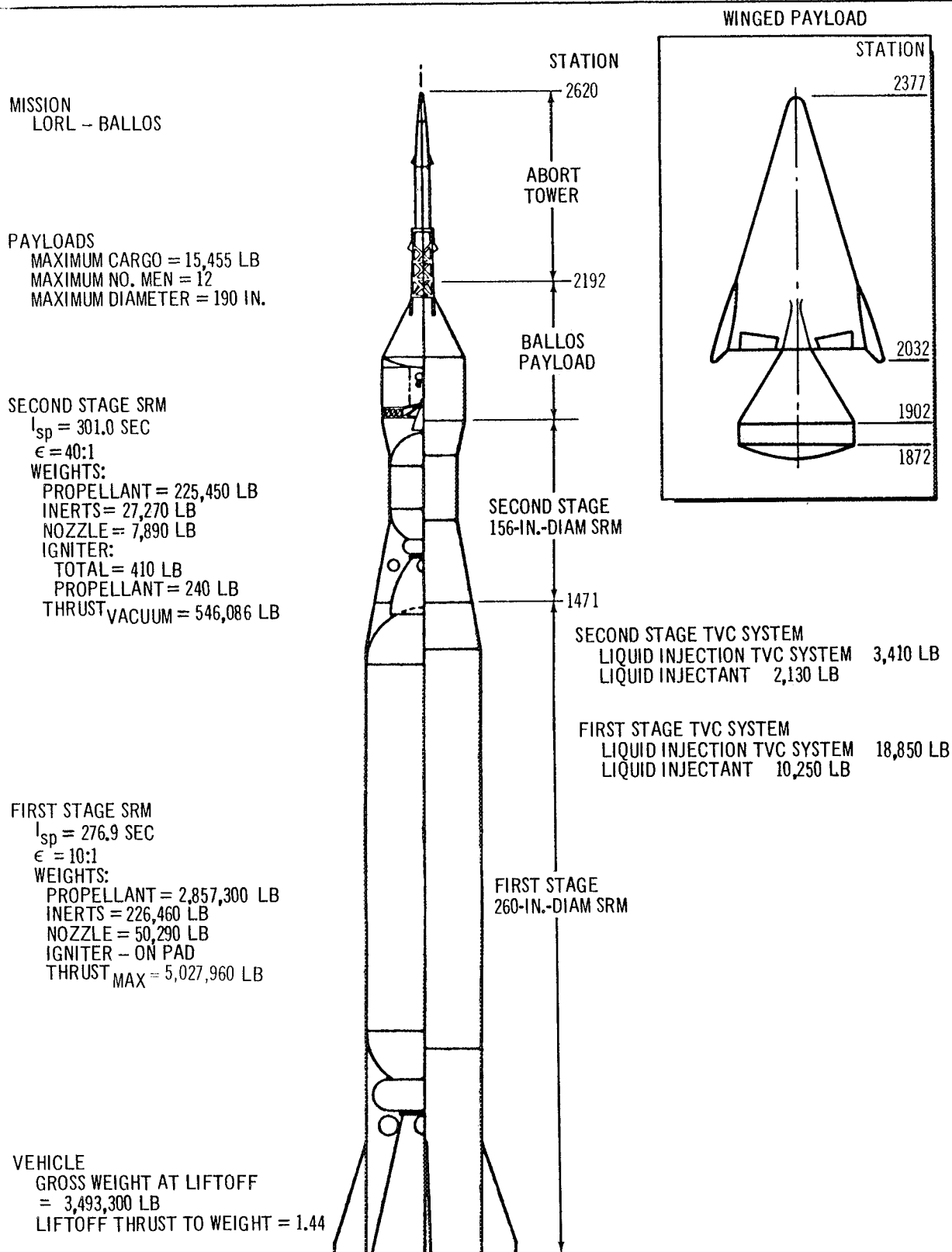


Figure 2-2. Basic Launch Vehicle and Payloads (Extracted from Phase II HES Study)

2.3 THRUST HISTORIES

First- and second-stage thrust is presented in Figure 2-3 as a function of action time. These are typical values because SRM's having the characteristics of those used in the basic launch vehicle have not been studied in detail.

2.4 TRAJECTORY DATA

Plots of pertinent trajectory parameters used in the control analysis are shown in Figures 2-4, 2-5, 2-6, and 2-7. This information was obtained from the trajectory analysis of the Phase II HES Study and represents the final and most refined data applicable to Configuration V.

2.5 WIND PROFILE

The 95% synthetic wind envelope of the Eastern Test Range (ETR) is shown in Figure 2-8. Also shown is the wind profile, which represents a wind buildup for a typical flight that has a maximum wind speed occurring at

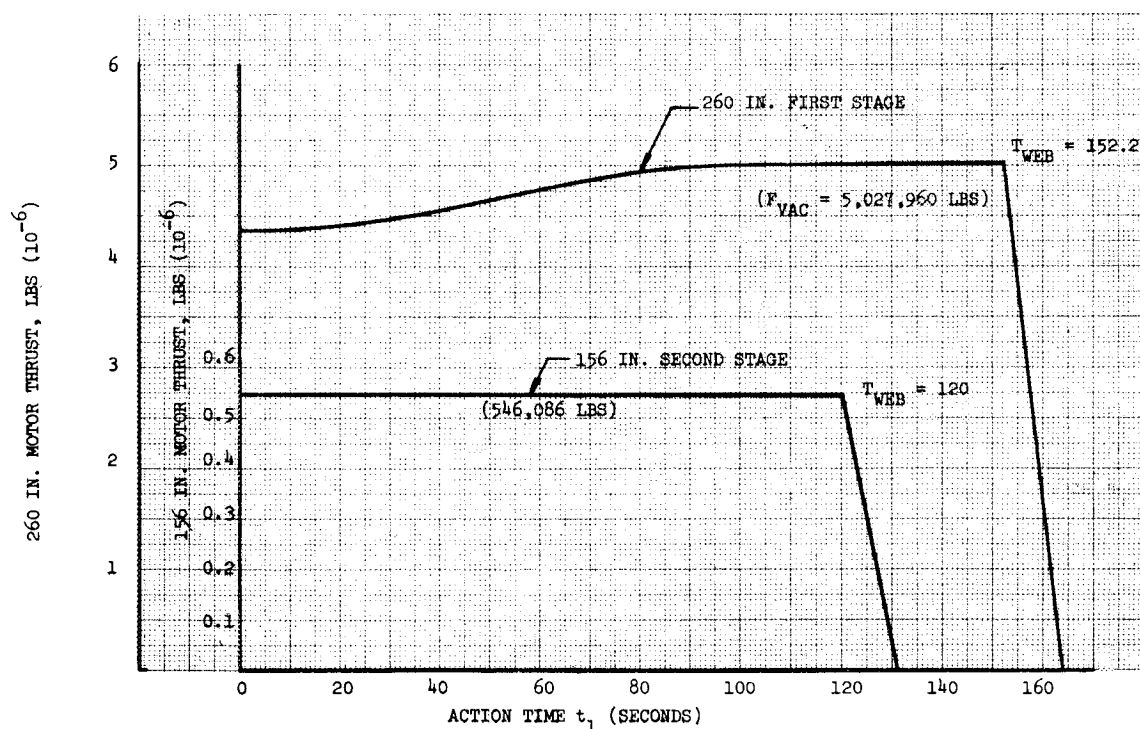


Figure 2-3. Thrust Profiles

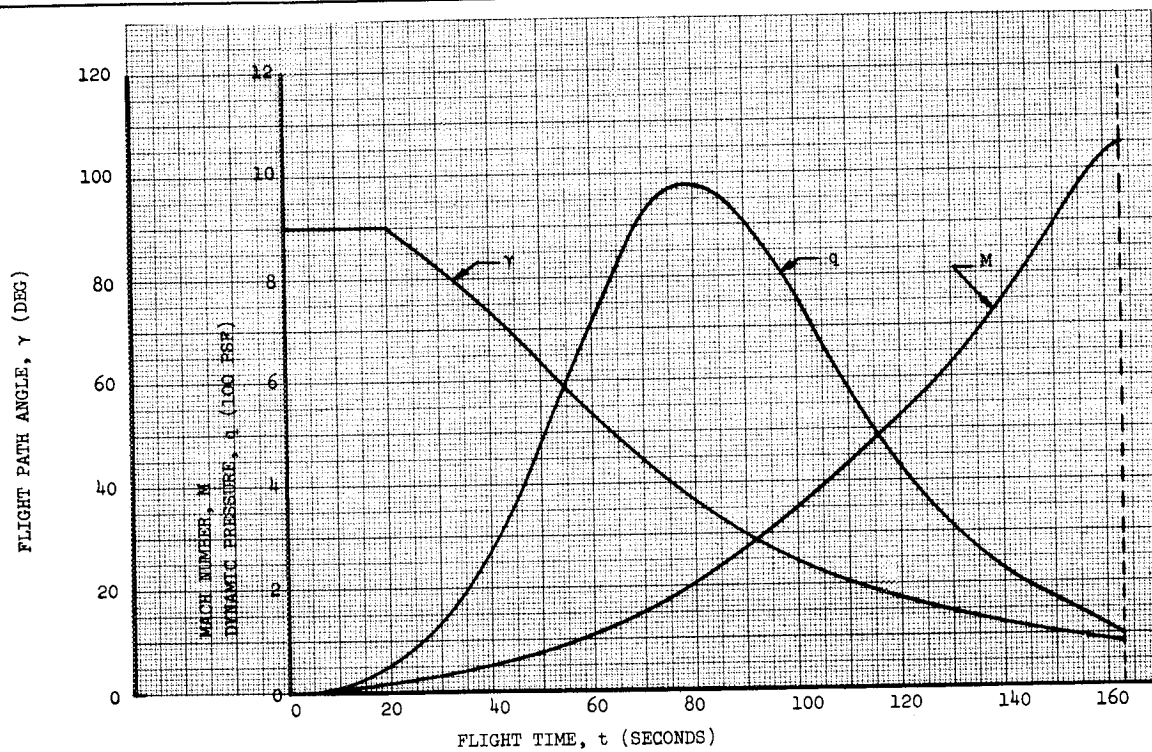


Figure 2-4. First-Stage Trajectory Parameters

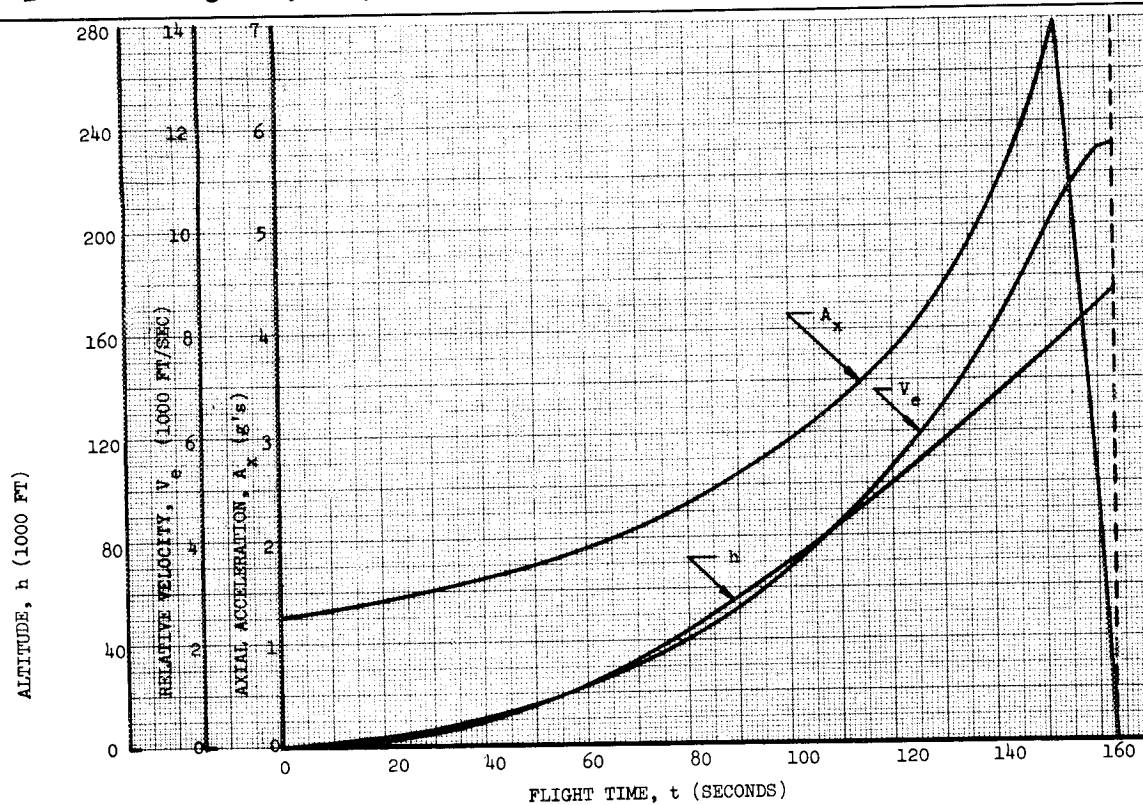


Figure 2-5. First-Stage Trajectory Parameters

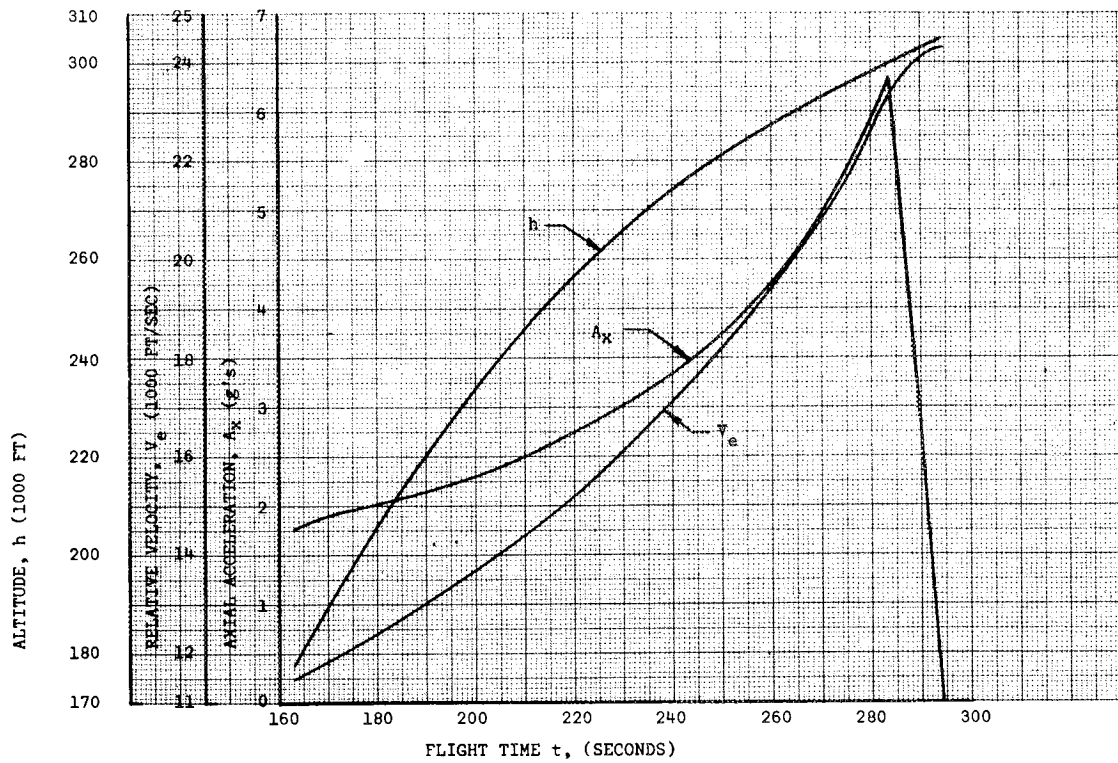


Figure 2-6 Second-Stage Trajectory Parameters

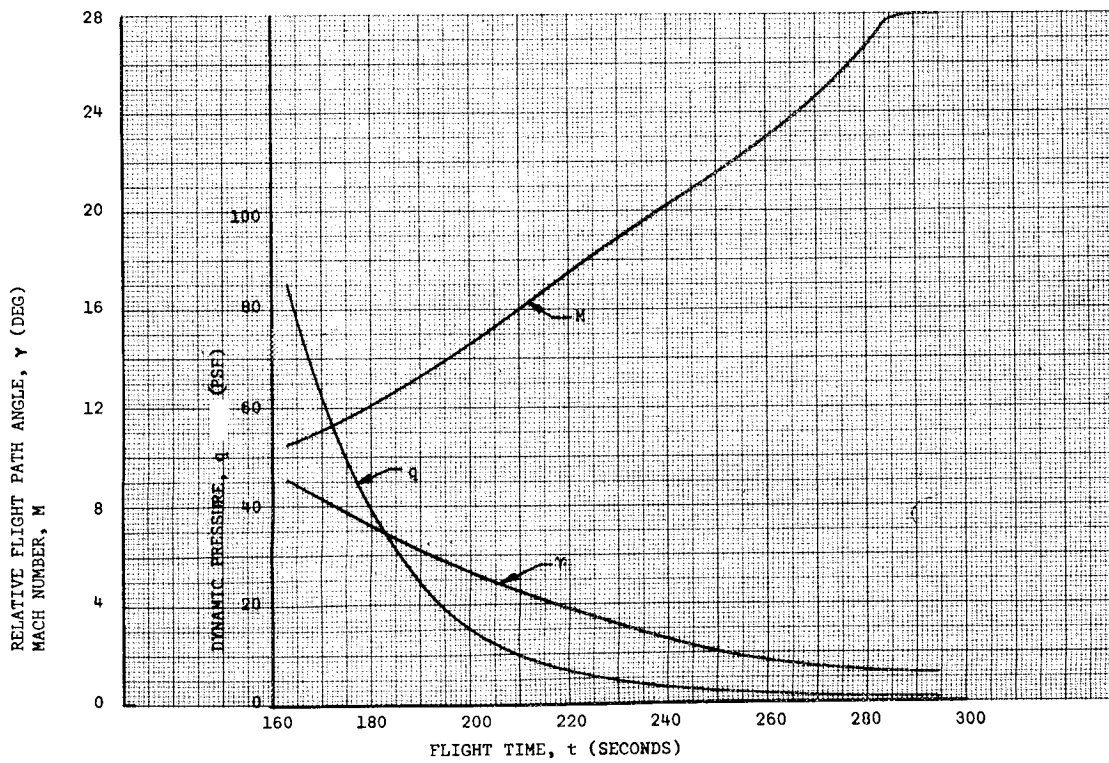


Figure 2-7 Second - Stage Trajectory Parameters

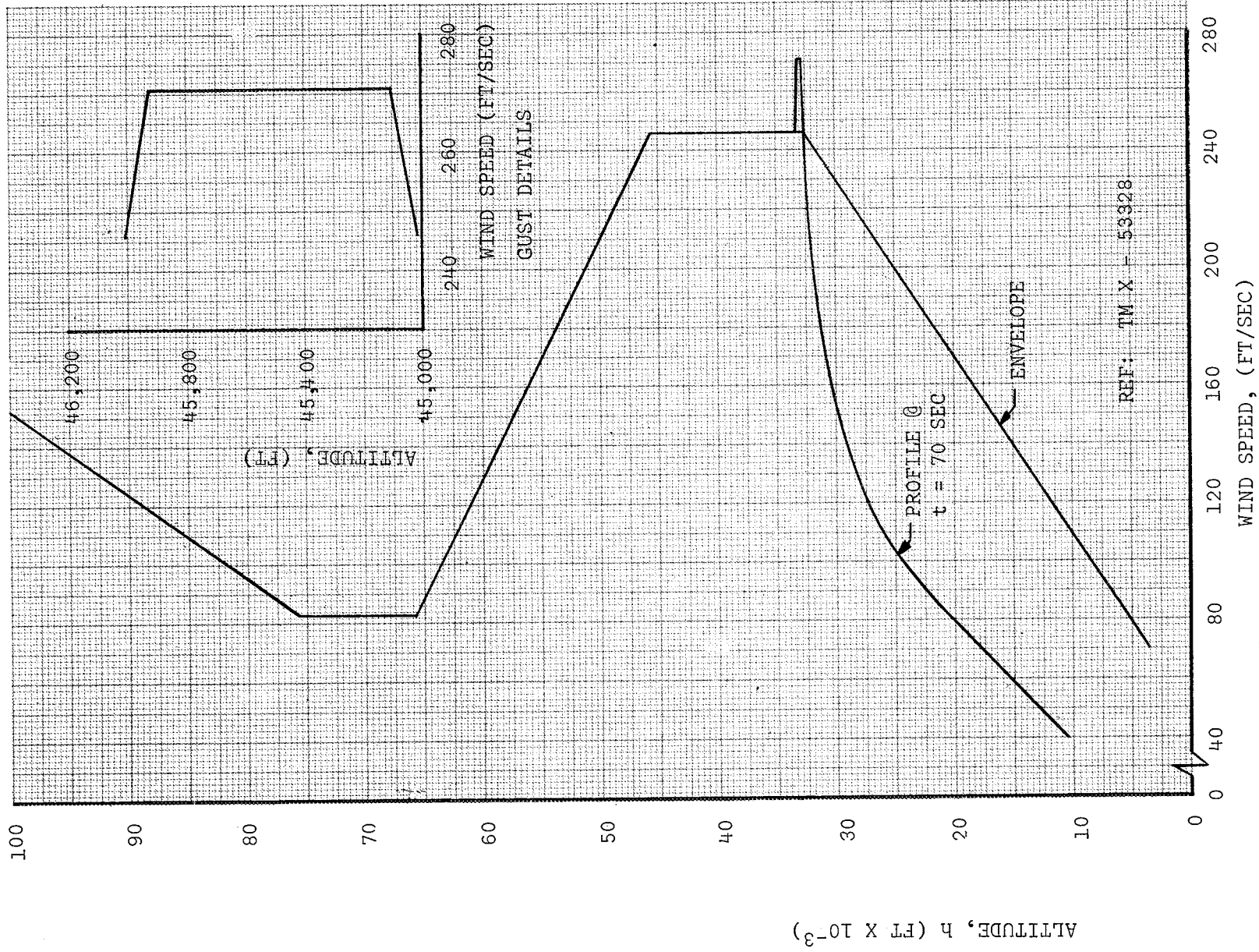


Figure 2-8. 95% Wind Profile

32,500 ft or 70 sec of flight time. Superimposed on this wind profile is a 99% gust reduced 15% as suggested in NASA TMX-53328. This wind profile is used in the vehicle load and control analyses. The envelope is also used in the control analysis.

2.6 MOTOR DETAILS

Table 2-1 shows the significant parameters associated with each SRM. Figures 2-9 and 2-10 show first- and second-stage motor and nozzle dimensions as well as nozzle location in the aft dome closers of each SRM. Table 2-2 is a detailed weight breakdown of the motors. Motor and propellant weights are based on data obtained from the Phase II HES Study. Corrections were made to the propellant weight where portions of the propellant are used for TVC, and aft dome weights are reduced because a large portion is removed to accommodate the deep nozzle submergence.

2.7 BASIC NOZZLE DESIGN

The first-stage SRM nozzle is conical with a half angle of 13° , an expansion ratio (A_e/A_t) of 10:1, and a throat area (A_t) of 4,506.3 sq in. The second-stage SRM nozzle has an optimum bell with an exit angle of 10° , an expansion ratio of 40:1, a throat area of 372 sq in., and a throat-to-exit length of 148 in. Sandwich structure of similar design is used for each nozzle. The face sheets are 0.038-in.-thick steel, and the core is 3-in.-thick aluminum honeycomb with a density of 3.1 lb/cu in. The mass properties of the basic nozzle, excluding the TVC system hardware, are shown in Table 2-3.

Table 2-1
BASIC SRM PARAMETERS

	260 in.	156 in.
Propellant Weight (lb)	2,857,300	225,450
Flame Temperature ($^\circ\text{F}$)	5,800	5,800
Chamber Pressure, meop (psia)	764	800
Motorcase Material	18% Ni-Maraging Steel	18% Ni-Maraging Steel
Wall Thickness (in.)	0.523	0.330
Specific Impulse (sec)	276.9	301.0

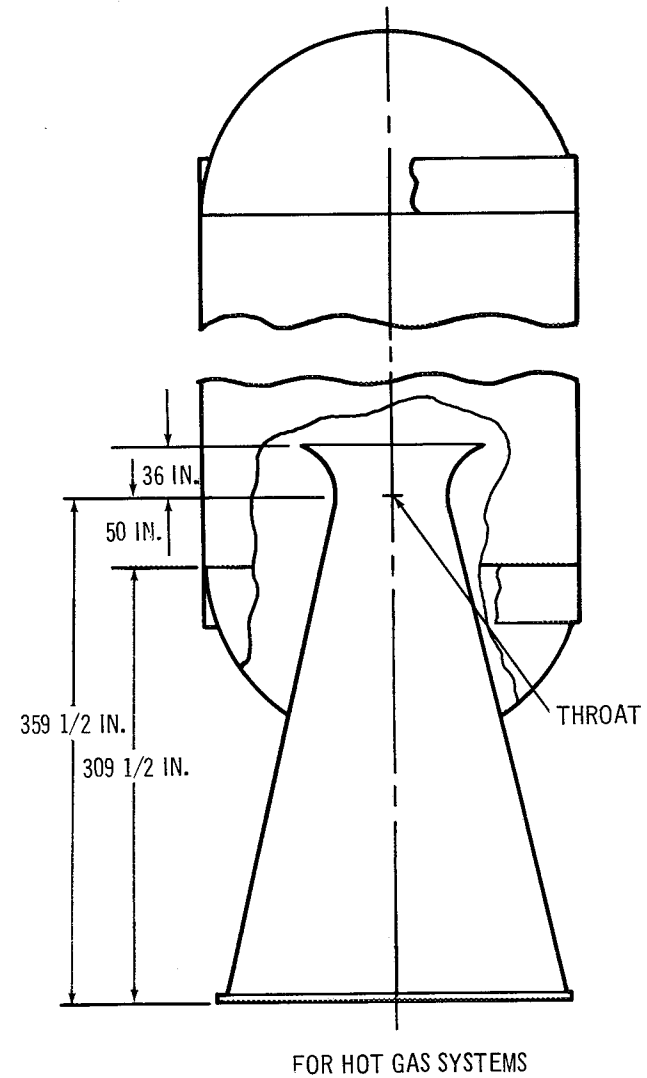
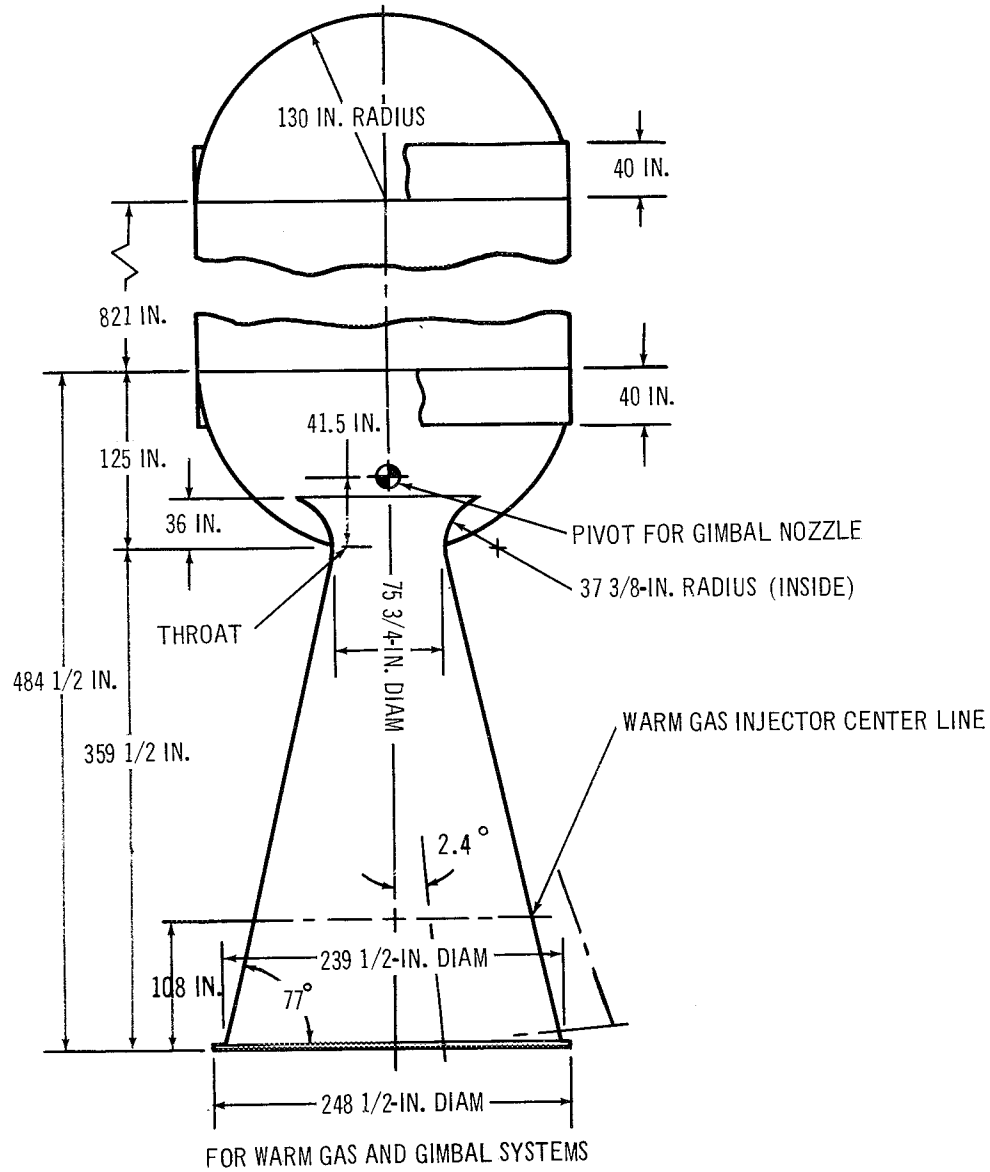


Figure 2-9 First-Stage 260-In.-Diam SRM

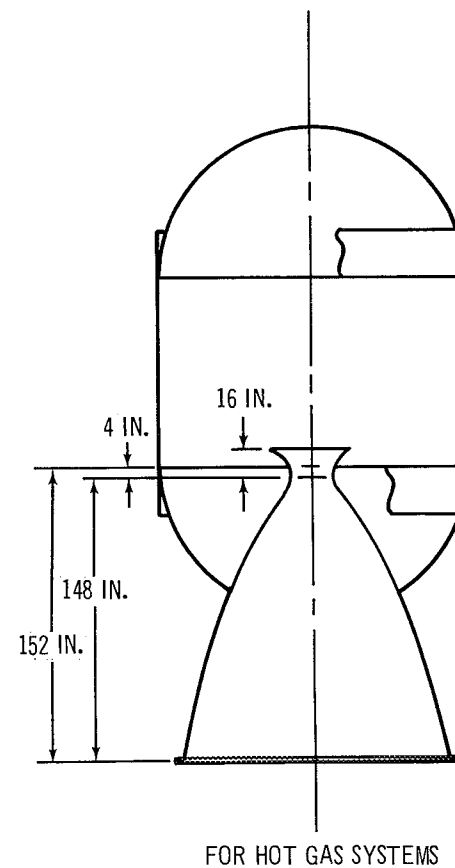
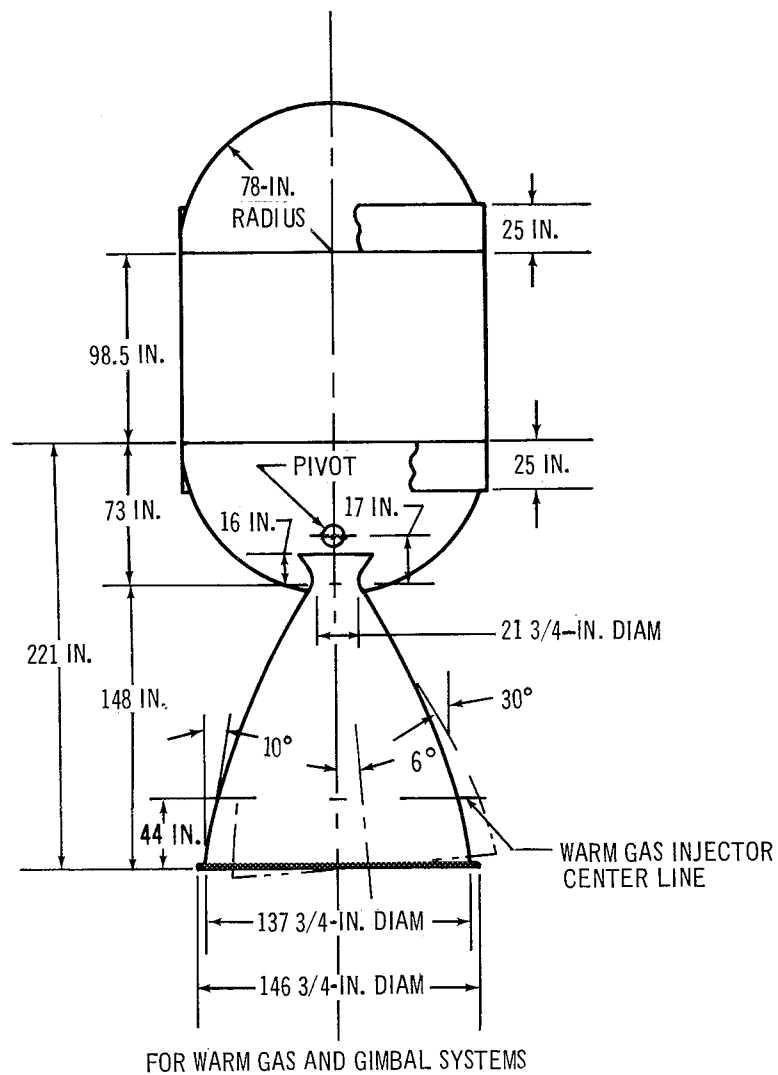


Figure 2-10 Second-Stage 156-In.-Diam SRM

Table 2-2
MOTOR WEIGHT BREAKDOWN (LB)

	156-in. -diam Gimbal and Warm Gas	260-in. -diam Gimbal and Warm Gas	156-in. -diam Hot Gas	260-in. -diam Hot Gas
Forward and Aft Dome	5,280	43,890	5,280	43,890
Sidewall	18,410	152,860	18,410	152,860
Insulation	3,580	29,710	3,580	29,710
Aft Dome Modification for Nozzle Submergence	---	---	-514	-3,948
Total Case Weight	27,270	226,460	26,756	222,512
Propellant	225,450	2,857,300	222,315	2,832,080
Propellant Allocated for TVC	---	---	3,135	25,220

Table 2-3
NOZZLE MASS CHARACTERISTICS

Nozzle Type	Weight (lb)	CG Inches Forward of Exit	Pitch MOI lb-in. ²
156-in. -diam Warm Gas and Gimbal	4,988	79	14.5×10^6
260-in. -diam Warm Gas and Gimbal	30,188	185	465.0×10^6
156-in. -diam Hot Gas	5,488	81	15.9×10^6
260-in. -diam Hot Gas	40,188	198	632.0×10^6

The increase in weight for the hot gas nozzle reflects the added structure needed to resist the external pressure acting on the submerged portion of the nozzle. The pressure distribution is assumed to be linear from zero at the throat to 731.6 psi at the nozzle-aft dome attach point which is 165.5 in. downstream of the throat for the 260-in. -diam SRM. The pressure distribution for the 156-in. -diam SRM nozzle is zero at the throat and linear to 794 psi at 63 in. downstream of the throat. These pressures resulted in structural changes for both nozzles. For the first-stage nozzle, the core thickness, t_c , is increased to 5 in. at nozzle station 165.5 in. with face thicknesses, t_f , of 0.465 in. These dimensions are straight tapered to the original design of $t_c = 3$ in. and $t_f = 0.038$ in. at the throat. The second-stage nozzle structure is changed to $t_f = 0.150$ in. at nozzle station 63 with straight taper to the original design at the throat.

Nozzle weight increases for warm gas TVC applications are the result of bosses that house injector nozzles. This weight increase is 607 lb for the 260-in. -diam SRM nozzle and 240 lb for the 156-in. -diam SRM nozzle. These weights are closely associated with the TVC system, therefore they are charged to the TVC system and not shown as a nozzle weight increase. These nozzle design mass characteristics reflect a safety factor of 1.4, which matches the vehicle factor of safety and which is considerably less than the nozzle factor of safety of 2.7 used in the Phase II HES Study. The nozzle used in the Phase II HES Study was designed for liquid injection TVC and this high factor of safety. The use of this heavy nozzle would effectively

nullify any weight change and comparison because of the installation of the candidate TVC systems. Using the basic nozzle design described above-- which does not have the TVC system weight included--the effect of structural reinforcement resulting from nozzle submergence can be shown.

The warm gas nozzle and gimbal-nozzle as shown in Figures 2-9 and 2-10 have the first- and second-stage nozzle throat submerged in the SRM end-dome closure 5 in. above the dome pole. The hot gas system shown in Figures 2-9 and 2-10 has the first-stage nozzle throat buried in the dome closure 180 in. above the dome pole, and the second-stage nozzle throat is buried 74 in. above the dome pole.

Nozzle submergence deviates from the nozzle/SRM design used in Phase II HES Study but was selected for use in this study because nearly all modern TVC/nozzle system designs include some extent of nozzle submergence for one or more of the following reasons:

1. Desired for TVC system optimization.
2. Required for feasible incorporation of TVC system.
3. Provides shorter overall vehicle.
4. Reduces skirt or interstage weight.
5. Yields lighter weight overall vehicle system.

The use of submerged nozzles for this study resulted primarily from the first two reasons, the second being particularly important for the hot gas and the Lockseal designs.

The hot gas submergence depth is primarily determined by the desired injection location, which is at 50% of the nozzle length. To eliminate the need for an excessively large plenum chamber, the nozzle must be submerged approximately the same depth. On the Lockseal system, however, only shallow submergence is necessary to provide for the seal installation. However, deep submergence is possible when using this design, but weight

of the Lockseal system increases with deep submergence. Data supplied by Lockheed, shown in Table 2-4, provide a weight comparison of two submerged nozzle concepts for the 260-in.-diam SRM shown in Figure 2-11.

Shallow submergence is used to avoid penalizing the concept. The pivot point location, forward of the throat, was also based on Lockheed data.

The warm gas system also benefits from nozzle submergence because a shorter interstage and skirt length is developed; therefore, vehicle weight is reduced. This system adapts to the nozzle submergence, used in the Lockseal design. Deep nozzle submergence is not feasible for the first stage because of space requirements for the gas generator. The nozzle can be submerged deeper in the second stage, but it was not incorporated to minimize the number of vehicle configurations.

2.8 TVC SYSTEM CONCEPTS

Four advanced TVC system concepts are studied to obtain comparative data pertaining to their use in large SRM's. Each of these systems control the vehicle by deflecting the thrust vector. The Lockheed Lockseal allows the

Table 2-4
260-IN. -DIAM SRM LOCKSEAL NOZZLE
WEIGHT SUMMARY (LB)

Deep Submergence	
Movable	32, 043
Fixed	5, 459
Adapter	38, 850
	<u>76, 352*</u>
Shallow Submergence	
Aft Flange	(+) 2, 770
Adapter, Insulation and Sleeve	(-) <u>42, 985</u>
Total	(net) <u>36, 137</u>

*These values are for comparison only; they are not used in the study.

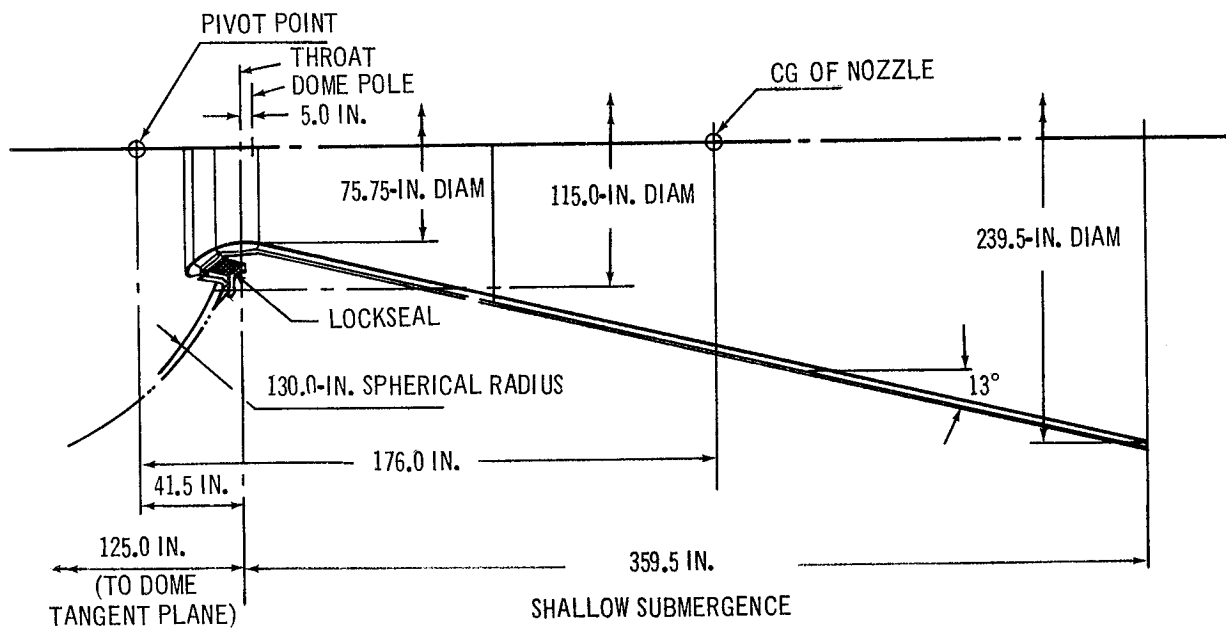
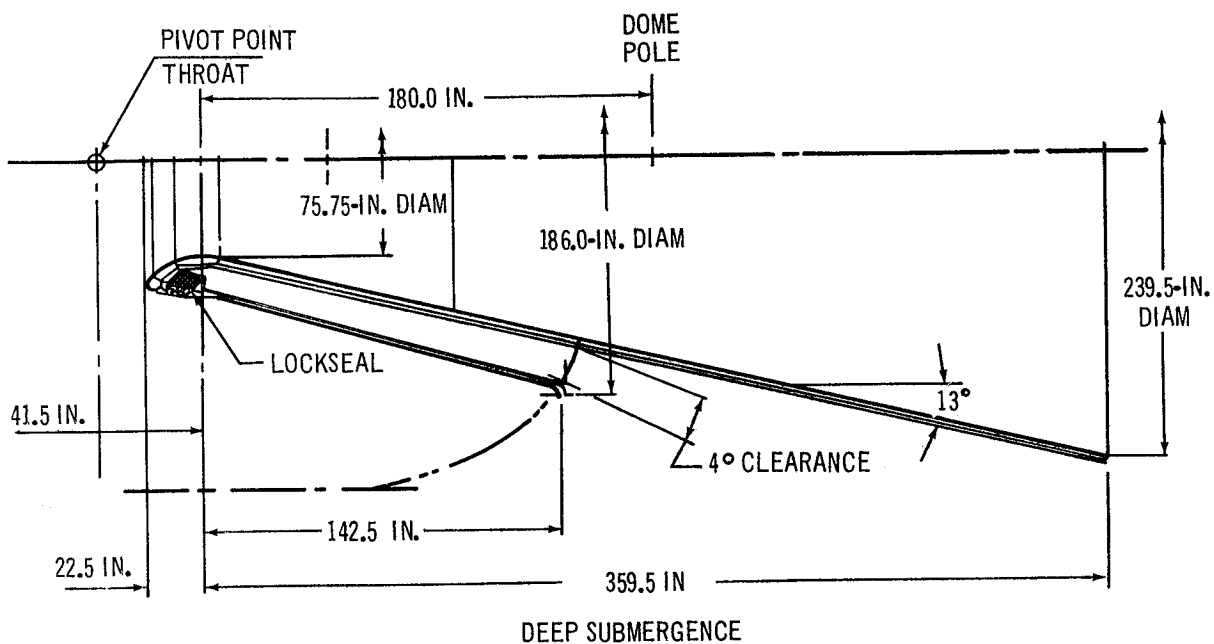


Figure 2-11. Nozzle Assembly: First-Stage 260-in.-Diam SRM

nozzle to gimbal and provides a static seal of chamber gas. The Vickers warm gas system injects gases, provided by a separate gas generator, continuously into the nozzle. The Thiokol and ABL hot gas systems inject main motor gases into the nozzle. Thiokol's design can operate at any valve-pintle position while the ABL design includes a valve that operates full-on or full-off. To obtain comparative data from a common base, each system was integrated with the two stages of the basic launch vehicle shown in Figure 2-2 and sized to provide attitude corrections caused by transient disturbing moments during flight and by steady-state perturbation such as CG offset and thrust misalignment. This section presents a description and the method of operation for each of the four TVC systems. Integration and sizing are discussed in Section 3.

2.8.1 Lockheed Lockseal TVC System

The Lockseal element consists of many alternate laminates of concentric metal spherical segments and elastomer vulcanized to form an integral unit. End rings attach to the motorcase and the nozzle. Thrust vector deflection or nozzle angular movement is allowed by shearing of the elastomer laminates. The metal laminates act as reinforcements and provide structural stability, high buckling strength, and limit axial deflection.

The basic seal assembly is protected from direct exposure to the motor thermal environment by a fixed insulator made of bonded plastic and a flexible insulator or boot constructed from elastomeric material. The boot is pressure-balanced to prevent chamber pressure from compressing it against the seal and causing an increase in actuation torque. The basic assembly and insulators are shown in Figure 2-12.

The primary Lockseal load is the axial ejection load caused by the motor chamber pressure on the nozzle entrance section. This load is carried in compression by the Lockseal elements. When rotated to effect TVC requirements, the Lockseal elastomeric pads deflect in shear. Under these two combined loadings, the Lockseal takes advantage of the properties of the elastomeric, that is, the effective bulk or compression modulus is approximately 1,000 times greater than the shear modulus. The Lockseal can sustain high axial loads with low axial deflections and can permit large angular deflections with low applied actuator forces.

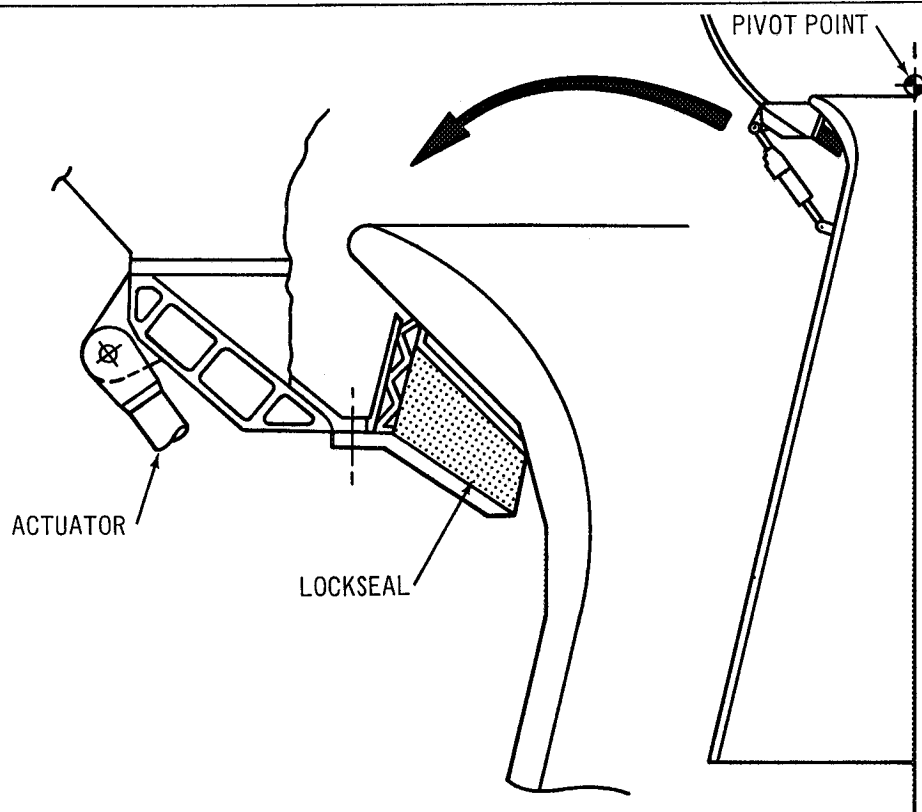


Figure 2-12. Gimbal Nozzle TVC (Lockheed)

2.8.2 Vickers Warm Gas TVC System

A schematic of this secondary injection system for one-axis TVC is shown in Figure 2-13. The TVC system for each axis includes a gas generator with solid-propellant grain and igniter system; a proportional, open center, high-temperature pneumatic control valve; secondary injection nozzles; gas manifolding between the gas generator and valve; and mounting frame and brackets. This is a continuous flowing system. The total gas flow from the generator is always injected into the motor nozzle downstream of the throat. The gas generator provides the source of warm gas ($2,000^{\circ}\text{F}$) to power this system. A load orifice is installed in the gas generator outlet flange to maintain a constant back pressure to the propellant, and gas flows continuously into the Vickers valve which is a spool design with a constant metering area. Gas flow is ported equally by the spool in the null position, thus providing zero net thrust-vector deflection when the flow is injected into the nozzle through diametrically opposite orifices. To produce jet deflection, spool position is shifted left or right, thereby reducing flow into the duct leading to one orifice, and increasing flow through the duct and orifice diametrically opposite. The

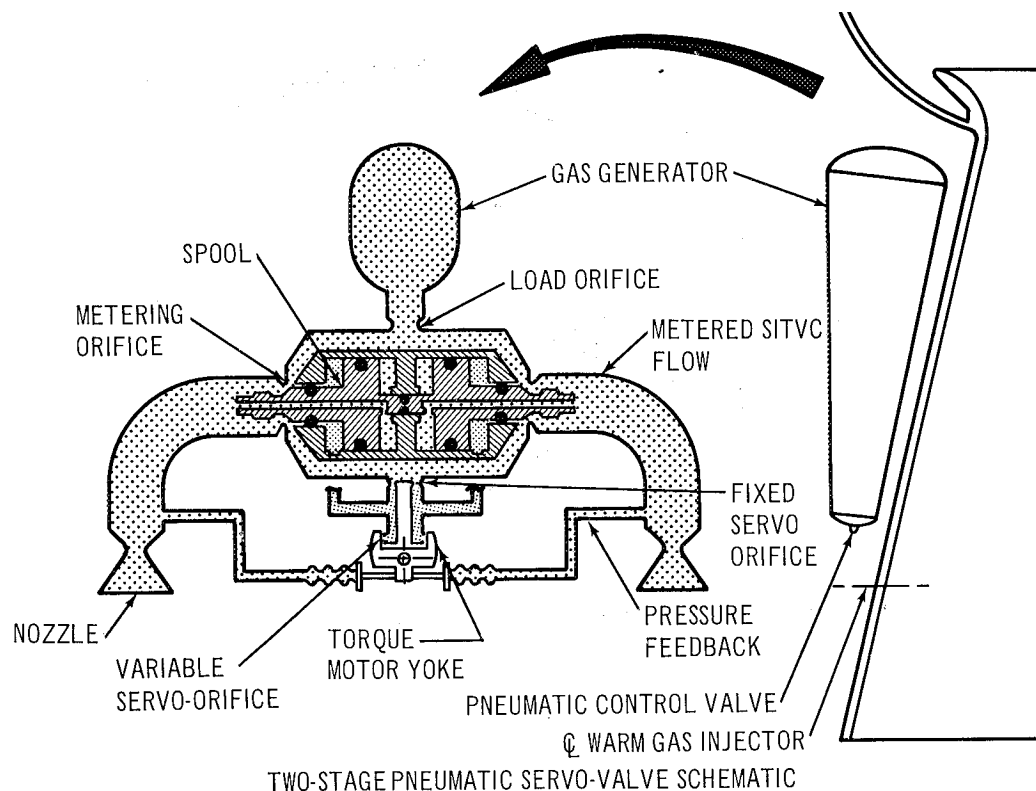


Figure 2-13. Warm Gas TVC (Vickers)

valve actuation force is provided by a tapoff flow from the gas generator which is approximately 3% of total flow. This flow may be dumped overboard or vented to a low-pressure region downstream. Actuation control comes from a torque-motor operated pilot yoke.

Manifold pipes and injection nozzles are made of heat-resisting steel alloys. The supersonic exit cone of the injection nozzles is submerged within the wall of the motor nozzle to prevent erosion by the rocket motor exhaust gases.

2.8.3 Thiokol and ABL Hot Gas TVC Systems

These hot-gas or chamber-bleed secondary injection TVC systems use high-temperature combustion gases that are bled off the main chamber and injected through metered orifices into the nozzle flow, downstream of the throat. The high-temperature (5,800°F), highly erosive combustion gases flow across the metering pintle and out through the injection orifices.

The Thiokol hot gas valve (Figure 2-14) has a thoriaated tungsten shell encasing the metering pintle which provides non-eroding surfaces. The pintle is pressure balanced through the use of a pressure-balanced cavity and bleed holes through the face of the pintle. Pintle position is hydraulically controlled by a servo valve (recommended as an integral part of the pintle valve with the hydraulic servo actuator mounted outside of the motorcase). Flow rate is varied as a function of deflection-angle demands. The higher the required deflection angle, the further the pintle is moved from the injection orifice, thereby increasing the injectant flow rate. The Thiokol pintle design has been tested in configurations that use both constant bleed and complete shutoff concepts. The latter uses a tungsten-to-tungsten seal which has been demonstrated at 6,000°F.

The ABL hot gas valve concept shown in Figure 2-15 meters the flow of chamber gases into the nozzle in pulses from zero to maximum; therefore, thrust deflections for vehicle control are produced by varying the pulse duration and cyclic frequency. It employs a graphite seat for the injection orifice and a rubber (Buna-S) nose on the mating pintle. Pintle actuation

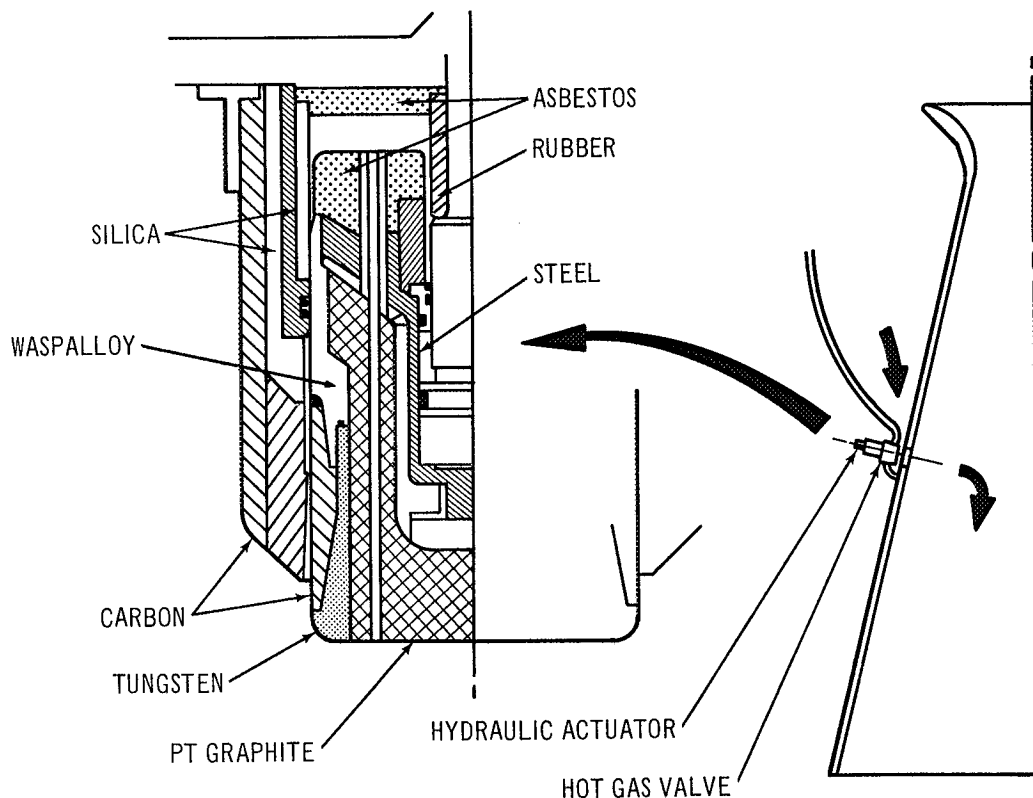


Figure 2-14. Hot Gas TVC (Thiokol) - Modulated

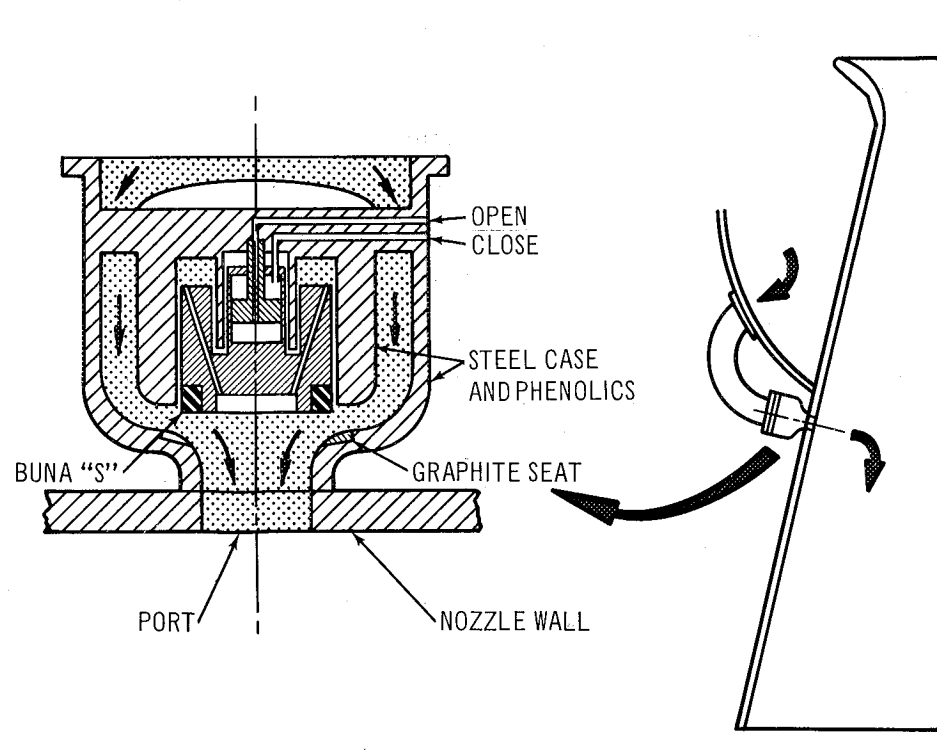


Figure 2-15. Hot Gas TVC (ABL) – Basic On-Off Design

loads are reduced through the use of a semibalanced pintle or plug. Combustion gases are bled past the pintle to a plug cavity on the backside, achieving the balancing effect. The hydraulic actuation cylinder is integral with the valve on the plug centerline, protected from the extreme temperature by a thick phenolic annulus. The valve is designed for positive seating and shutoff; however, some deformation and char of the rubber portion of the pintle as a function of duty cycle does occur. The ducts required in this mode of operation can be constructed using a tungsten inner liner, a graphite core, and a tantalum external surface coating. The duct design has been developed and tested at temperature of 5,800°F. The complete evaluation of this TVC system was not made because its use and feasibility as a control system for large launch vehicles is not established, and in consultation with ABL it was their recommendation to modify this basic on-off valve design to provide modulation capability (see Appendix A.5) when using this technique for the control of large solid-propellant launch vehicles. A silver-infiltrated tungsten plug and seat are recommended to eliminate plug erosion when the on-off valve is modified. A schematic is shown in Appendix A.5.

Section 3

LAUNCH VEHICLE SYSTEM COMPARISONS

Six launch vehicle configurations were established to obtain the necessary design and aerodynamic data to perform the TVC stability and control analyses, and to show the structural/configurational differences that exist because of the use of each candidate TVC systems and two payload shapes. These configurations, shown in Figure 3-1, are derivatives of the basic launch vehicle. Configurations I and IA use only warm gas TVC systems, Configurations II and IIA use only gimbal nozzle TVC systems, and Configurations III and IIIA use only hot gas TVC systems. A pictorial representation of all possible first and second stage combinations is not shown because of the close similarity of the second-stage vehicles. The Ballos payload is the primary payload, and the HL-10 type wing payload is an alternate. The basic launch vehicle and the two payload shapes are shown in Figure 2-2. The first- and second-stage SRM and nozzle installations are shown in Figures 2-9 and 2-10.

Since the SRM's used in both stages are fixed by the basic launch vehicle, the only structural differences that exist are changes in interstage and skirt geometry. Associated with this change in geometry is a weight change. Geometry variations are shown in Figure 3-1. Weight variations require a design and analysis of each component. The objectives and scope of the study did not warrant an analysis of each vehicle configuration; therefore, a representative vehicle was selected for analysis, and the weight changes for other configurations were obtained by a ratio of surface areas.

3.1 STRUCTURAL DESIGN CRITERIA

The interstage and skirts are designed using the following criteria to establish lengths, shapes, and separation planes:

1. First-Stage Skirt.
 - A. The skirt extends to the nozzle exit plane to facilitate launch pad support and handling.

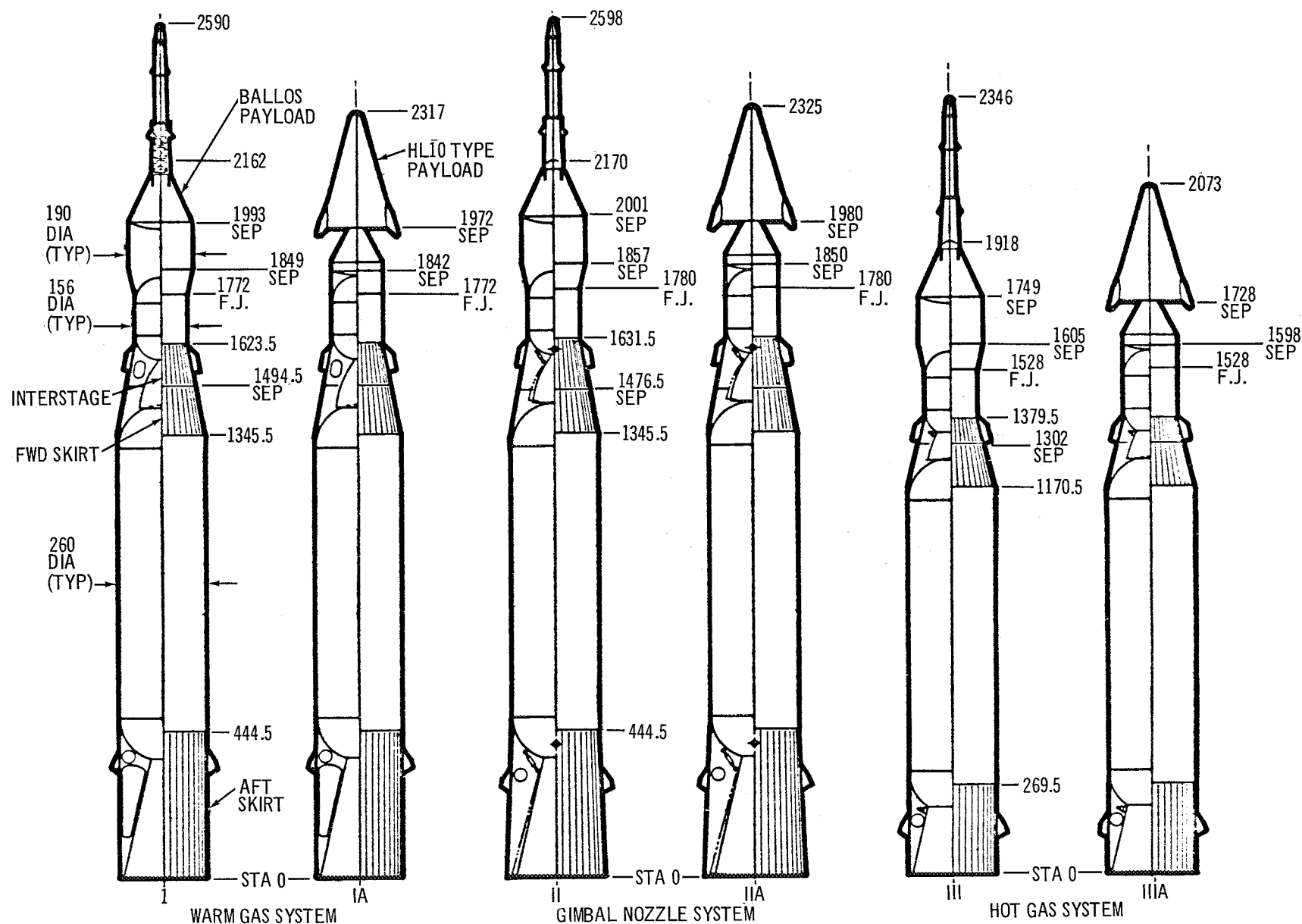


Figure 3-1. SRM TVC System Configurations

	CONDITION	
	MAX $q \alpha$	BURNOUT
ALTITUDE (FT)	45,000	154,000
t (SEC)	80	152.2
q (PSF)	975	155
M	2.0	9.2
α (DEG)	8°	$1^\circ 44'$
F_s (LB)	151,000	4,320
T (LB)	4,950,000	5,030,000
WEIGHT (LB)	2,181,946	704,616
I (IN.-LB SEC ²)	10.568×10^8	6.343×10^8
CG (IN.)	992.9	1188.4
η_z (G)	0.150	0.0127
η_x (G)	-2.122	-7.086
$\ddot{\theta}$ (RAD/SEC ²)	0	0.003

NOTE: FOR GROUND WIND CONDITION, STATION 0 IS 408 IN. ABOVE THE GROUND ON THE LAUNCH PAD.

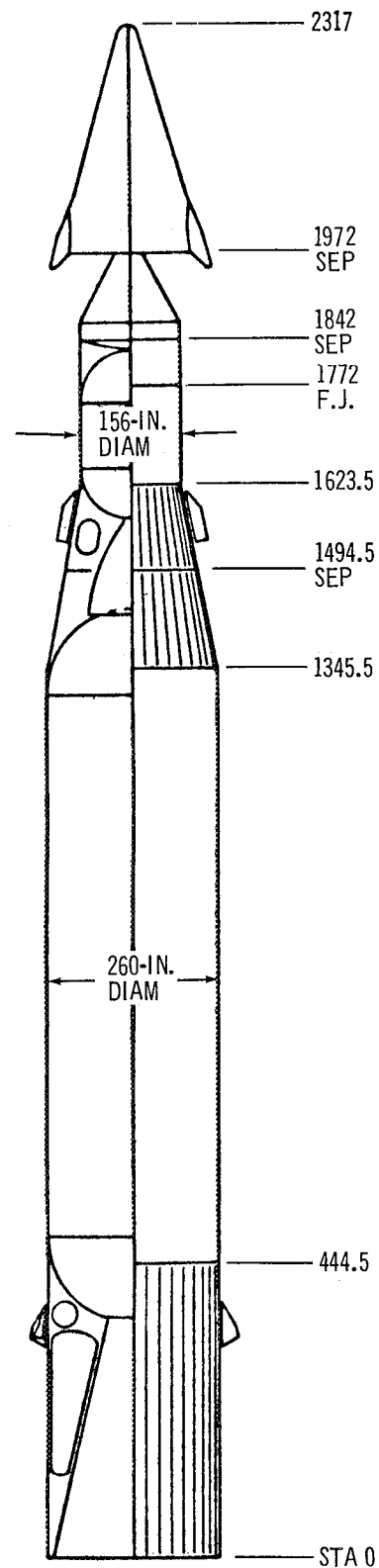


Figure 3-2. Preliminary Loads – Configuration IA

- B. Nongimballed nozzle configurations use cylindrical skirts.
 - C. Gimballed nozzle configurations use truncated conical skirts that provide satisfactory nozzle clearance in the gimballed position.
 - D. No skirt separation.
2. Second Stage Interstage.
- A. The interstage/skirt and stage forward skirt are cone frustrums with end diameters that match the 260-in.-diam and 156-in.-diam SRM's.
 - B. The forward dome closure of the 260-in.-diam SRM protrudes 8 in. into the nozzle opening of non-gimballed nozzles.
 - C. The forward-dome closure of the 260-in.-diam SRM is not permitted to protrude into the nozzle opening of the gimballed nozzle when in the neutral position.
 - D. The separation plane is established using the following approximate S-IVB criteria:
 - (1) 15° clearance angle from the vertical.
 - (2) Angle apex at the outermost nozzle point (maximum gimbal position for the gimballed nozzle).
 - (3) Maximum gimbal angle of 6° in the corner of a square gimbal pattern.

3.1.1 Loads

Interstage and skirt structural weights are developed from designs for Configuration IA. This configuration was selected because it should produce the highest loads of all the configurations shown in Figure 3-1. Its mass distribution is such that it tends to reduce the relieving inertia bending moment, and its winged payload produces high airloads. Therefore, the structural weights obtained from a ratio of surface areas should be conservative.

To determine critical design loads, calculations of vehicle shears, moments and axial loads were made for three conditions: ground wind, maximum $q\alpha$, and first-stage burnout. Figure 3-2 shows vehicle geometry and a summation of the significant parameters used and developed in this analysis.

3.1.1.1 Ground Wind Condition

Ground wind loads are shown on Figure 3-3. The vehicle is free standing, fully loaded, and subjected to a 99.9% ETR surface wind. These loads are

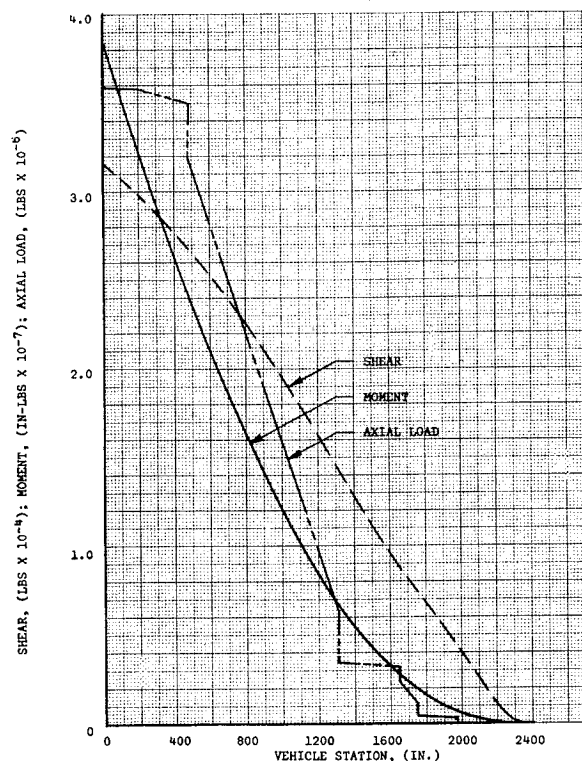


Figure 3-3. Ground Wind Loads

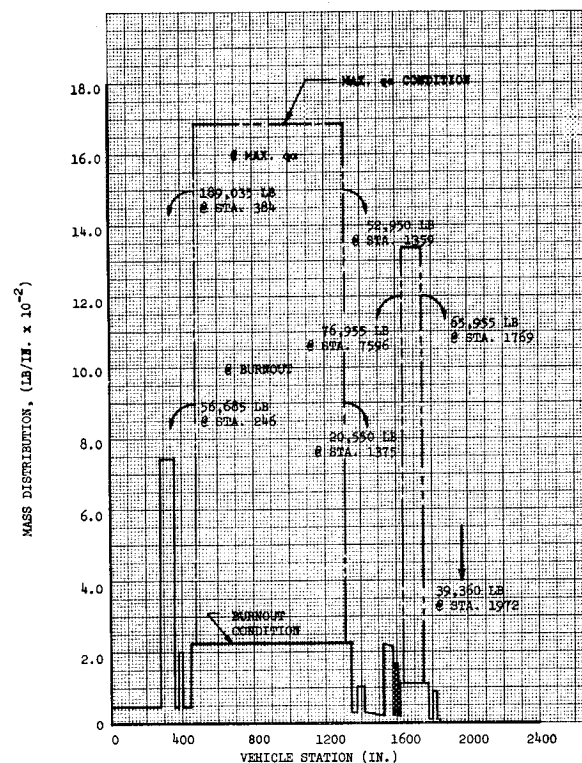


Figure 3-4. Mass Distribution – Configuration IA

calculated on the basis of steady-state winds and the effect of vortex shielding (Von Karmon Effect).

3.1.1.2 Flight Loads Conditions

Loads for the two flight conditions (maximum $q\alpha$ and first stage burnout) were calculated on the basis of the mass distribution and vehicle aerodynamics consistent with these two events. The mass distributions are shown on Figure 3-4. Vehicle "dry weight" is shown by the solid line, and propellant weight is represented by dashed lines. Axial force coefficients and normal forces coefficients are shown in Figures 3-5, 3-6, and 3-7. Two values for the base drag coefficient are shown on Figure 3-5, power on and power off. Power-on values were used in the analyses for both flight conditions, for the burnout condition was considered to occur an instant prior to thrust tail-off. Vehicle loads for these two flight conditions are shown on Figures 3-8, 3-9, and 3-10.

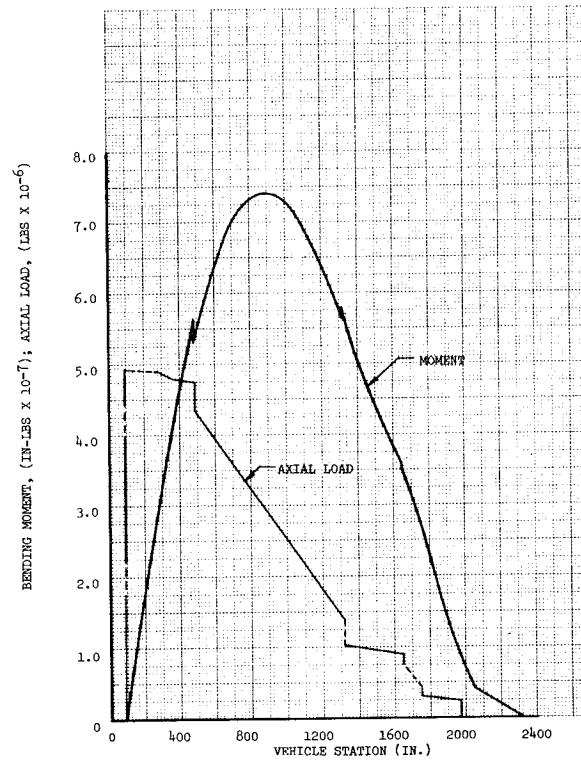


Figure 3-9. Bending-Moment and Axial-Load Diagram,
Max q_a Condition

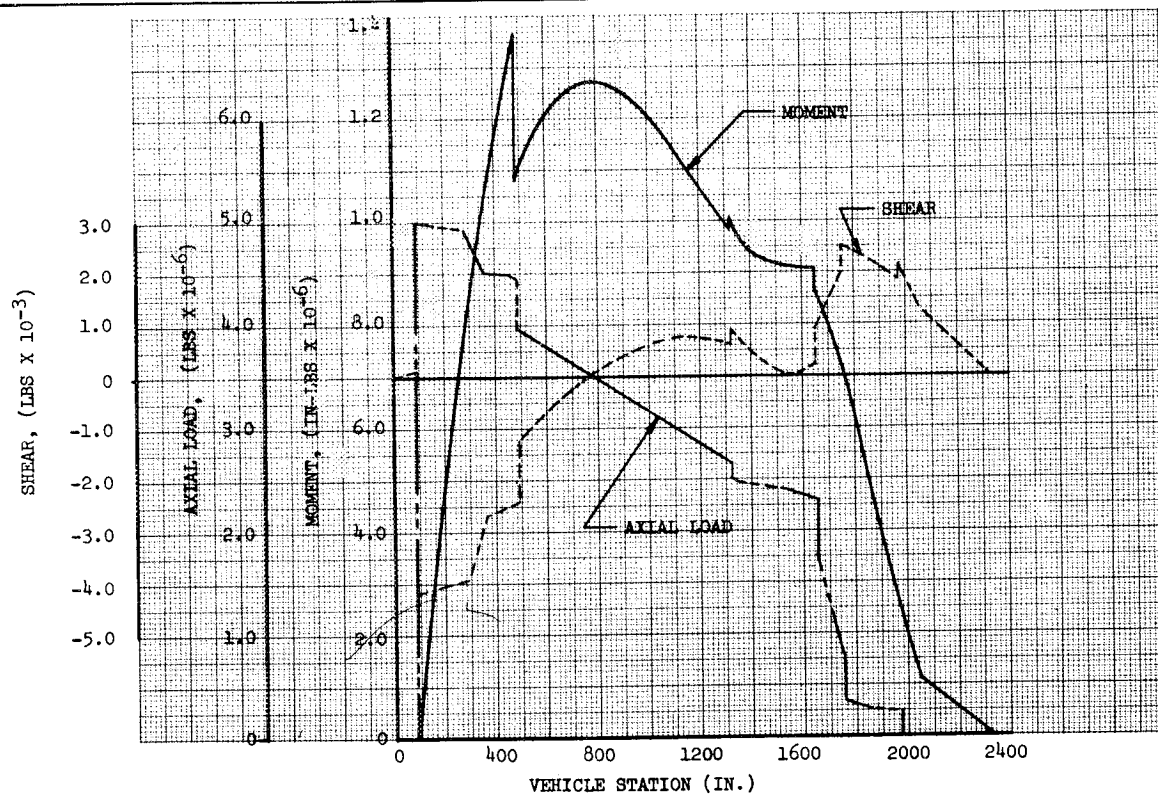


Figure 3-10. Flight Loads – Burnout Condition

3.2 STRUCTURAL DESIGN

Structural design and detailed sizing were accomplished to obtain accurate weights for the first-stage forward and aft skirt and the second-stage inter-stage of Configuration IA. In addition, an EI distribution is calculated for use in the body-bending analysis.

Semimonocoque construction and 7075-T6 aluminum are used in all designs.

3.2.1 Aft Skirt-260-in.-diam SRM

The aft skirt is a cylindrical section having a diameter of 260-in. and a length of 444.5 in. as shown in Figure 3-11. The semimonocoque construction includes external stringers and internal frames. The critical compression loading intensity (N_c) occurs at the ground wind condition. An average $N_c = 6,815$ lb/in. was used to size the stringers and frames.

The skin gage selected is 0.050 in. The skin thickness increases to 0.200 in. locally at the eight aft-pad points and step-tapers back to 0.050 in. over a length of 90 in. and a width of 65 in. This local increase of skin gage distributes the launch-stand loads evenly into the aft interstage.

Eighty stringers are used for the aft skirt and are equally spaced at 10.20 in. around the circumference. The resultant compressive load per stringer is 69,500 lb. The stringer shape designed for this load is shown in Figure 3-11. Seventy-two of the 80 stringers have an area of 1.055 sq in. Eight stringers which have an area of 10 sq in. locally at the aft end hard points. These 8 stringers are tapered back to an area of 1.055 sq in. over a 90-in. length where the loads are evenly distributed.

The frames were designed to prevent general instability. The required inertia (I) value was calculated on the basis of the following equation, and the frame design is shown in Figure 3-11.

$$\begin{aligned} I_{\text{REQUIRED}} &= \frac{(C_f)(N_c)(D^4)(\pi)}{4 EL} = \frac{(62.5 \times 10^{-6})(6815)(260)^4(\pi)}{(4)(10.5 \times 10^6)(29.5)} \\ &= 4.93 \text{ IN}^4 \end{aligned}$$

where

$$L (\text{optimum}) = 0.115D = 0.115 (260) = 29.9 \text{ in.}$$

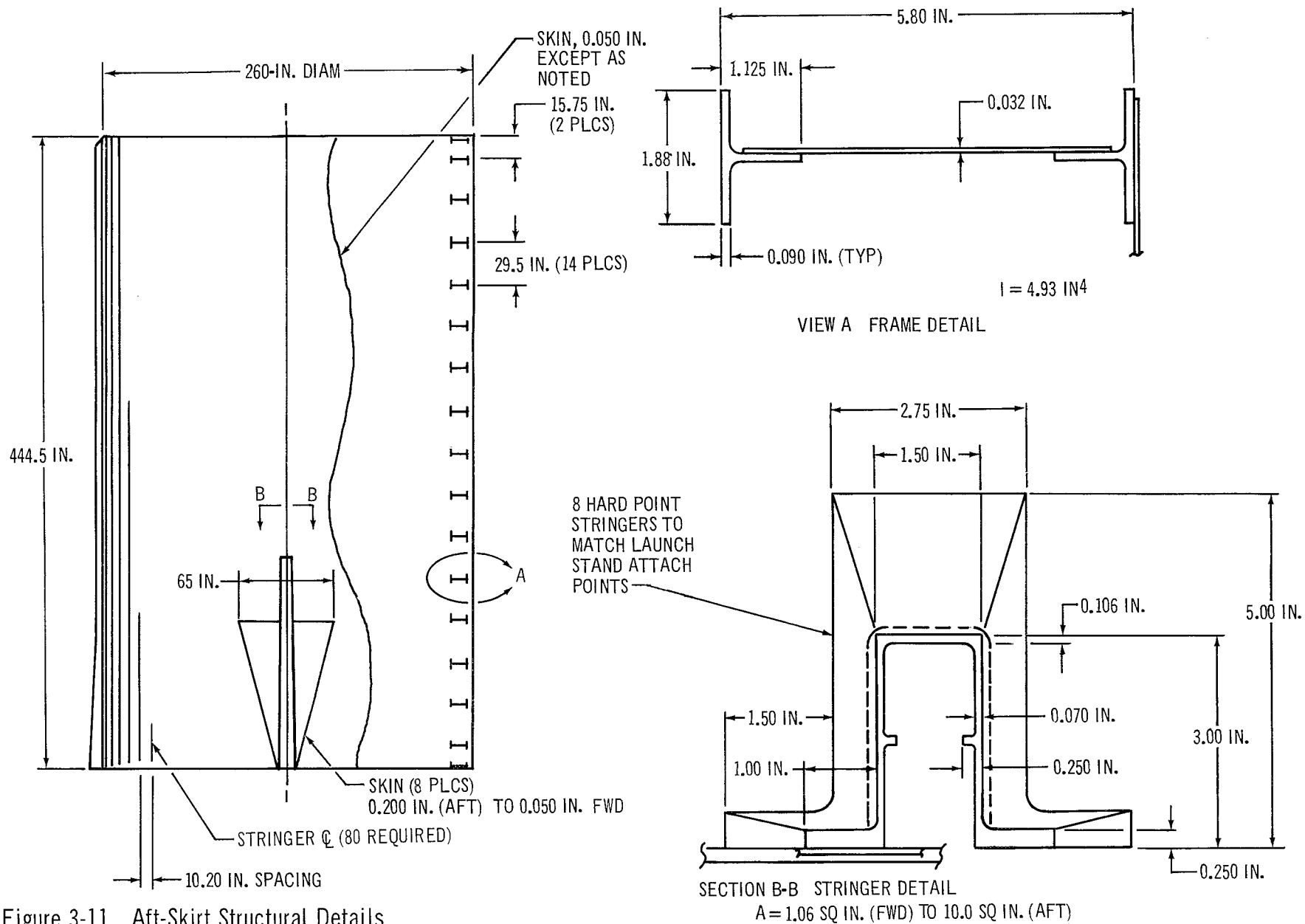


Figure 3-11. Aft-Skirt Structural Details

The frame spaced is 29.5 in. with the 2 end bays having a spacing of 15.75 in.

3.2.2 First-Stage Forward Skirt and Second-Stage Interstage

The first-stage forward skirt and the second-stage interstage are truncated conical sections. The skirt has an aft diameter of 260 in. and a vertical length of 149 in., and the interstage has a forward diameter of 156 in. and a vertical length of 129 in. These components are constructed with external stringers and internal frames. The critical compression loading condition occurs at first-stage burnout and was used to size the stringers and frames.

The skin thickness varies between 0.025 in. at the 156-in. -diam and 0.050 in. at the 260-in. -diam.

The skirt and interstage have 80 external stringers that are equally spaced around the circumference of the conical sections. The stringer spacing varies from 6.13 in. at the forward end to 10.20 in. at the aft end. The compressive load per stringer is 41,700 lb (forward) and 44,400 lb (aft). The stringer sized by these loads is shown in Figure 3-12.

To prevent general instability, frames were designed by the method shown for the aft skirt. Design loads and frame dimensions are summarized in Table 3-1 for three stations. Frame spacings and a cross section is shown in Figure 3-12.

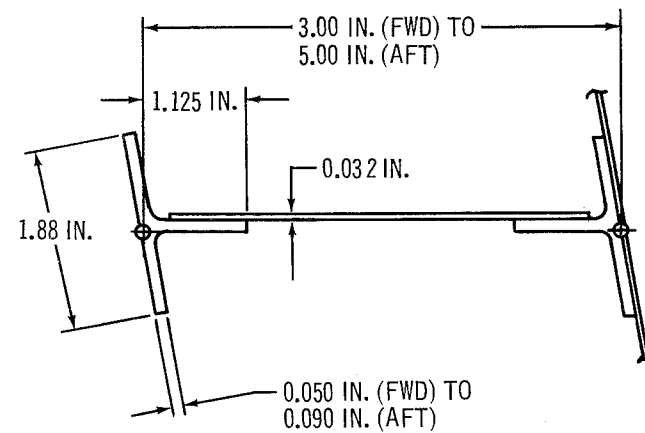
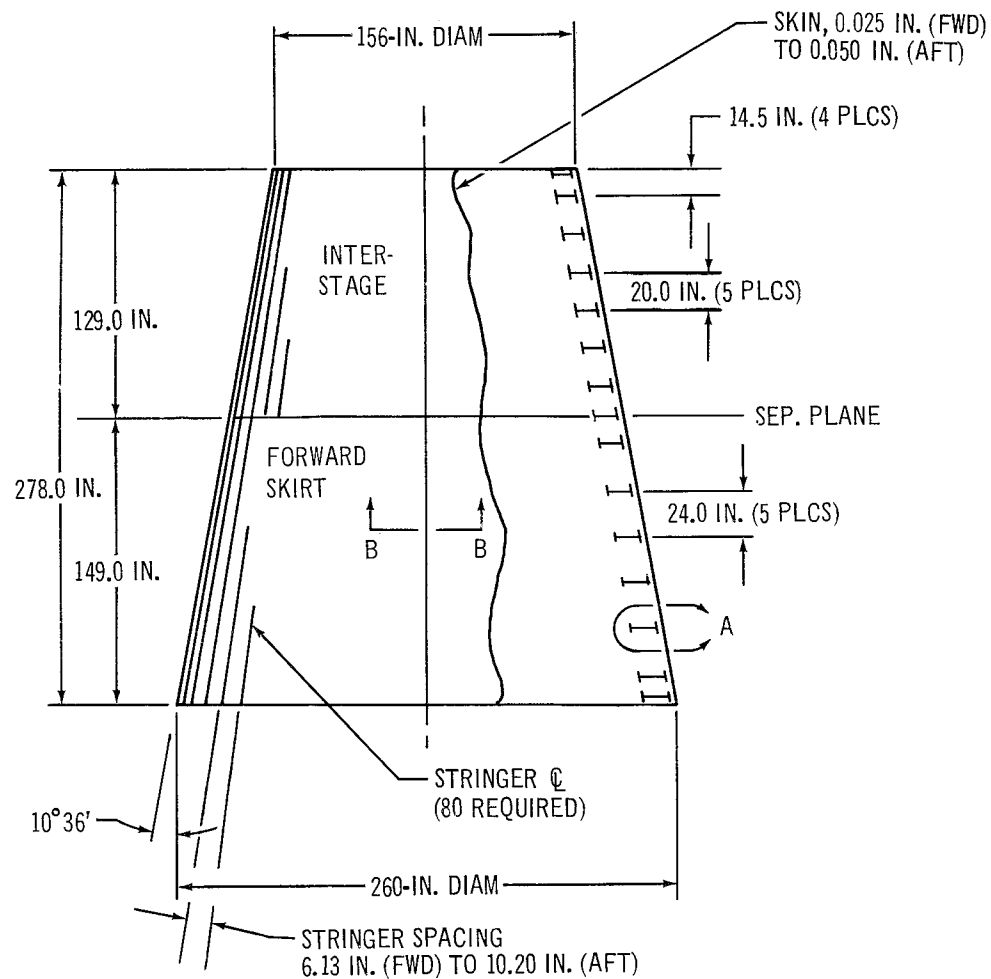
3.2.3 Vehicle Stiffness (EI Distribution)

Vehicle stiffness or EI distribution is calculated for the three configurations with the Ballos payload (Figure 3-13). This distribution also applies to the winged payload configurations except in the region of the payload.

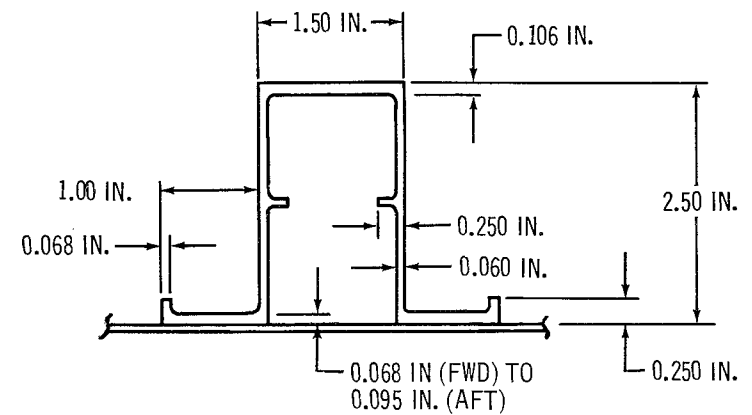
3.3 INTEGRATION OF TVC DESIGNS

Figure 3-14 (Douglas Drawing No. 1B67823) shows the preliminary structural design and the integration of the major subsystems of each TVC system on the first and second stages of the launch vehicle.

Sheet 1 of Figure 3-14 shows a launch vehicle using a warm gas TVC system on both first and second stage. The eight first-stage gas generator tanks are made in the shape of cone frustrums with Cassinian domes in order to fit



VIEW A FRAME DETAIL
 $I = 0.92 \text{ IN}^4$ (FWD) TO 3.81 IN^4 (AFT)



SECTION B-B STRINGER DETAIL
 $A = 0.629 \text{ SQ. IN.}$ (FWD) TO 0.675 SQ. IN. (AFT)

Figure 3-12. Forward-Skirt Interstage Structural Details

Table 3-1
FRAME DIMENSIONS

Station (in.)	N_c (lb/in.)	I_{REQUIRED} (in. ⁴)	Frame Height (in.)	Cap Thickness (in.)
1,345.5	4,275	3.81	5.0	0.090
1,494.5	5,360	2.07	4.0	0.070
1,623.5	6,680	0.92	3.0	0.050

inside the cylindrical aft skirt volume. The gas valves are attached to the bottom of the tanks. The four second-stage gas generator tanks are made in the more conventional cylinder-hemispherical dome tanks shape. This is possible because the smaller tank size and the flared interstage volume does not require the "sardine packing" of the first stage. As in the first stage, the gas valves and actuators are attached to the bottom of the tanks and control diametrically opposed injector nozzles.

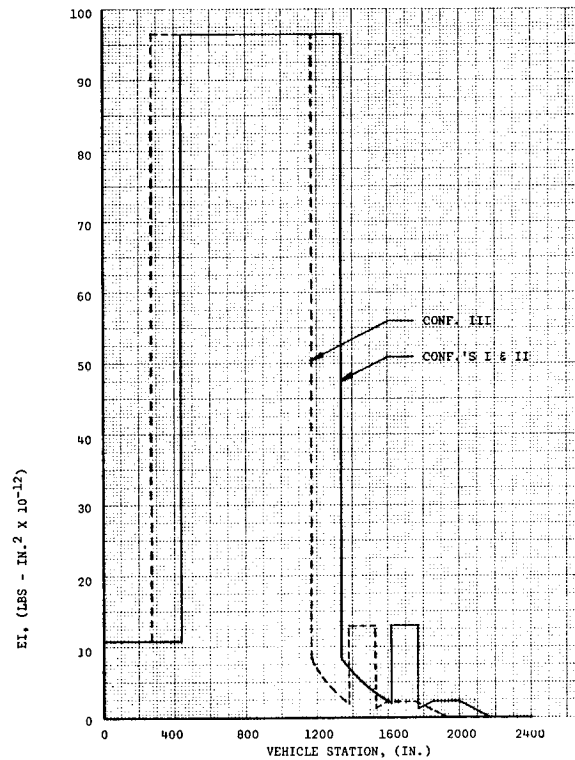
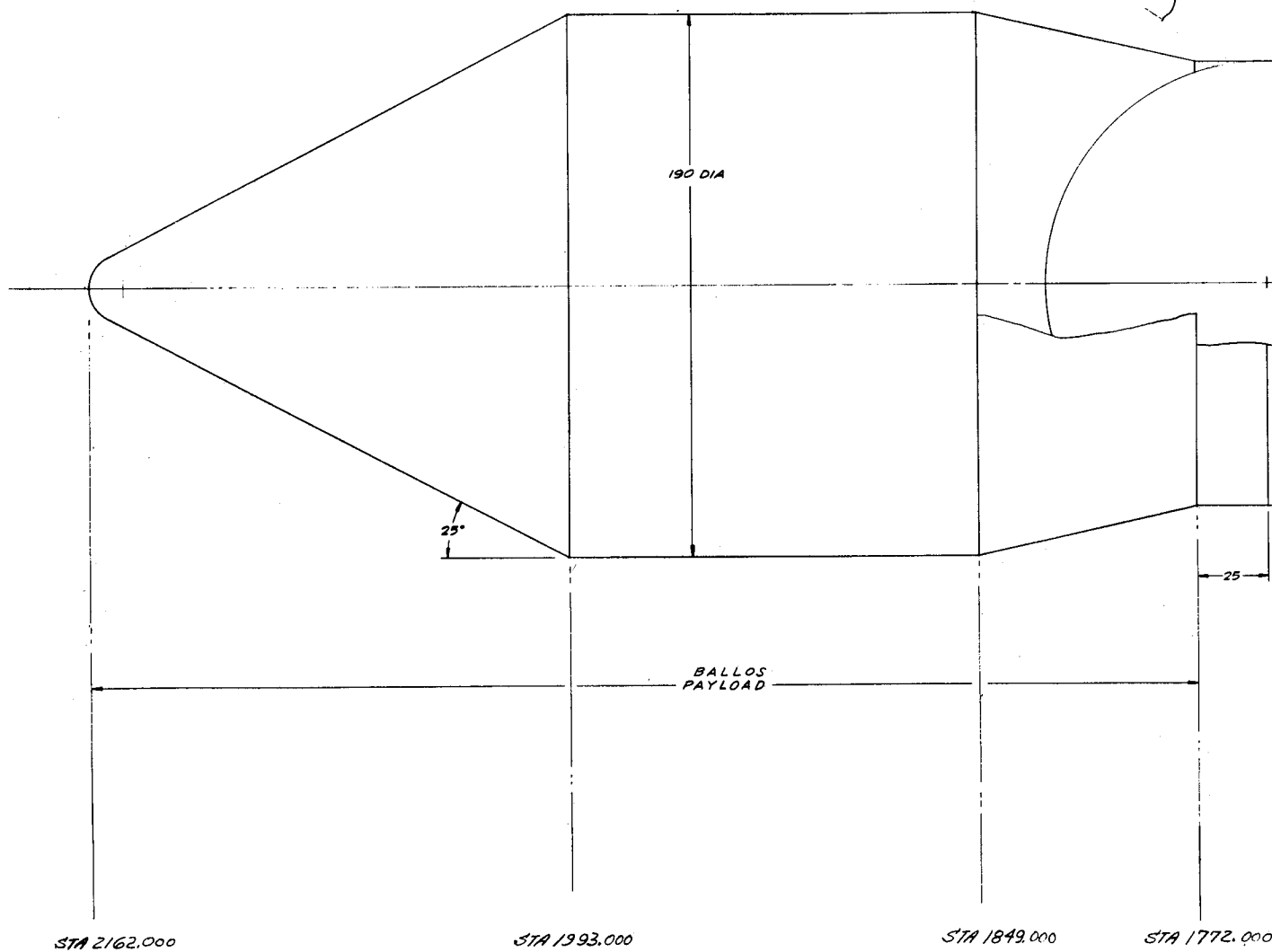
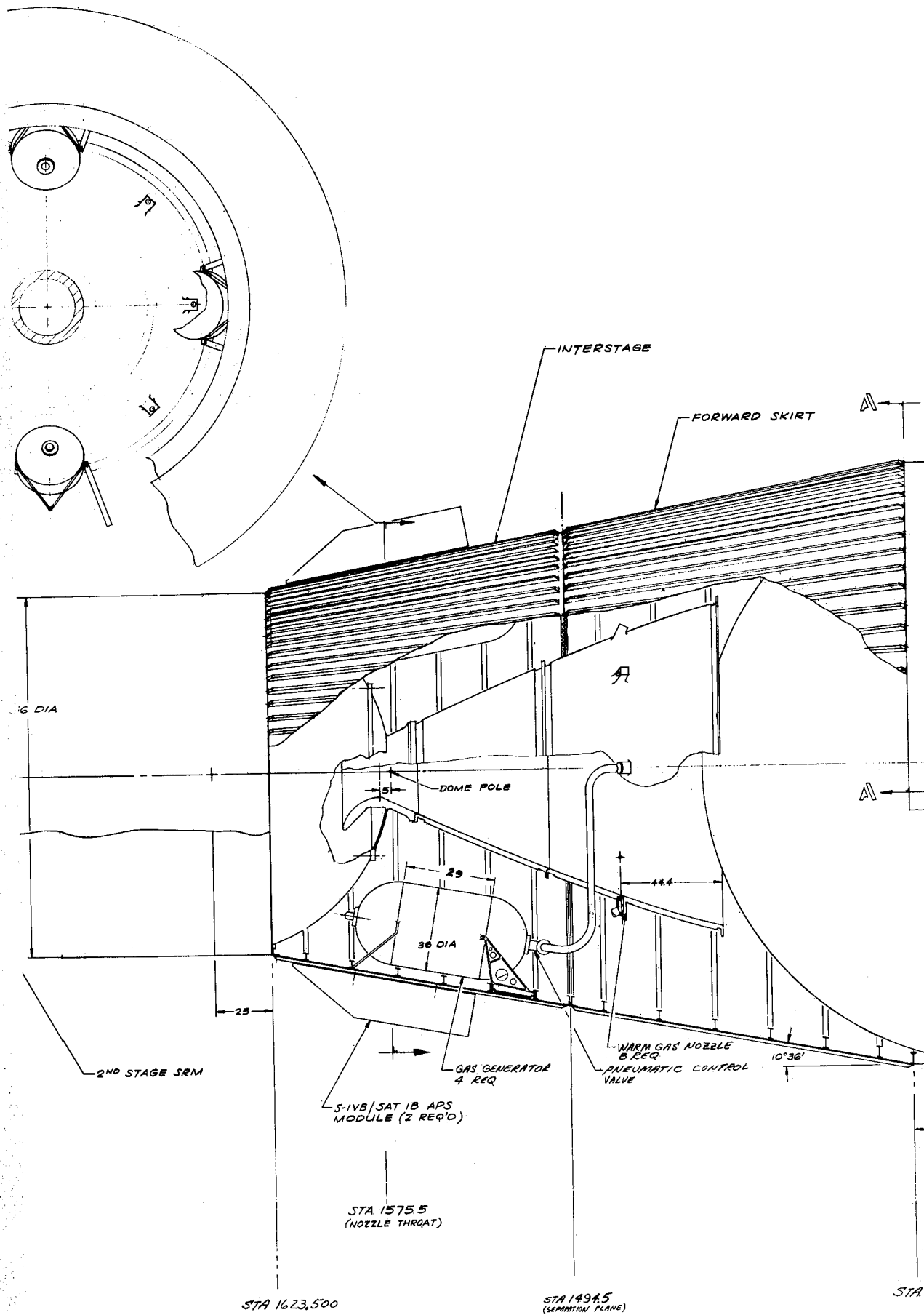
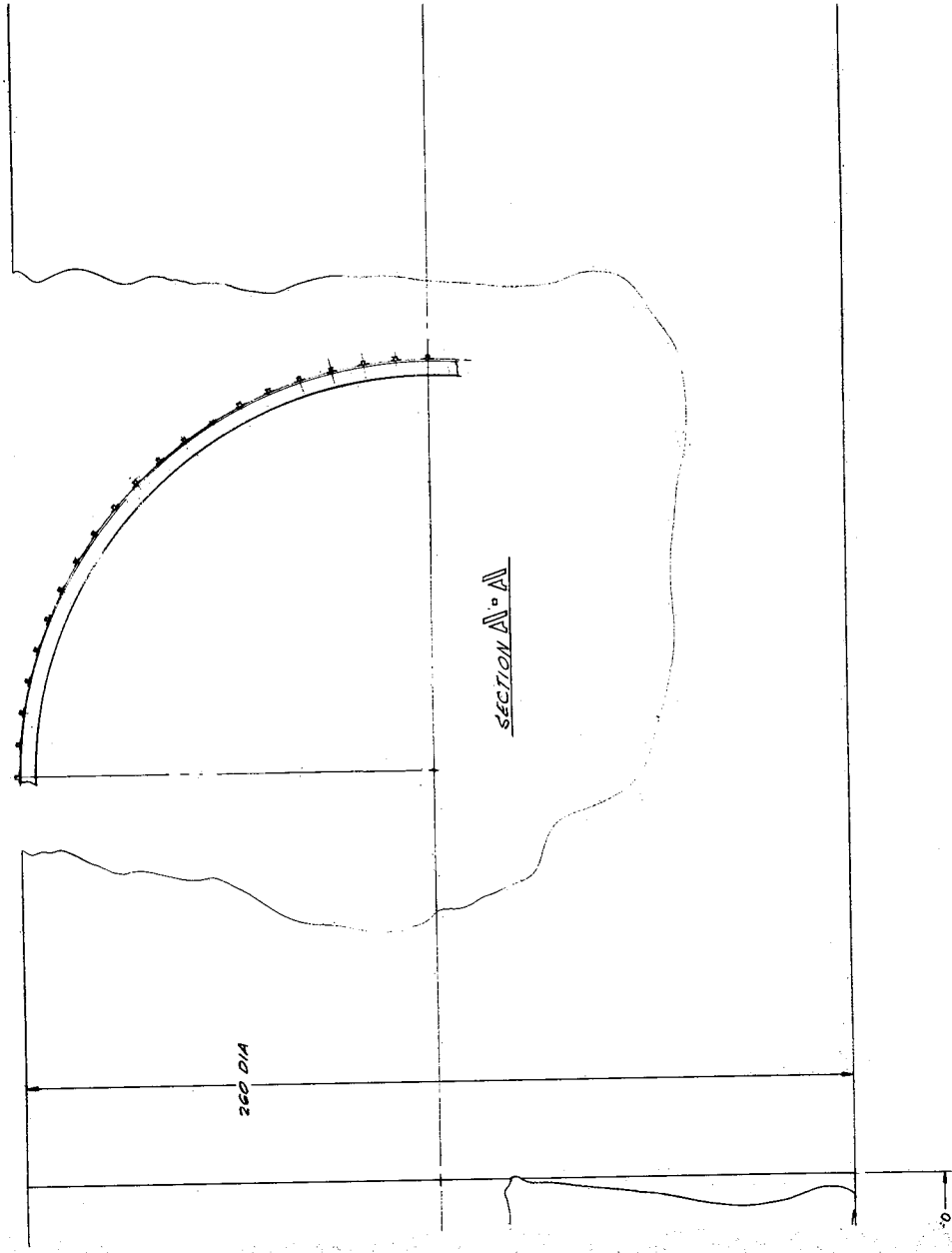
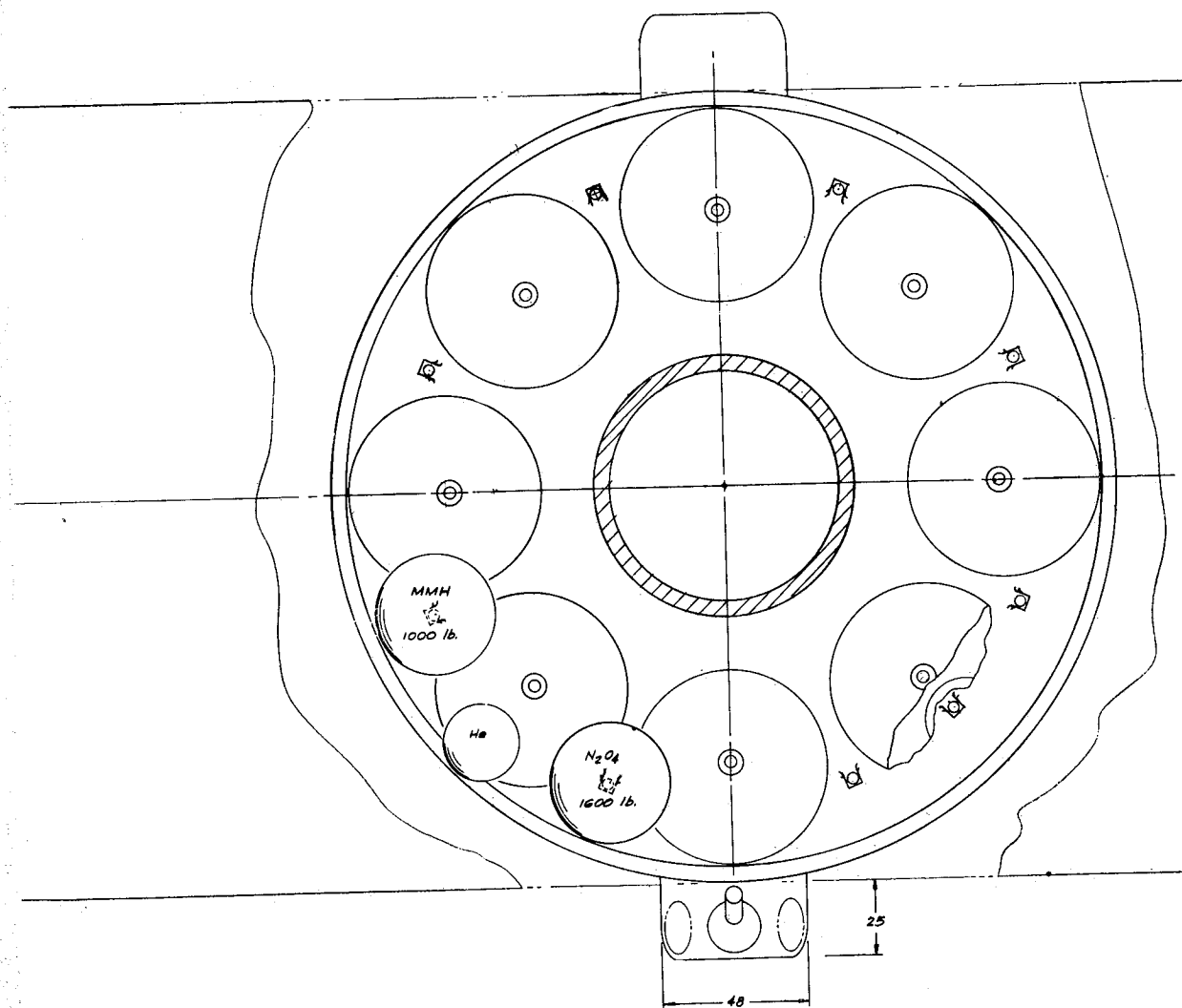


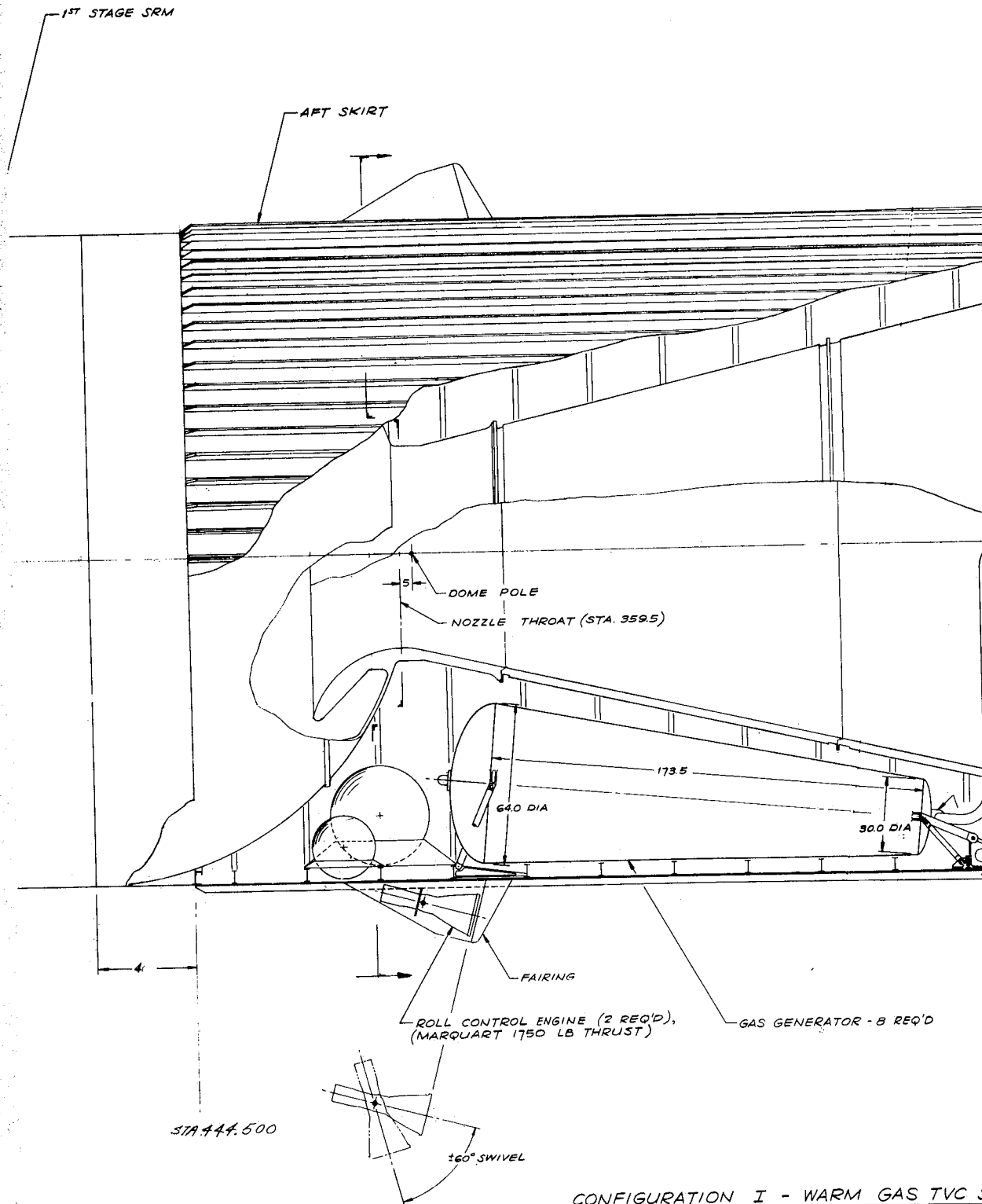
Figure 3-13. EI Distribution











CONFIGURATION I - WARM GAS TVC

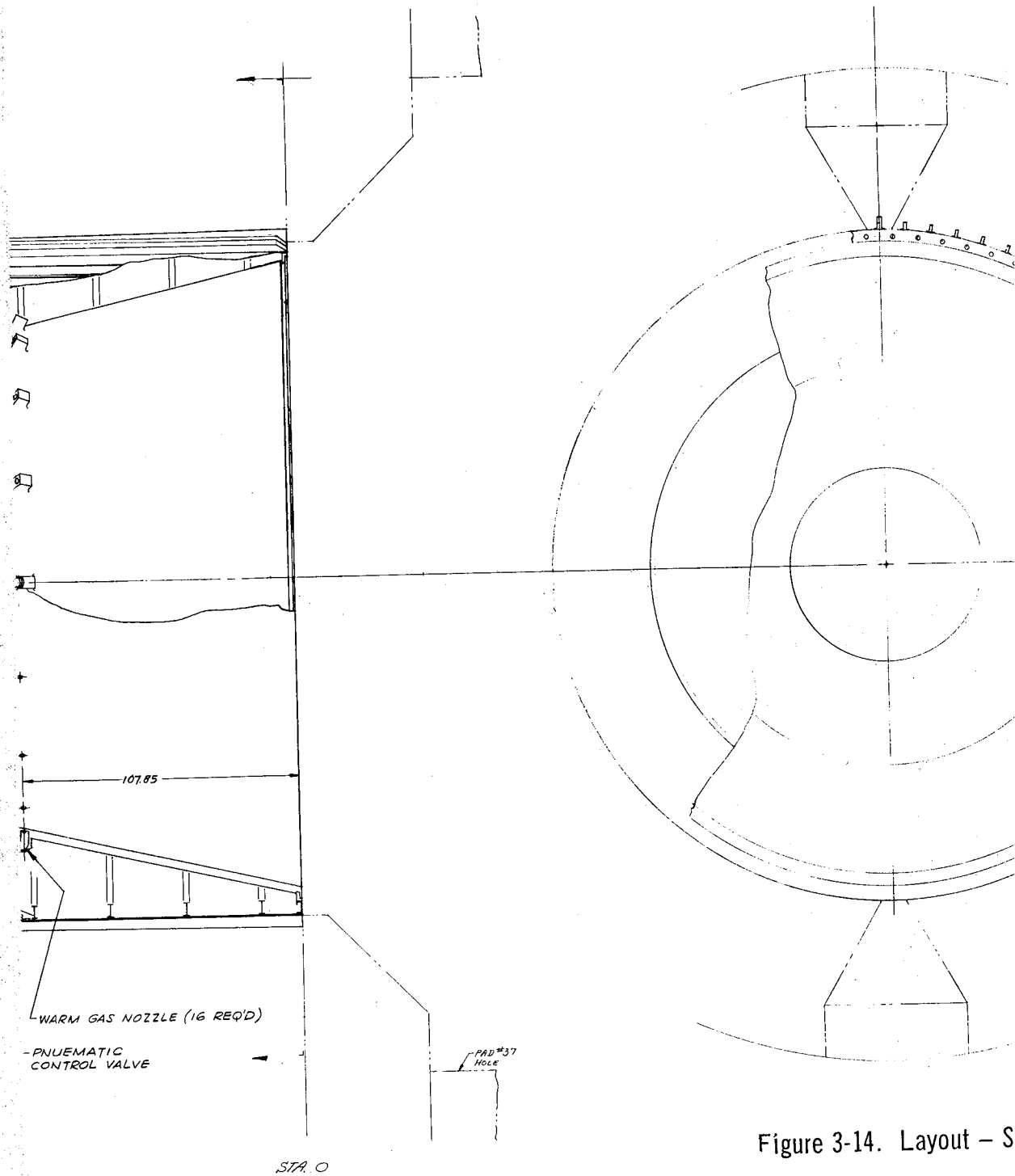
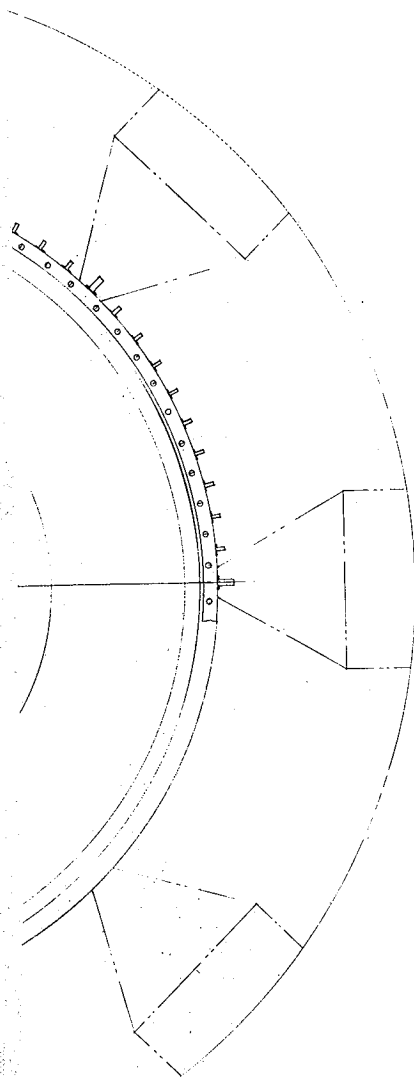


Figure 3-14. Layout - S



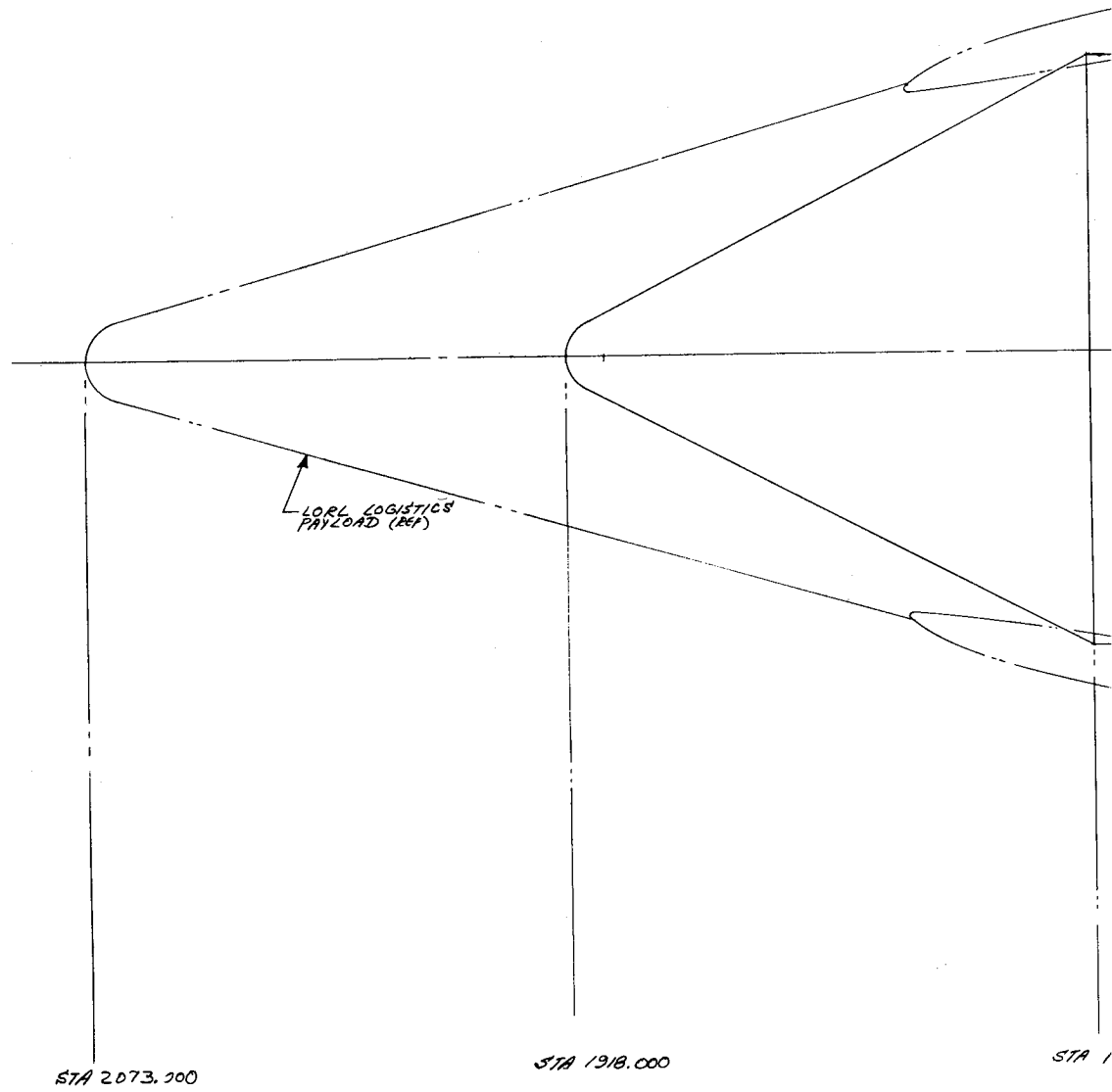
0 50 100

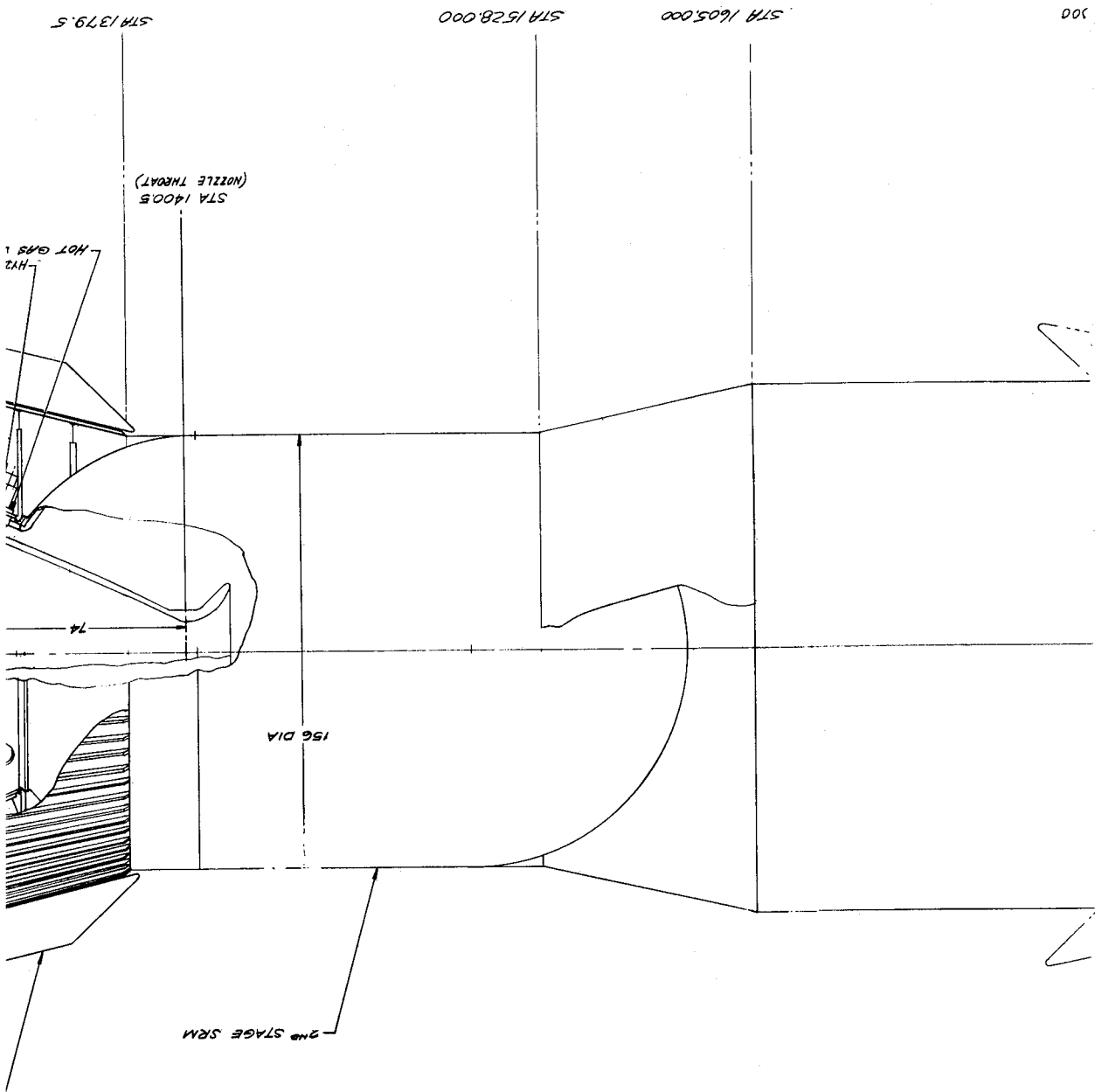
SCALE: 1 = 20

1B67823

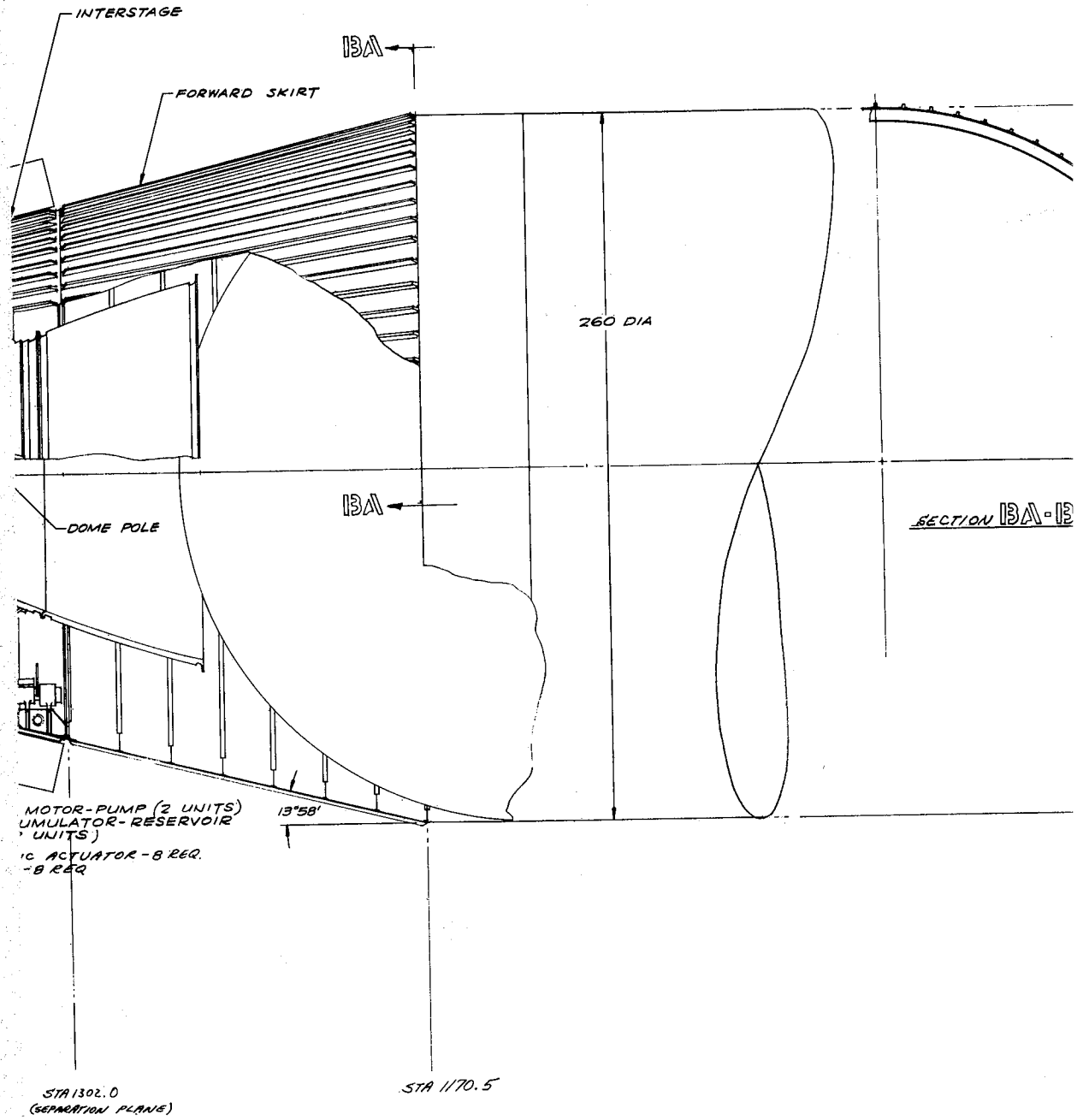
Motor TVC System Configurations (Page 1 of 3)

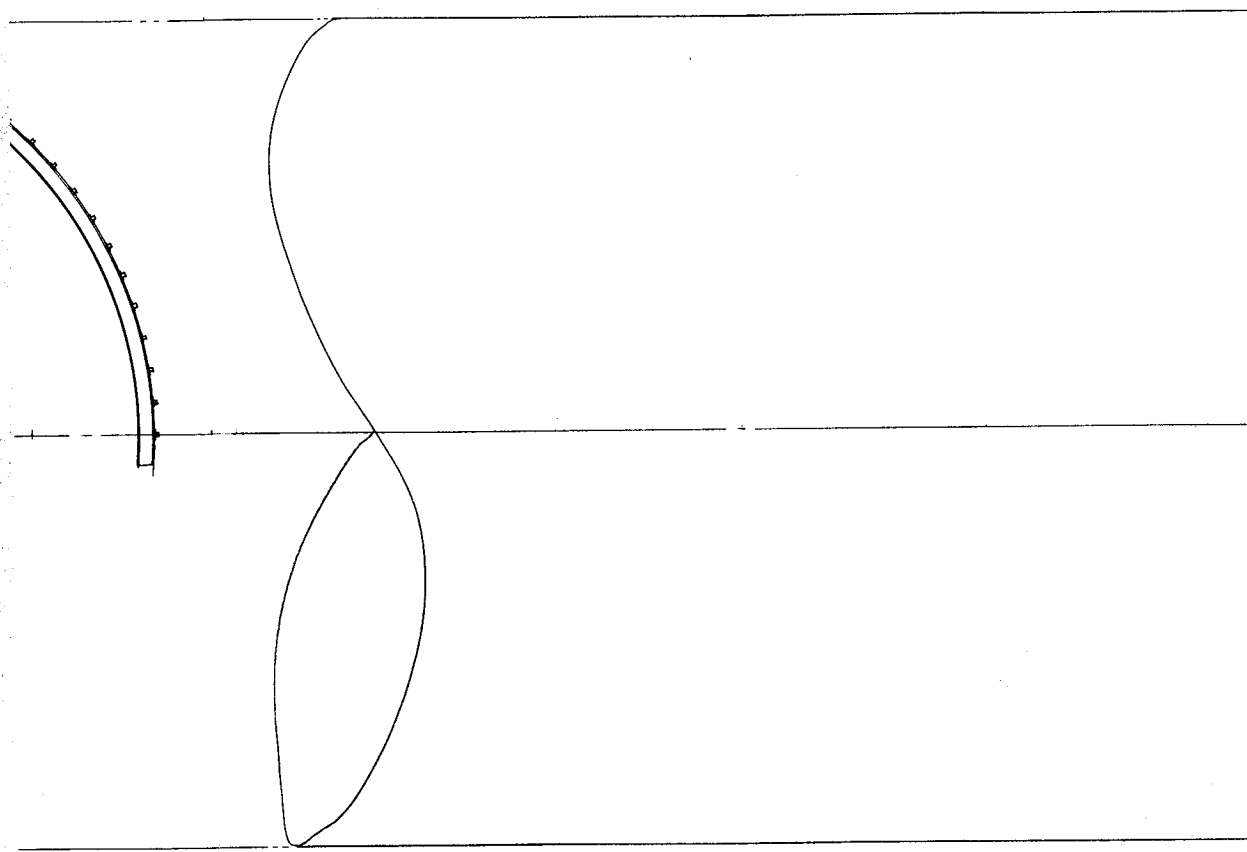
MATERIAL		DOUGLAS SANTA MONICA, CALIFORNIA	
WT CHK		AIRCRAFT COMPANY, INC	
STR CHK			
CHECK		LAYOUT, SOLID MOTOR TVC	
PR ENGR		SYSTEM CONFIGURATIONS	
DES ENGR			
GR ENGR			
PREP BY C. LIPPOLD 3/1/66			
DESIGN ACTIVITY APPROVAL		CODE IDENT NO SIZE	1B67823
CUSTOMER APPROVAL		SCALE A-11-D	SHEET 1 OF 3

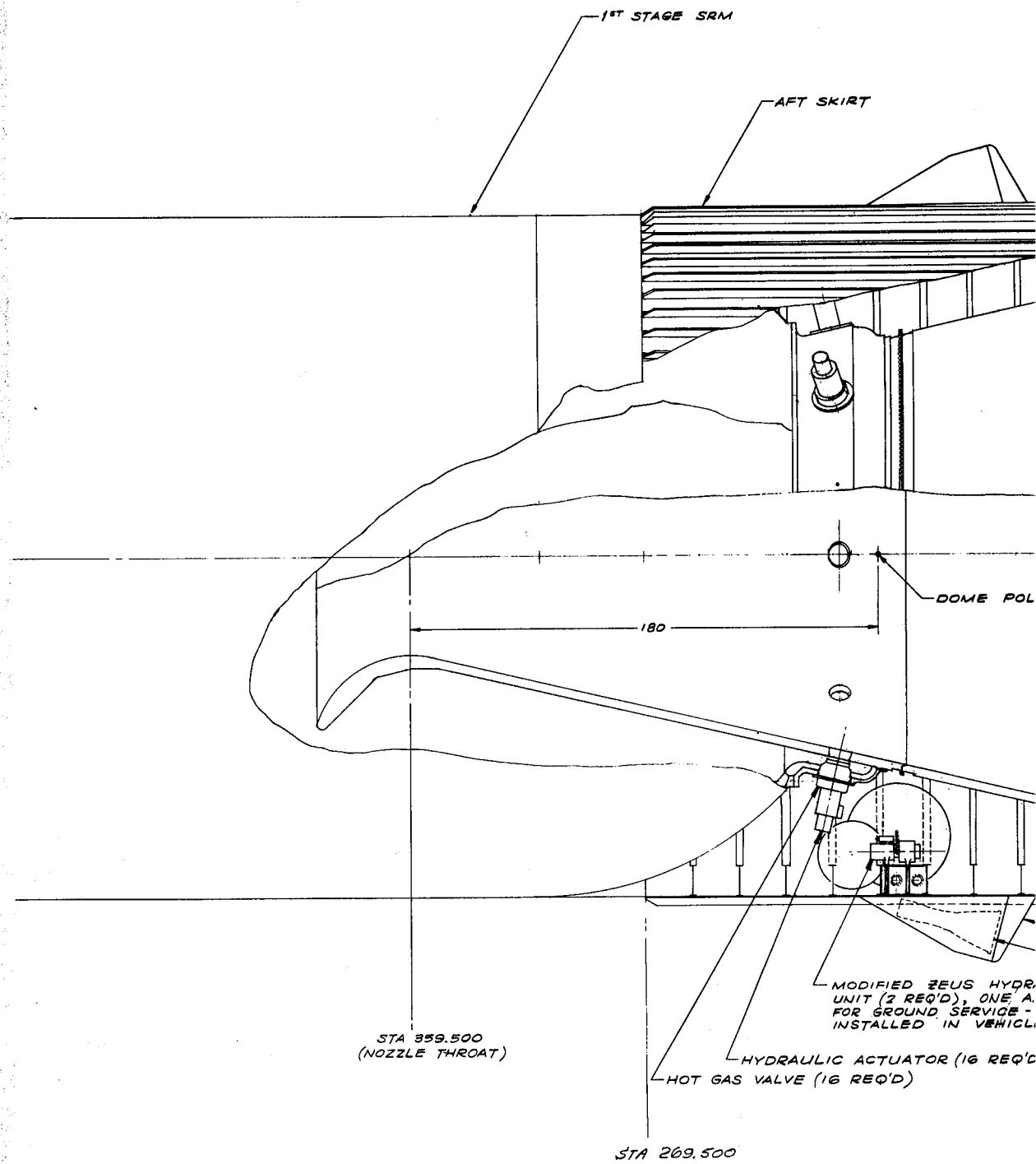




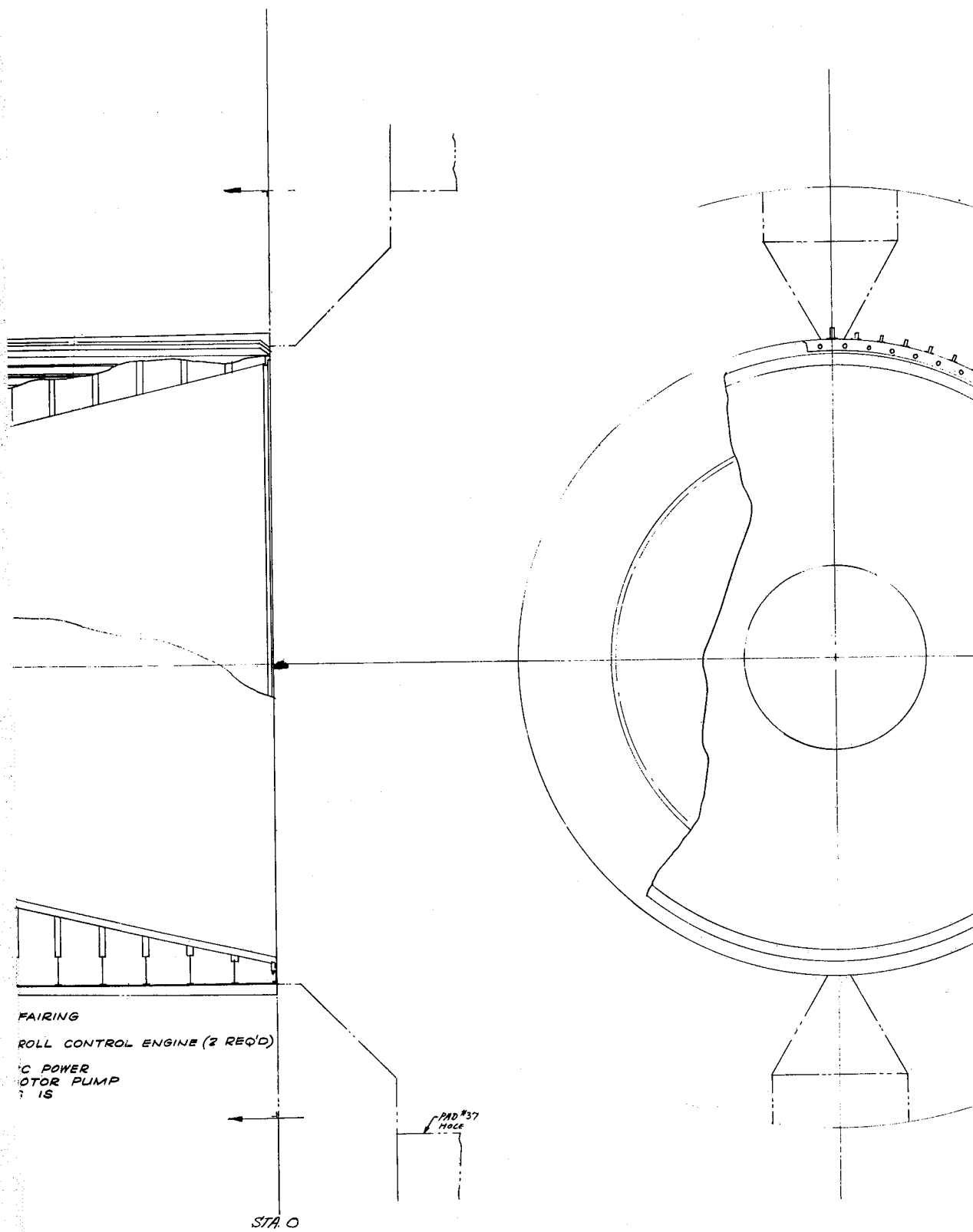
S-IVB / SAT 1B APS
MODULE (2 REQ'D)





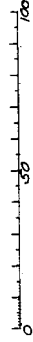
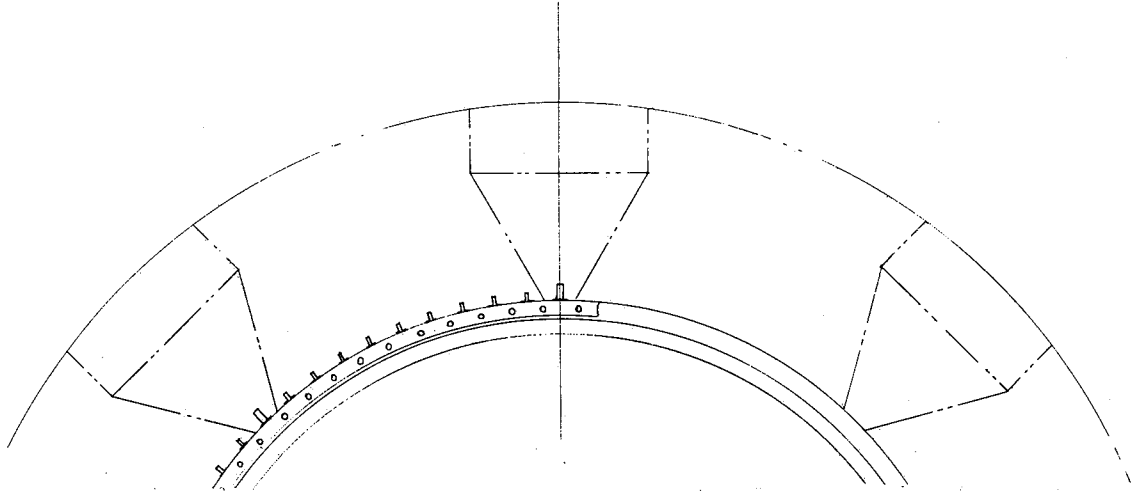


CONFIGURATION III - HOT GAS TVC SY



SM

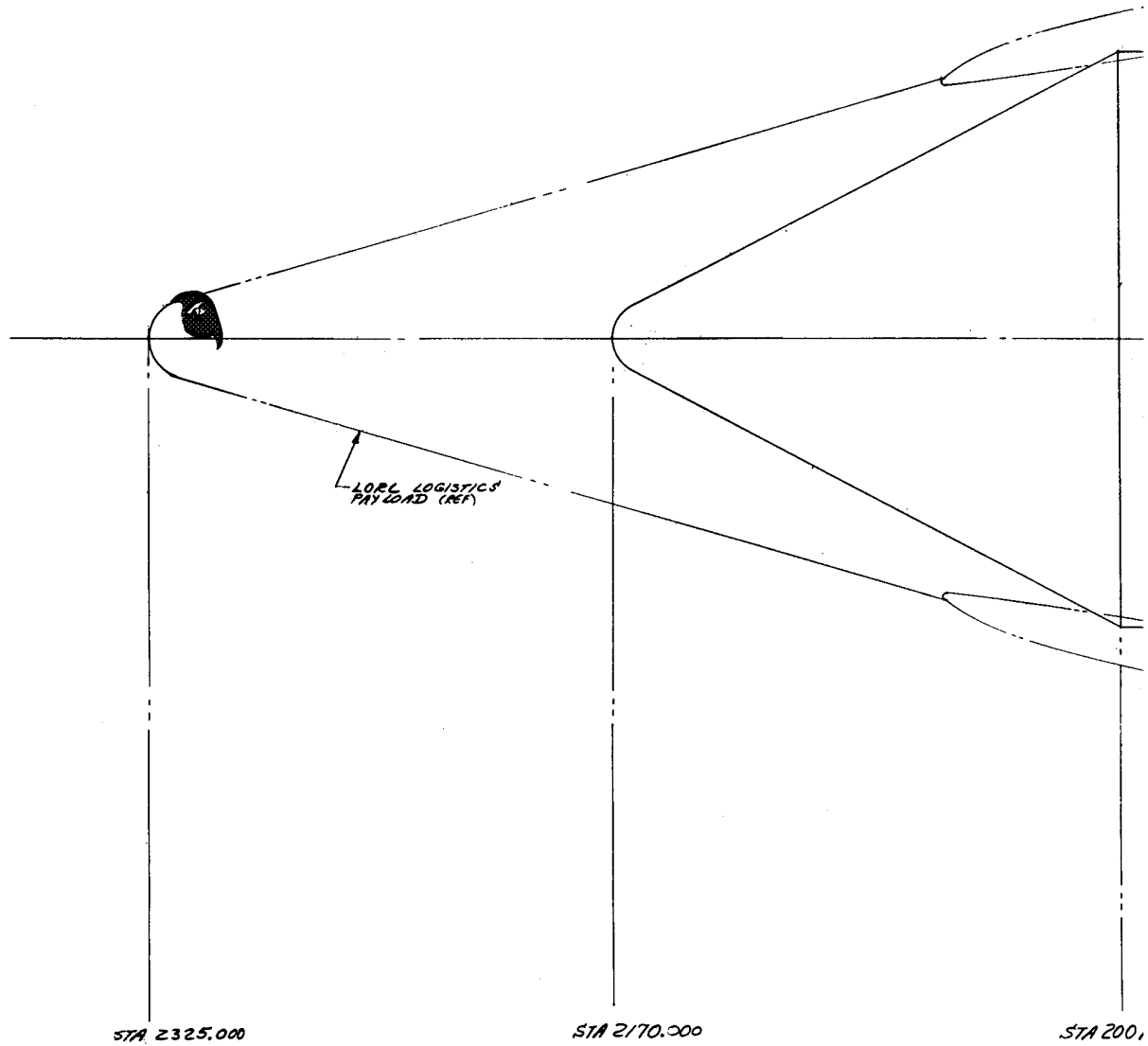
Figure 3-14

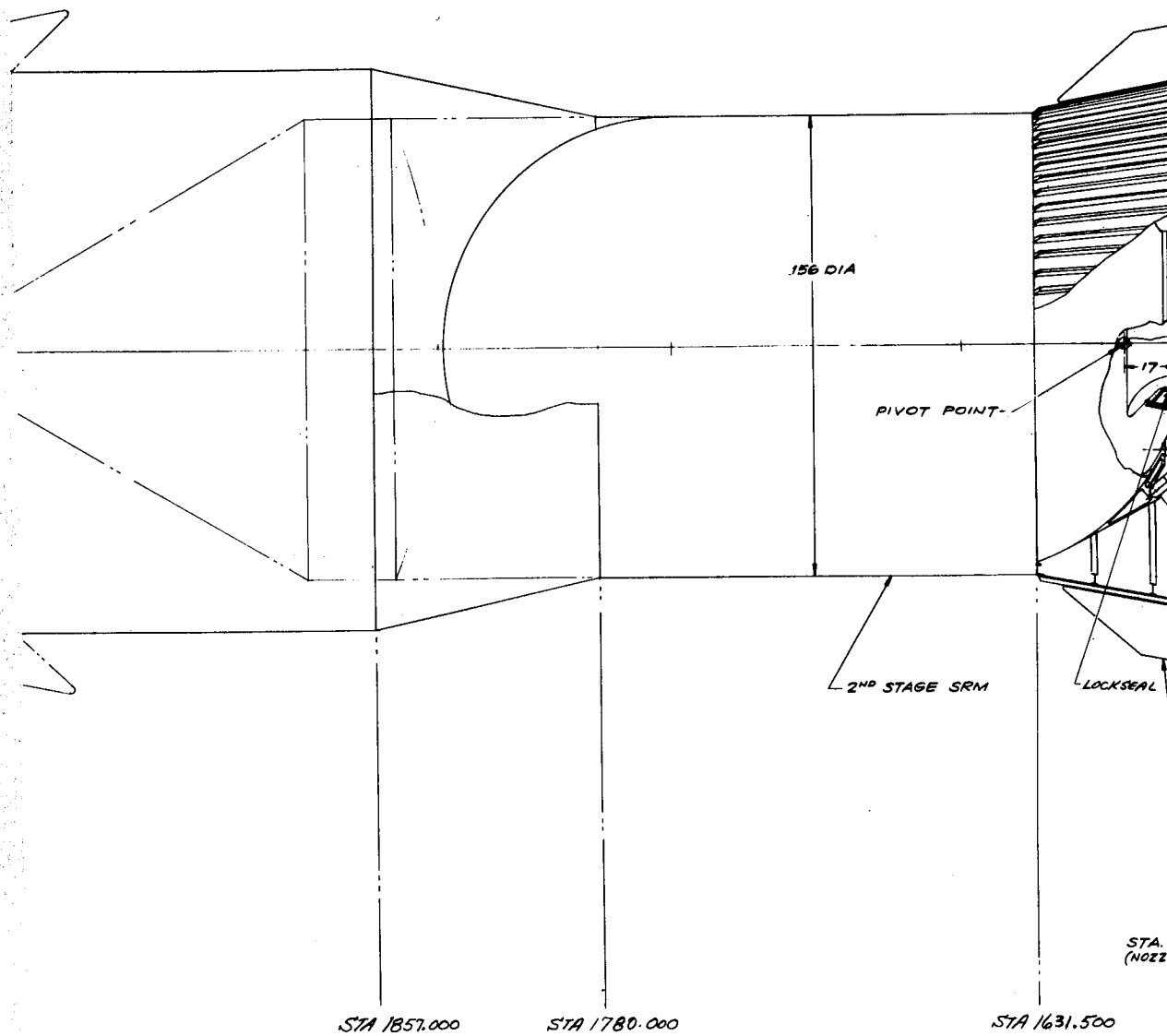


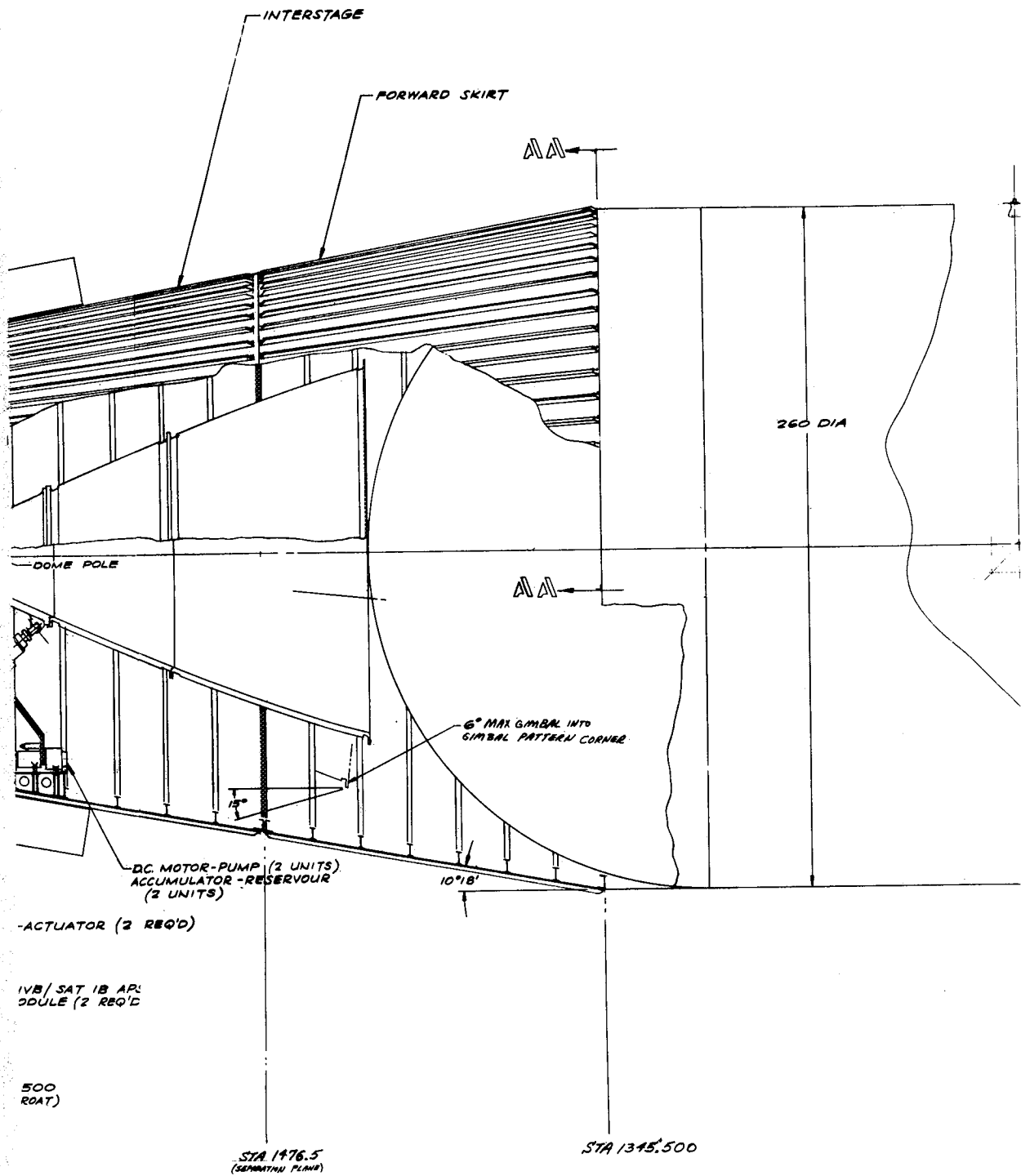
SCALE: 1" = 20'

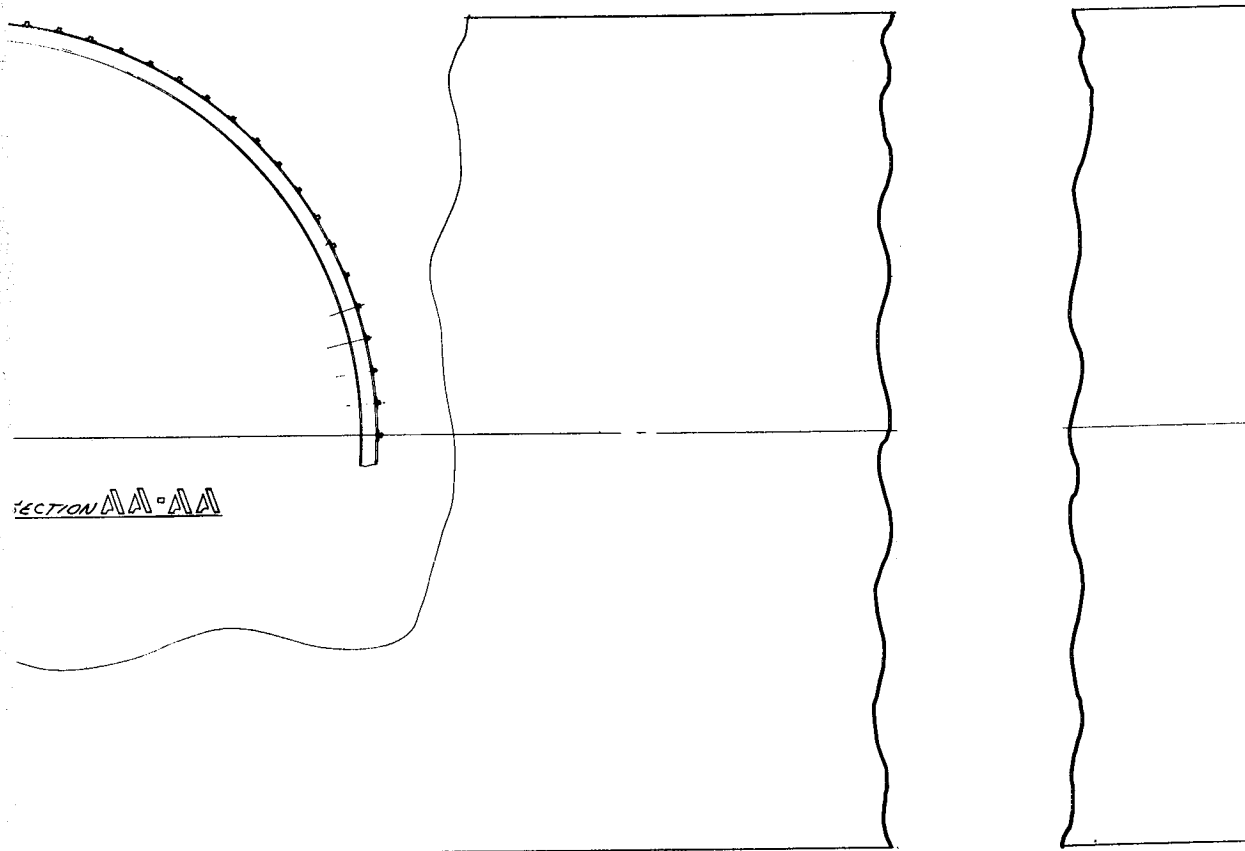
1867823

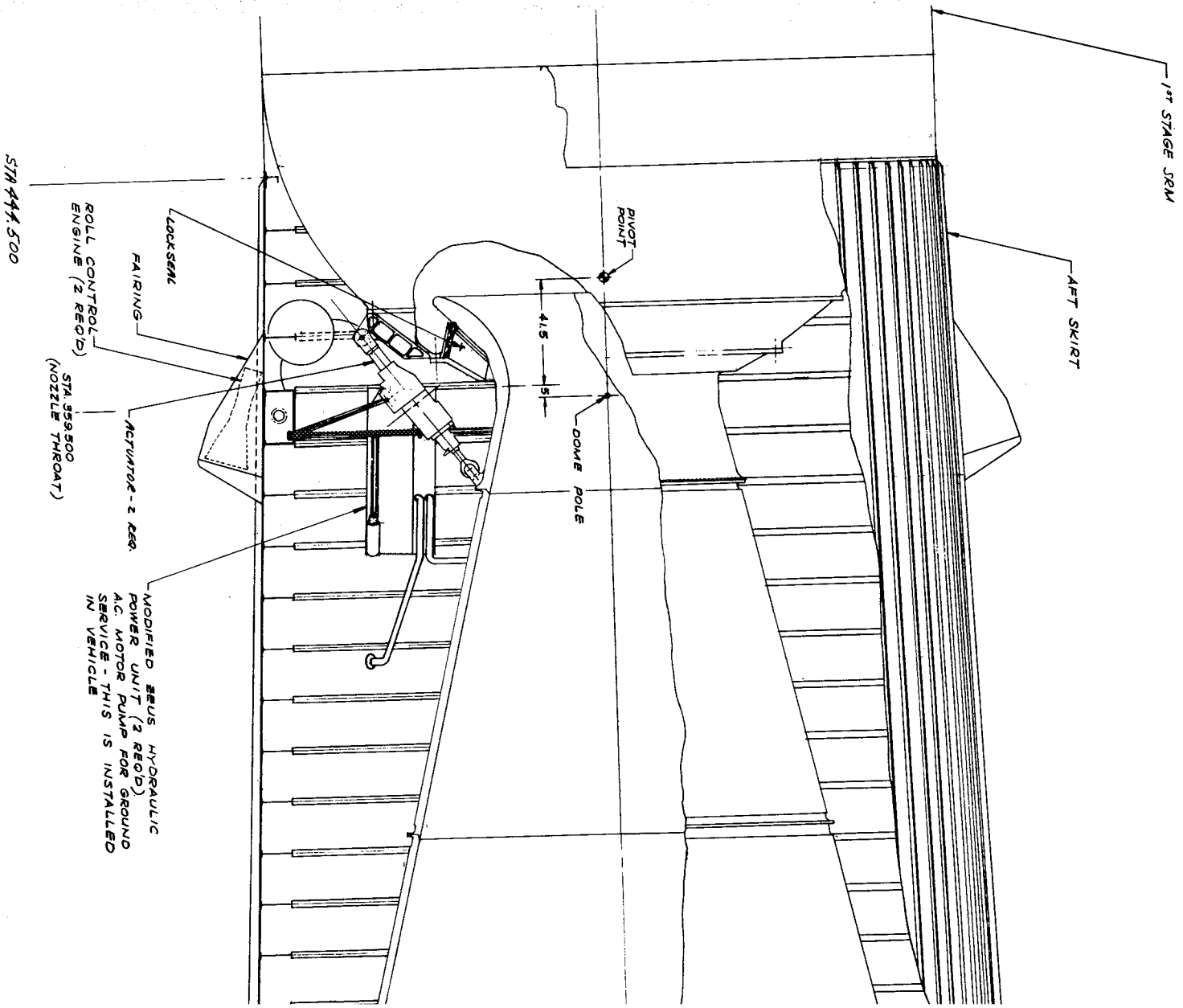
LAYOUT - SOLID MOTOR TVC SYSTEM CONFIGURATION	
RAVALAS AIRPORT CONSULTING, INC.	
SANTA MONICA, CALIFORNIA	
FOOTPRINT NO. 18385	1867823
SCALE: 1" = 20'	SHEET 3











CONFIGURATION II - GIMBAL NOZZLE

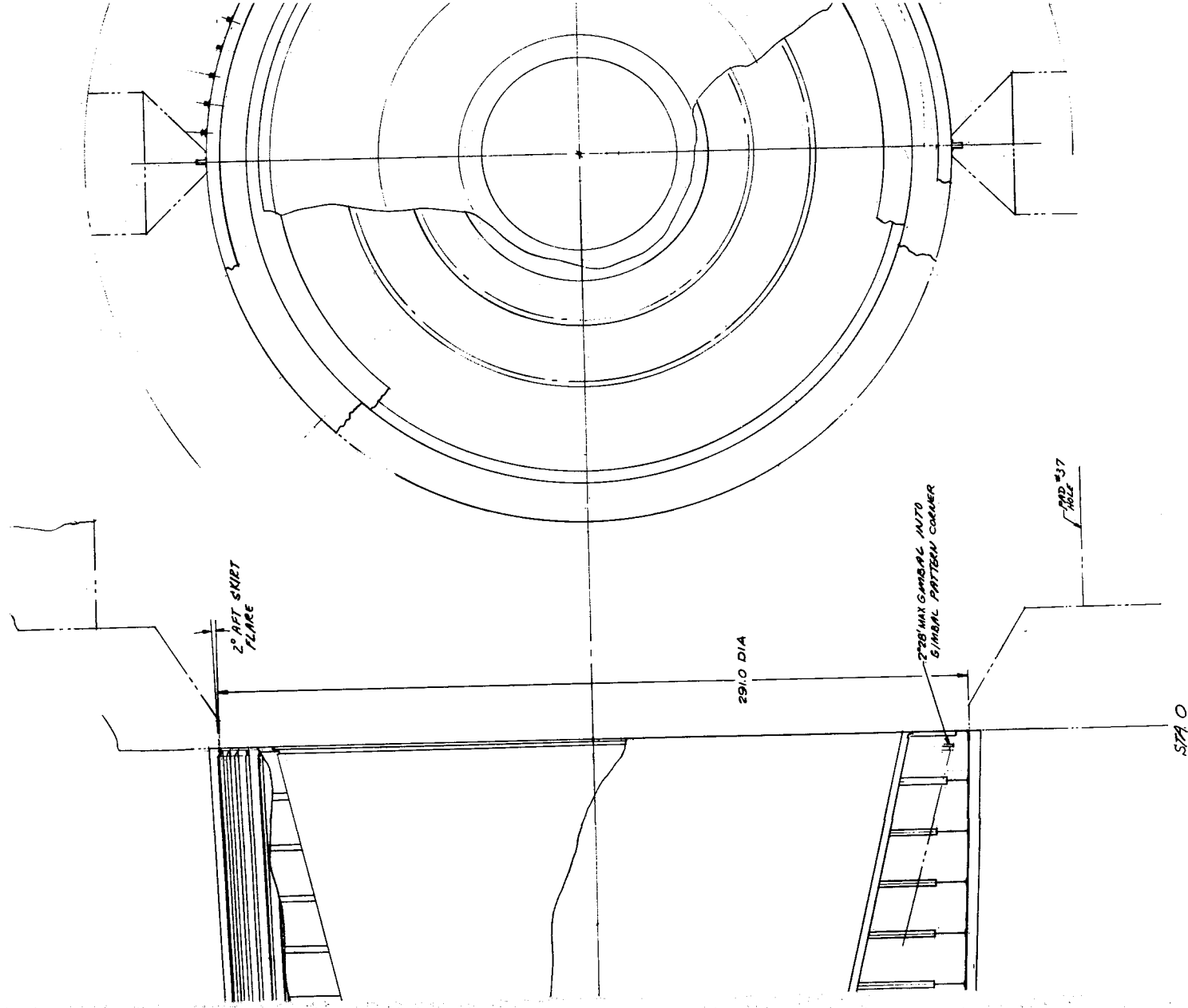
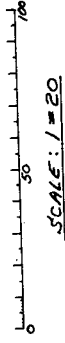
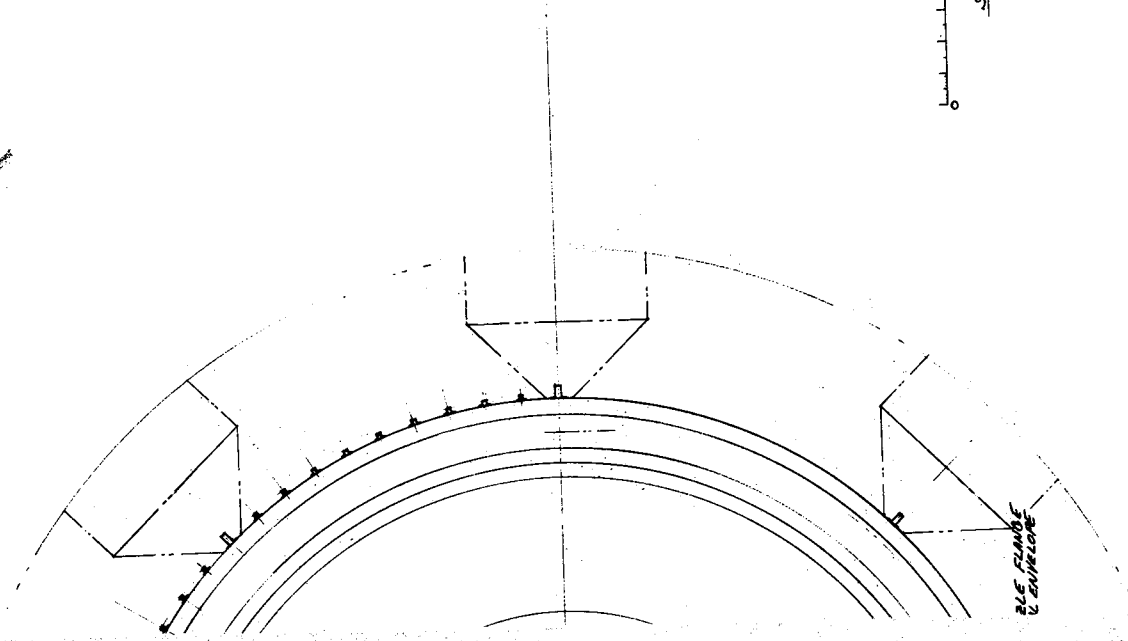


Figure 3-14.



SCALE: 1" = 20'

1867823

LAYOUT - SOLID MOTOR TVC SYSTEM CONFIGURATIONS	
DOUGLAS SANTA MONICA, CALIFORNIA	
DATE: 10/1/82	1867823
10355	10355
SCALE: 1" = 20'	10355

out - Solid Motor TVC System Configurations (Page 3 of 3)

Sheet 3 of Figure 3-14 shows the gimballed nozzle TVC system installed on the first and second stage. The two actuators are supported on each stage by the motorcase and nozzle. They are positioned on the pitch and yaw planes with their centerline perpendicular to a radial line passing through the actuator center and the nozzle gimbal point. This positioning gives equal actuator travel from neutral to maximum nozzle gimbal. Each stage also has two actuator power units attached to the stage skirt.

Sheet 2 of Figure 3-14 shows a hot gas TVC on both the first and second stages. The nozzles have been buried deeply to reduce the length of plenum chamber from motorcase dome to injector nozzles. The 16 injector valves on the first stage and 8 injectors on the second are mounted on the plenum chamber case as are their valve actuators. Hydraulic actuator power for each of the stage valves is provided by two variable-delivery pump-motor-reservoir units mounted on the stage skirts.

3.4 STAGE WEIGHT BREAKDOWNS

Table 3-2 shows the weight breakdown for the six stages that are used in the three launch vehicles. For comparison purposes, the stage weights for Configuration V from Phase II HES are also shown.

Table 3-3 is a weight breakdown of the various subsystems not directly involved in the TVC system comparison.

3.5 VEHICLE PERFORMANCE

Vehicle performance, in this section, is measured by the change in weight injected and circularized into the 260-nmi (LORL) orbit. This change in weight is expected because of variations in launch vehicle weight and specific impulse caused by TVC modifications to the basic launch vehicle. A sensitivity analysis was conducted to determine the relative effect of the various combinations of TVC systems on the nominal weight in orbit.

Ballos structure and the propellant necessary for orbital transfer and injection is not perturbed, therefore the derived weight changes are changes in the cargo-carrying ability of the Ballos spacecraft. (15,455 lb of the total nominal weight is cargo.) Trade factors that allow the evaluation of the penalties

Table 3-2 (Page 1 of 2)
VEHICLE WEIGHT COMPARISON (LB)

	Hot Gas	Warm Gas	Gimbal Nozzle	Phase II HES Study Configuration V (Min. Control Moment Fins)
First Stage				
Aft Stage	5, 541	7, 959	8, 353	21, 150
Fins	---	---	---	2, 000
Nozzle	40, 188	30, 188	30, 188	50, 290
Motorcase	222, 512	226, 460	226, 460	226, 460
Forward Fairing	1, 932	2, 075	1, 944	2, 250
TVC System	5, 808	54, 279	7, 500	8, 600
TVC Control System	100	100	100	---
Tunnels	248	242	248	---
Equipment and Instrumentation	6, 271	6, 271	6, 271	---
Contingencies* (%)	<u>6, 300</u>	<u>7, 995</u>	<u>6, 225</u>	<u>---</u>
Stage Weight (empty)	288, 900	335, 575	287, 289	310, 750
First Stage				
Main Propellant	2, 832, 080	2, 857, 300	2, 857, 300	2, 857, 300
TVC Propellant	25, 220	102, 352	---	10, 250
Roll Control Propellant	2, 609	2, 609	2, 609	---
Retrorocket Propellant	<u>2, 150</u>	<u>2, 150</u>	<u>2, 150</u>	<u>---</u>
Stage Weight (loaded)	3, 150, 959	3, 299, 986	3, 149, 348	3, 178, 300

*2% for structure; 5% for equipment, 20% for instrumentation.

Table 3-2 (Page 2 of 2)

	Hot Gas	Warm Gas	Gimbal Nozzle	Phase II HES Study Configuration V (Min. Control Moment Fins)
Second Stage				
Aft Skirt	803	1,318	1,532	3,180
Nozzle	5,488	4,988	4,988	7,890
Motorcase	26,756	27,270	27,270	27,270
Igniter	170	170	170	170
TVC System	1,755	5,500	1,273	1,280
TVC Control System	100	100	100	---
Tunnels	47	47	47	---
Equipment and Instrumentation	4,388	4,388	4,388	---
Contingencies	<u>1,445</u>	<u>1,612</u>	<u>1,440</u>	<u>240</u>
Stage Weight (empty)	40,952	45,393	41,208	40,030
Igniter Propellant	240	240	240	---
Main Propellant	222,315	225,450	225,450	225,450
TVC Propellant	3,135	8,788	---	2,130
Roll Control Propellant	<u>131</u>	<u>131</u>	<u>131</u>	<u>---</u>
Stage Weight (loaded)	266,773	280,002	267,029	267,610

or gains associated with cargo weight were computed for stage weight, specific impulse, and propellant weight sensitivities for both the first and second stages. These are presented in the following figures; Figures 3-15, 3-16, and 3-17 present the payload sensitivities for first stage inert weight, specific impulse, and propellant weight. Figures 3-18, 3-19, and 3-20 present the payload sensitivity for second-stage inert weight, specific impulse, and propellant weight.

Table 3-3
EQUIPMENT AND INSTRUMENTATION WEIGHT BREAKDOWN (LB)

	First Stage	Second Stage
Igniter	N/A	170
Equipment Mounting	458	458
Environmental Control	326	326
Telemetry System	2, 124	1, 998
Electrical System	501	501
Tracking System	47	47
Abort Detection System	38	38
Sequencing System	103	103
Range Safety	73	73
Separation System	15	15
Roll Control System	571	646
Systems for total vehicle	183	183
Retrorockets	<u>1, 832</u>	<u>N/A</u>
Equipment Weight (empty)	6, 271	4, 558
Roll Control Propellant	2, 600	128
Helium for Pressurization	9	3
Retrorocket Propellant	2, 150	N/A
Igniter Propellant	<u>N/A</u>	<u>240</u>
Equipment Weight (loaded)	11, 030	4, 929

The vehicle parameters were compared to nominal values obtained from the baseline vehicle (shown in Table 3-4) to obtain payload changes.

The analysis was performed with the three-dimensional trajectory simulation computer program used in the Phase II HES Study to simulate the boost flight of both the first and second stages. The injection into the 105-nmi parking orbit, Hohmann transfer, and injection into the 260-nmi orbit was done by impulsive calculations.

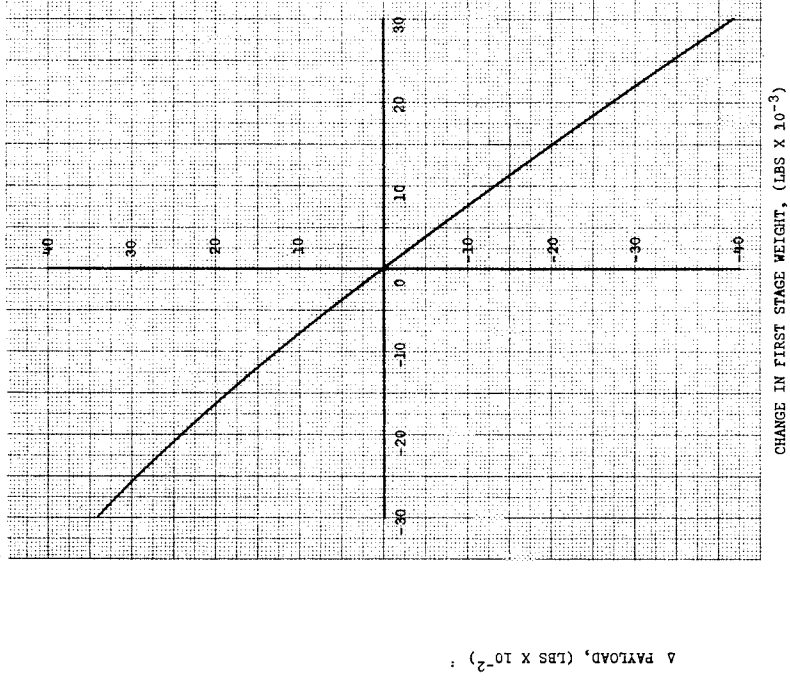


Figure 3-15. Payload Sensitivity to First-Stage Weight

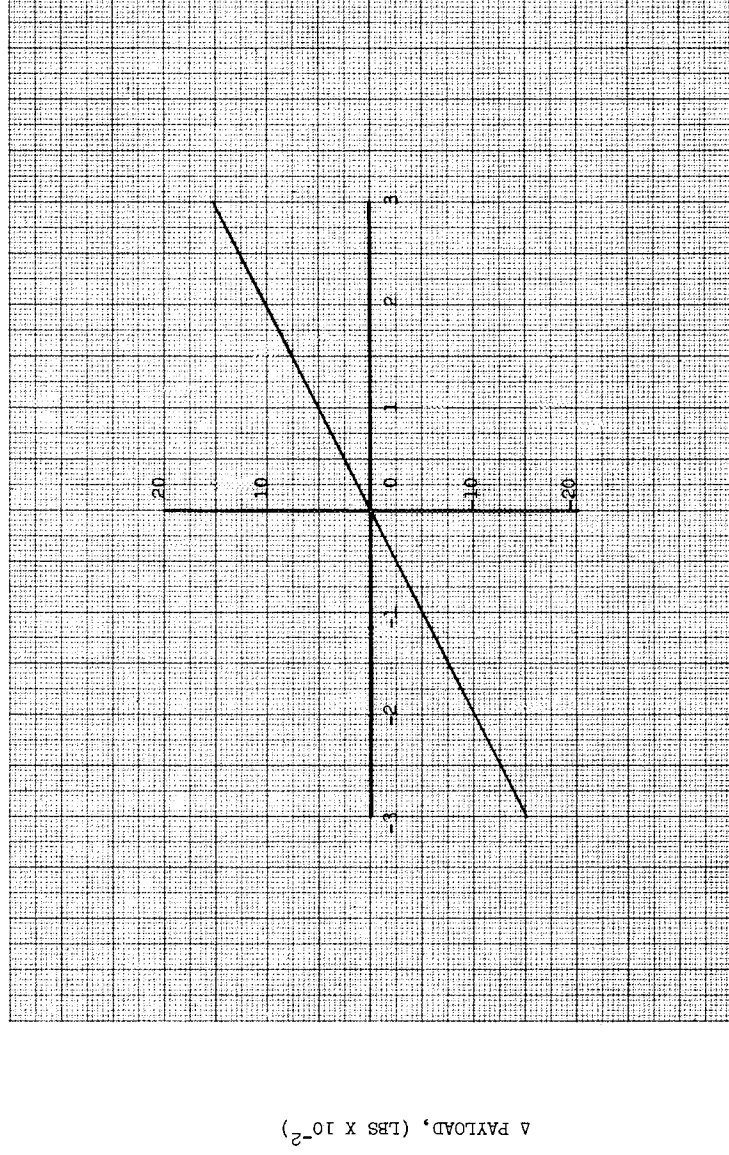
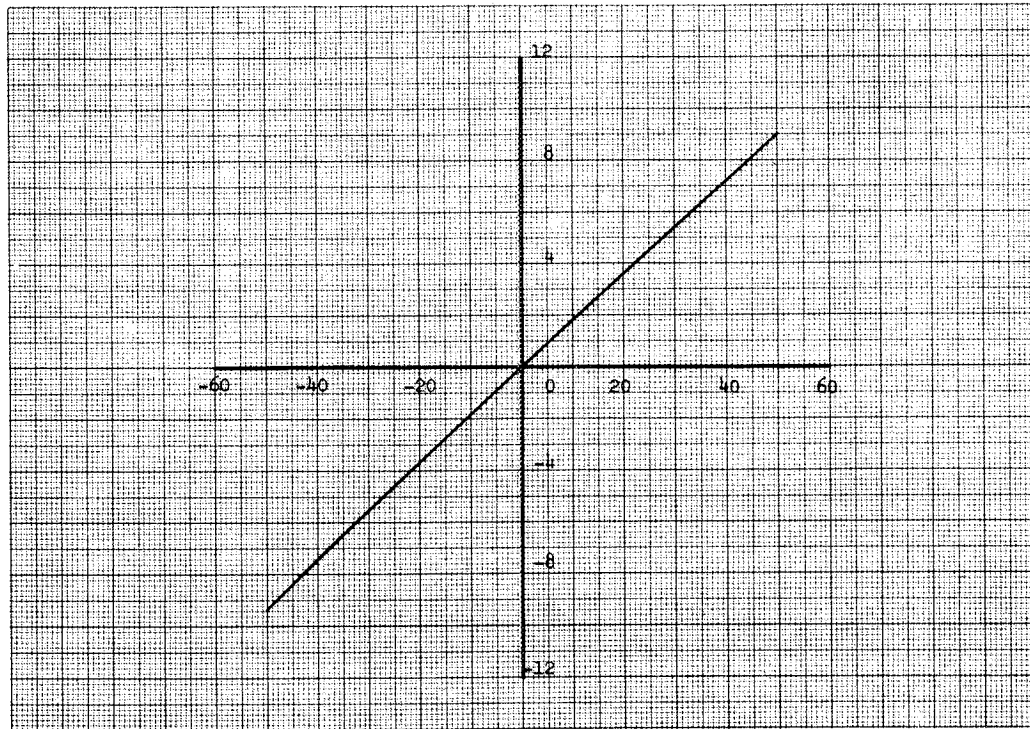


Figure 3-16. Payload Sensitivity to First-Stage Specific Impulse

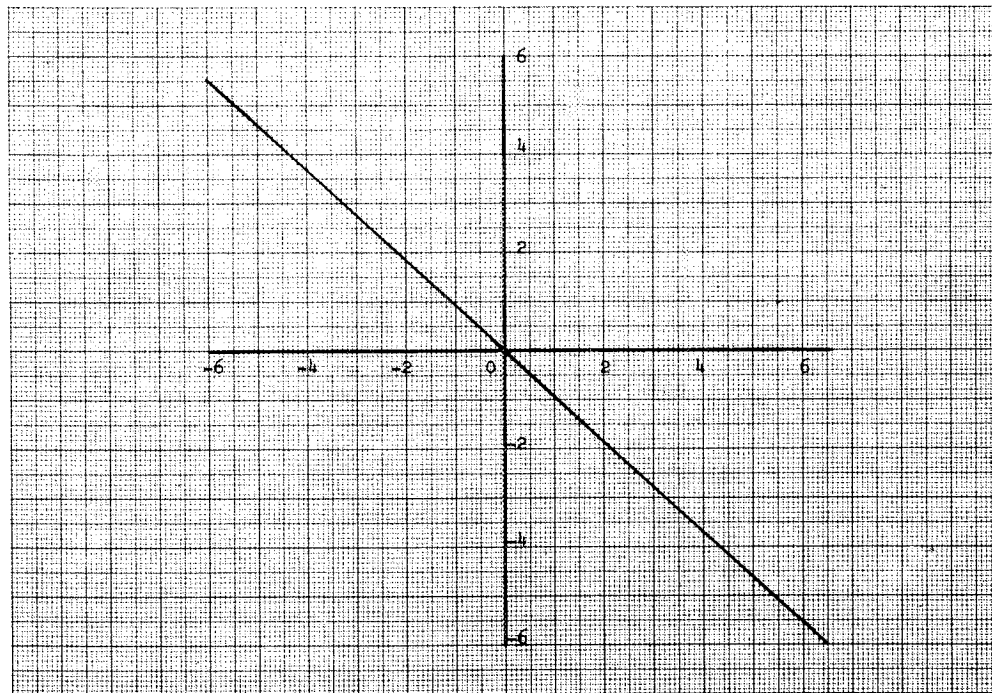
Δ PAYLOAD, (LBS $\times 10^{-2}$)



CHANGE IN FIRST STAGE PROPELLANT WEIGHT, (LBS $\times 10^{-3}$)

Figure 3-17. Payload Sensitivity to First-Stage Propellant Weight

Δ PAYLOAD (LBS $\times 10^{-3}$)



CHANGE IN SECOND STAGE WEIGHT (LBS $\times 10^{-3}$)

Figure 3-18. Payload Sensitivity to Second-Stage Weight

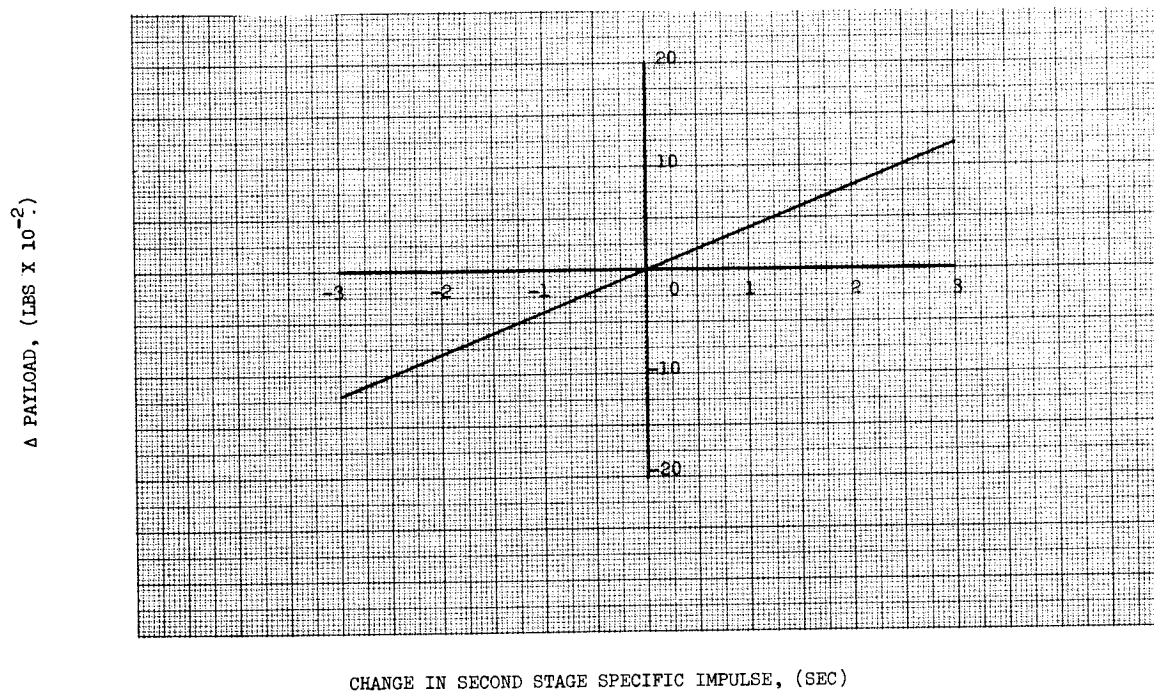


Figure 3-19. Payload Sensitivity to Second-Stage Specific Impulse

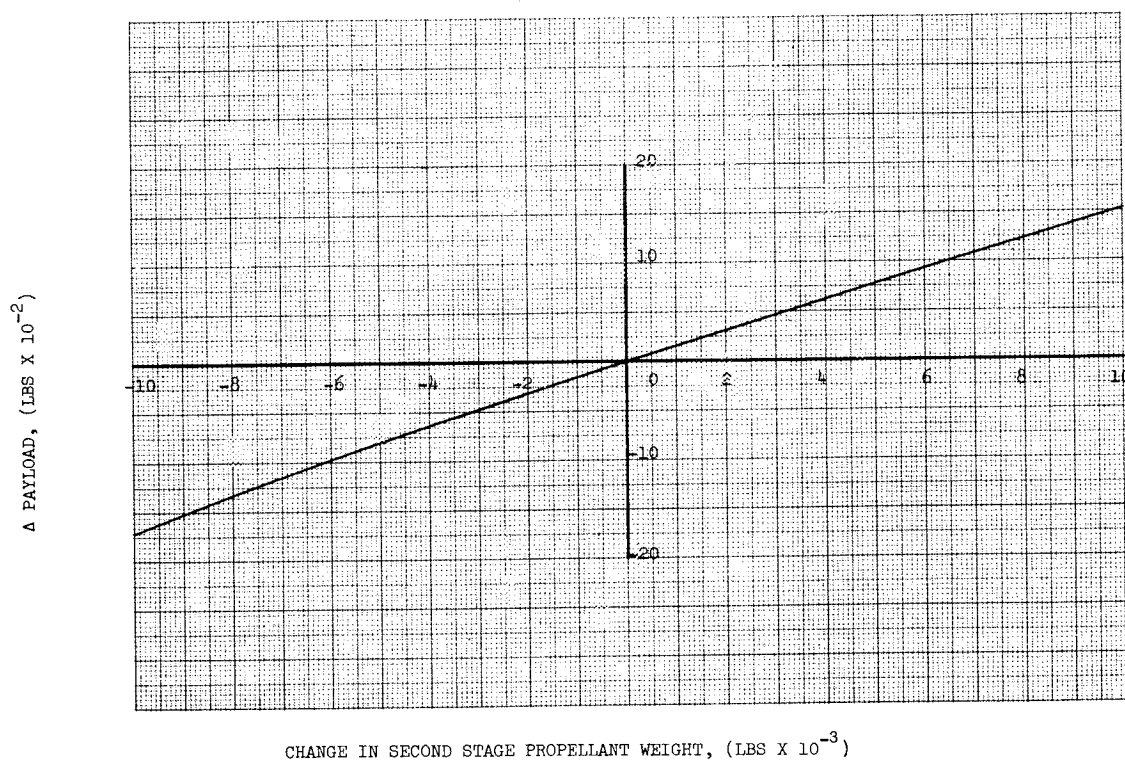


Figure 3-20. Payload Sensitivity to Second-Stage Propellant Weight

Table 3-4
NOMINAL STAGE WEIGHT, PROPELLANT WEIGHT, AND I_{SP}

	Propellant Weight (lb)	Stage Weight (lb)	Specific Impulse (sec)
First Stage	2, 857, 300	310, 750	276. 910
Second Stage	225, 450	40, 030	301. 006
Ballos Payload	---	45, 365	305. 0

3.6 STABILITY AND CONTROL ANALYSIS

The guidelines and assumptions used in the steering analysis to obtain TVC control requirements are shown below. Basically, they are the same as those used in the Phase II HES Study:

1. A nominal-attitude flight is maintained through the specified wind-profile envelope. In addition, two cases are analyzed with some divergence to determine what effect this mode has on TVC.
2. The wind-profile envelope used is the 95% ETR envelope with standard gust velocities superimposed (see Section 2.5).
3. Control capability is required for both full headwinds and full side-winds considered to be acting separately.
4. Steering response capabilities correspond to a second-order system, with a natural frequency of 0.15 cps and a 0.7 damping ratio.
5. Maneuvering moment requirements provide the capability of proportionally following step changes in attitude rate commands of 0.35°/sec in pitch and 0.1°/sec in yaw.
6. The sources of disturbing moments to be considered and their assumed uncertainty levels are as shown in Figure 3-21.

3.6.1 TVC Requirements

Duty-cycle, total control impulse, maximum thrust-vector deflection angle, and roll-moment requirements were calculated for both stages of all the launch vehicles shown in Figure 3-1. First-stage values and second-stage roll moments were obtained through the use of the static-balance analytical method developed for the HES Studies, while second-stage TVC requirements were obtained by means of a dynamic response analysis.

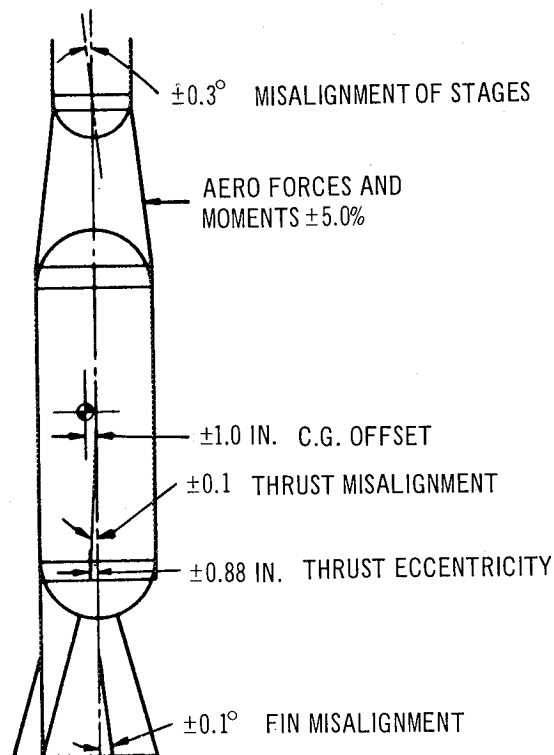


Figure 3-21. Sources of Disturbing Moments and Their Uncertainty Levels

The static analysis (which is described in detail in Appendix B) assumed that the vehicle follows the nominal trajectory, but a 1° average error in angle of attack (α) and side slip angle (β) are considered to act continuously. When fins are used on the launch vehicle, an additional 1° error caused by dihedral effects is introduced. These errors are negligible in pitch and yaw and were used only to determine roll moments. Two wind conditions, or directions, were investigated: headwinds and side-winds. To these conditions, root-sum-squared positive and negative uncertainties were superimposed, resulting in four basic conditions from which an envelope of maximum values for thrust deflection and duty cycle was obtained. The maneuvering capability for proportionally following step changes in attitude rate commands of $0.35^\circ/\text{sec}$ in pitch and $0.1^\circ/\text{sec}$ in yaw was added to these conditions. This analysis was performed for both stages; however, it did not account for second-stage separation transients and was therefore not used in establishing maximum thrust-vector deflection and rate requirements.

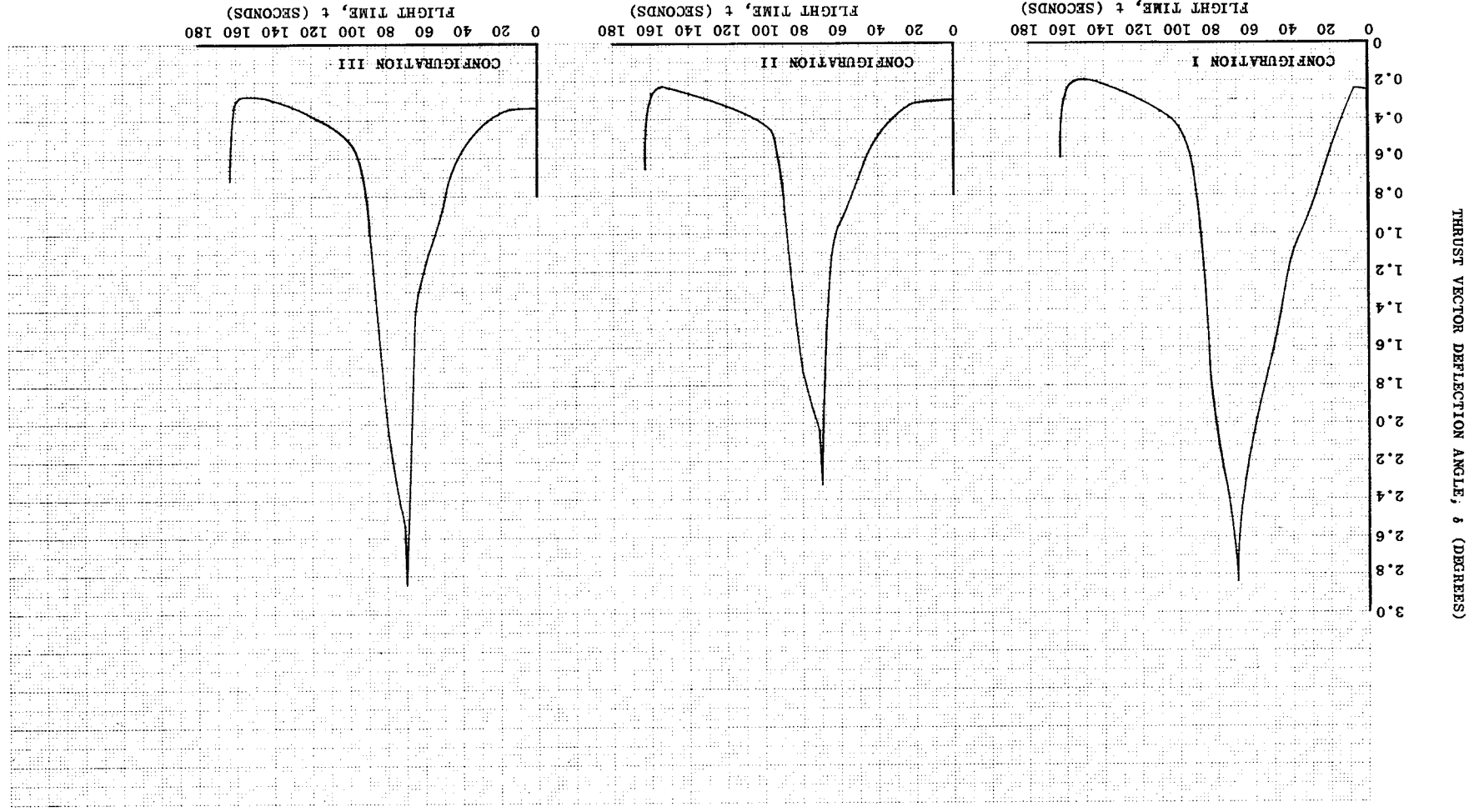
Figures 3-22 through 3-25 show the control system duty-cycle requirement for each launch vehicle configuration with both the Ballos payload and a winged payload. In all cases, the control side force was considered to act at the throat as a reference station. This criteria was used to provide consistent data for the TVC performance analysis (discussed in Section 4), which located injector planes for the warm gas and hot gas TVC systems. In the TVC system design effort, the plane of the side force was corrected from this reference station to the actual station as defined by the pivot point for the movable-nozzle technique and the nozzle injection location for the gas injection systems.

Control-system duty cycles for vehicles with a winged payload were calculated to allow a comparison of the degree of control necessary for stable flight between a winged and ballistic payload shape. This comparison can be seen in Table 3-5. First-stage flight control data for vehicles using the Ballos payload are shown in Figure 3-22. These were used in the design effort.

The duty cycle for Configuration I, which uses warm gas injection TVC, differs from those of Configurations II and III, because it is derived using the 95% wind envelope while the others use a discrete 95% wind profile. The envelope of maximum winds does not represent a realistic wind environment for a given flight, as does the discrete wind profile; it is used however, in the analysis of vehicles using warm gas TVC because of the continuous flow characteristics of this design; that is, flow rates at any time in flight must be sufficient to provide control for vehicles encountering maximum winds at that time.

The maximum deflection angle for Configurations I and III are nearly identical, yet Configuration III is approximately 11% shorter. The shortening is brought about by the submergence of the first- and second-stage nozzles. However, almost exactly as much shortening occurs forward of the CG as it does aft of it; thus, the ratio of moment arms of the CP and control side force from the CG remains nearly the same. Since aerodynamic moments are predominant during first-stage burn, the control requirements are essentially the same for the two configurations. Configuration II has lower requirements because of the stabilizing effect of the aft-skirt flare. This effectively moves the CP aft, thus reducing aerodynamic moments. Because of the aerodynamic

Figure 3-22. First-Stage Duty Cycle - Ballos Payload



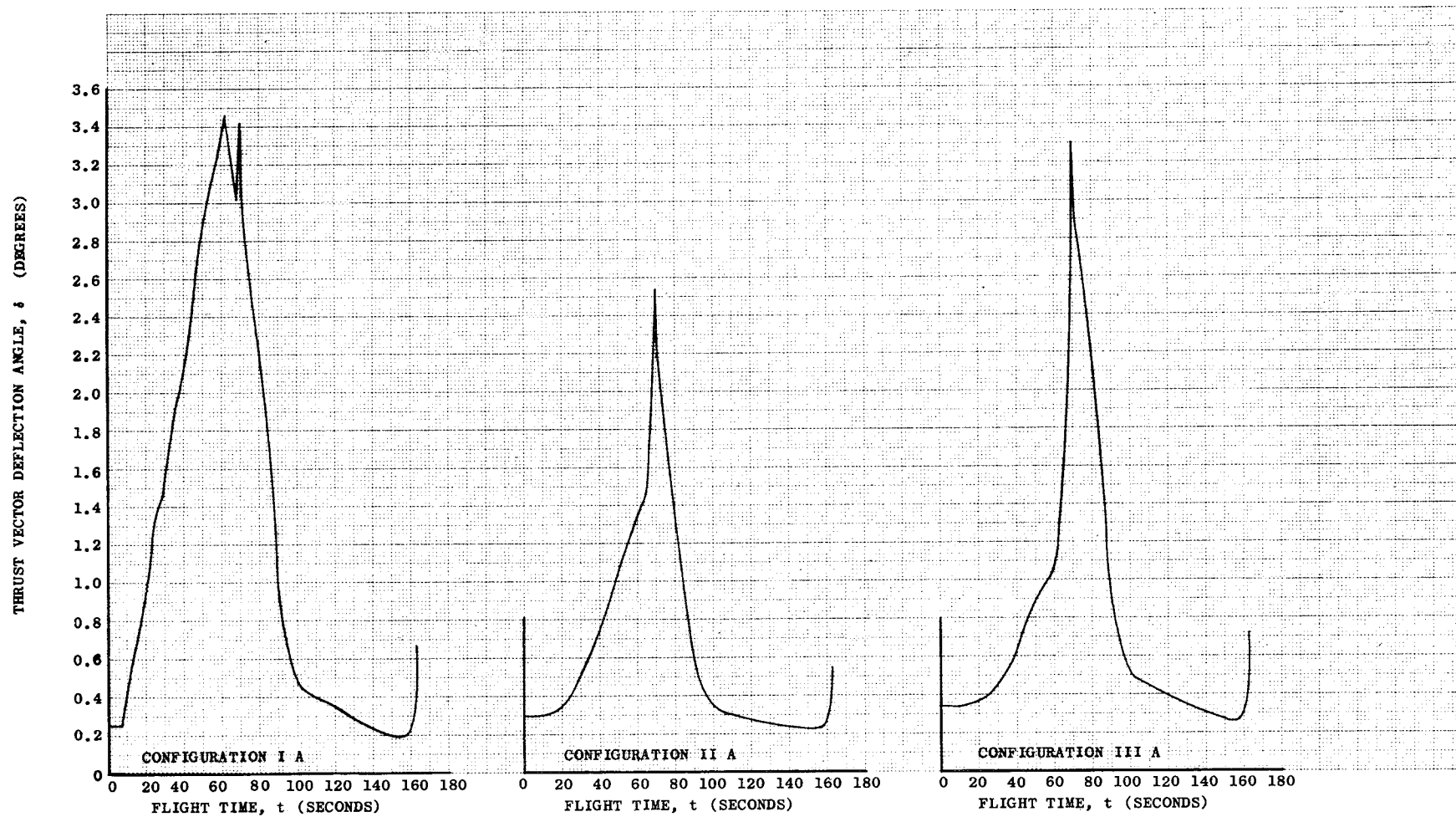


Figure 3-23. First-Stage Duty Cycle – Winged Payload

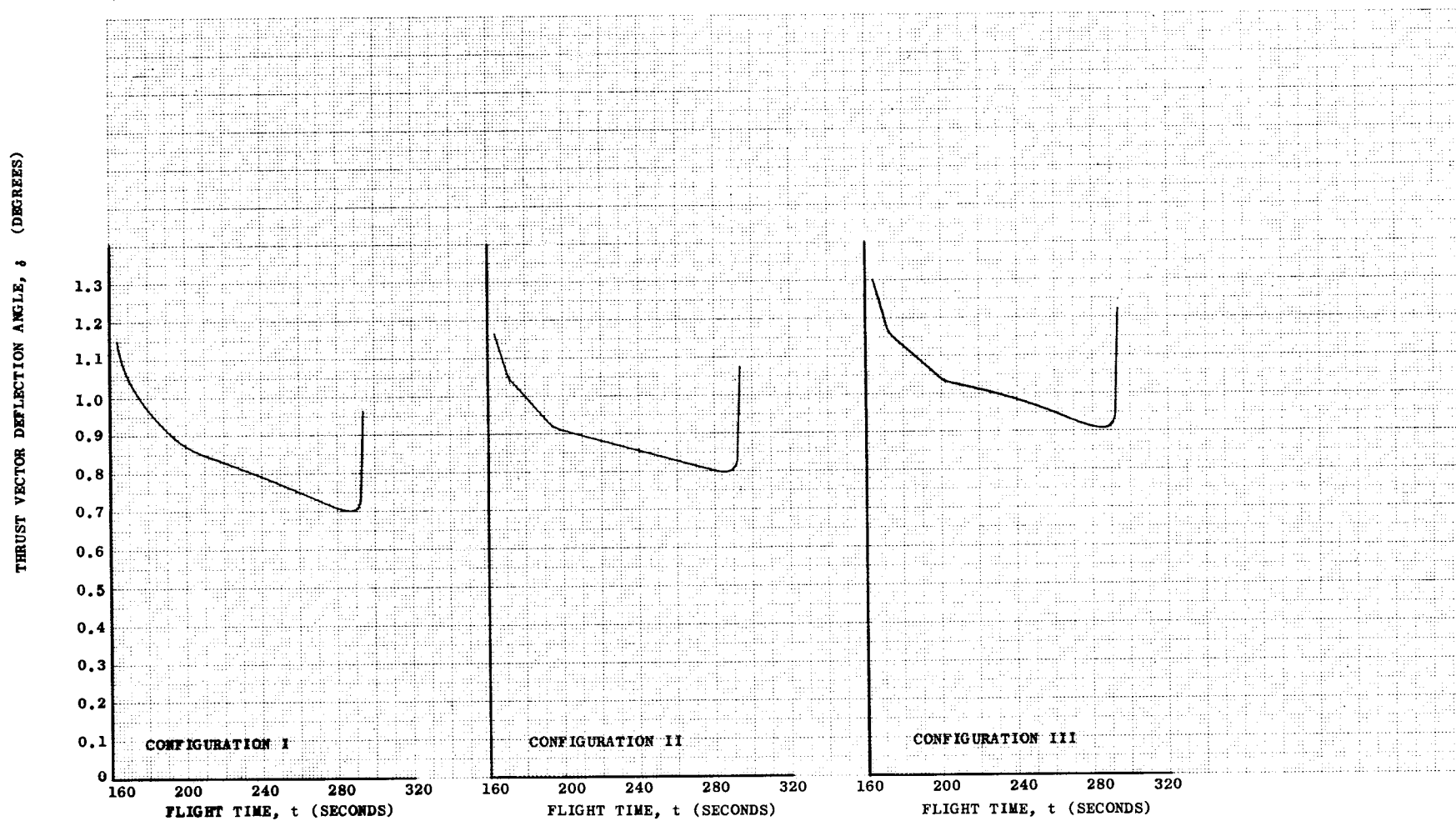


Figure 3-24. Second-Stage Duty Cycle – Ballos Payload

Figure 3-25. Second-Stage Duty Cycle - Winged Payload

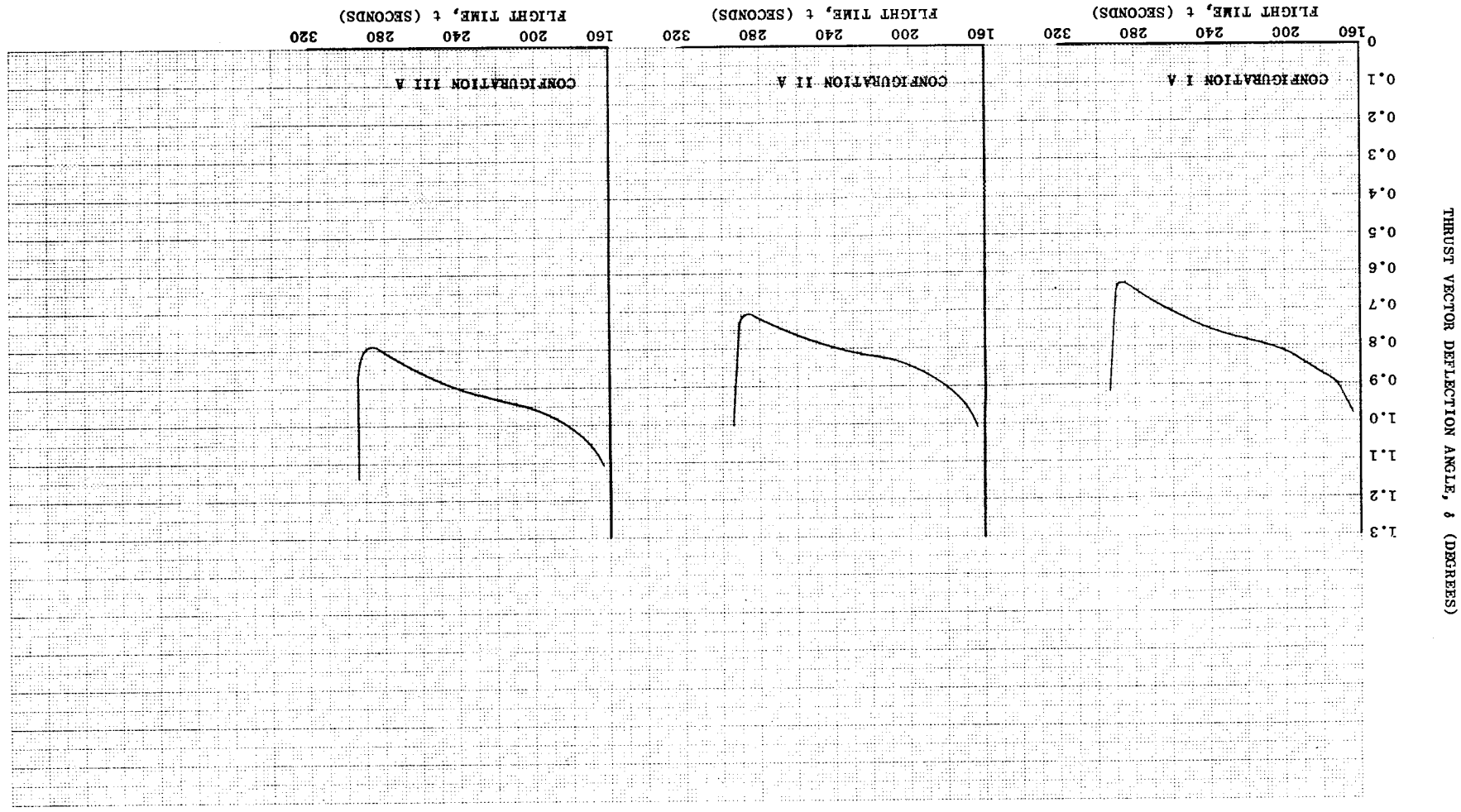


Table 3-5
COMPARISON OF CONTROL-SYSTEM DUTY CYCLES

Config- uration	A_{DC} (deg-sec)	δ_{Max} (deg)	A_{Roll} (ft-lb-sec)	$M_{R Max}$ (ft-lb)
First Stage				
I	144.05	2.842	463,920	17,541
IA	187.89	3.460	564,220	21,500
II	97.48	2.307	382,890	14,026
IIA	101.21	2.705	444,080	16,607
IIAF	45.18	0.355	1,419,200	38,774
III	115.36	2.843	465,220	17,391
IIIA	122.76	3.461	551.080	21,373
Second Stage				
I	108.38	0.965	6441.2	278.6
IA	100.35	0.779	4438.0	166.7
II	116.11	0.979	6593.3	281.6
IIA	106.31	0.806	4556.2	173.9
IIAF	106.31	0.806	4556.2	173.9
III	131.98	1.070	6679.6	281.5
IIIA	119.29	0.854	4139.6	147.6
A_{DC} = Duty Cycle Area. δ_{Max} = Maximum Thrust-Vector Deflection Angle. A_{Roll} = Roll Duty Cycle. $M_{R Max}$ = Maximum Roll Moment. A = Indicates HL-10 Payload. F = Indicates Fins on First Stage.				

destabilizing effects of the HL-10, first-stage requirements (shown in Figure 3-23) are more stringent than those of the configurations with the Ballos payload. Although the general shape of the curves is the same, a double peak now occurs during first-stage flight. The peak at 70 sec is caused by the wind gust. The peak at 62 sec is brought about by the different aerodynamic characteristics of the HL-10 as opposed to the Ballos and the use of envelope wind velocities.

The static analytical method assumes that the vehicle flight path does not deviate from the nominal trajectory. To comply with the guideline of investigating some divergence, a first-stage control-system dynamic response was performed for Configuration II. This analysis considered the effects of lags in the control system on thrust-vector deflection and associated vehicle attitude divergence. Winds in the yaw plane were assumed for this analysis since they produce maximum requirements. The control system included attitude error, body rate, and angle-of-attack feedback, with control gains programmed to satisfy the drift minimum principle.

Figure 3-26 shows yaw attitude divergence during first stage flight. This is not uncontrolled divergence, for the vehicle is controlled during this phase of flight; however, the vehicle is responding to transient forcing functions and not statically balanced at any instant in flight. The resulting maximum vector deflection angle predicted is lower than that calculated when the static balance technique is used. Figure 3-27 shows the deflection history in the yaw plane during first-stage flight with a maximum of 2.1° occurring at the time of peak winds. The maximum deflection predicted by the static method is 2.3° in the yaw plane. A comparison of the results of both analytical representations of vehicle flight shows that close correlation exists, and, that when vehicle dynamics which include attitude divergence are considered, TVC angular requirements are somewhat relieved.

The peak thrust-vector deflection rate requirement was obtained from the thrust-vector deflection transient shown in Figure 3-27. The peak rate requirement is approximately $7^\circ/\text{sec}$. The thrust-vector deflection acceleration requirement was assumed to be $30^\circ/\text{sec}^2$. This acceleration is consistent with results of previous analyses performed for a similar vehicle.

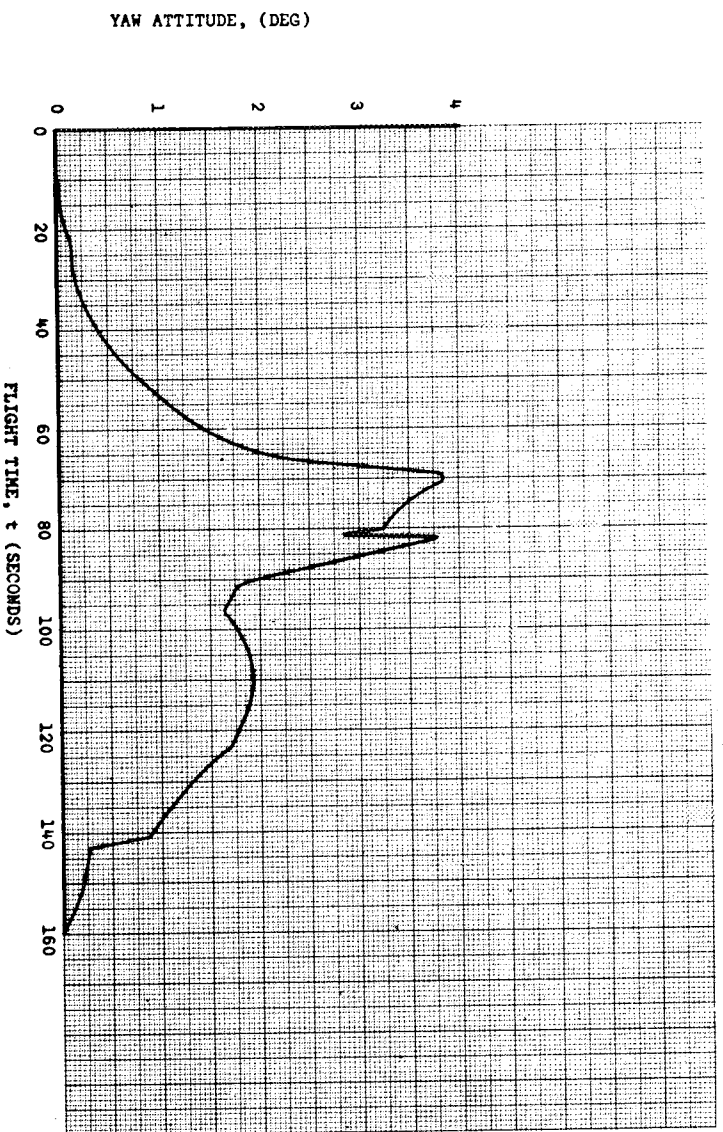


Figure 3-26. Yaw Attitude - Gimbal Nozzle Vehicle

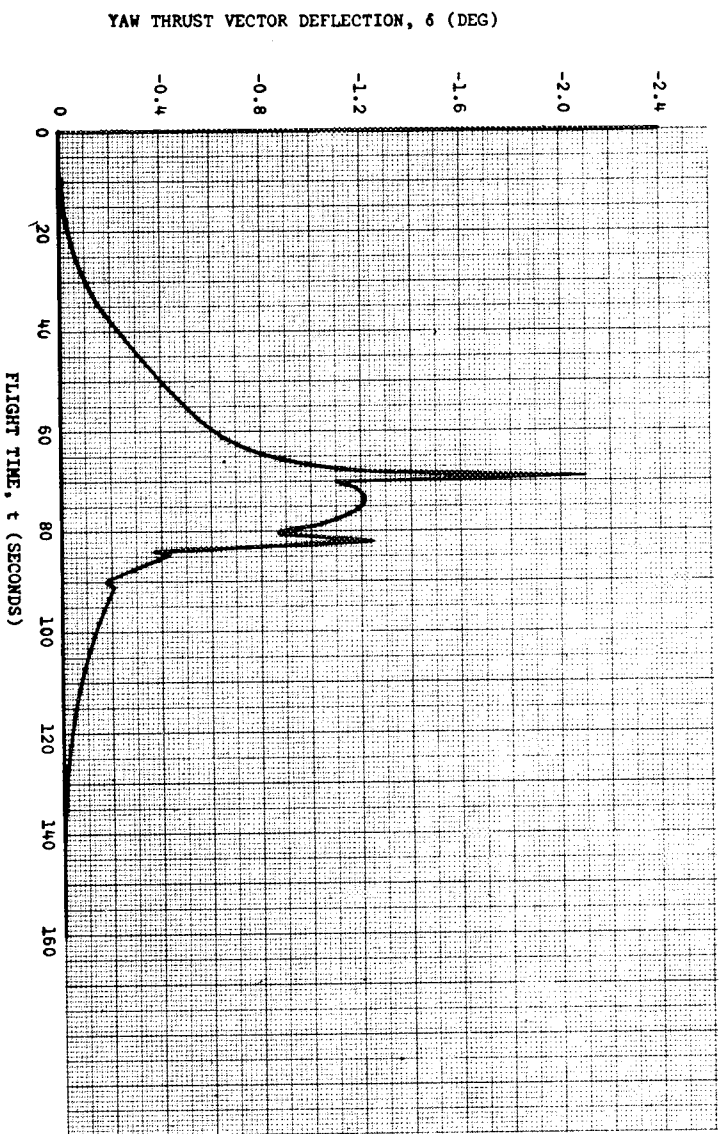


Figure 3-27. Yaw Thrust-Vector Deflection - Gimbal Nozzle Vehicle

Second-stage TVC deflections were also calculated with the static balance method. These deflections are shown in Figure 3-24 for vehicles with the Ballos payload and in Figure 3-25 for vehicles with the winged payload.

Since the second-stage Configurations I and II are nearly identical, it would be expected that their deflections would be nearly the same. This is true initially; however, as the gas generators in the aft-skirt area of Configuration I are depleted, the CG moves forward faster, and deflections for Configuration I become less because of the increased control moment arm. Configuration III, because of the submerged nozzle, has the shortest control moment arm and, thus, the highest deflections. Second-stage deflection differences due to the two payload shapes are less pronounced than those for the first stage, because dynamic pressure is low and aerodynamic moments are negligible in comparison to thrust eccentricity and misalignment. Total second-stage moments are nearly the same for both payload shapes, and the duty cycle for the second stage with the Ballos is less than those for the HL-10 type winged vehicles because the winged shape produces a longer control-moment arm. These deflections, however, are not the governing factors for second-stage control requirements. Second-stage dynamic response to initial conditions existing at separation determine maximum thrust-vector deflection and deflection rate requirements. The second-stage separation analysis is used in TVC system design.

Second-stage separation occurs at approximately 163.5 sec into the flight at an altitude of 175,000 ft. A 1-sec uncontrolled coast period was allowed for the second-stage nozzle to clear the interstage structure. Control-system activation and engine ignition occurred after this coast period. The engine thrust was assumed to build up linearly to full thrust (546,086 lb) in 0.3 sec. The initial angular rate and angle-of-attack used to determine the stability boundaries were $0.25^{\circ}/\text{sec}$ and 3.0° , respectively. These have been reduced from those used for the S-IVB because disturbances encountered during first-stage engine thrust tailoff will be smaller for the single engine configuration. Control-system stability boundaries are defined for each configuration in terms of the thrust-vector deflection limit as a function of the thrust-vector deflection rate limit. Figure 3-28 is a typical representation that applies to Configuration II. The lower stability boundary represents the minimum thrust-vector deflection with which divergence (caused by

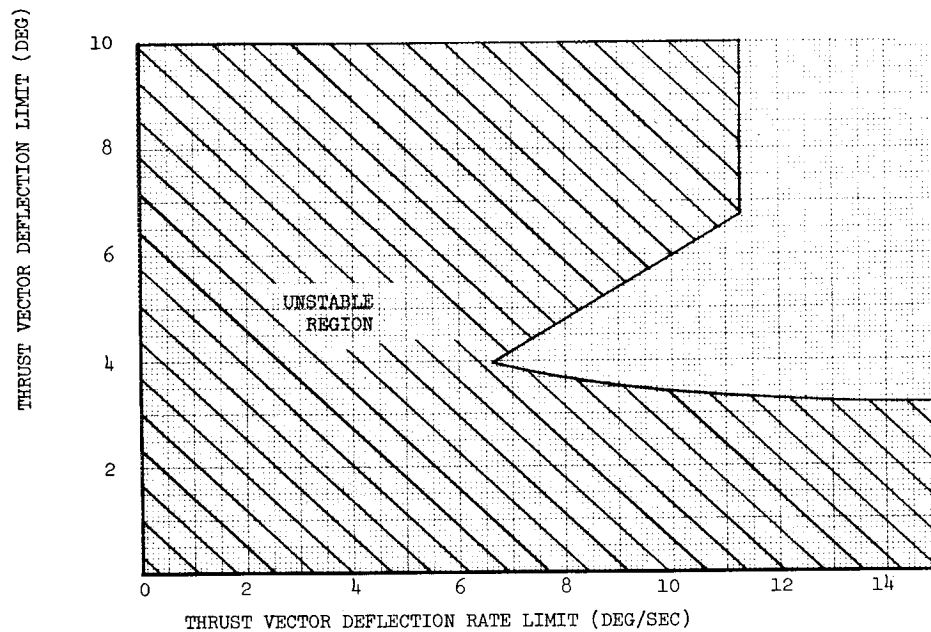


Figure 3-28. Second-Stage Control System Stability Boundaries – Configuration II

aerodynamic moments) can be prevented. The minimum thrust-vector deflection decreases slightly with increasing thrust-vector deflection rate. The upper stability boundary represents the minimum deflection rate limit for which an instability caused by rate saturation, will not occur. The minimum acceptable requirement (based on minimum acceptable deflection rate) is given in Table 3-6 for each configuration. Configuration I has the maximum deflection and deflection rate requirement. Configurations IIA and IIIA have lower minimum stability boundaries because of a higher pitch moment of inertia; therefore, less divergence occurs during the 1-sec uncontrolled coast period even though the aerodynamic normal force coefficient ($C_{z\alpha}$) is larger than that of the Ballos payload. These requirements are higher than those predicted by the static balance analysis because the vehicle is allowed to diverge during the 1-sec uncontrolled coast period, which results in a large vehicle angle-of-attack and body rate at control-system activation.

Table 3-6
MINIMUM ACCEPTABLE SECOND-STAGE TVC
SYSTEM DESIGN REQUIREMENTS

Configuration	Thrust- Vector Deflection (deg)	Thrust- Vector Deflector Rate (deg/sec)
Ballos Payloads		
I	4.3	7.3
II	4.0	6.7
III	3.3	5.6
Winged Payloads		
IIA	3.2	5.4
IIIA	2.0	3.8

It is not realistic to pick as the TVC design point the minimum requirement since a slight increase in the initial angle-of-attack or body rate could result in a control-system instability. Therefore, a second-stage TVC system design point of 6° and $15^\circ/\text{sec}$ for deflection and deflection rate limits were chosen. The same design point was used for all configurations since the minimum requirements are not significantly different. The thrust-vector deflection transient using the 6° and $15^\circ/\text{sec}$ limits for Configuration II is shown in Figure 3-29, and the attitude error transient is shown in Figure 3-30. Similar transients for Configuration IIA are shown in Figures 3-31 and 3-32. A nozzle acceleration of $200^\circ/\text{sec}^2$ is selected for use in system design.

No analysis of the structural clearance required during separation was undertaken. It has been assumed that separation can be accomplished (in 1 sec) if retrorockets are used to decelerate the first stage. If the coast period must be extended beyond the assumed 1 sec to allow for additional clearance, then the minimum acceptable deflection limit would also increase since it is a function of the coast period. However, the TVC system design point has been chosen well away from the stability boundary, so no instability is expected.

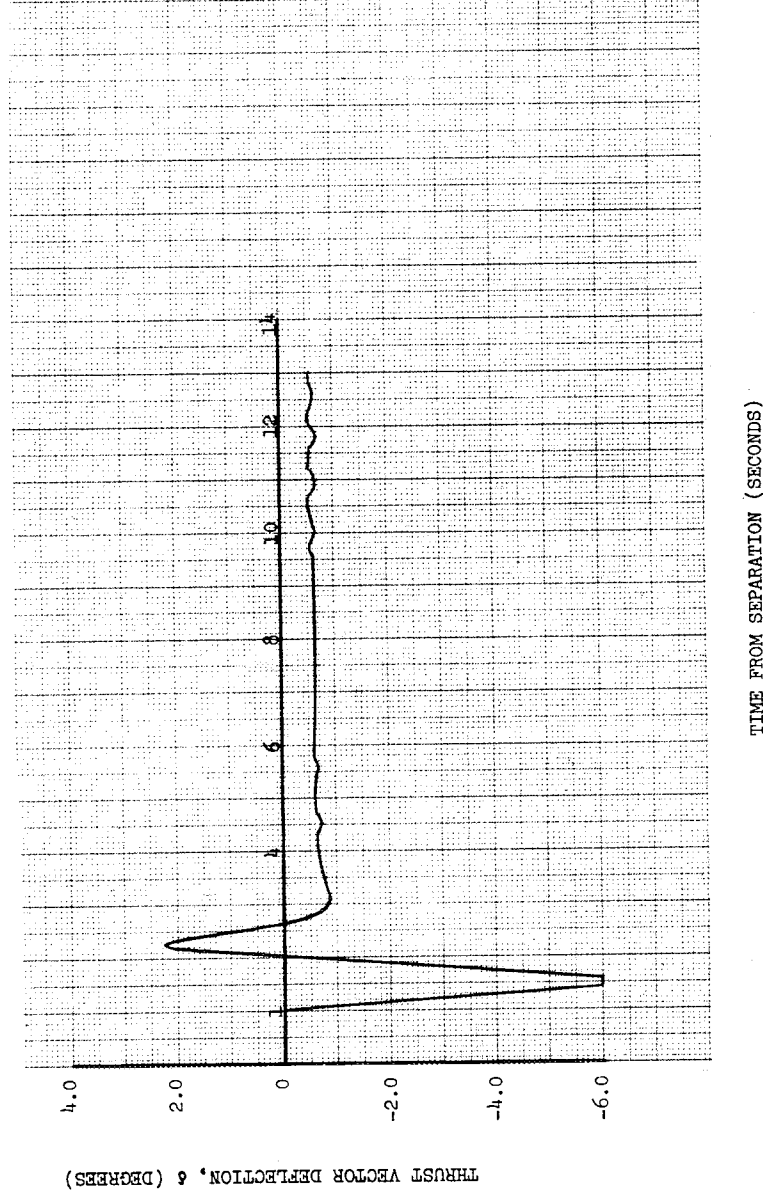


Figure 3-29. Second-Stage Thrust-Vector Deflection Angle Transient

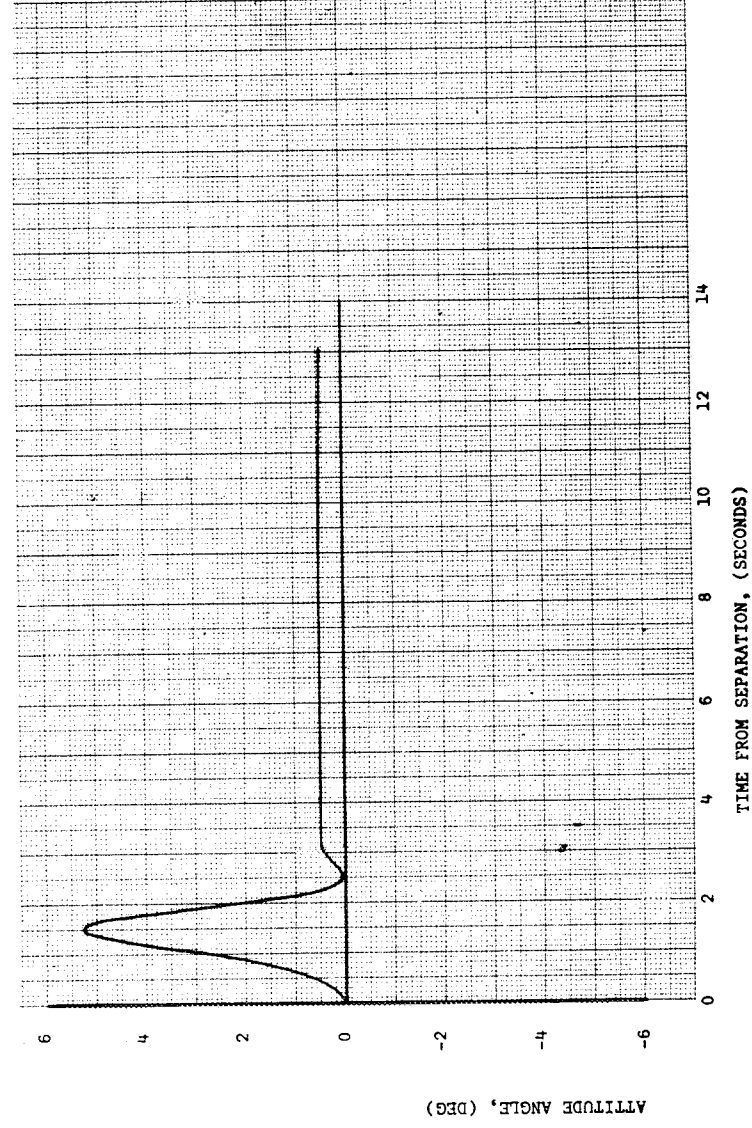


Figure 3-30. Attitude Angle Transient Following Separation: Configuration II – Ballos Payload

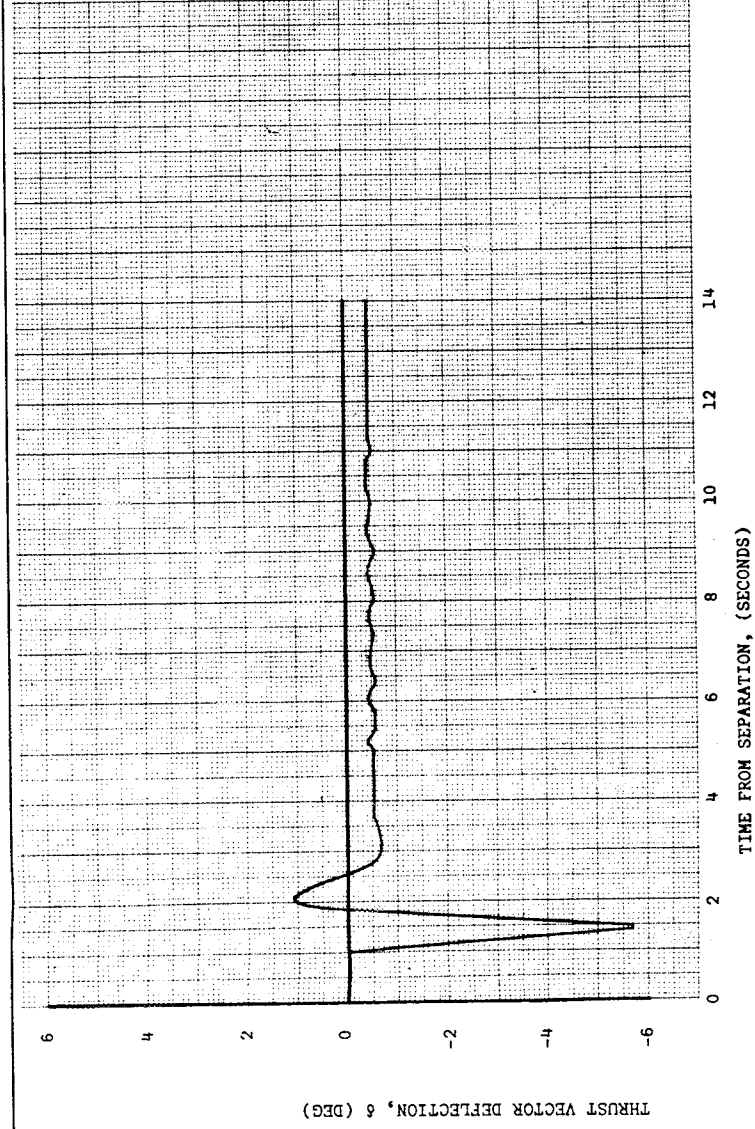


Figure 3-31. Thrust-Vector Deflection Angle Transient Following Separation: Configuration IIA HL-10 Payload

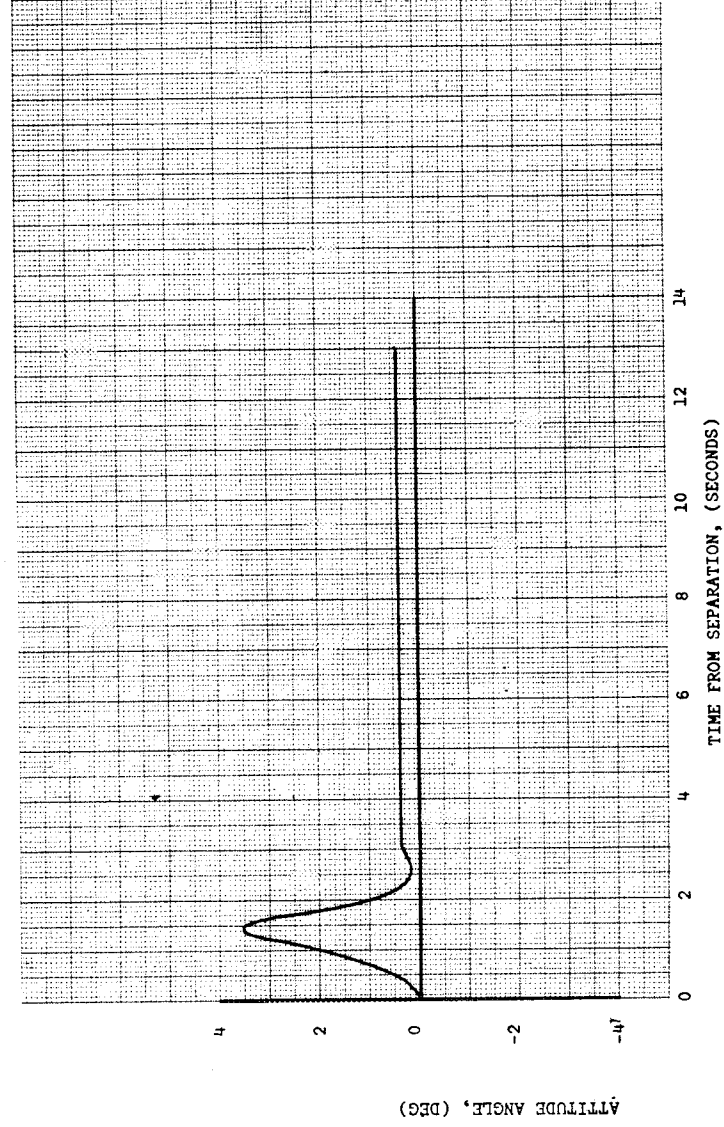


Figure 3-32. Attitude Angle Transient Following Separation: Configuration IIA-HL-10 Payload

3.6.2 Roll Control Requirements

Roll moments are derived from two sources: (1) aerodynamics and (2) moments resulting from thrust eccentricity and CG offset. The aerodynamic moments occur because of fin misalignment and dihedral effects when fins are used. Moments caused by thrust eccentricity and CG offset are equal to thrust times the sine of the thrust-vector deflection angle times the magnitude of the eccentricity CG offset combination. (See Appendix B for the actual derivation.) For small thrust-vector angles, roll moments for vehicles without fins are proportional to thrust magnitude and thrust-deflection angle; therefore, the roll-moment duty cycle curves are of the same form as the TVC duty cycles shown in Figures 3-22 through 3-25. For this reason, these curves are not plotted, but maximum roll moments and total roll impulse are tabulated in Table 3-5.

3.6.3 Effect of Fins and Fin Size Variation on First-Stage Maximum Deflection and Duty-Cycle Requirements

The addition of fins to the first stage has the effect of making the vehicle more stable in the same manner as the flared skirt did for Configuration II. The maximum deflection angle and duty-cycle requirements in pitch and yaw are thereby decreased at the expense of added structural weight. This decrease in deflection angle also causes a decrease in roll moment caused by thrust eccentricity and CG offset, but fins incur additional roll moments because of fin misalignment and dihedral effect. The magnitude of the first of these moments is dependent upon the individual fin sizes, while the second is a function of the size of the pitch fins relative to the yaw fins. Whether the net roll moment is increased or decreased by the addition of fins, therefore, depends upon the particular configuration of the vehicle for which both pitch and yaw fins must be defined. It will be noted in Table 3-5, however, that for Configuration IIA, which has the HL-10 type winged payload, the addition of fins more than triples the roll total impulse requirement. Pitch and yaw fins were sized for this configuration, for it is typical of the launch vehicles in this study. The conclusions reached would be similar had any of the other configurations been selected. However, a vehicle having a winged payload--which required more TVC for first stage flight--tends to accentuate the results.

Fin sizing is accomplished by varying the pitch and yaw span and aspect ratio to minimize the aerodynamic moment in pitch and yaw respectively. The effect of these fins can be seen by comparing Figures 3-23 and 3-33 and by reference to Tables 3-5 and 3-7. Figure 3-33 shows that the maximum thrust vector deflection required for a vehicle with optimum fins is 0.355° . While Figure 3-23 shows a maximum deflection of 2.54° for the same vehicle without fins. Table 3-7 which is a detailed breakdown of the components that produce the total control moment required, shows a similar trend for total control impulse. Total control impulse is reduced from $101.21^\circ/\text{sec}$ for the vehicle with no fins to $45.18^\circ/\text{sec}$ for the same vehicle with optimum fins.

Several other pitch fin areas were evaluated. Since there are many combinations of fin span and aspect ratio for a given area, it was necessary to define a particular optimum combination of these for each area. This was done by means of varying span and aspect ratio in such a manner as to maintain a constant area and minimize the body pitching moment. The yaw fin was held constant at its previously determined value which was obtained from optimum

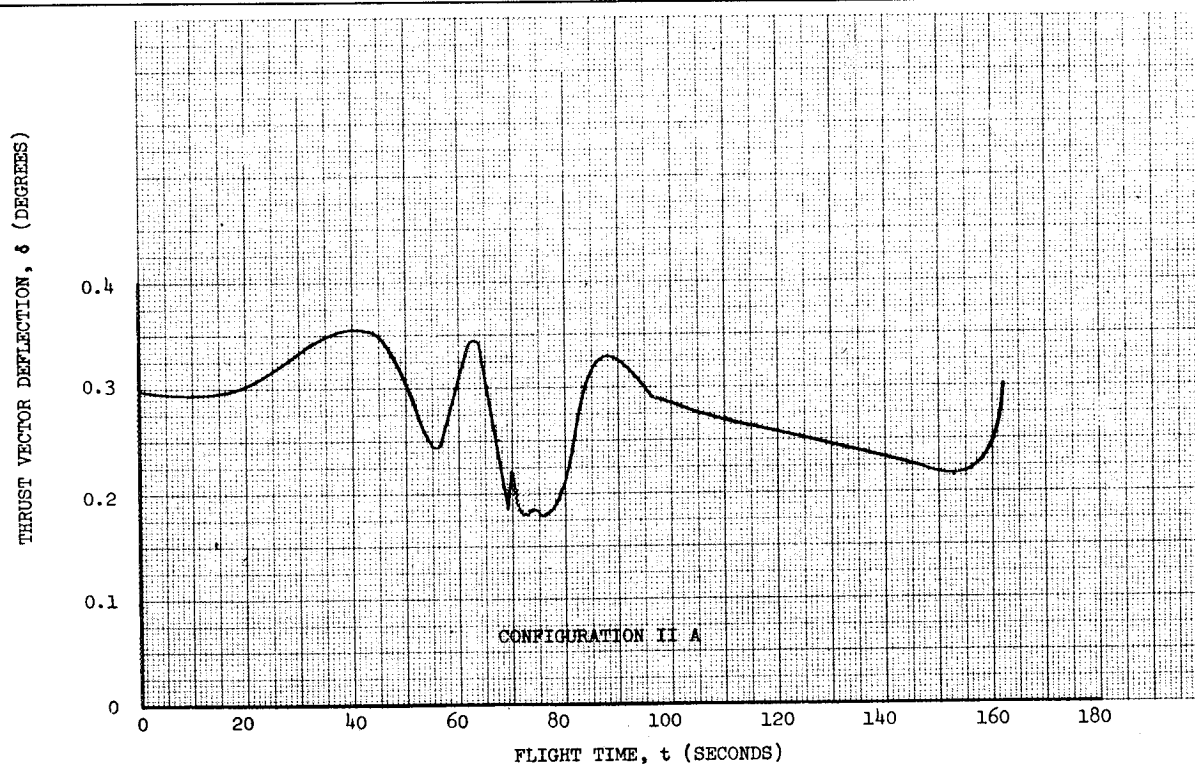


Figure 3-33. First-Stage Duty Cycle – Optimum Fins and Winged Payload

Table 3-7
DUTY-CYCLE AREA BREAKDOWN

Items	Configuration IIA First Stage	Configuration IIAF First Stage
Pitch Impulse in Deg-Sec Due to the Following:		
Wind	61.946	6.623
Total Uncertainties	25.397	24.956
Aerodynamic	3.097	0.331
Fin Misalignment	0.000	0.804
Thrust Offset and Angle	24.899	24.899
Maneuvering	7.805	7.805
Yaw Impulse (deg-sec)		
Total Uncertainties	24.899	24.929
Fin Misalignment	0.000	0.670
Thrust Offset and Angle	24.899	24.899
Maneuvering	2.223	2.223
Total Impulse - Pitch-Yaw (deg-sec)	101.21	45.18
Roll (ft-lb-sec)		
Dihedral Effect	0	397,310
Pitch Fin Misalignment	0	501,560
Yaw Fin Misalignment	0	463,470
Thrust Offset	444,080	52,360
Total Area - Roll (ft-lb-sec)	444,080	1,419,200

fin calculations for Configuration IIA. The results of this study are shown in Figure 3-34. As fin size decreases, both required pitch-control impulse and maximum pitch-deflection angle increase.

The maximum deflection angle becomes so small with optimum fins that the nominal deflections may well be below the threshold level of any but very sophisticated control systems. It is for this reason that fins were not included on the launch vehicle configurations developed for this TVC comparison study.

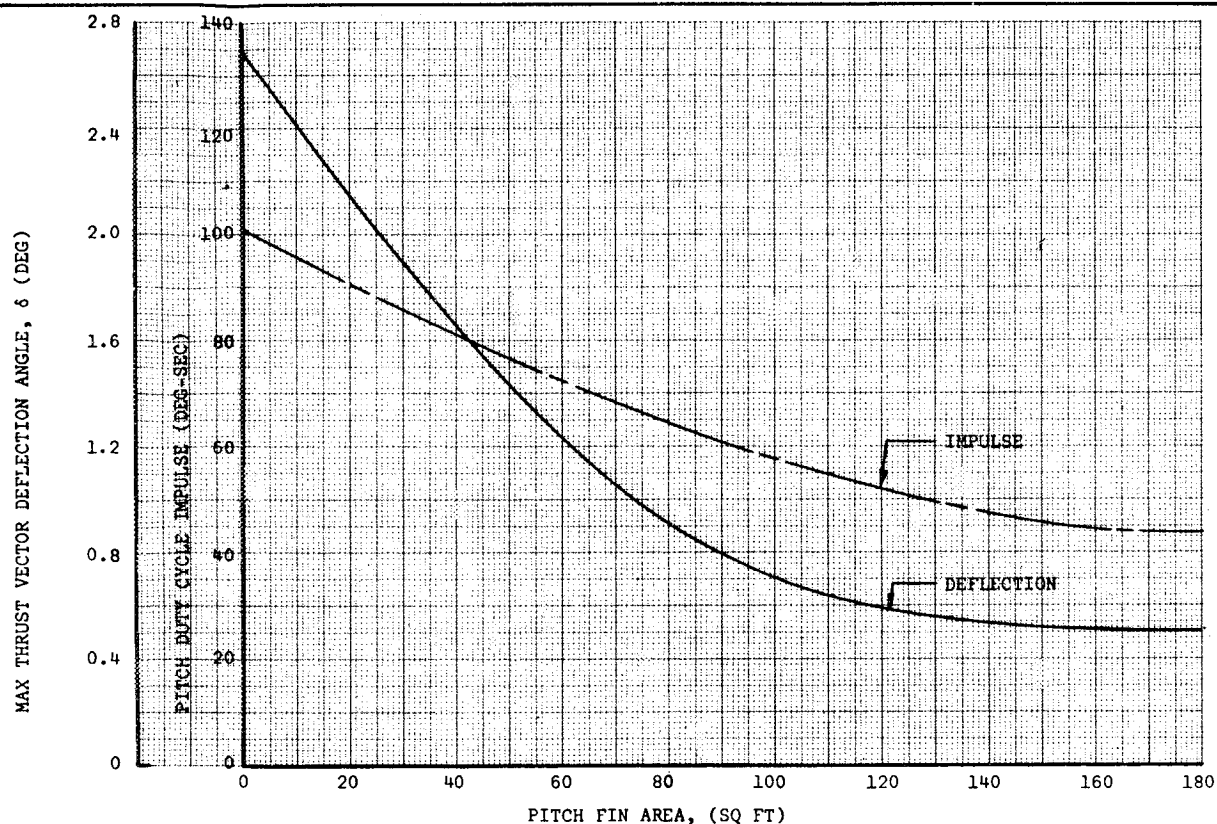


Figure 3-34. Fin Performance

3.6.4 Stability Characteristics

Launch vehicle lateral bending characteristics were analyzed to evaluate the effects of body-bending dynamics on control-system stability. One of the primary requirements of the control system is to provide satisfactory stability in the body-bending frequency range. Body-bending vibrations are sensed by the attitude reference system and rate gyros. Control-system response to body-bending vibrations must be stable so that the vibrations will be damped and structural loads, because of bending will not become excessive.

Bending characteristics were determined for Configurations I and III with both payload shapes. Since Configuration II is similar to Configuration I, the data resulting from the analysis of Configuration I apply to Configuration II. The mass distribution and stiffness characteristics for each configuration investigated are obtained from Figures 3-4 and 3-13. The lowest three-body bending-mode frequencies are shown in Table 3-8. These data were generated for a flight time corresponding to maximum dynamic pressure. The minimum body-bending frequency is 3.44 cps and occurs for Configuration IA. The mode shapes for the first three modes are shown in Figure 3-35. Since

Table 3-8
BODY-BENDING FREQUENCIES (cps)

Mode	Configuration I and IA (Warm Gas)		Configuration III and IIIA (Hot Gas)	
	Ballos Payload	Winged Payload	Ballos Payload	Winged Payload
1	3.71	3.44	4.20	3.90
2	12.02	10.42	13.16	11.64
3	19.12	15.83	22.82	17.76

the minimum bending frequency is approximately a factor of 10 higher than the control-system natural frequency, it will be possible to stabilize all of the vehicles using current techniques, such as passive filter networks in the control system, with little or no control system response degradation.

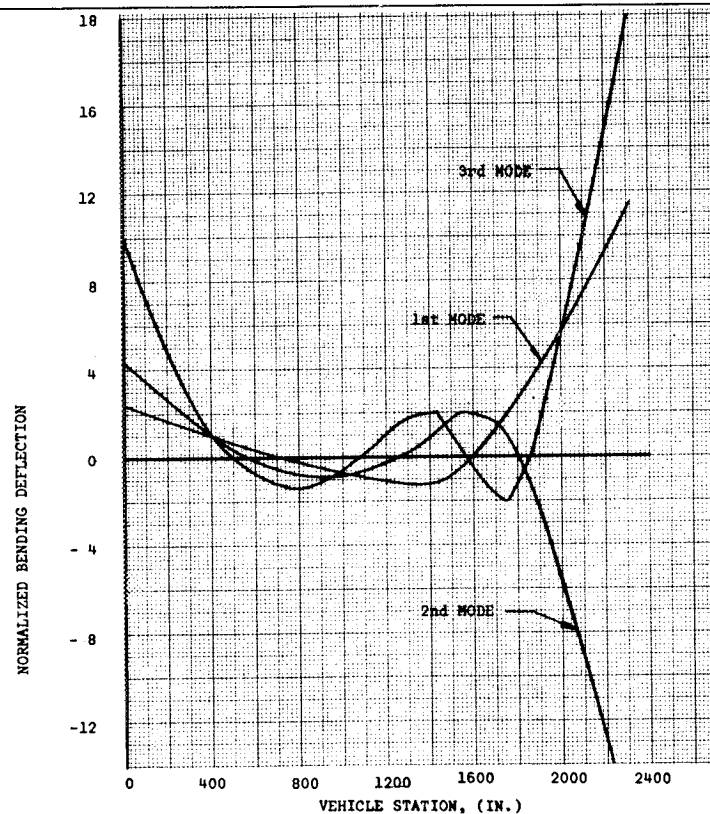


Figure 3-35. Body Bending Modes for Configuration IA

3.6.5 Control System Sensitivity

Since neither the hot gas or warm gas injection TVC system must resist the large inertia of the nozzle, as is the case for the gimbaled nozzle TVC system, the response time of the gas injection systems is faster than that of the gimbaled nozzle system. An analog computer study was performed to determine if this fast response can be used to reduce thrust-vector deflection requirement. The analysis also included an evaluation of vehicle bending moment in order to determine if this parameter can be reduced by using the fast response capabilities of the gas injection systems.

The yaw plane was chosen to evaluate the control-system response because the winds in the yaw plane generally cause the most stringent control requirements. Two control schemes were considered in the study: attitude error plus body-rate feedback, and attitude error, body rate, and angle-of-attack feedback. In both cases, the control gains were programmed to maintain a constant (with flight time) control-system natural frequency and damping ratio. A control-system damping ratio of 75% was used, and the natural frequency was varied from 0.2 cps to 1.0 cps. The TVC loop was simulated with the use of a second-order differential equation. The TVC loop damping was 75% of critical, and the natural frequency was varied from 5 to 50 times the control-system natural frequency. TVC loop natural frequency for a gimbaled nozzle is normally in the range of from approximately 5 cps to 10 cps and is limited by the moment-of-inertia of the gimbaled nozzle. Since neither the hot gas or warm gas injection TVC system must move a large inertia, the natural frequency will be limited by only the lags associated with the mechanical and electrical equipment of the system and will be much higher than the gimbaled nozzle system. To take advantage of this capability, the control-system natural frequency may be increased beyond that normally used. An equation for the peak bending moment was included in this simulation to evaluate the effect of the control schemes and control frequencies on this parameter. The equation is a summation of the bending moments resulting from angle-of-attack, lateral acceleration, and angular acceleration, and is valid only in the region of maximum dynamic pressure. A single wind profile with a gust occurring at maximum dynamic pressure was used throughout the study.

The results of the simulation are presented in terms of peak angle-of-attack, peak thrust-vector deflection angle, and peak bending moment as a function of control-system natural frequency in Figures 3-36 through 3-38. The data have been normalized to the results obtained using angle-of-attack feedback with a control frequency of 0.2 cps. The cross-hatched area represents the variations resulting from variations in TVC-loop natural frequency. A TVC-loop natural frequency of 50 times the control-system natural frequency results in the minimum requirement.

With attitude error and body rate feedback the angle-of-attack, thrust vector deflection and bending moment are sharply reduced by increasing the control frequency from 0.2 cps to 0.5 cps. The increased control frequency reduces the rotation of the vehicle away from the wind vector by increasing the tightness of the attitude control loop. A further increase in the control frequency causes little decrease in angle of attack, thrust vector deflection or bending moment. Since the gimballed nozzle TVC system is capable of responding to control system commands up to at least 0.5 cps, this system will provide the same overall system response characteristics as either the hot gas or warm gas TVC systems.

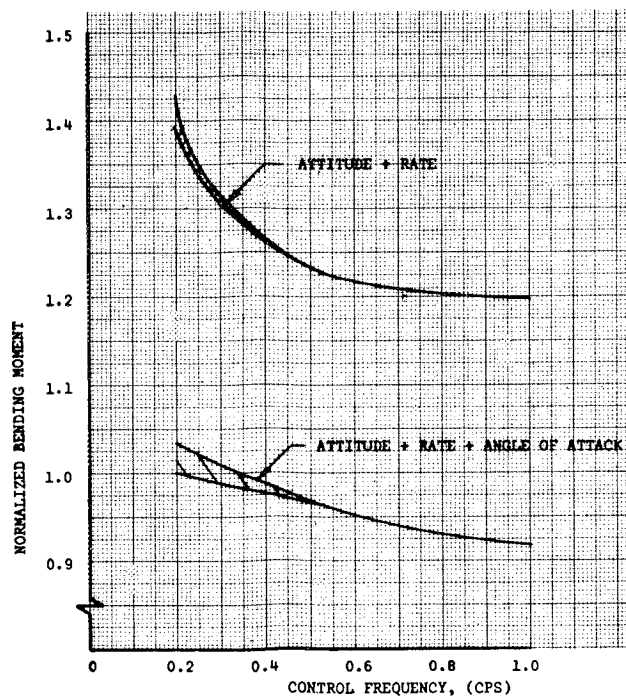


Figure 3-36. Peak Bending Moment as a Function of Control Frequency

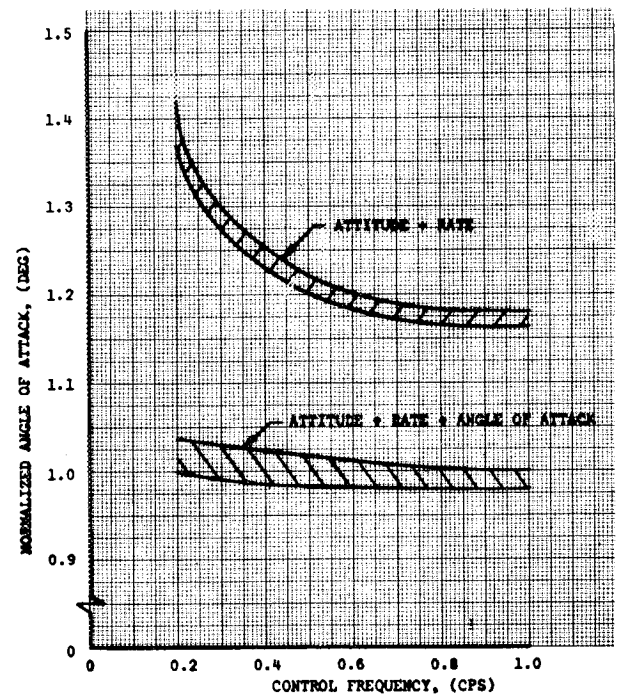


Figure 3-37. Peak Angle-of-Attack as a Function of Control Frequency

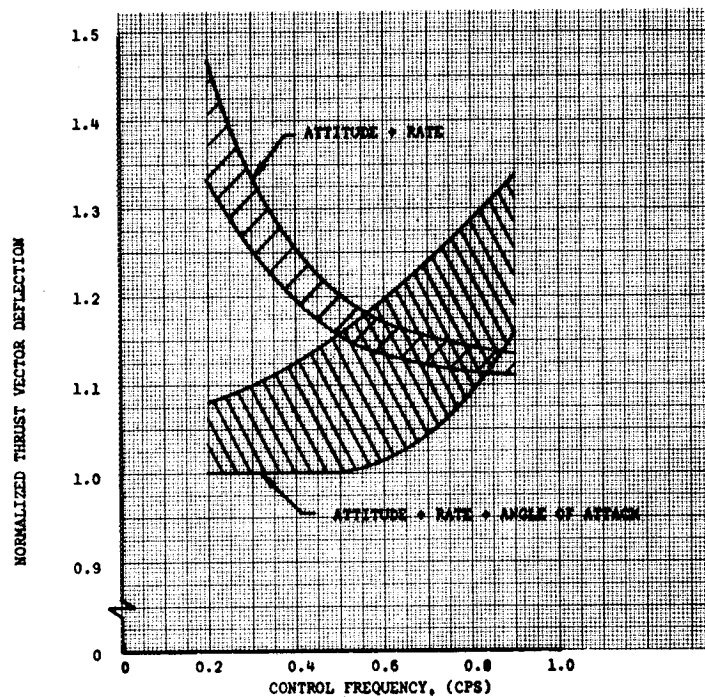


Figure 3-38. Peak Thrust-Vector Deflection as a Function of Control Frequency

The inclusion of angle of attack feedback along with attitude error and body rate feedback resulted in a much lower bending moment at all control frequencies. This lower bending moment results because angle of attack control allows the vehicle to turn into the wind, reducing the angle of attack. It should be noted (from Figure 3-38) that increased control frequency results in increased thrust-vector deflection. For this case, the decrease in bending moment due to increased control system natural frequency is less than 10%.

It was concluded from this analysis that the bending moment could be reduced by increasing the control frequency beyond the nominal value of 0.2 cps with an attitude error and body rate feedback control system. If angle of attack feedback is added and the control gains programmed to satisfy the drift-minimum criterion, the maximum bending moment does not vary significantly with control frequency, and is substantially lower at all control frequencies because of reduced angle of attack. Since the latter control mode reduces the bending moment virtually independent of the control frequency, it is considered to be more optimum. Therefore, high response characteristics of the hot gas or warm gas injection system have no particular advantage over a gimballed nozzle system at control frequencies below approximately 0.5 cps.

Section 4

TVC SYSTEMS COMPARISON

The Lockheed Lockseal gimballed nozzle, the Thiokol hot gas injection, and the Vickers warm gas injection TVC concepts were expanded into workable designs for use with the 260-in. -diam and the 156-in. -diam SRM's. Only the design requirements of launch vehicles with the primary Ballos payload were considered in this task, and the design effort concentrated on parameters necessary for vehicle control and not a detail design of seal or valve elements. The resulting designs and analysis were used to generate comparisons of vehicle and TVC system reliability, performance, and weight.

4.1 LOCKSEAL DESIGN REQUIREMENTS

Gimballed nozzle TVC system designs for both stages are straightforward and center about actuator and power system sizing and the electronics systems necessary to perform TVC. Lockseal details, such as pivot-point location, lockseal geometry, weights, and seal torques, were obtained from the data supplied by the Lockheed Propulsion Company. Nozzle torques produced by the flight environment were established from requirements determined by the stability and control analysis. Table 4-1 summarizes these requirements.

Table 4-1
GIMBAL NOZZLE TVC SYSTEM DESIGN REQUIREMENTS

Items	First-Stage 260-in. -diam SRM	Second-Stage 156-in. -diam SRM
Maximum Deflection (Deg)	2.474	6.0
Deflection Rate (Deg/Sec)	7.5	15.0
Angular Acceleration (Deg/Sec ²)	30	200

The maximum deflection shown for the first stage is adjusted to reflect the actual pivot-point location. Reference Section 3.5.1 $\delta = \delta_T \left(\frac{\ell_T}{\ell_p} \right)$

where

δ_T = maximum deflection based on the nozzle throat as the pivot point

ℓ_T = distance from CG to the throat

ℓ_p = distance from CG to actual pivot point

4.2 GAS INJECTION TVC DESIGN DATA

To satisfy stability and control requirements, designs for the hot gas and warm gas injection TVC systems required a determination of (1) injector locations, (2) main motor I_{sp} changes due to TVC, (3) flow rates, and (4) number of valves per quadrant. To determine the injector location, it was first necessary to evaluate the parameters that might significantly affect it. The parameters in question were (1) injection Mach number, M_j , (2) injection angle, ϵ , (3) number of valves per quadrant, N , and (4) recovery and amplification factors. This evaluation was performed with the use of a preliminary design computer program (H-236). This program was developed to evaluate candidate nozzle/TVC systems and for making system tradeoff studies. Its validity has been checked against similar methods for analytical performance prediction developed by Vickers and Thiokol/Vidya as well as correlated with test results within 15% for a wide range of test conditions.

4.2.1 Injector Location

The initial investigation showed that injection nozzle location had no significant effect on side-force ratio when side force was used as the major parameter. Further evaluation of injection Mach number, injection angle, and number of valves per quadrant showed similar results. (See Figures 4-1 and 4-2.) More significant results were obtained when a performance parameter which considers both side-force and axial-thrust efficiency was evaluated for its effect on injector location. Main-motor specific-impulse degradation is at a minimum when $(1 - K_A K_R)$ approaches zero, where K_A is the amplification factor defined as the ratio of side specific impulse to axial

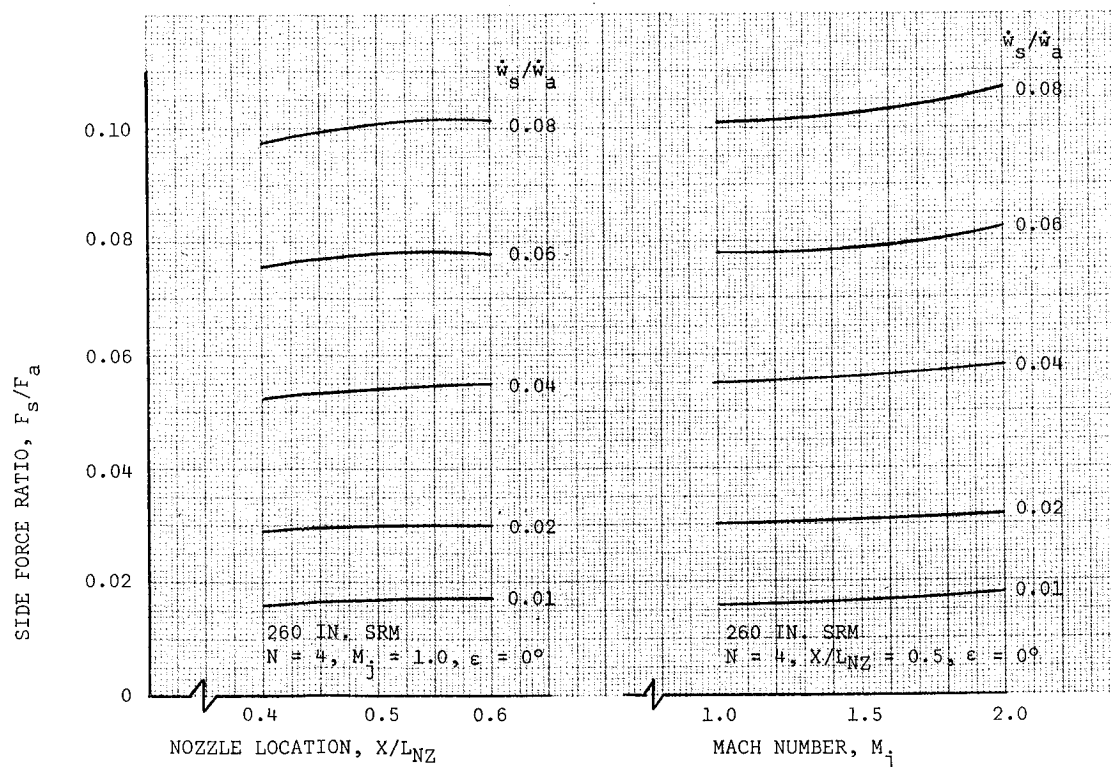


Figure 4-1. Effect of Injector Nozzle Location and Mach Number on Side-Force Performance

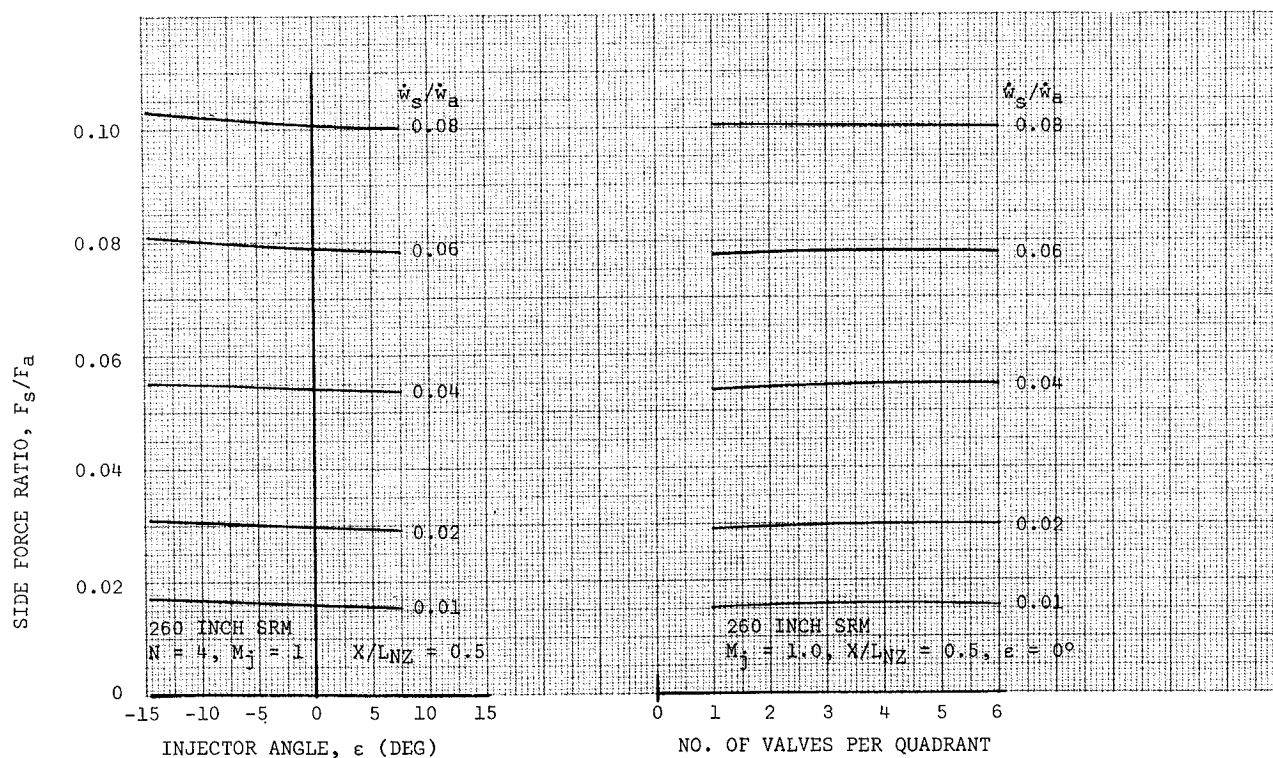


Figure 4-2. Effect of Injector Angle and Number of Valves Per Quadrant on Side Force Performance

main motor specific impulse $\frac{I_{sps}}{I_{spm}}$ and K_R is the recovery factor defined as the ratio of change in axial force to side force ($\Delta F_a / F_s$). Therefore, a plot of $K_A K_R$ versus nozzle injector location for the 260-in. -diam SRM hot gas case was developed. As seen in Figure 4-3, improved performance can be obtained by locating the injection station at low nozzle area ratios, that is, low (X/L_{NZ}) . However, before the actual nozzle injector location could be determined, specific design requirements associated with the particular application of the TVC systems were included in the computer program for analysis. Factors such as duty cycle, deflection angle, motor pressure level and action time, and injectant velocity were included in the analysis. The resulting gain performance curve for the 260-in. -diam SRM with hot gas injections is presented in Figure 4-4. Two (X/L_{NZ}) ratios were analyzed, 0.4, which Figure 4-3 suggested as providing better performance than 0.5, and 0.5 which Thiokol suggested for use in our design. In addition, the gain performance using the Thiokol analytical method and suggested X/L_{NZ} was calculated. A nozzle injector location (X/L_{NZ}) of 0.5 was selected on the basis of this analysis for it showed superior

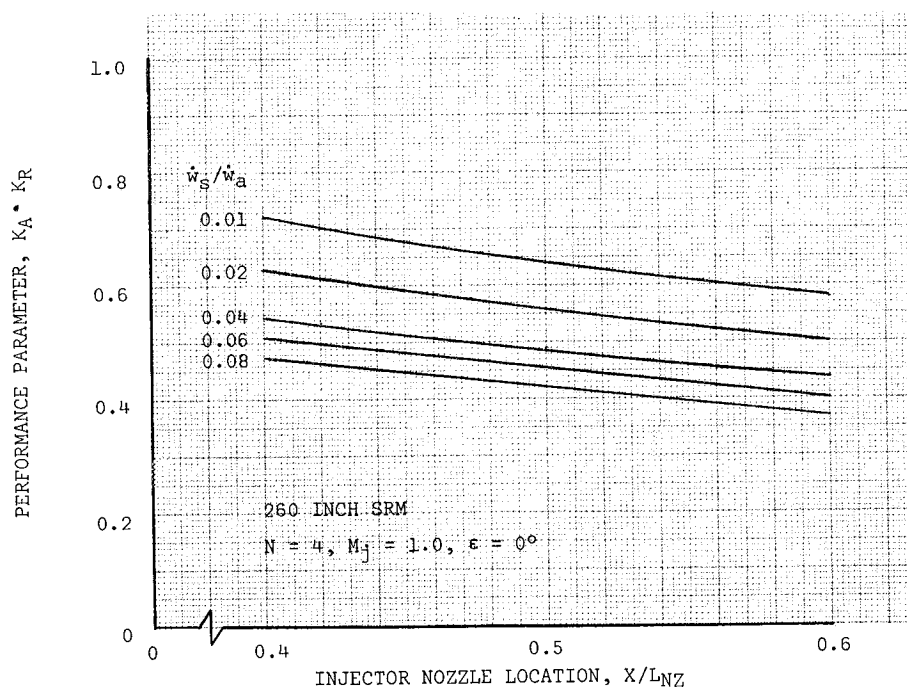


Figure 4-3. Effect of Injector Location on Hot Gas Performance Parameter

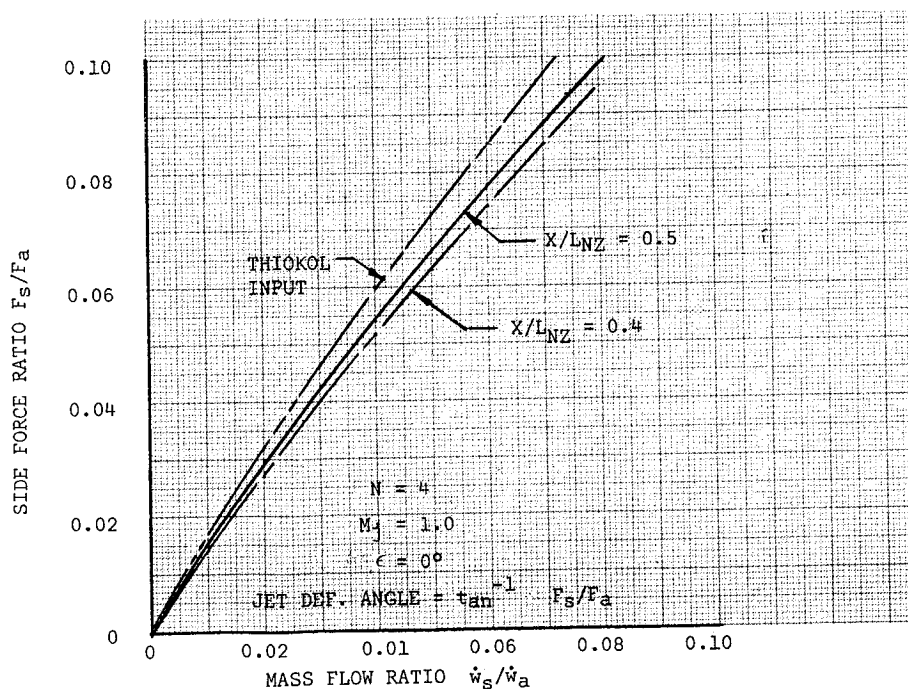


Figure 4-4. 260-in.-Diameter Hot Gas TVC Gain Performance

performance to that of a 0.4 injector location and it correlated with the Thiokol prediction. The jet deflection angles capable of being produced by this TVC system can be obtained from this figure.

Amplification factor and recovery factor are calculated as a function of deflection angle and shown in Figure 4-5. These values are used to obtain the change in I_{sp} due to secondary gas injection TVC.

Similarly, the gain performance curves, recovery factor, and amplification factor were calculated for the 156-in.-diam SRM hot gas injection TVC system. Figures 4-6 and 4-7 present the results.

Selection of nozzle injector location for the warm gas TVC systems was performed in a similar manner to that used to locate hot gas TVC injectors. Since amplification factor was found to be a significant performance parameter, it was plotted as a function of injector location. These results, shown

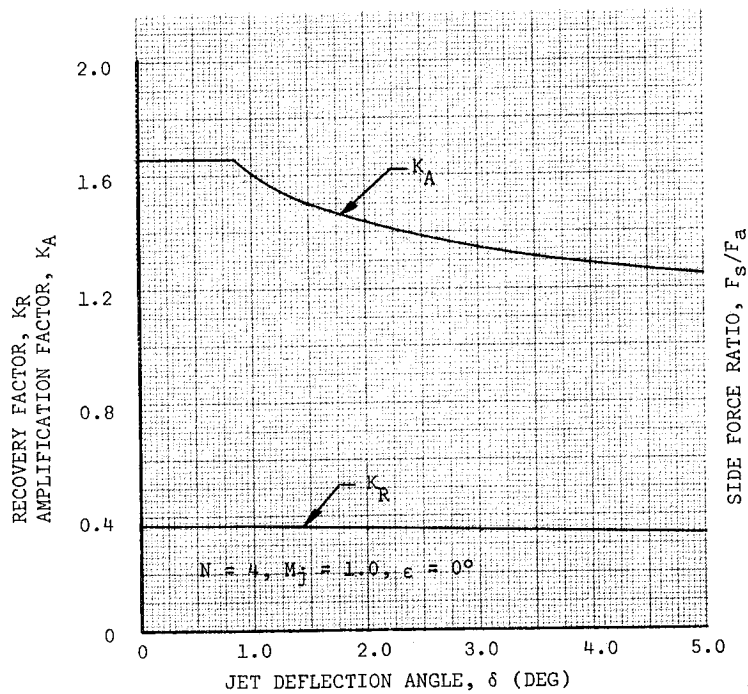


Figure 4-5 260-in. Diameter Hot Gas Performance Factors

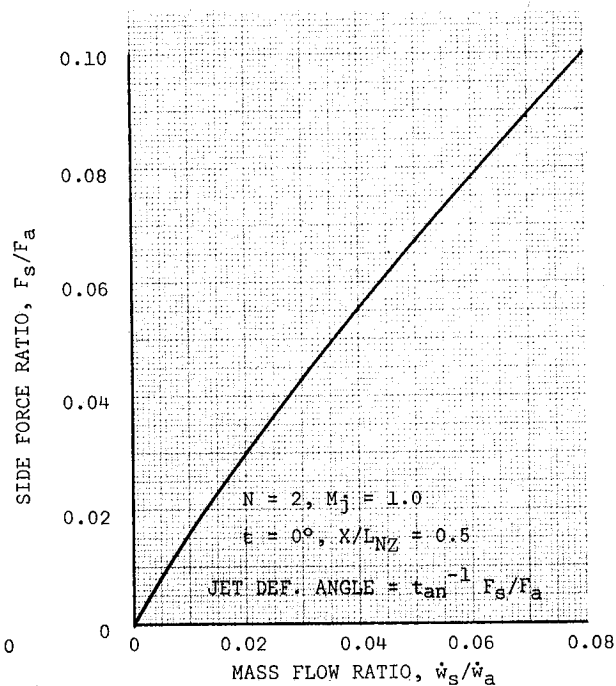


Figure 4-6 156-in. Diameter Hot Gas TVC Gain Performance

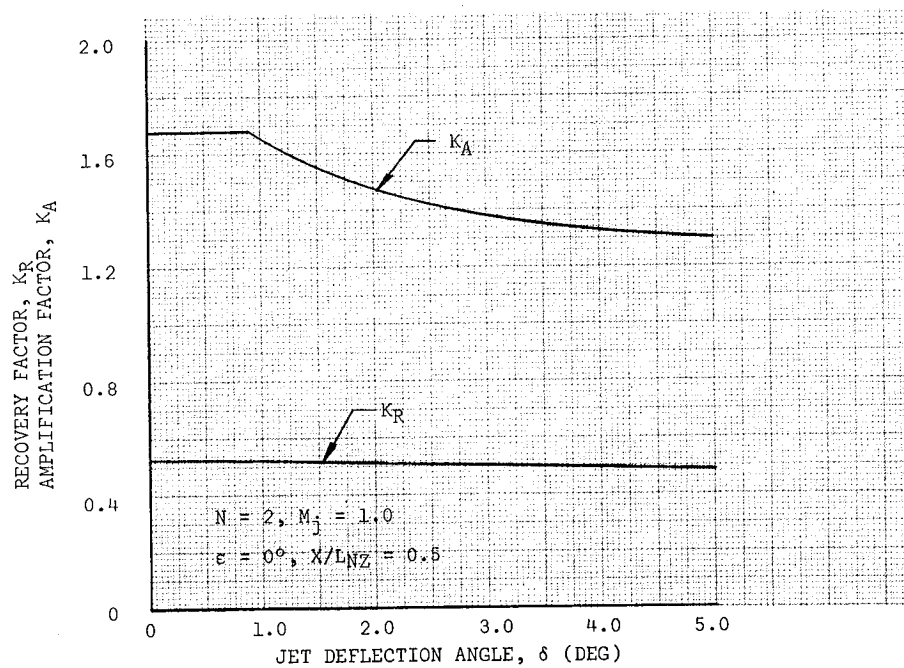


Figure 4-7. 156-in.-Diameter Hot Gas TVC Performance Factors

in Figure 4-8, indicate that maximum performance will occur at $(X/L_{NZ}) = 0.6$; and additional investigation of this parameter with recovery factor showed minimum system I_{sp} loss occurs at $(X/L_{NZ}) = 0.55$. However, Vickers specified that best performance would occur at $(X/L_{NZ}) = 0.75$. When the influence of a longer moment arm due to larger values of (X/L_{NZ}) were included in this analysis, as shown in the gain performance curve in Figure 4-9, a nozzle injector location of 0.7 was selected. Again the Douglas analysis was verified by superimposing the results of a similar analysis using the Vickers approach and suggested (X/L_{NZ}) location. The gain performance curve for the 156-in. -diam SRM warm gas injection TVC system was calculated by using the nozzle injection location of the 260-in. -diam SRM. Figure 4-10 shows the results of this analysis and the excellent correlation that exists with the Vickers analytical method; therefore, this nozzle injector location is selected for both stages. The recovery factors and amplification factors as a function of thrust-vector deflection angle are shown for both stages in Figures 4-11 and 4-12.

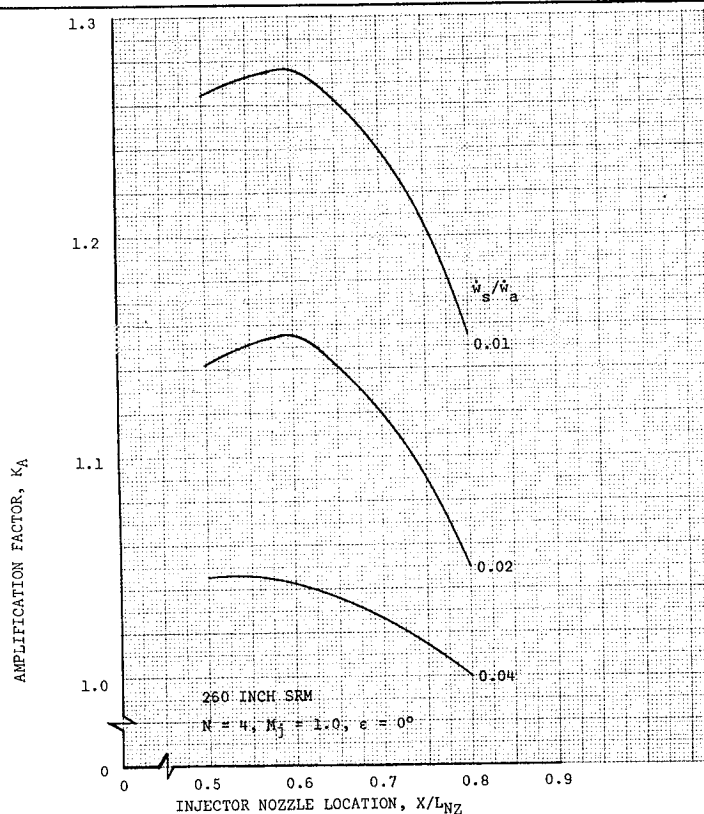


Figure 4-8. Effect of Nozzle Location on Warm Gas TVC Performance

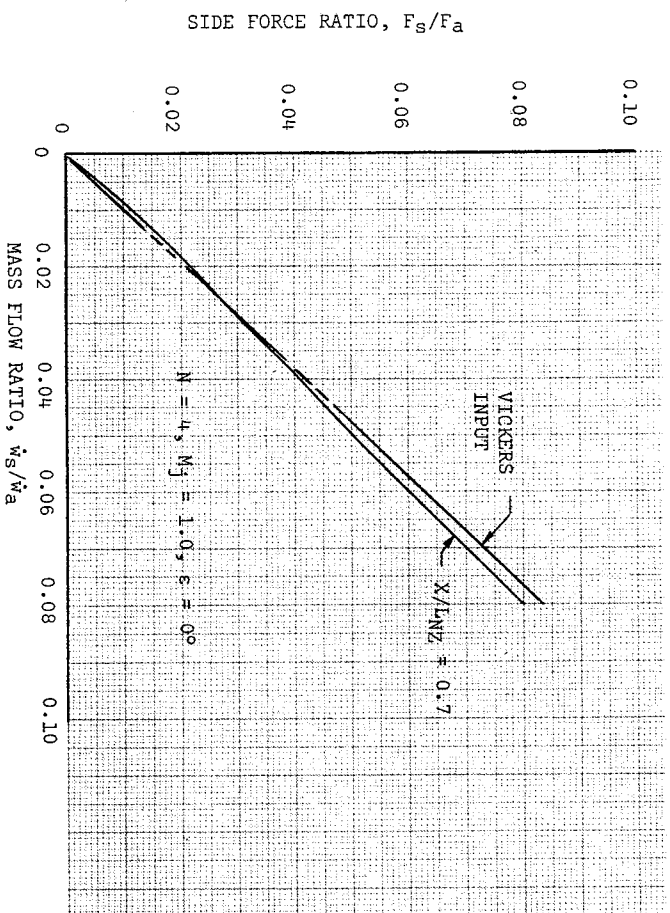


Figure 4-9. 260-in. Diameter Warm Gas TVC Gain Performance

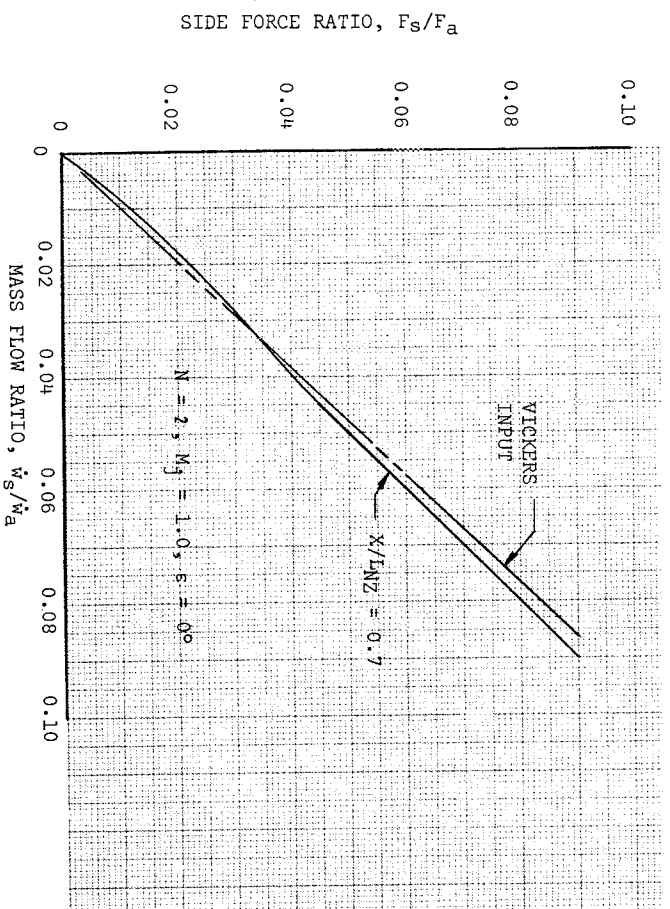


Figure 4-10. 156-in.-Diameter Warm Gas TVC Gain Performance

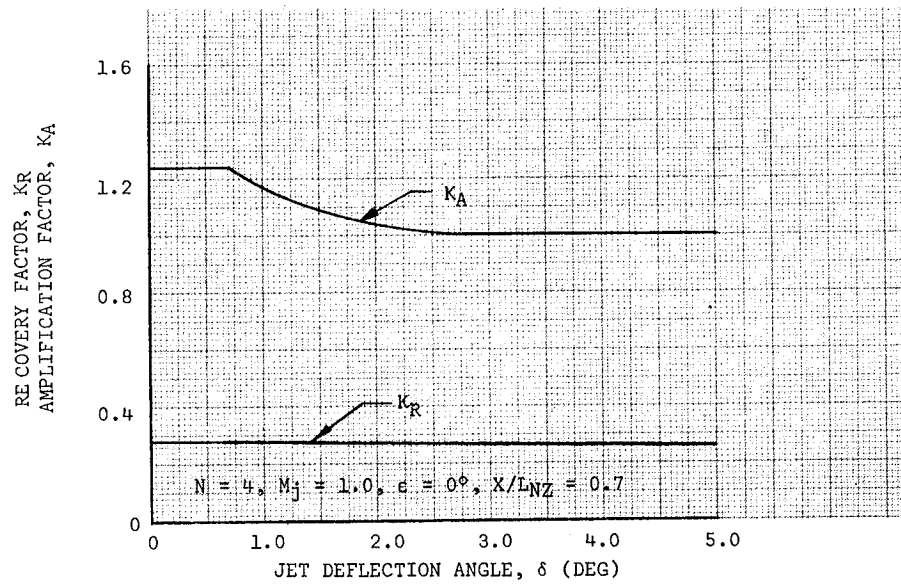


Figure 4-11. 260-in. Diameter Warm Gas TVC Performance Factors

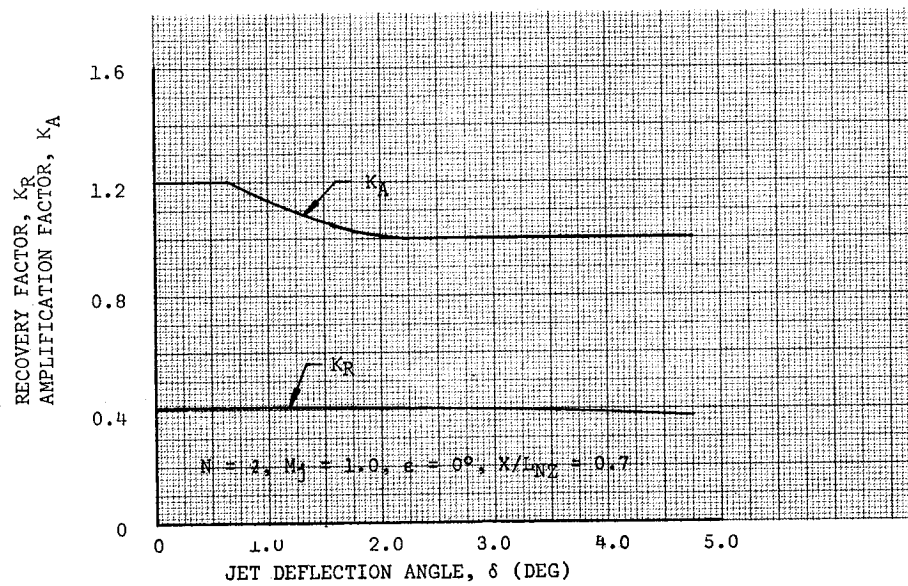


Figure 4-12. 156-in.-Diameter Warm Gas Performance Factors

4.2.2 Specific Impulse Change Caused by TVC

Specific impulse losses resulting from gas injections TVC were calculated using the following equations:

For hot gas injection TVC,

$$\Delta I_{sp} = I_{spm} \left(\frac{\dot{w}_s}{\dot{w}_a} \right) (1 - K_A K_R) \quad (1)$$

For warm gas injection TVC,

$$\Delta I_{sp} = I_{spm} \left(\frac{\dot{w}_s}{\dot{w}_a + \dot{w}_w} \right) (1 - K_A K_R) \quad (2)$$

where

I_{spm} = initial value of motor I_{sp}

\dot{w}_w = total flow rate of the gas generators

The derivation of these equations is shown in Appendix A. To evaluate these equations it is necessary to obtain average thrust-vector deflections and side forces so values for the parameters shown in the equations can be obtained. K_A and K_R were determined from Figures 4-5 and 4-7 for the hot gas case and Figures 4-11 and 4-12 for the warm gas case. Values of $\frac{\dot{w}_s}{\dot{w}_a}$ were determined from Figures 4-4 and 4-6, while the flow rate ratios for the warm gas case are calculated.

The average side force, \bar{F} , is obtained by converting the duty cycles shown in the stability and control analysis into side force as a function of time, adjusting first-stage values to reflect the actual pivot point. Total side impulse is obtained by integrating these values. Dividing total impulse by motor-action time yields average thrust which can then be converted to average deflection from the gain curves. A summary of these calculations is shown in Table 4-1A. The I_{sp} change resulting from gimballed nozzle TVC is trivial and was considered to be zero in this study. The maximum side forces developed for Configuration II are 217,000 lb for the first stage and 12,880 lb for the second stage.

Table 4-1A
TVC DESIGN SUMMARY

		Configuration I		Configuration III	
		First Stage	Second Stage	First Stage	Second Stage
Maximum Deflection Angle	(deg)	2.023*	6	2.088*	6
Maximum Side Force	(lb)	177,488	6,098	183,200	7,850
Total Side Impulse	(lb-sec)	7.14×10^6	0.601×10^6	7.65×10^6	0.788×10^6
Motor Action Time	(sec)	163	131	163	131
Average Side Force	(lb)	43,800	4,590	46,900	6,020
Motor Thrust	(lb)	5.028×10^6	0.546×10^6	5.028×10^6	0.546×10^6
Average Deflections	(deg)	0.53	0.82	0.53	0.82
Mass Flow Ratio		0.0080	0.0071	0.0057	0.00865
I_{sp}	(sec)	276.9	301.0	276.9	301.0
K_A		1.240	1.20	1.64	1.67
K_R		0.28	0.41	0.38	0.545
Change in I_{sp}	(sec)	-1.45	-1.09	-0.59	-0.23

*These deflection angles reflect actual side-force plane locations $X/L_{NC} = 0.5$
for hot gas TVC and $X/L_{NZ} = 0.70$ for warm gas TVC.

4.2.3 Flow Rates and Number of Valves Required for TVC

Valve sizes for the hot gas and warm gas TVC systems are dependent on maximum flow-rate requirements and physical constraints. For this analysis, hot gas valve development and arrangement of the gas generators were prominent factors in the selection of individual valve flow rates. Maximum flow-rate requirements per quadrant were determined as follows:

$$\dot{w}_s = \frac{F_a \tan \delta}{I_{sps}}$$

where

\dot{w}_s = maximum side flow, lb/sec

F_a = axial force, lb

δ = maximum deflection angle, deg

I_{sps} = side specific impulse, sec = $I_{sp} K_A$

Table 4-2 shows design data for these valves.

The number of valves shown in parentheses is the total number of valves needed to provide the maximum gas flow in a quadrant. Once ignited, the

Table 4-2
WARM GAS AND HOT GAS VALVE DESIGN DATA

	Configuration I Warm Gas TVC		Configuration III Hot Gas TVC	
	First Stage	Second Stage	First Stage	Second Stage
Maximum flow rate per quadrant (lb/sec)	560	180	445	147
Flow rate per valve (lb/sec)	140	90	115	75
Number of valves per quadrant	2(4)	1(2)	4	2
Number of injectors per quadrant	4	2	4	2
Total number of valves	8	4	16	8

gas generators operate continuously, and the flow of gas is proportioned (from zero to maximum) to opposing quadrants of the nozzle. Therefore, even though there are two valves physically located in each quadrant, there are four injectors that can provide maximum flow.

4.2.4 Warm Gas Generator Design

Gas generators must provide flow rates adequate to meet the control requirements. Two methods of providing the necessary flow as a function of flight time are available: (1) size the generators to provide a continuous flow rate based on a peak control requirement or (2) tailor the flow rate to the maximum control demands that exist at any altitude. The second method was selected in order to minimize the size of the gas generator and this consequently rules out the use of an end burner.

Details of the gas generator sizing are shown in Appendix A. Solid-propellant gas generators were selected for use in both stages. The propellant is OMAX 453D with a density of 0.053 lb/cu in. Gas temperature is 2,000°F, and chamber pressure is 2,000 psia. The total propellant weight is 102,352 lb for the first stage and 8,790 lb for the second. Eight generators having a propellant weight of 12,794 lb were positioned in the aft skirt of the first stage and four with a propellant weight of 2,197 lb in the aft skirt of the second stage. Figure 3-14, Sheet 1, shows the general arrangement and shape of the generators. Each generator provides gas for one control valve. The size of the valve inlet from the gas generator to the valve of the warm gas system is of 8-in. -diam for the first stage and 7-in. -diam for the second. A low Mach number was used in the design to prevent the valve from burning up. The size of the duct from the valve to the injector of the warm gas system is 4-in. -diam for the first stage and 3-in. -diam for the second. The design of ducts required by this system is also shown in Appendix A.

4.3 LOCKSEAL ACTUATOR DESIGN

A hydraulic servo-actuator system was chosen to gimbal the nozzles because it has a number of advantages: (1) it has great power-carrying capability produced from a relatively compact unit; (2) for continuous operation, it

offers a minimum horsepower-to-weight ratio; (3) for intermittent operation, it produces large amounts of power from an accumulator with a minimum of storage volume. In addition to the design criteria established by flight environment (that is, maximum deflection angle duty cycle rate and accelerations), the hydraulic system is conservatively designed to sustain limit cycling. Servo-actuator leakage flows are also accounted for in the design.

Two linear, double-acting hydraulic actuators mounted 90° apart and attached to the nozzle and the aft dome of the motorcase are used to provide the gimbaling force. Sheet 2 of Figure 3-14 shows the installation of the complete system for both stages. One actuator controls movement in the pitch plane and the other in the yaw plane. Differential actuation of both actuators provides omnidirectional movement.

The vehicle's flight path is controlled by guidance signals sent to the hydraulic servo-valve to control actuator position. The servo-valve directs hydraulic flow to the appropriate side of the actuator piston when a change in actuator length is required, or it prevents flow to or from the actuator piston. The rate of flow is proportional to input current. The direction of flow is controlled by the sign of the guidance signal which changes direction of rotation of the servo-torque motor. The torque motor has two identical coils connected in parallel. The servo-valve's first stage, which is inherently the weakest part of the valve because of fluid contamination, has its reliability improved by operating three first-stage channels in parallel. If one channel fails, the two remaining channels overpower the defective channel permitting continuation of control. The servo-valve incorporates negative pressure feedback to increase damping at the load resonant frequency. Positive pressure feedback is used to eliminate steady-state actuator position errors caused by actuator and load compliant effects. Actuator piston position is mechanically fed back through a cam-actuated mechanism to a summing point in the servo-valve torque motor. Mechanical feedback is used in lieu of electrical feedback since it offers higher reliability. A linear piston position transducer is contained in each actuator for telemetry purposes. Figure 4-13 is a schematic of the hydraulic servo-actuator assembly. It applies to both the 260-in. -diam SRM and the 156-in. -diam SRM.

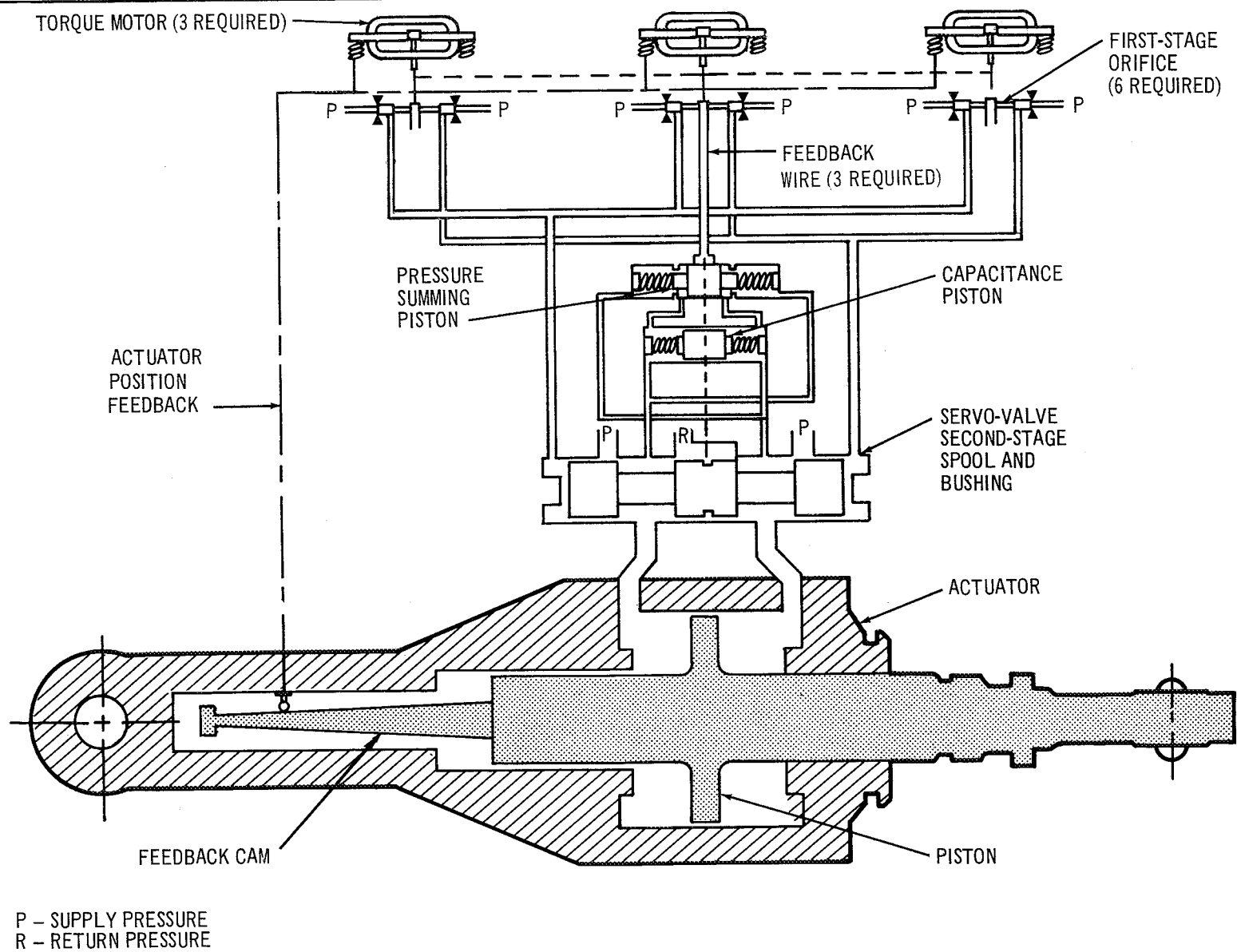


Figure 4-13. Schematic of Hydraulic Servo-Actuator Assembly

Once the main engine is fired, axial loads are applied to the Lockseal, which causes the seal to deflect. Actuator length at neutral is therefore adjusted to bring the engine to zero deflection under full thrust load.

4.3.1 Actuator Torques

The servo-actuators are sized to meet the maximum nozzle deflection, rate of movement, and nozzle acceleration required for vehicle stability. Required actuator area or force is determined through the consideration of the following torques acting on the nozzle.

4.3.1.1 Lockseal Spring Torque

Lockheed provided a Lockseal spring torque of 2,340,000 in.-lb developed at 3.5° of nozzle deflection for the 260-in.-diam SRM first stage. This torque is proportional to deflection if design deflection limits have not been exceeded; thus, for the first-stage deflection of 2.47° , the torque is 1,650,000 in.-lb. Data for the 156-in.-diam SRM second stage were obtained from Lockheed which showed spring torque as a function of thrust deflection and having a slope of 31,666 in.-lb/deg; thus, for a 6° deflection, second-stage Lockseal torque is 190,000 in.-lb.

4.3.1.2 Internal Aerodynamic Torque

An internal aerodynamic torque of 2,000,000 in.-lb developed at 3.5° of nozzle deflection was provided by Lockheed for the 260-in.-diam SRM first stage. This torque is assumed to be proportional to deflection; thus, at a deflection of 2.47° , the torque is 1,410,000 in.-lb. A 156-in.-diam SRM second stage torque of 51,000 in.-lb at 4° of deflection was converted similarly to 76,500 in.-lb for 6° of deflection.

4.3.1.3 Vehicle Axial Acceleration Torque

Axial acceleration produces a restoring torque which attempts to center the nozzle. The equation used to calculate this value for both stages is

$$T = R_{CG} \tan \delta \left(\frac{W_n}{g} \right) a$$

where

R_{CG} = distance from gimbal point to nozzle center of gravity

δ = nozzle deflection

W_n = nozzle weight

a = vehicle axial acceleration

The calculated values for both stages are

First stage, T_1 , = 485,000 in.-lb

Second stage, T_1 , = 65,700 in.-lb

4.3.1.4 Nozzle Acceleration Torque

A torque must be generated by the actuators to accelerate the nozzle mass at $\ddot{\theta}_{\max.} = 30^\circ/\text{sec}^2$ for the first stage and $200^\circ/\text{sec}^2$ for the second stage. The equation $T_2 = I \ddot{\theta}_{\max.}$ gives a torque of 2,020,000 in.-lb for the first stage and 510,000 in.-lb for the second.

4.3.1.5 Vehicle Lateral and Angular Acceleration Torque

Vehicle lateral and angular acceleration about its CG generates nozzle torques that assist the actuator forces. The first-stage torque equation resulting from vehicle angular acceleration is

$$T_3 = -(\ddot{\theta}_v L_{CG} \frac{W_n}{g} R_{CG})$$

The torque equation resulting from vehicle lateral acceleration is

$$T_4 = -\left(\frac{W}{g}\right) a_L R_{CG}$$

where

$\ddot{\theta}$ = vehicle angular acceleration

L_{CG} = distance from vehicle CG to nozzle CG

a_L = vehicle lateral acceleration

First and second stage values are

	<u>260-in. -diam SRM First Stage</u>	<u>156-in. -diam SRM Second Stage</u>
T_3	-217,000 in.-lb	-26,500 in.-lb
T_4	-825,000 in.-lb	-6,500 in.-lb

4.3.1.6 Nozzle Eccentricity Torque

Nozzle eccentricity is caused by the nozzle being offset from the centerline of the vehicle. Eccentricity torque is the product of a 0.88-in. moment arm, ℓ , and a force of 40% of generated thrust which is the approximate load acting on the nozzle case. The equation $T_5 = 0.4 F_a \ell$ gives a torque of 1,710,000 in.-lb for the first stage and 192,000 in.-lb for the second.

The maximum torque the hydraulic actuator must deliver is the sum of these torques; therefore, at 2.47° of nozzle deflection, first-stage maximum torque = 6,233,000 in.-lb and second-stage torque, at 6.0° nozzle deflection, is 1,001,300 in.-lb. For a safety factor, the actuators are sized to deliver 1.2 times this torque. Table 4-3 show actuator and servo valve design data.

Table 4-3

LOCKSEAL ACTUATOR AND SERVO-VALVE DESIGN DATA

Items	Configuration II	
	260-in. -diam SRM	156-in. -diam SRM
Actuator		
Maximum required actuator torque (in. -lb)	6, 233, 000	1, 001, 300
Actuator moment arm (in.)	90	50
Actuator stroke (in.)	7. 74	10. 51
Actuator area (sq in.)	59. 5	12
Hydraulic supply press (lb/sq in.)	1, 800	3, 000
Hydraulic return press (lb/sq in.)	200	200
Maximum required actuator load (lb)	69, 300	20, 026
Maximum actuator stall load (lb)	95, 250	33, 600
Number servo-actuators	2	2
Servo Valve		
Servo-torque motor rated current (mA)	50	50
Servo-torque motor input impedance (ohms)	100	100
Servo-valve torque limit, $T_{e \text{ lim}}$ (in. -lb)	0. 0646	0. 0205
Servo-valve torque motor gain, K_{vt} (in. -lb/mA)	0. 050	0. 050
Servo-valve flow gain, K_{vz} ($\frac{\text{cu in. /sec}}{\text{in. -lb}}$)	10, 810	7, 660
Actuator piston feedback gain, K_{fb} (in. -lb/in.)	0. 617	0. 428

The following equations were used to obtain servo valve design data:

$$T_{e \text{ lim}} = I_c K_{vt}$$

$$K_{v2} = \frac{\omega_p A}{K_{fb}}$$

$$K_{fb} = \frac{0.9 I_{c \text{ max}} K_{vt}}{X_{p \text{ max}}}$$

where

I_c = servo input signal

ω_p = position open-loop gain

A = actuator piston area

X_p = actuator piston position

4.4 LOCKSEAL HYDRAULIC POWER SYSTEMS

Hydraulic power systems were developed for both stages of Configuration II to supply the high-pressure fluid needed to move the actuators. Each system design supplies fluid at rates that meet stage-control demands, possible limit cycling, and actuator leakage. Figure 4-14 presents the hydraulic flow requirements during maximum-demand condition which occurs at peak winds for the first stage. Maximum hydraulic-energy requirements for the second stage occurs over a relatively short interval of time, approximately 2 sec, during stage separation. Figure 4-15 shows the flow requirements.

4.4.1 Power System Flow Requirements

Leakage flows are estimates, and based on Saturn S-IC actuator-design flow and leakage rates. Limit cycle flow is calculated from the equation

$$Q_{lc} = 0.637 (A)(D)(\pi)(f)(N)$$

where 0.637 = the average area under a sinusoidal curve.

A = Actuator piston area

D = Actuator stroke (peak to peak)

f = Actuator cycling rate

N = Number of actuators

Duty cycle flows are calculated from stability and control duty cycle requirements in Figures 3-24 and 3-31 using the equation

$$Q_{dc} = 1.414 A \dot{X}_p$$

where

$$\dot{X}_p = \text{actuator piston velocity}$$

Maximum flow requirements for both stages are shown in Table 4-4.

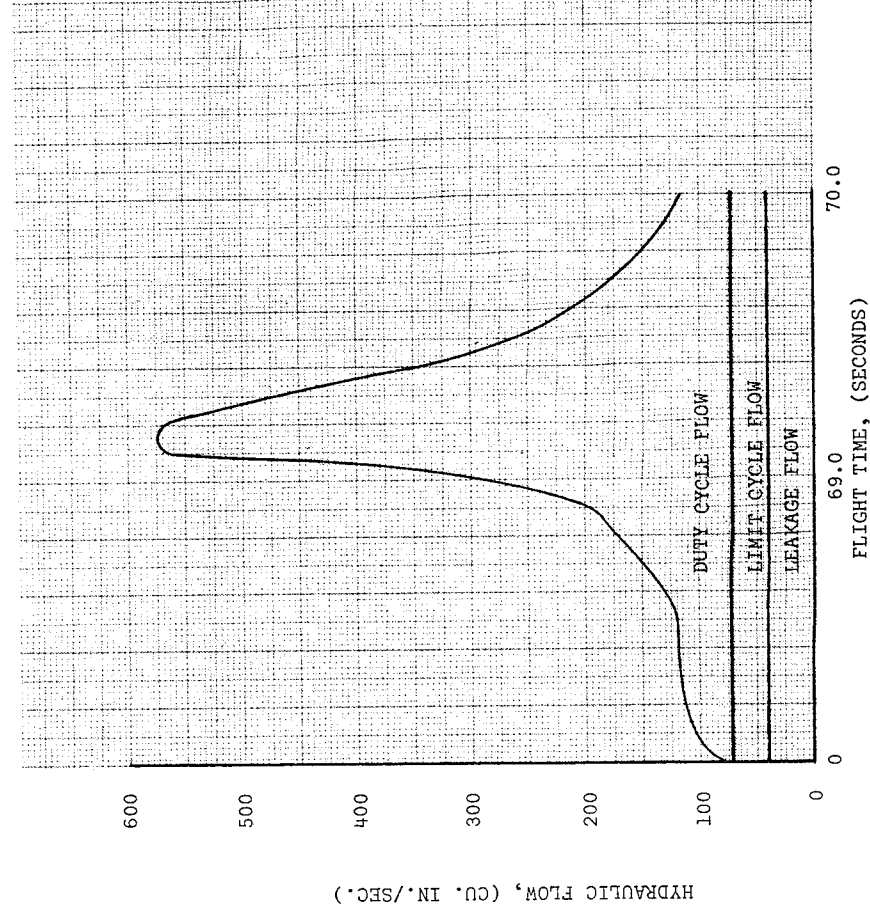


Figure 4-14. Hydraulic Flow Requirements for Lockseal Gimbal
Design - 260-in.-Diam SRM First Stage

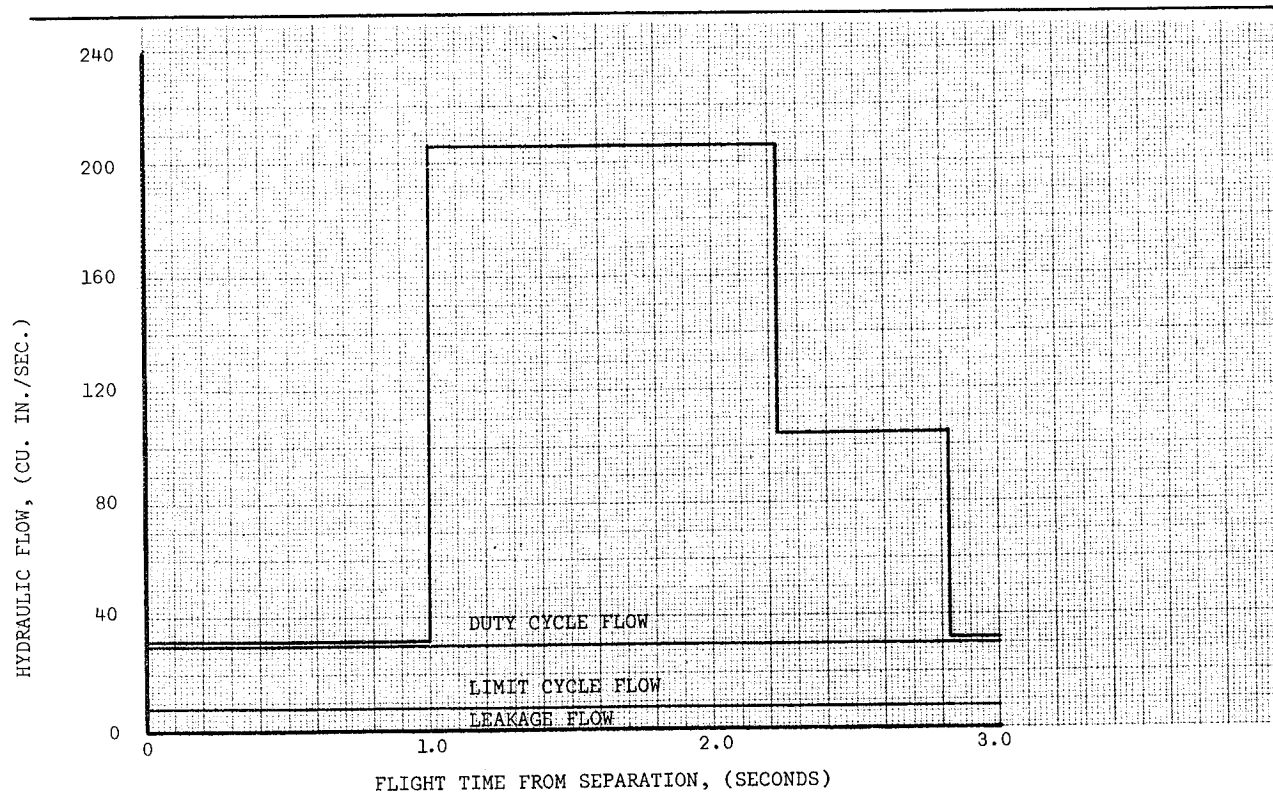


Figure 4-15. Hydraulic Flow Requirements for Lockseal Gimbal Design – 156-in.-Diam Second Stage

Table 4-4
MAXIMUM FLOW RATES REQUIRED

Item	260-in. -diam First Stage	156-in. -diam Second Stage
Actuator leakage	41 cu in. /sec	8 cu in. /sec
Limit cycling	31 cu in. /sec	22 cu in. /sec
Duty cycle	500 cu in. /sec	176 cu in. /sec
Total	572 cu in. /sec	206 cu in. /sec

4.4.2 Power Unit Designs

Two Nike Zeus hydraulic-power units manifolded together, as seen in Figure 4-16, are used for first-stage power. A complete unit consists of a solid-propellant gas generator, dual-igniter squibs, gas turbine, burn-rate control valve, gearbox, fixed-displacement hydraulic pump, check valves, filter, accumulator, reservoir, and pressure-regulating and relief valve. Dual squibs ignite the solid propellant in the gas generator. The burn-rate control valve controls the hot gas flowing from the generator to the gas turbine. The turbine drives a fixed-displacement hydraulic pump through a speed-reduction gearbox. The pressurized hydraulic fluid passes through a check valve and filter into a high pressure accumulator. Excess flow is returned to the low-pressure side of the system through a relief valve. A pressure-regulating valve regulates the hydraulic pressure delivered to the servo-actuators. A reservoir is used to obtain system inlet pressure and to store hydraulic fluid. An ac-motor-driven pump using ground power only is used for hydraulic system tests and for initial filling of the accumulators during launch operations. Use of this on-board power supply for tests during launch operations minimizes the possibility of contamination of the hydraulic system.

One Zeus power unit with a flow of 85 cu in. /sec exceeds average requirements, but the large duty-cycle flow of 500 cu in. /sec requires the use of accumulators to handle the increased flow demands. For redundancy, two complete Zeus power units are used connected in parallel. Their turbine-driven fixed-displacement pumps charge the accumulators to 3,800 psig with a total oil volume of 520 cu in. A pressure-regulating valve regulates the hydraulic pressure delivered to the servo-actuators to between 1,600 and 1,800 psig. The burn-time of the gas generators is extended to 166 sec minimum, providing 160 sec for the duty cycle and 6 sec for checkout prior to firing of the main motor.

For ground servicing, a 60 cu in. /sec ac-motor pump is used to supply actuator leakage, and it will fill the accumulators in 28 sec. Ground checkout transient response tests of the hydraulic control system depends mainly on the accumulators for fluid flow.

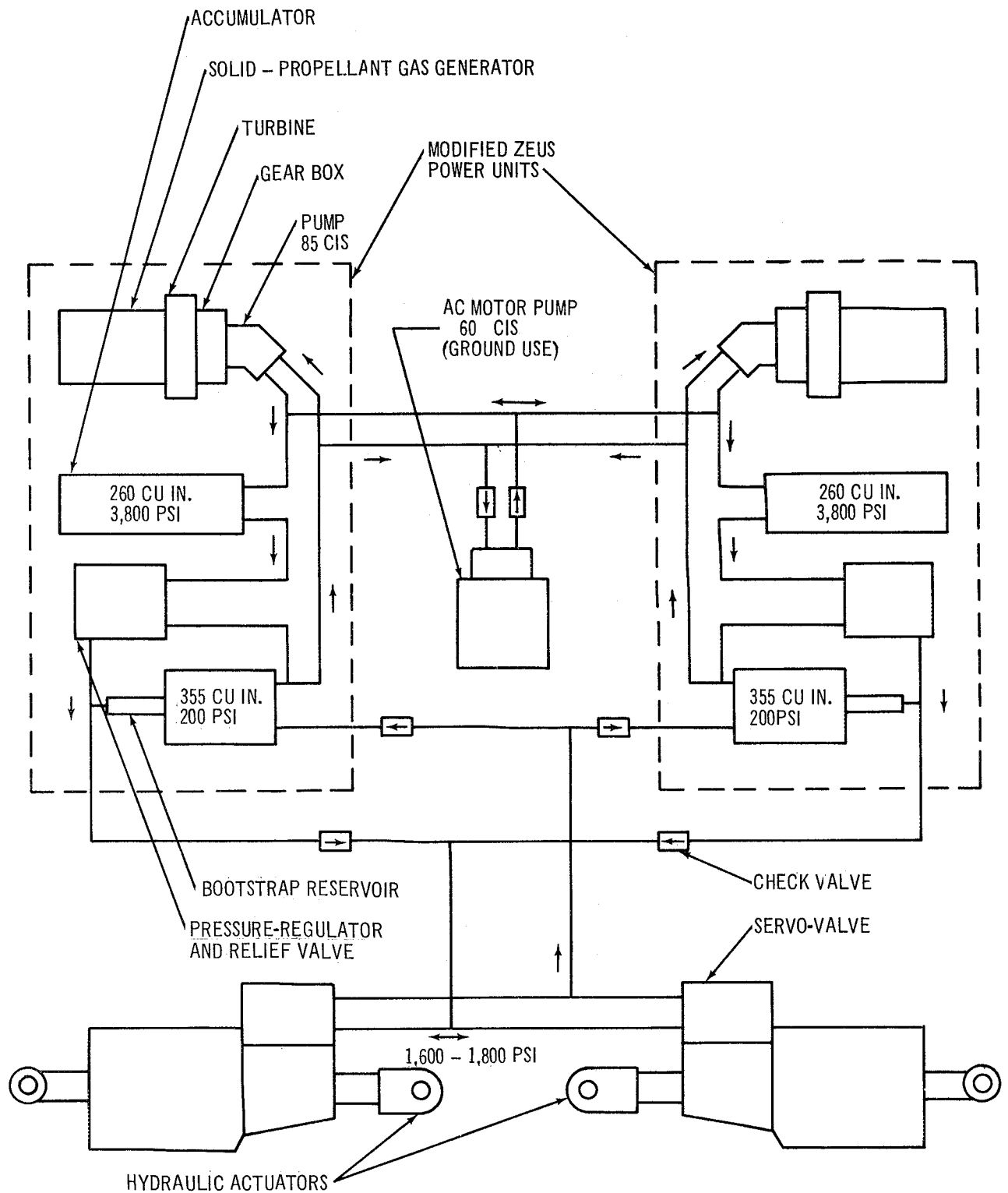


Figure 4-16. First-Stage Hydraulic Power System Schematic

The hydraulic power system for the second stage is a 3,000-psi closed-loop system consisting of two variable-delivery hydraulic pumps operating in parallel, each driven by a dc compound-wound motor, an accumulator-reservoir assembly, and a manifold assembly which contains the main supply filter, necessary check valves, relief valves, and ground service disconnects. Figure 4-17 is a schematic of the hydraulic power system.

An accumulator is used to store hydraulic fluid under pressure and is sized to have sufficient energy in reserve to supply the peak demands with only one of the two system pumps in operation. The accumulator is recharged by the hydraulic pumps after the separation transients have subsided. The accumulator-reservoir is a typical S-IVB design which incorporates a chamber pressurized with gas at 2,000 psi to precharge the hydraulic system. Variable-delivery pumps are used to minimize energy consumption over a major portion of the flight since maximum pump output is only required over a short interval of time. Pump output is controlled by means of rotating a valve plate to vary pump delivery. The valve plate is positioned by an actuator piston which is controlled by sensing the differential pressure across the pump. To obtain high starting torque and good speed regulation, series and shunt fields are used in the dc-motor design.

In flight, silver-zinc batteries furnish the dc-pump power requirements. For system checkout during prelaunch operations, the motor pump receives its electrical power from ground service. This eliminates opening the hydraulic system to connect a ground power unit since the flight hydraulic power unit is used for system checkout. This feature significantly reduces the probability of system contamination present in a system requiring circulation through the GSE; furthermore, these conditions more nearly simulate the flight configuration.

4.5 THIOKOL HOT GAS TVC ACTUATOR DESIGN

The hot gas pintle is hydraulically positioned and controlled by a servo-actuator which is in line with the pintle valve. The actuator cylinder is an integral part of the pintle which is inside the motor plenum chamber. The telemetry transducer, feedback cam, and servo-valve are mounted outside

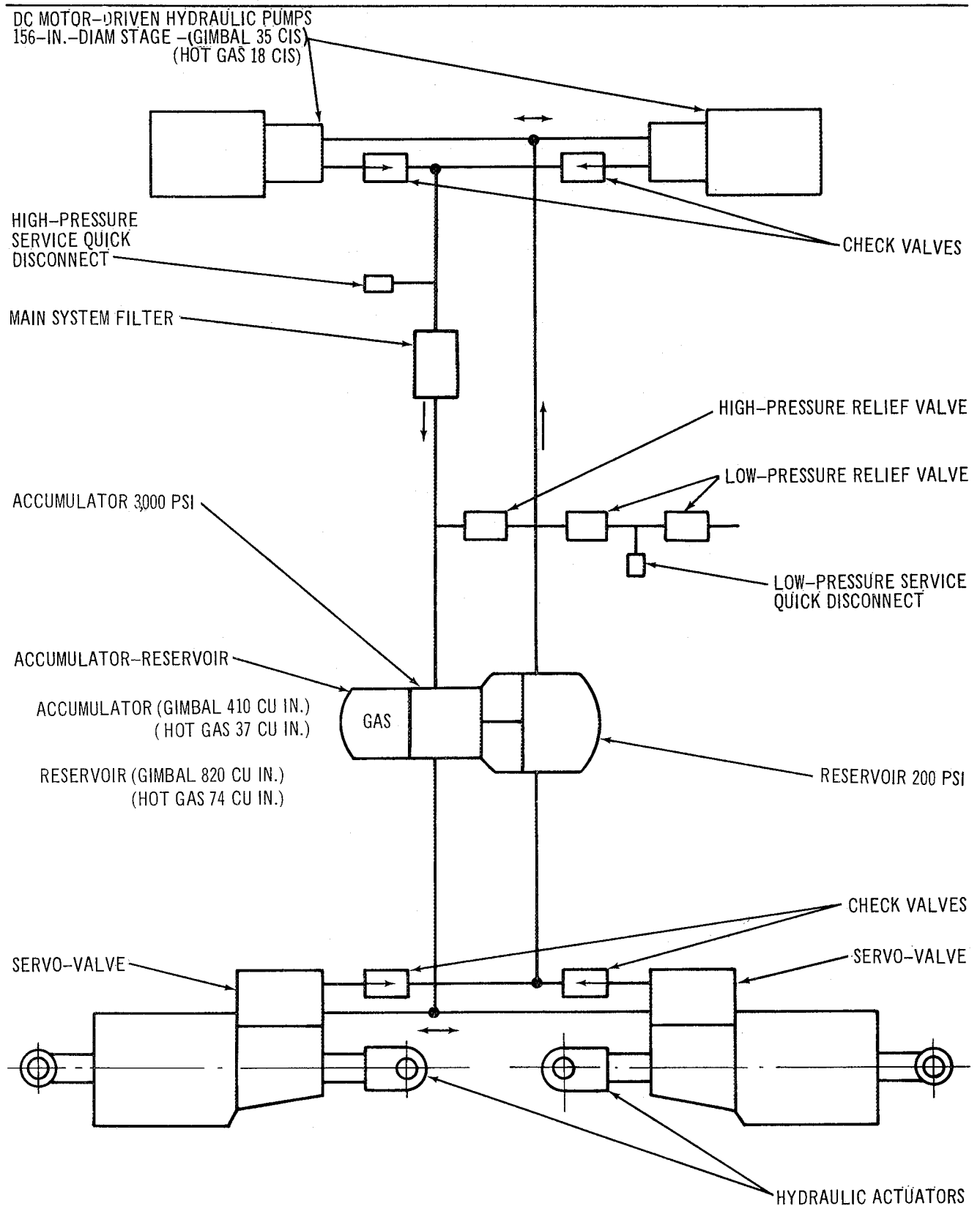


Figure 4-17. Second-Stage Hydraulic Power System Schematic

the plenum chamber in the ambient environment where these components can be easily maintained during ground checkout.

All valves in a nozzle quadrant respond simultaneously to guidance signals for TVC. When a change in pintle position is required, these signals position the servo-valve spool to direct hydraulic fluid to the appropriate side of the actuator piston. Pintle position is fed back mechanically through a cam-actuated mechanism to a summing point in the servo-valve torque motor. Mechanical feedback is used in place of electrical feedback since it offers higher reliability. A linear piston position transducer is contained in each actuator for telemetry purposes. Figure 4-18 is a schematic of the hydraulic servo-actuator pintle assembly, and design data are presented in Table 4-5. The forces necessary to operate the valves for each stage were obtained from Thiokol.

4.6 THIOKOL HOT GAS VALVE POWER SYSTEMS

Power system designs for both stages of Configuration III are similar to those used for the gimballed nozzle TVC systems. Since the forces necessary to

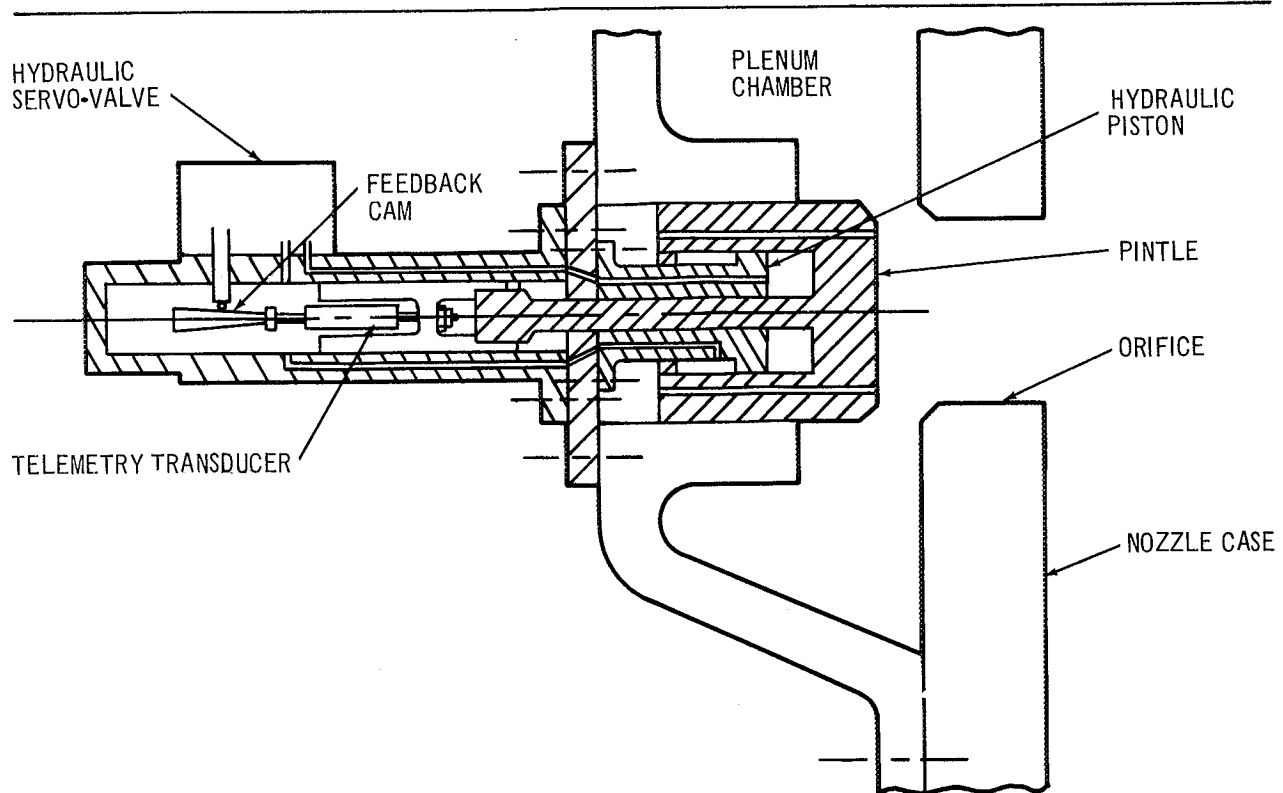


Figure 4-18. Hydraulic Servo-Actuator Hot-Gas Pintle Assembly

Table 4-5
THIOKOL HOT GAS TVC SERVO-ACTUATOR DESIGN DATA

Items	Configuration III	
	260-in. -diam First Stage	156-in. -diam Second Stage
Secondary injection pintle diameter (in.)	6.8	5.4
Secondary injection orifice diameter (in.)	6.0	4.8
Actuator data		
Actuator stroke (in.)	1.575	1.125
Actuator area (sq in.)	5.6	2.7
Hydraulic supply press (lb/sq in.)	1,800	3,000
Hydraulic return press (lb/sq in.)	200	200
Maximum actuator stall load (lb)	8,960	7,560
Number of servo-actuators	16	8
Servo data		
Servo-torque motor rated current (mA)	50	50
Servo-torque motor input impedance (ohms)	100	100
Servo-valve torque limit (in. -lb)	0.076	0.0205
Servo-valve torque motor gain (in. -lb/mA)	0.050	0.050
Servo-valve flow gain ($\frac{\text{cu in. /sec}}{\text{in. -lb}}$)	413	370
Actuator piston feedback gain (in. -lb/in.)	1.43	2.00

move the actuators are much lower than those of the gimballed nozzle TVC system, the flow rates to actuate the hot gas pintle are much lower. Figures 4-19 and 4-20 show flow rate requirements for both stages during the period of maximum fluid demand. The system leakage flow appears large when compared to the gimballed nozzle values, but there are 16 actuators in the first stage and 8 in the second, each incorporating a triple-redundant, first-stage servo-valve of the same size as that used in the gimballed nozzle design. Table 4-6 shows the maximum flow requirements for both stages of the launch vehicle.

One Zeus power unit is adequate to furnish the first-stage flow demands; however, for redundancy, two complete units are used in parallel. The accumulator reservoir is reduced to 1/4 of that used for the gimbal nozzle design.

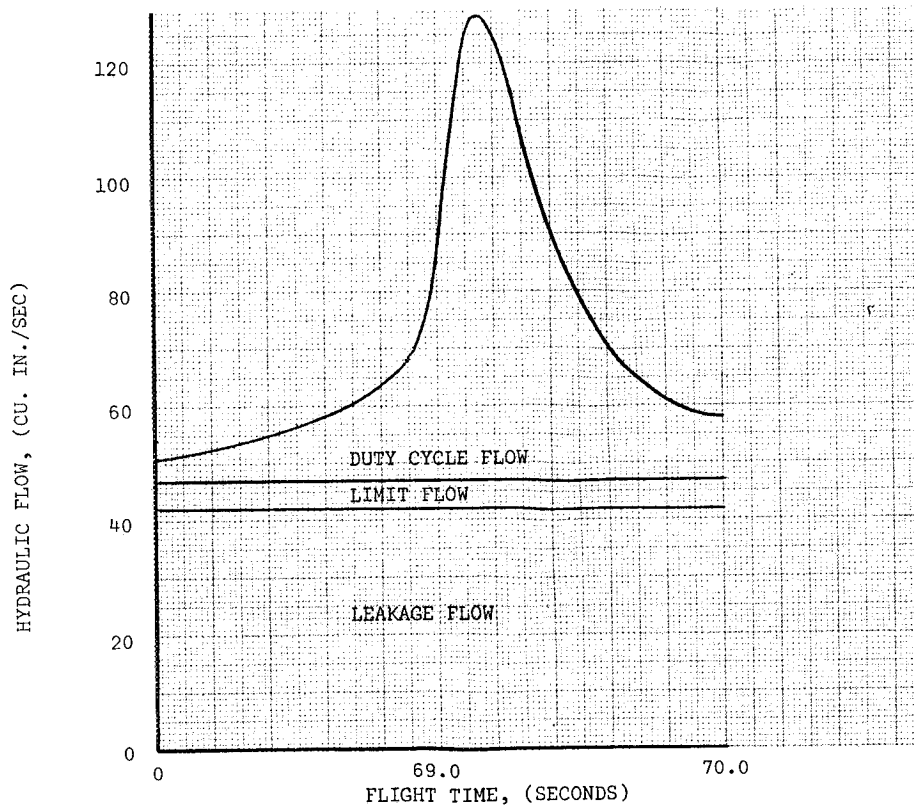


Figure 4-19. Hydraulic Flow Requirements for Thiokol Hot Gas Design – 260-in.-Diam SRM First Stage

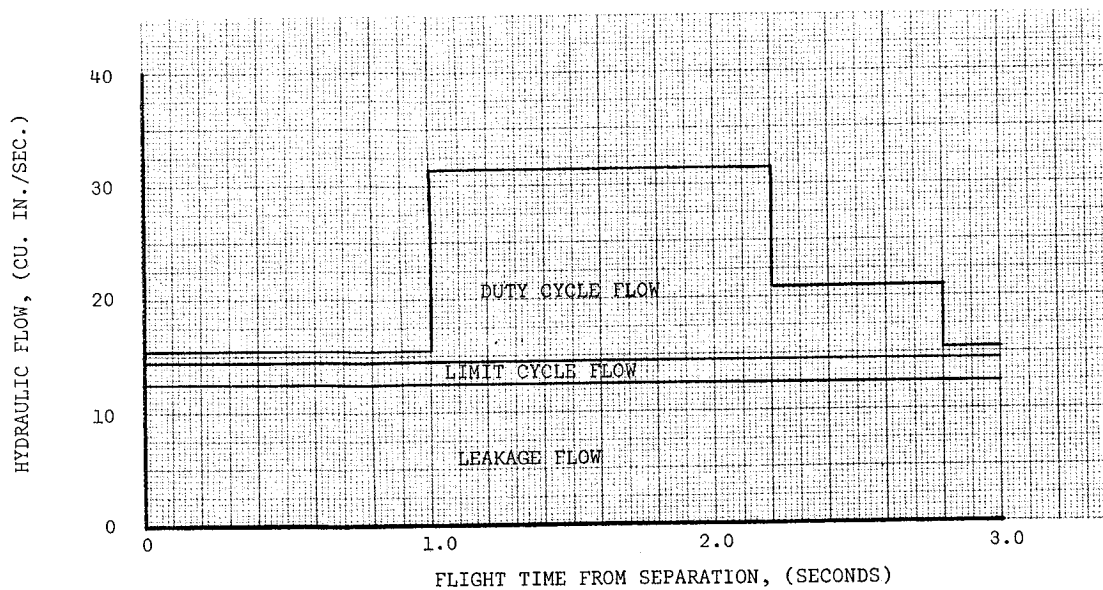


Figure 4-20. Hydraulic Flow Requirements for Thiokol Hot Gas Design 156-in.-Diam SRM Second Stage

Table 4-6
MAXIMUM FLOW RATES REQUIRED

Items	Configuration III	
	260-in. -diam First Stage	156-in. -diam Second Stage
Actuator leakage	42 cu in. /sec	12.5 cu in. /sec
Limit cycling	5 cu in. /sec	2.0 cu in. /sec
Duty cycle	77 cu in. /sec	17.0 cu in. /sec
Total	124 cu in. /sec	31.5 cu in. /sec

An 8.2-hp pump with a fluid flow capability of 18 cu in. /sec is used in the second stage to provide leakage and limit cycling flow. Two pumps operating in parallel are installed to increase reliability. An accumulator is installed in the system to handle peak flow demands.

4.7 VICKERS WARM GAS PNEUMATIC VALVE

Pneumatic control valves, installed in the outlet of the gas generators, are used to proportion the mass of warm gas (2,000°F) flowing through the injection orifices which are located in the main nozzle downstream of the throat. An electrical command signal to the pneumatic control valve positions an open center spool to provide a proportional modulation of the gas flow to two injection nozzles. A null input signal to the servo results in evenly splitting the continuously flowing gas from the generator to each injector. An off-null signal causes the spool to move increasing the gas flow to one injector and decreasing the gas flow to the opposing injector. At the maximum signal, one side of the valve is completely closed, and the total gas flow is ported to only one injector, causing maximum deflection of the thrust vector. A torque motor responds to resultant electrical command and feedback signals to position a yoke-type flapper. The feedback torque is proportional to the output pressures of the pneumatic valve. To obtain a proportional output from the control valve, pneumatic rate is incorporated in

the main stage. The output pressure differential is applied across the main spool resulting in a force balance on the spool creating a positive pneumatic spring rate. Four 140 lb/sec valves are used per control axis in the first stage and two 90 lb/sec valves are used in the second stage. Each control valve receives gas from its own generator and controls the gas flowing to opposing injection orifices. Figures 4-21 and 4-22 show the general piping arrangement between the injectors and the pneumatic control valves. The 16 first-stage injection orifices are located $22\text{-}1/2^\circ$ apart around the circumference of the nozzle. The 8 second-stage injection orifices are spaced 45° .

4.8 TVC SYSTEM WEIGHT

Table 4-7 is a detailed weight summary of the hot gas TVC system for both the 156-in. -diam and the 260-in. -diam stages. Table 4-8 is the weight summary for the warm gas TVC system, and Table 4-9 is the weight summary for the gimbal nozzle TVC system.

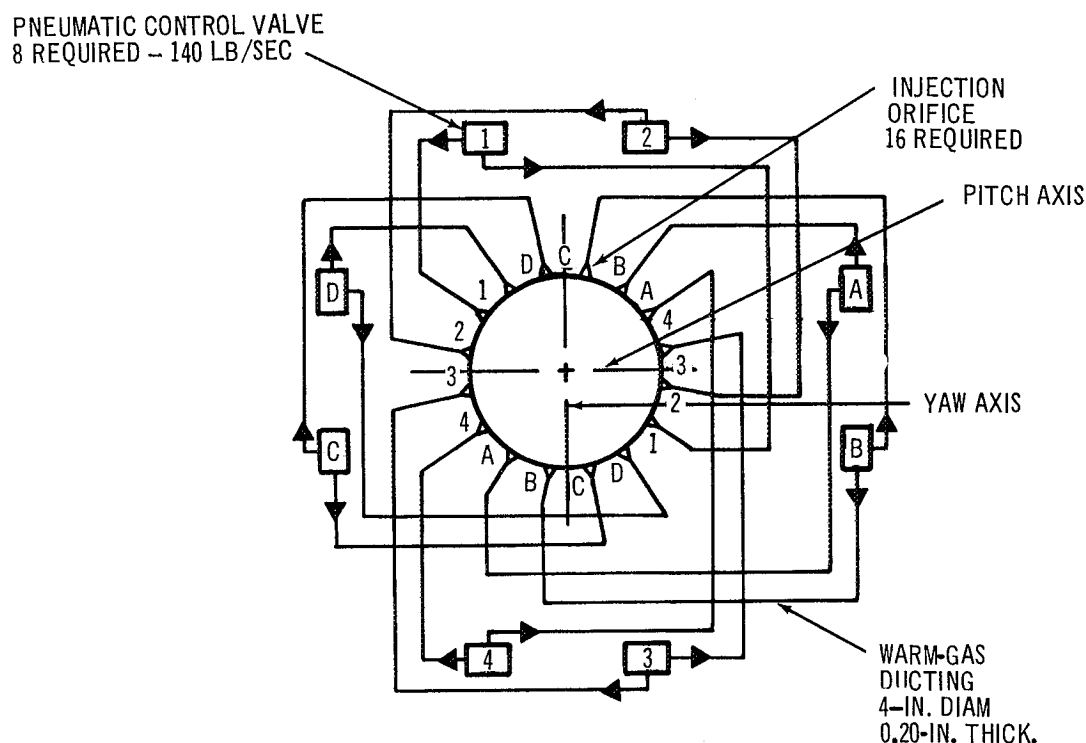


Figure 4-21. Warm Gas Ducting for the 260-in.-Diam SRM First Stage

PNEUMATIC CONTROL VALVE
4 REQUIRED - 90 LB/SEC

INJECTION
ORIFICE
8 REQUIRED

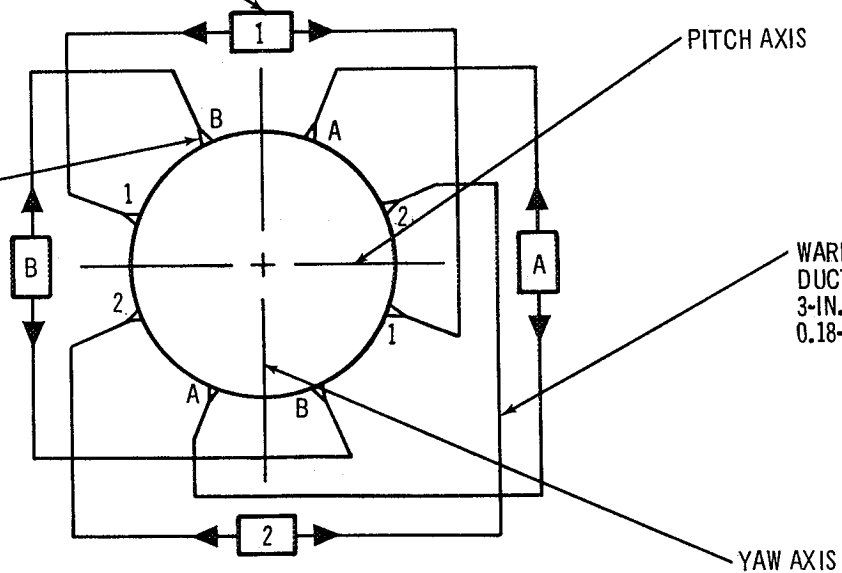


Figure 4-22. Warm Gas Ducting for the 156-in.-Diam SRM Second Stage

Table 4-7
HOT GAS TVC SYSTEM WEIGHT SUMMARY (LB)

Items	260-in. -diam	156-in. -diam
Zeus power unit	282	NA
Servo-actuators (8)	1,680	720
Orifices (8)	528	180
Plenum chamber	3,000	600
AC pump and motor	92	73
Battery	NA	65
Accumulator	NA	26
Fittings and mounts	<u>226</u>	<u>91</u>
Total system weight	5,808	1,755
Allocation of main propellant	25,220	3,135

Table 4-8
WARM GAS TVC SYSTEM WEIGHT SUMMARY (LB)

Items	260-in. -diam	156-in. -diam
Propellant containers and insulation	24,960	1,624
Control valves	12,800	2,560
Ducting	1,600	296
Orifices	607	240
Fittings and mounts	14,312	780
Total system weight	54,279	5,500
Propellant loaded	102,352	8,788

Table 4-9
LOCKSEAL TVC SYSTEM WEIGHT SUMMARY (LB)

Items	260-in. -diam	156-in. -diam
Lockseal assembly	5,949	463
Zeus power package (2)	400	NA
Electric pump	NA	142
Ground power pump (2)	101	NA
Accumulator reservoir	NA	282
Actuator	660	156
Actuator support	200	
Hydraulic fluid	74	52
Battery	NA	120
Hydraulic line mounts and fittings	116	58
Total system weight	7,500	1,273

4.9 ELECTRONIC DESIGN

A multistaged, solid-fueled, launch vehicle requires an instrumentation unit (IU) to provide navigation, guidance and control signals, data transmission between vehicle and ground stations, tracking, checkout and monitoring of vehicle functions in orbit, and detection of emergency situations. The IU described herein is identical to that used on the Saturn V with modifications required to permit full operation of the two-stage solid-fueled launch vehicle; it can be a separate unit or a stage-integrated unit. It contains an inertial platform assembly, a launch-vehicle digital computer (LVDC), a launch-vehicle data adapter (LVDA), and a flight-control computer and rate gyros. The launch-vehicle digital computer performs computations for navigation, guidance, and control functions. The position and velocity of the vehicle is obtained by means of combining accelerometer measurements with computed gravitational acceleration. This information is the input to the guidance computations which determine the required TVC orientation and engine cutoff time according to the guidance scheme stored in the memory of the LVDC. The inertial platform assembly provides the inertial reference coordinates, integrated acceleration data, and vehicle attitude measurements with respect to those coordinates for navigation, guidance, and control of launch vehicles.

Control of the launch vehicle can be divided into two categories, attitude control and discrete control functions. For attitude control, the instantaneous attitude of the vehicle is compared with the desired vehicle attitude. This comparison is done in the LVDC. Attitude correction signals are derived from the difference between the existing attitude angles (gimbal angles) and the desired attitude angles. In the flight control computer, these attitude correction signals are combined with signals from control sensors (rate gyros) to generate the pitch, yaw, and roll-control commands for the engine actuator or TVC control servo-valves. Commands for all discrete control functions are generated in the LVDC according to a stored program. These commands are transferred to the switch selector of the

corresponding vehicle stage. The switch selector in the addressed stage activates the necessary circuits to perform such commanded functions as engine ignition, cutoff, and stage separation. The operation of all attitude-control functions requiring analog parameters is assigned to the flight control computer. All discrete-control functions of each stage are assigned to the switch selectors of each stage. Analog devices such as hydraulic actuators are dependent upon the analog error signals generated in the flight control computer to operate, whereas the turning on and off of the roll control engines of the 260-in. -diam solid stage requires a discrete voltage level input supplied by a switch selector.

Each vehicle stage is equipped with a measuring and telemetry system, including RF transmitters and antennas. For efficient utilization of available bandwidth and to obtain the required accuracy, three different modulation techniques are used in each stage telemetry system. These three are frequency modulation/frequency modulation (FM/FM), pulse code modulation/frequency modulation (PCM/FM), and single sideband/frequency modulation (SSB/FM). SSB/FM is employed in research and development flights only. The PCM/FM telemetry data of the 156-in. -diam stage and the IU are interconnected to provide a redundant transmission path and to make the 156-in. -diam stage measurements available to the LVDA. Telemetry data are transmitted from the vehicle to ground in the VHF band. All flight control data are transmitted through the PCM system. The IU command system permits data transmission from the ground stations to the IU for insertion into the LVDA.

As in the Saturn IB vehicle, the offset Doppler tracking system (ODOP) is located in the first stage, thereby providing data immediately following lift-off while other tracking systems cannot "see" the vehicle or their accuracy is reduced by multipath preparation during the early phase of the flight. The IU is equipped with two C-band radar transponders, an AZUSA transponder, and an S-band tracking system.

An emergency detection system collects special measurements from each stage of the launch vehicle. On the basis of these measurements, critical

states of the vehicle which may require mission abort are detected and, depending upon the criticality factor, the initiation of automatic abort.

The flight-vehicle electronic systems for each stage is based on design concepts of equipment proven on the S-IVB vehicle. Each electronic subsystem of the S-IVB has been evaluated and modified as required to operate the candidate TVC systems and acquire and transmit data pertaining to their performance to Earth for detailed evaluation and analysis. The electronics systems of each stage consists of (1) a measuring and telemetry system, (2) a switch selector/sequencer unit, power supply, and power distribution system. The measuring subsystem acquires and performs all signal conditioning required to adequately prepare the vehicle sensor data for data transmission to ground stations through the telemetry system. The power-supply systems used on each stage consists of silver-zinc batteries identical to those used on all Saturn V vehicles. These were selected because of their proven high reliability and efficiency. The power-distribution system is designed around the Saturn S-IVB/IB configuration with modifications as required to operate the given electronic/electrical system. The electronic systems required to operate each TVC system is described in the following pages of this report.

4.9.1 Lockseal TVC System

Pitch and yaw commands for the Lockseal TVC system actuators are provided by the flight-control computer of the IU. Servo-amplifiers within the flight-control computer govern the position of the main-engine actuators by controlling the position of the servo-valve. In the 260-in. -diam SRM (Figure 4-23), a single servo-amplifier is required for each engine actuator on the stage (that is, one pitch servo-amplifier and one yaw servo-amplifier). The three yaw output control signals ($\psi_Y \phi_Y \gamma_Y$) to the flight-control computer are fed into the yaw amplifier. Correspondingly, the three pitch channels are connected to the pitch amplifier. The two roll input signals (ψ_R and ϕ_R) are sent to the roll-control actuator servo-amplifier.

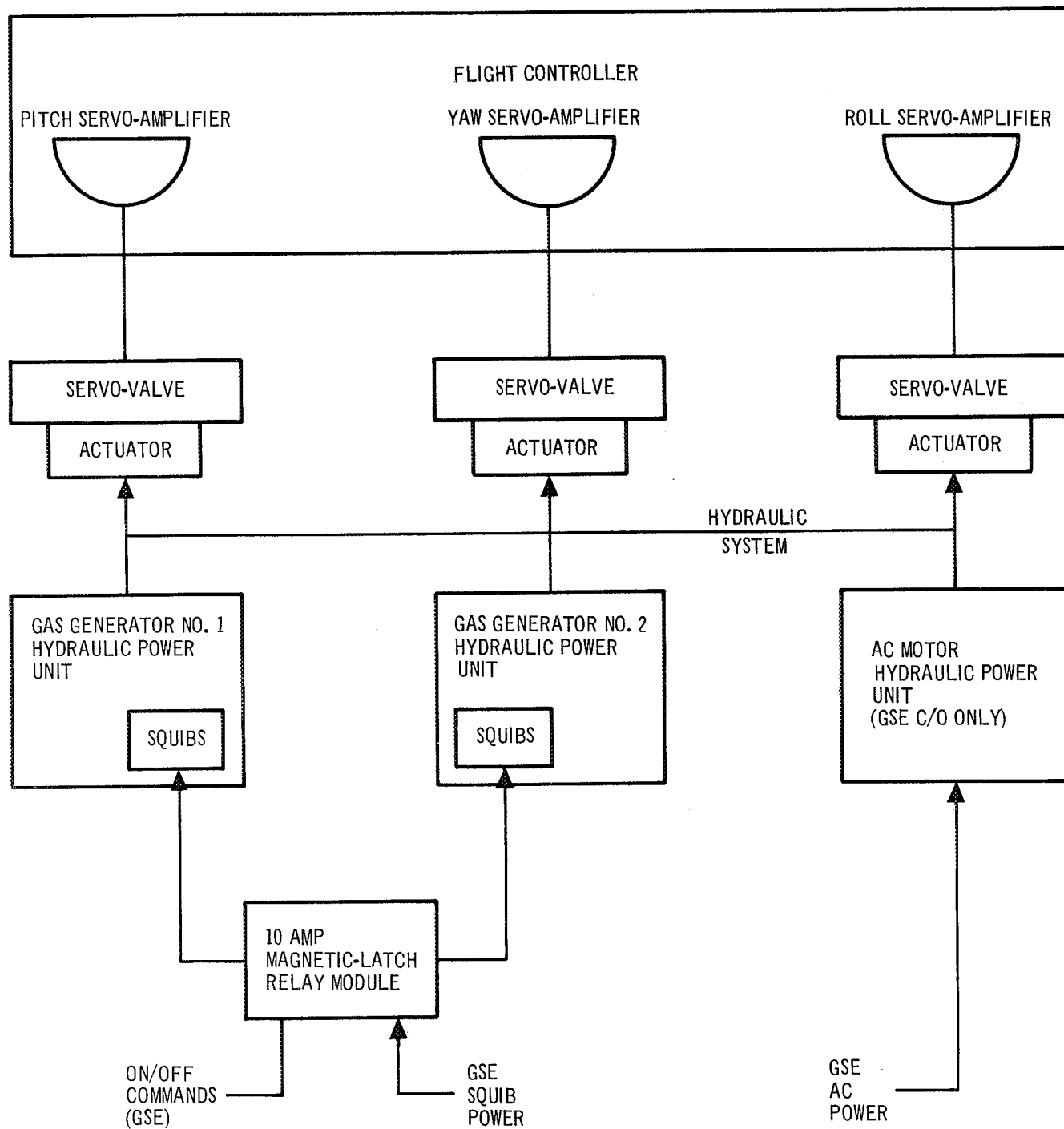


Figure 4-23. Lockseal Control System – 260-in.-Diam SRM

On the 156-in. -diam SRM Lockseal TVC system (Figure 4-24), the 6 servo-amplifiers of the pitch and yaw control system are used in a triple-redundant configuration to control the two servo-actuators of the main-engine nozzle. This scheme was selected because of its proven capability and reliability on the S-IVB. In this scheme, the output signals of two yaw servo-amplifiers are compared and if they agree, one is used to control the servo-actuator. If these two signals disagree, the output of the third yaw servo-amplifier is switched to the actuator. The same scheme applies to the pitch channel.

In both the 260-in. - and 156-in. -diam stages, each amplifier provides a maximum output current of 50 mA to the motor-operated control valves of the actuators.

4.9.2 Hot-Gas--Thiokol TVC System

Electrical control of the 16 hot gas TVC servo-valves of the 260-in. -diam SRM is provided by 8 push-pull amplifiers in the flight-control computer, and a group of 4 valves are driven by a pair of push-pull amplifiers as shown in Figure 4-25. This system was selected to provide redundancy in the event one amplifier fails. In the 156-in. -diam SRM, the 8 TVC servo-valves are driven by 4 push-pull amplifiers. As in the 260-in. -diam stage, each amplifier drives 2 servo-valves. The diode array on the output of the amplifiers provides a method whereby positive current will be input to only (+) pitch servo-valves. This will ensure that any faults in the servo-valves on the (+) side will not affect the negative side, and vice versa. On the hot gas TVC system, the amplifiers drive the servo-valves in one quadrant or the other, but never both sets, whereas the Lockseal amplifiers drive each servo-valve from one extreme to the other.

Controls to the 2 roll-control engines on the 260-in. -diam stage is provided from a single servo-amplifier dividing the 2 servo-control valves of the roll-control actuators. When the servo-amplifiers outputs a positive roll signal, both servo-control valves will move their actuators into the + roll plane. In the 156-in. -diam stage, roll control is identical to that of the S-IVB, with the flight-control computer roll-control amplifier operating the S-IVB APS relay package. Gating of all gases for roll control is under full disciplines of the stage switch selectors.

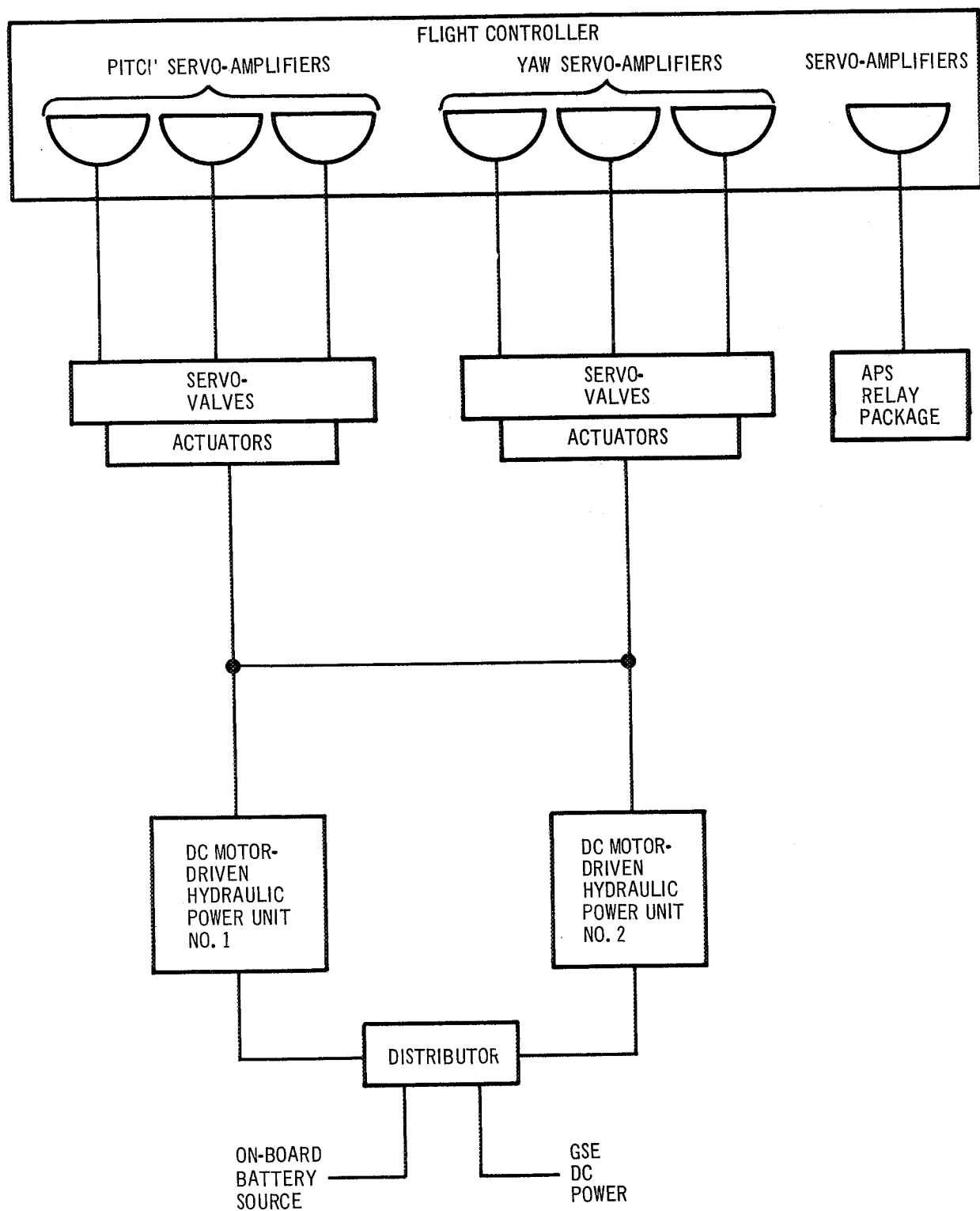


Figure 4-24. Lockseal Control System – 156-in.-Diam SRM

The diagram illustrates the hydraulic control system for the pitch actuator. It consists of five P Amplifiers and one Roll Amplifier, each connected to a network of servo-valves. The first four amplifiers control Pitch Actuators 1 through 4, each with positive and negative lines. The fifth amplifier controls a Roll Actuator with two lines. The servo-valves are represented by rectangular blocks with internal valve symbols.

- (1) ALL 4^+ PITCH ACTUATORS ARE LOCATED IN A GROUP IN 1 QUADRANT.
- (2) ALL 4^- PITCH ACTUATORS ARE LOCATED 180° FROM THE $+$ PITCH ACTUATORS.
- (3) THE YAW PITCH ACTUATOR-AMPLIFIER SYSTEM IS IDENTICAL TO THE PITCH SYSTEM

4-40

4.9.3 Warm Gas TVC

In the 260-in. -diam SRM warm gas TVC electronic control system (Figure 4-26), torque motors for a pair of pneumatic valves is driven by an amplifier. Two of the four provide pitch attitude control signals, and the other two amplifiers provide yaw-control signals. By inserting a positive error signal to the torque motor, the valve spool will be moved to the positive error end of the valve in direct relationship to the amount of current output by the amplifier.

The 156-in. -diam SRM warm gas TVC electronic system (Figure 4-27), operates identically to the 260-in. -diam stage. Each of the pneumatic valves is driven by an electronic amplifier on the 156-in. -diam stage.

Roll control for the 260-in. -diam SRM warm gas system is provided by a single servo-amplifier driving the two roll-control servo-valves. The on-off function required of these continuous burn engines is provided by the stage switch selector unit. In the 156-in. -diam stage, roll control is provided by a single amplifier in the flight-control computer driving two S-IVB APS units. The roll-control system for the 156-in. -diam stage is identical in all three TVC schemes. These APS units may be operated on a demand basis only or in a continuous operation mode providing + roll, - roll, or propulsive modes of operation throughout the powered flight of that stage.

To monitor and evaluate the critical parameters of the stage by ground mission control, each stage is equipped with a measuring and telemetry system including transmitters and antennas. All flight data is transmitted to ground through the pulse coded modulated/frequency modulated (PCM/FM) telemetry system. The PCM/FM telemetry system will be utilized to transmit such data as that pertaining to the operation of the stage TVC system, roll control, and so forth.

4.9.4 Power Profile

An analysis of the power systems of each of the three candidate TVC systems for each stage is described below.

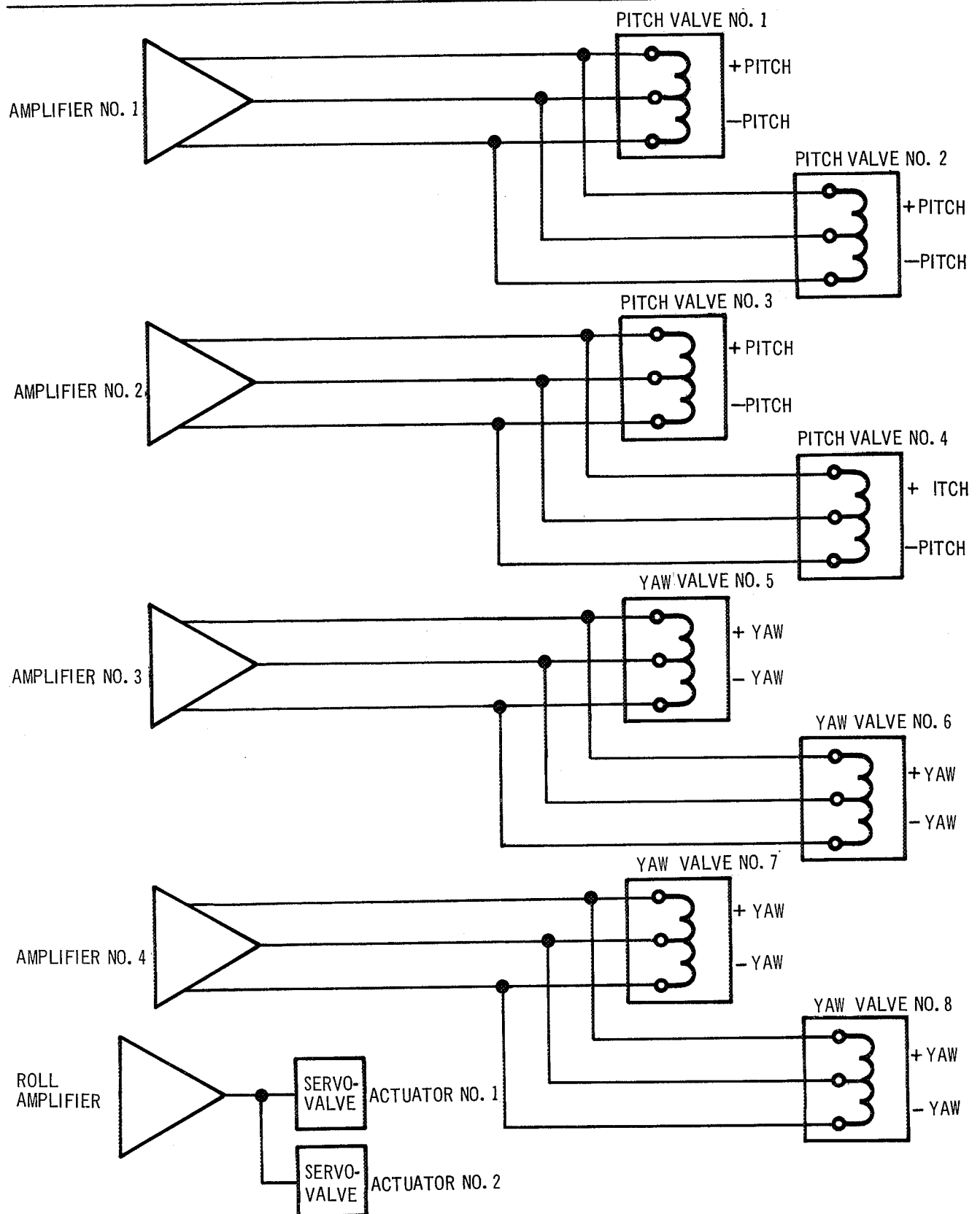


Figure 4-26. Warm Gas Control System – 260-in.-Diam SRM

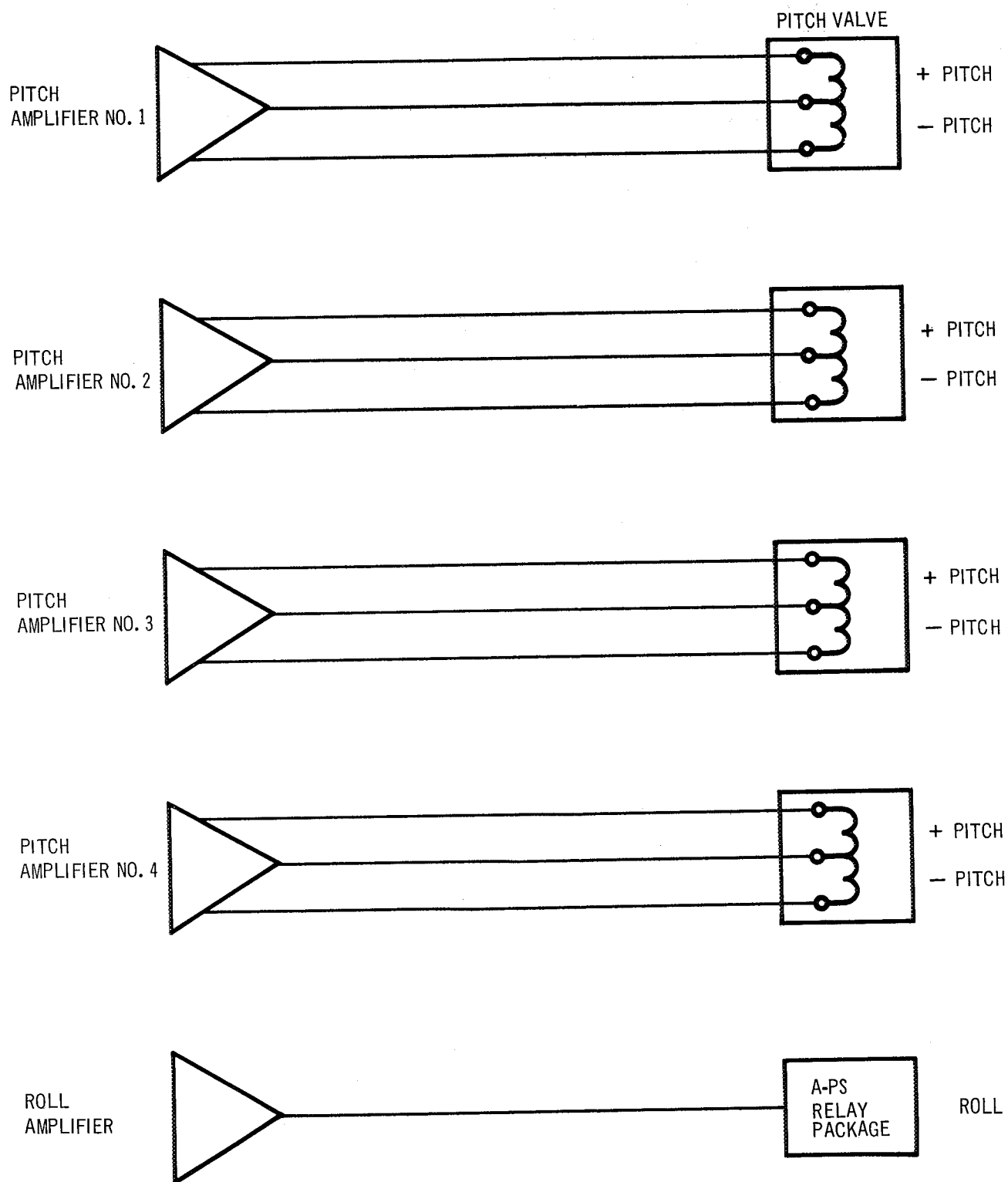


Figure 4-27. Warm Gas Control System – 156-In.-Diam SRM

4.9.4.1 Lockseal and Hot Gas

An analysis of the electronic and electrical systems for the Lockseal and hot gas TVC systems requires an estimated 200 W for the first stage and 150 W for the second stage, excluding the hydraulic pump power requirements. An estimated 300 W, expended within 20 sec, is required to pressurize the hydraulic system of the second stage. This occurs just prior to separation. Operation of the 2 dc motor-driven pumps in this hydraulic system requires 100 lb of battery weight. Battery and support weight for both stages are 50 lb and 150 lb, respectively.

Ignition of the 260-in. -diam SRM is by GSE power while the 156-in. -diam SRM is ignited by on-board battery power. This is common to all vehicle configurations and TVC systems.

4.9.4.2 Warm Gas

Electrically initiating squibs with GSE power ignite the 8 gas generators in the first stage. The 4 gas generators of the second stage are initiated by switching a current from the vehicle power base through a protective device such as a squib switch. This current switch will be relay controlled from the switch selector-guidance sequencing unit.

The electronic equipment power requirement for the first stage is 200 to 250 W, and 175 to 200 W for the second stage. The differential is the result of the different number of pneumatic valves and different roll-control systems used in each stage. An estimated 50 lb of batteries will supply the requirements of both stages.

4.9.5 Data Acquisition

To evaluate the TVC systems during prelaunch, launch and postlaunch, it will be necessary to monitor certain instrumentation parameters. A summary of critical measurements indicate that the Lockseal TVC system will require $\cong 74$ measurements for the first stage and $\cong 62$ measurements for the second; the warm gas TVC system requires $\cong 116$ and $\cong 74$ measurements on the first and second stages, respectively; and the hot gas TVC system and first- and second-stage measures $\cong 88$ and 62 respectively. A listing of these measurements are presented in Tables 4-10, 4-11, and 4-12, and a summary of electronics data for all TVC systems is shown in Table 4-13.

Table 4-10
CRITICAL MEASUREMENTS FOR LOCKSEAL TVC SYSTEM

Equipment	Number of Measurements
260-in. -diam	
Gas generators (2)	
Temperature and pressure	8
Flow rates	2
Valve position	6
Hydraulic (2)	
Temperature and pressure	12
Hydraulic valve position	16
Nozzle thrust (1)	
Temperature and pressure	8
Actuator (2)	
Position	2
Hypergolic engine (2)	
Valve position	4
Engine temperature and pressure	4
Fuel and oxidizer temperature and pressure	2
Flow rates	2
Actuator position	2
	74
156-in. -diam	
Dc motor generator (2)	
Current and voltage	4
RPM	2
Hydraulic system (2)	
Temperature and pressure	8
Hydraulic valve position	8
Nozzle thrust (1)	
Temperature and pressure	8
Actuator	
Position	2
Hypergolic engine	
Valve position	4
Engine temperature and pressure	4
Hypergolic temperature and pressure	8
Flow rates	2
Nozzle temperature	6
Nozzle valve	6
	62

Table 4-11
CRITICAL MEASUREMENTS FOR WARM GAS TVC SYSTEM

Equipment	Number of Measurements
260-in. -diam	
Gas generators (8)	32
Temperature and pressure	8
Flow rates	16
Valve position	16
Nozzle temperature	16
Hydraulic (2)	8
Temperature and pressure	8
Hydraulic valve position	8
Main thrust nozzle (1)	8
Temperature and pressure	8
Actuators--roll (2)	2
Position	2
Hypergolic engines (2)	4
Valve position	4
Engine temperature and pressure	8
Fuel temperature and pressure	2
Flow rates	<u>2</u>
	116
156-in. -diam	
Gas generators (4)	16
Temperature and pressure	4
Flow rates	8
Valve position	8
Nozzle temperature	8
Nozzle thrust (1)	8
Temperature and pressure	8
Hypergolic engine (2)	4
Valve position--fuel solid	4
Engine temperature and pressure	8
Hypergolic temperature and pressure	2
Flow rates	6
Nozzle temperature	6
Valve position of thruster	<u>6</u>
	74

Table 4-12
CRITICAL MEASUREMENTS FOR HOT GAS TVC SYSTEM

Equipment	Number of Measurements
260-in. -diam	
Gas generators (2)	
Temperature and pressure	8
Flow rates	2
Valve position	6
Hydraulic (2)	
Temperature and pressure	12
Hydraulic valve position	16
Control valves (16)	
Position	16
Nozzle--main (1)	
Temperature and pressure	8
Actuator--roll (2)	
Position	2
Hypergolic engine (2)	
Valve position	4
Engine temperature and pressure	4
Hypergolic temperature and pressure	8
Flow rates	2
	<u>88</u>
156-in. -diam	
Dc motor pumps (2)	
Current and voltage	4
RPM	2
Hydraulic system (2)	
Temperature and pressure	8
Hydraulic valve position	8
Nozzle--thrust (1)	
Temperature and pressure	8
Actuator, roll (2)	
Position	2
Hypergolic engine (S-IVB (2)	
Valve position	4
Engine temperature and pressure	4
Hypergolic temperature and pressure	8
Flow rates	2
Nozzle temperature	6
Nozzle valve position	6
	<u>62</u>

Table 4-13
ELECTRONIC COMPARISON

Systems	Lockseal		Warm Gas		Hot Gas	
	260-in. -diam	156-in. -diam	260-in. -diam	156-in. -diam	260-in. -diam	156-in. -diam
Instrumentation (estimated number of parameters)	75 to 80	60 to 65	115 to 120	75 to 80	85 to 90	60 to 65
Power						
Electronics	200 to 250 W	150 to 200 W	200 to 250 W	175 to 200 W	200 to 250 W	200 to 250 W
GSE complexity of modification (lowest number easiest change)	1	2	6	5	4	3
Battery weights	50 lb	150 lb	50 lb	50 lb	50 lb	50 lb

4.10 FIRST- AND SECOND-STAGE TVC SYSTEMS RELIABILITY ANALYSIS

The primary purpose of this preliminary reliability analysis was to independently evaluate the first- and second-stage application of the selected TVC. The results--with respect to failure modes and effects, mission criticality, and confidence--are summarized in the following paragraphs.

4.10.1 Gimbal Nozzle TVC

The gimbal nozzle TVC system, as presently conceived for either a first- or second-stage application, consists of four major components which are (1) the Lockseal element, (2) a hydraulic power unit (HPU), (3) servoactuators, and (4) an electrical control network. The main difference between the first- and second-stage application is the method for providing hydraulic power which is a gas-propelled, turbine-driven, fixed-displacement pump for the first stage and an electrically driven, variable-delivery pump for the second stage. Other differences are mainly with respect to sizing and duty cycle.

The reliability analysis of this TVC system evaluated the basic failure modes of each major component with respect to the design features which tended to eliminate or at least significantly reduce their probability of occurrence. From the results of this evaluation, in addition to the factors of complexity, the status of technology, and the reliability history of similar configurations and applications, the flight reliability of the system is estimated to be 0.998792 for the first stage and 0.99884 for the second.

The Lockseal consists of an elastomeric seal (which is a bonded sandwich arrangement of elastomer and metal reinforcement rings), forward and aft metallic flanges, and an insulating boot. The primary failure modes of this element are (1) structural breakdowns and (2) burn through of the insulating boot caused by heat and erosion. Since the Lockseal is essentially a structural element, its reliability will be a function of the design safety margins and materials compatibility with the environment. Based on the reliability analysis conducted by Lockheed under NASA contract these failure modes are well recognized, and adequate measures are being or will be instituted to ensure high reliability.

The servo-actuators are similar to those developed for use in the Saturn V Program. The major modifications are (1) to accommodate different stroke requirements and (2) to incorporate a triple-redundant, majority voting, flow-control servo-valve. The basic design, which presently incorporates such high reliability features as mechanical feedback and a hydraulic load-damping network, is unaltered. This TVC system uses two servo-actuators, one each in the pitch and yaw planes. The primary failure modes of a servo-actuator are (1) failure of the servo-valve to either change or maintain the position of the actuator and (2) failure of the actuator to respond when commanded. Failure histories of similar items indicate that the servo-valve is the most unreliable element of this component (that is, the S-IVB servo-actuators have a criticality of 1,200--1,100 of which is attributed to the servo-valves). With this in mind, redundancy is provided by the technique known as majority voting. This valve is a three-stage hydraulic amplifier with three parallel, majority voting first-stage channels. Majority voting is based on automatic agreement by a majority before responding to a given command, thereby eliminating the ability of single channel to fail the system or inadvertently respond to a spurious signal. The probability of second- or third-stage failure because of spool jamming from particle contamination or manufacturing burrs is reduced by oversize piston areas and high applied forces in addition to well-designed filtration techniques.

The First-stage HPU is essentially the same as one designed and developed for the Nike Zeus Program. The TVC system incorporates two of these units manifolded together in such a manner that the failure of one unit does not affect the other. Based on their capability, these units are redundant throughout 98% of the flight. Therefore, the only single-point failure modes would be structural in nature, such as burst or burn through. The second-stage HPU consists of redundant, battery-powered, dc-electric, motor-driven pumps and an accumulator reservoir assembly. For most of the mission, the accumulator reservoir and pump assemblies can be considered triple redundant. Thus, the probability of mission loss because of the single failure of one of these elements is reduced by the conditional probability

of encountering the failure prior to staging. Based on the history of similar configurations and applications, such as the S-IVB and the aforementioned conditional probability, high reliability can be achieved.

The electrical requirements for the first-stage TVC system are power for firing the dual-initiator squibs of the solid-propellant gas generator (SPGG) and command signals to the servo-actuators. The second-stage requirements are power for the dc-motor-driven pump assemblies and command signals to the servo-actuators. Power for both stages will be provided by silver-zinc batteries, while primary guidance and control is assumed to be a function of an IU. For both stages, six servo-amplifiers, (one for each of the triple-redundant first-stage servo-actuator channels) will be incorporated. The only single-point failures are those associated with power supply and distribution. However, for the first stage these are not considered flight critical since SPGG start-up is programmed approximately 6 sec prior to stage ignition; therefore, failure would only result in launch delay.

It should be noted that the Lockseal, which is the gimbal-bearing element, contributes in excess of 80% of the unreliability for both the first- and second-stage TVC systems. However, if it can be assumed that Lockheed's current reliability assessment is a conservative estimate based on the status of development technology and is not inherent in the concept, then significant reliability growth can be expected.

4.10.2 Hot Gas Secondary Injection

The reliability analysis of the Thiokol hot-gas secondary injection TVC system considered the integral functional relationships of the major components with respect to both first- and second-stage success. This TVC system, as presently conceived, will consist of (1) hot gas injector valves, (2) injection orifices, (3) hydraulic servo-actuators, and (4) an HPU. The basic difference between the first- and second-stage designs is the size and number of components required.

This system incorporates 16 servo-actuator injector-valve assemblies for the first stage and 8 for the second. Each assembly is independently actuated as required to provide the proper TVC. The servo-actuators

incorporate both triple-redundant servo-valves and mechanical piston-position feedback to improve reliability by protecting against the fail-open mode which could result in mission degradation or even mission loss. This failure mode is of primary concern since it is a single failure point for each of the injector-valve assemblies. The effects of this failure mode would be induced pitch or yaw disturbances which would have to be counteracted by a flight-control command to open additional injectors. Depending on the magnitude of these induced disturbances and whether they are additive or subtractive from the environmental disturbances, launch success could be seriously degraded or even aborted. It should be noted that this failure mode is not only prevalent with respect to the servo-actuator but also with respect to the valve pintle and its associated orifices. A pintle sticking open or an orifice burn through would probably result in the same effect. The main reason for concern is the number of these servo-actuator injector-valve assemblies involved (16 on the first stage and 8 on the second, any one of which failing in this mode could have these results). Since the system is designed for worst-case control conditions, the fail-closed mode for any one assembly is only of concern if these specific control conditions are present. These conditions are analogous to the probability of a double failure, that is, the worst-case control conditions must be present on the same flight that involves a fail-closed for one of the servo-actuator injector assemblies.

The HPU's for both the first and second stages are essentially the same as those proposed for the first and second stages of the Lockseal system.

The first- and second-stage electrical power requirements are also essentially the same as for the Lockseal system. However, the control network is somewhat different. The control scheme is to be orthogonal in nature and will consist of diode arrays which will control positive and negative electrical inputs to appropriate pitch and yaw actuators. The critical failure mode is an electrical failure which results in an error signal commanding the injector valves open. This failure mode is similar in effect to the fail-open mode for the servo-actuator injector-valve assemblies previously described.

Based on the results of the reliability analysis of this system, the estimated reliability is 0.991409 for the first stage and 0.995044 for the second. As expected, because of the status of technology and the number of injector valves required, the hot gas valve is the major contributor to the system unreliability. Therefore, any effort toward reliability improvement in this area would be effective. Furthermore, normal progression in the technology coupled with the elimination, through experience, of initial design, manufacturing, and testing errors, should also provide significant reliability growth. However, the reliability of this system will always be limited by the number of independent components that can cause system failure.

4.10.3 Warm Gas Secondary Injection

The reliability of the Vickers warm-gas secondary injection TVC system is dependent on the integral functional relationships among (1) the solid propellant gas generators, (2) the pneumatic flow control servo valves, (3) the injection orifices, and (4) the electrical power and control valves, (3) the with the other TVC systems, the basic difference between the first- and second-stage application is the size and number of components required. A typical assembly consists of an SPGG which continuously supplies warm gas for secondary injection to a pneumatic flow control servo-valve which ports the injectant gas proportional to an input guidance command signal to two geometrically opposed injection nozzles. The 260-in. -diam SRM first stage requires 8 of these assemblies while the 156-in. -diam SRM second stage requires 4.

Each of the system components have failure modes that are mission critical. The generators can fail to ignite, fail to supply adequate pressure or flow, or burst or burn through. Failure to ignite or provide adequate pressure or flow is not critical for the first stage because start-up can be programmed prior to mainstage ignition, thereby resulting only in a launch delay if a failure occurs. This failure mode is obviously more significant for the second stage. However, since the system has been designed for worst-case flight control conditions, it may or may not result in mission degradation or loss depending on the specific launch conditions. Therefore, the probability of mission success is increased by considering the conditional probability of

failure during a mission requiring maximum flight control. The burst or burn-through failure mode, however, is equally critical and possibly catastrophic for each of the 12 gas generators. This failure mode would also be significant for manned missions. It would be difficult if not impossible to completely protect against this failure mode. Therefore, each of the 12 gas generators presents a mission critical and/or catastrophic single failure point.

The injectant flow-control valve is a proportional two-stage pneumatic valve. This valve, as presently designed, does not incorporate the triple-redundant majority-voting feature present in current hydraulic servo-valve designs. However, it does incorporate high reliability pressure feedback. As previously pointed out, failure histories indicate that servo-valves are inherently unreliable and their primary failure modes are (1) failure to respond or over response to an input signal and (2) inadvertent response. Since this valve design does not protect against these failure modes, these modes are considered single failure points. Furthermore, the failure mode of concern for this system, like the hot gas system, is an induced disturbance resulting from a valve failure in an off-center position. Also, like the hot gas system, this condition could result in mission degradation or abort depending on the magnitude of the induced disturbance in conjunction with the natural environmental disturbances. The injection nozzles do not present the significant problem with respect to burn through as is present with the hot gas orifices. This is primarily because of lower injectant gas temperatures (2,000°F versus 5,800°F).

The electrical control signals to the valves is provided by redundant push-pull servo-amplifiers responding to guidance and control commands from the IU. Of primary concern are electrical failures inducing spurious signals to the servo-valves. Because the valves are of a simplex design, any one spurious or error signal will induce an inadvertent response.

Based on the results of this analysis, the reliability of the Vickers warm gas secondary injection TVC systems is estimated at 0.988937 and 0.993959 for first- and second-stage applications, respectively. As expected, the flow-control valves are the major contributors to system unreliability, contributing approximately 70%. Incorporation of triple-redundant, majority-voting servo-valves offers the potential for significant reliability improvement and should be considered as a future modification.

4.11 RELIABILITY COMPARISON

Table 4-14 presents a comparison of the reliability estimates for first- and second-stage TVC applications.

4.12 DEGREE OF DEVELOPMENT

The degree of development that exists for each of the candidate TVC system concepts is best described by the extent and nature of the testing program. All of these concepts have been under development for some time and have a history of hardware tests. Many tests were performed by the TVC system contractors resulting from their own development program, and government development contracts have provided an extensive series of test data. Tables 4-15, 4-16, and 4-17 show test data resulting from government development contracts only.

Table 4-15 show lockseal test data as well as the results of a test of the Thiokol Flexible Bearing, which uses the same principle used for the development of Lockseal designs. These data are presented because they

Table 4-14
TVC SYSTEM RELIABILITY COMPARISONS

Items	Lockseal Gimbal Nozzle	Hot Gas Secondary Injection	Warm Gas Secondary Injection
First-Stage	0.998792	0.991409	0.988937
Second-Stage	0.998840	0.995044	0.993959

Test No. / Motor Used/Test Date	Throat Diameter (in.)	Deflection	Maximum Chamber Pressure (psia)	Burn Time (sec)	Maximu Deflecti Angle (deg)
1. 36-in. -diam Char Motor ⁽¹⁾ /8-27/65 (AFRPL)	2. 308	Omnidirectional	620	58	4. 2
2. 36-in. -diam Char Motor/10-8-65 (AFRPL)	2. 308	Omnidirectional	620	125	3. 9 3. 3
3. 84-in. -diam Char Motor/2-11-66	8. 40	Omnidirectional	560	37	4. 0
4. 36-in. -diam Char Motor/5-10-66 (NOL)	1. 50	Single-Plane Actuation	1, 410	31	15 15
5. 36-in. -diam Char Motor/1-26-67 (NOL)	1. 50	Single-Plane Actuation	2, 450	25	6. 4
6. Modified Minuteman Test Motor (TU-437)/ 3-23-67 ⁽²⁾ (Poseidon)	11. 56	Omnidirectional	720	56	2. 5
7. Modified Minuteman Test Motor (TU-437)/ 1967 (Poseidon)	11. 56	Omnidirectional	720	56	5
8. Modified Minuteman Test Motor (TU-437)/ 1967 (Poseidon)	11. 56	Omnidirectional	420	56	5
9. NCI-Conducted Tests	2. 512	Single-Plane Actuation	700	33	8
10. 156-in. -diam/5-26-67	34. 54	Omnidirectional	656	77	>3

- (1) Char Motor is an endburning gas generator utilizing propellant without curatives.
 (2) Based on "Preliminary Data" from Project Engineers' trip report.
 (3) Tests 1 through 9: Lockheed; Test 10: Thiokol.

4-15
FIRING HISTORY

Maximum Rate (deg/sec)	Maximum Torque (in. -lb)	Actuation System	Remarks
3.95	6,500	Hydraulic actuators/ linear displacement transducers/electrical servovalve controls	Satisfactory test. LPC Report No. 689 Q-1, AFRPL TR 65-108
3.85	8,100	Same as above	Satisfactory test. LPC Report No. 689 Q-2, AFRPL TR 65-173
4.0	43,000	Same as above	Burnthrough in exit cone at 37 sec, followed by exit cone ejection. Lockseal successful. LPC Report No. 689 Q-3, AFRPL TR-65-243
320	+3,350	Same as above	Lost nozzle throat insert at 16.4 sec, followed by throat insulator. Lockseal functioned satisfactorily. LPC Report No. 689-F, AFRPL TR-66-112
135	+9,400	Same as above	Actuator linkage failed as a result of chamber overpressure and consequent buckled seal element. LPC Report No. 689-F, AFRPL TR-66-112
13.0	32,400	Same as above	Apparently satisfactory test.
13.0	45,000	Same as above	Apparently satisfactory test.
13.0	45,000	Same as above	Apparently satisfactory test. No published reports (2)
---	2,200	Linear electric actuators	Approximately 9 tests conducted at NCI; Lockseal 100% successful. LPC Dwg 201010, NCI DO 200012.
Approx 24	1,640,000	Hydraulic	Satisfactory test. Thiokol Report No. TE2-183-6-7; 27 June 1967.

Test No.	1	2	3	
Test Date	10/9/64	11/23/64	3/18/65	
Motor used, diam (in.)	14	65	65	
Duration (sec)	39.4	54.0	64.4	
Chamber pressure (psia)	800	280 to 587	639.9 Avg	
Thrust (lb)	NA	NA	16,316 Avg	16
Propulsion weight (lb)	203	195	4,712	4
% aluminum	16	16	16	
% solids	86	86	86	
Flame temperature (°F)	5,700 to 5,800	5,700 to 5,800	5,700 to 5,800	5,7
Nozzle type	None Used	None Used	Flight type, subm	
Actuator	Not actuated	Conventional	Conventional	Cor
Location	---	External (facility)	Within support structure	Wit str
Motion	---	Linear, proportional	Linear, proportional	Lin pro
Fluid	---	Hydraulic oil	Hydraulic oil	Hyc
Servo location and type	---	Integral with actuator, 4-way	Integral with valve, 4-way	Rer 3-w
Pintle & Actuator protection	Molded carbon fiber phenolic	Molded carbon fiber phenolic	Composite molded an carbon cloth and V-4	
Valve	Simulated clearance	Fully modulating, clearance		Ful ting and
Weight (lb)	---	NA	17.5	12
Quantity	1	1	1	
Flow rate (lb/sec)	3.77	2.42 at 700 psi	2.65 at 700 psi	2.8
Mounting arrangement	←	Plenum mounted internal on closure		---
Duty cycle	Held full open	Tape input	Tape input	Ta
Number of cycles	---	18	40	
Maximum cyclic rate (cps)	---	1	4	
Thrust deflection (deg)	NA	NA	2.79	
Maximum extend load(6) (lb)	---	248	525	Sea Cle
Maximum retract load (lb)	---	16	450	Sea Cle
Stroke to full open (in.)	0.381	0.381	0.381	Sea Cle

Notes: 1. Tests 1-4: AF 04(694)-334. 4. Tests 10-12: AF 04(611)-11408.
2. Tests 5-6: AF 04(694)-774. 5. Schedule test date; all performance
3. Tests 7-9: AF 04(611)-11627. 6. Extended load is actuator stall load

Table 4-16
THIOKOL HOT-GAS VALVE TEST SUMMARY

4	5	6	7	8
6/65	12/16/65	2/3/65	11/18/65	1/26/67
14	14	14	14	65
67.9	56.0	64.0	53.0	52.0
616.1 Avg	225 to 900	230 to 680	275 to 780	275 to 740
199 Avg	NA	NA	NA	NA
767	260	258	288	288
16	20	20	21	21
86	88.6	88.6	← Classified Information	← Classified Information
to 5,800	6,100	6,100	6,500	6,500
argued	None Used	None Used	None Used	None Used
ventional	Conventional	Conventional	Conventional	Conventional
n support	External	External	External	External--
ure				flight weight
r,	Linear,	Linear,	Linear,	Linear,
rtional	proportional	proportional	proportional	proportional
ulic oil	Hydraulic oil	Hydraulic oil	Hydraulic oil	Hydraulic oil
te	Remote	Remote	Remote	Remote
y	3-way	3-way	3-way	3-way
tape wrap	Composite molded and tape wrap carbon cloth			Molded silicon
rubber				cloth over-
				wrapped with
				carbon cloth
				tape
modula-	Fully modula-	Fully modula-	Fully modula-	Fully modula-
clearance	ting, seating	ting, seating	ting, seating	ting, seating
ating				
nd 17	← NA, heavy weight design →			
2	1	1	1	1
at 700 psi	3.5 at 700 psi	3.1 at 700 psi	3.1 at 700 psi	3.0 at 700
→	Plenum	Plenum	Plenum	Plenum
input	Tape input	Tape input	Tape input	Tape input
15	12	17	7	57
1.25	1	1	1	>5
3.06	NA	NA	NA	NA
avg 2,000	1,750	1,150	1,750	1,800
ance 209				
avg 1,130	150	350	300	250
ance 470				
avg 0.325	0.600	0.450	0.450	0.4
ance 0.381				

Values are predicted.
All valves seated.

	9(5)	10	11	12(5)
	1/67	9/8/66	1/20/67	8/67
	65	65	65	120
	65.0	48.0	101.0	120.0
	700	130 to 480	180 to 760	700
	22,000	NA	NA	500,000
	5,000	6,260	8,376	212,520
	21	16	16	16
ation →	86	86	86	86
	6,500	5,700	5,700	5,700
	Submerged	None Used	None Used	Highly submerged
	Conventional	Conventional	Reversed	Reversed
	External--	External	Internal flight	Internal flight
	flight weight	(facility)	type	type
	Linear,	Linear,	Linear,	Linear,
	proportional	proportional	proportional	proportional
	Hydraulic oil	Hydraulic oil	Hydraulic oil	Hydraulic oil
	Integral with	Integral with	Remote	Remote
	actuator, 3-way	actuator, 4-way	4-way	4-way
	Tape wrapped	Silica cloth tape	Silica cloth tape overwrapped	
	silica cloth	overwrapped	with carbon cloth tape and	
	overwrapped	with carbon	V-44 rubber	
	with carbon	cloth tape		
	cloth tape			
-	Fully modula-	Fully modula-	Fully modula-	Fully modula-
	ting, seating	ting, seating	ting, seating	ting, seating
	8.13	NA	280	260
	4	2	2	4
	3	78	100 at 700 psi	110
	Plenum	Plenum	Internal on closure	Internal on nozzle
	Tape input	One fixed open	Tape Input	Tape input
		one w/tape input		
	19	9	11 and 4	6
	>10	0.5	0.5	1.5
	3.0	NA	NA	3.5
	---	12,000	17,000	---
	---	0	Valve #3 0	---
			Valve #4 950	
	0.400	2.00	1.750	1.750

Tes

Test

Motor used

Duration (sec)
Chamber pressure (psia)
Thrust, Avg (lb)
Mass flow (lb/sec)
Propellant weight (lb)

Injection nozzle

Axial location (X/L)
Injection angle (deg)
Throat area (in. ²)
Exit area (in. ²)
Maximum chamber pressure (psi)
Gas total temperature (°F)

Gas generator

Average pressure (psia)
Mass flow (lb/sec)
Total gas temperature (°F)

Valve

Actuator

Notes: 1. Tests 1-6: NAS1-20
 2. Tests 7-9: NAS1-40
 3. Tests 1-5: Single-ax
 4. Tests 6-9: Two-ax
 5. Tests 3-6: Success

Table 4-17
VICKERS WARM-GAS STATIC TEST SUMMARY

No.	1	2	3	4	5
Date	1/23/64	4/29/64	12/2/64	1/21/65	3/10/65
	EM 72	EM 72	EM 72	EM 72	EM 72
	25.26	9.96	45.46	44.80	42.91
	590	645	523	533	534
	2,873	2,820	2,506	2,557	2,582
	12.6	13.2	11.4	11.6	11.5
	---	---	520	520	520
	Sonic	Supersonic	Sonic	Supersonic	Supersonic
	0.75	0.75	0.75	0.60	0.75
	0	0	0	0	20° upstream
	0.0738	0.0674	0.1353	0.1124	0.11
	0.0738	0.1024	0.1353	0.1261	0.13
	519	857	510	575	544
	1,630	1,560	1,885	1,915	1,915
	2,300	2,690	2,650	2,670	2,700
	0.608	0.615	0.606	0.617	0.61
	1,820	1,880	2,000	2,015	---
	Electrically driven p				Hydraulic -

--Phase I.
injection and control.
injection and control.
firing.

6. Test 1: Gas-generator igniter housin
7. Test 2: Motor malfunctioned at 10 se
8. Test 7: Motor leak developed at 16 s
9. Test 8: Flow separation at 21 sec.
10. Test 9: Intermittent flow separation.

6	7	8	9
6/10/65	7/29/65	10/22/65	1/12/66
EM 72	EM 72	EM 72	EM 72
42.32	22.357	42.803	42.087
554	542	529	543
2,770	3,313	3,063	3,189
12.4	12.1	12.3	12.4
560	558	560	562
Yaw Axis	Pitch Axis		
Supersonic	Supersonic	Sypersonic	Supersonic
← 0.75 →	0.75	0.67	0.75
20° upstream	0	0	25
← 0.1128 →	0.1047	0.1047	0.0983
← 0.1385 →	0.304	0.2545	0.271
572 590	505	592	655
1,880 1,860	1,870	1,920	1,870
2,600 2,610	2,430	2,480	2,630
0.625	0.584	0.585	0.587
1,980 1,960	1,970	1,970	1,950
matic			

ailed at 10 sec.

represent the first firing of a 156-in. -diam SRM with an omniaxial flexible-seal nozzle. The detailed report of this test is contained in Thiokol Report No. TE 2-183-6-7, AF 156-9, Flexible Seal Nozzle Demonstration (U), 27 June 1967, Thiokol Chemical Corporation, Wasatch Division. The design components for this test were (1) 156-in. -diam SRM with a monolithic 18% Ni/steel case, (2) submerged movable 35-in. -diam throat nozzle, (3) 276,515 lb of propellant, (4) 70-sec duration, and (5) 1,000,000-lb thrust.

Table 4-16 shows test data for the Thiokol hot gas pintle valve. The most recent test of this concept occurred on 30 August 1967. The design components were (1) 4 internally mounted 110 lb/sec valves with 1 valve per quadrant, (2) 120-in. -diam SRM, 160-sec duration, 500,000 lb thrust, and a chamber pressure of 700 psia. The test was not successful because of a burn through of the nozzle injector orifice. However, prior to burn through, good side force and valve actuation data were obtained, and all four valves operated at over their design flow rates. Two of the 4 internally mounted valves were ejected after burn through, and the 2 remaining valves were subsequently cold flow tested at 1.5 times their rated flow. No data were obtained on the thrust-modulation feature associated with opening all valves simultaneously, because this test was programmed for a time period after nozzle burn through occurred.

Table 4-17 shows Vickers warm gas valve test data.

Section 5

ROLL CONTROL SYSTEM

Two roll control concepts were investigated: an independent system and a dependent system. The independent system uses subsystems and propulsion units that are independent of main-motor TVC. This concept is considered as the prime roll control method in this study and was applied to all vehicle configurations regardless of the TVC system used. The selection of the roll control systems (RCS) for each stage was based on data availability and functional requirements. They do not represent optimum systems.

The dependent system uses inherent roll control capabilities associated with the hot gas and warm gas TVC systems, and does not apply to vehicles using gimbal nozzle TVC.

5.1 INDEPENDENT ROLL CONTROL SYSTEM

The first-stage RCS selected uses two hypergolic engines pivoted in one plane only and a regulated pressure supply, chosen over a blowdown method to avoid the degradation of engine performance that would result if a gradual drop in chamber pressure occurred.

This RCS was taken from the final design reported in Phase II of the Solid-Boosted S-IVB Study. The hypergolic engines were basically the 1,750-lb-thrust engines formerly being developed by Marquardt for the Saturn V/S-IVB auxiliary propulsion system (APS) unit. This selection was made because the system was designed for a slightly larger 260-in. diam solid booster and because data were available on its design and operating characteristics.

Investigation of various motor-mounting configurations showed that a payload gain could be realized if 2 pivoted engines were used in place of the 4 fixed-engines configuration. The engines are mounted 180° apart, but would point aft and would pivot in one plane through a total-included angle of 120° to

provide roll control capability. The installation of this system in the first stage is shown in Figure 3-14.

To adapt the Marquardt 1750 hypergolic engine for use in this RCS, the engine was uprated and modified for sea-level use. The basic chamber pressure was raised from 100 to 150 psia for a substantial thrust increase. To prevent flow separation during near-sea-level operation and to provide a considerable increase in actual thrust throughout most of the booster flight, the nozzle was shortened from an expansion ratio of 20 to an expansion ratio of 6. The engines are required to swivel $\pm 60^\circ$ in one plane for roll control. They are pivoted about their CG to minimize actuation system force requirements. A slight increase in capacity of the on-board hydraulic power system used for TVC is adequate for meeting RCS requirements. Reliable operation is achieved by providing constant pressure-regulated propellant to the engine inlet and allowing the engine to burn continuously after start. A single set of propellant and pressurant tanks feeds both engines. A schematic of this system is shown on Figure 5-1.

The roll control propellants are fed from a common set of tanks to both engines through 1/2-in. -diam stainless steel tubing. Flexible metal hoses connect this tubing to the engine inlet hard-mount points on the aft skirt. Hand valves located immediately upstream of the engine valve permit filling with minimum gas entrapment. The same valves allow purging prior to the fill operation and draining of propellant, if required. Propellant flow is controlled by the engine valve complex.

A 4.5-cu-ft sphere supplies helium to both propellant tanks. The regulation module consists of a regulator which provides a constant 400 psi at its outlet, a pressure-switch-actuated solenoid valve which provides backup regulation in the event of regulator failure, a plenum chamber, and a hand valve for venting the line downstream of the regulator during functional checks. Downstream of the plenum chamber, the 1/4-in. -diam pressurization line separates into 2 branches, 1 for each propellant tank. Complete isolation of these branches is achieved by a series combination of initially closed squib valves,

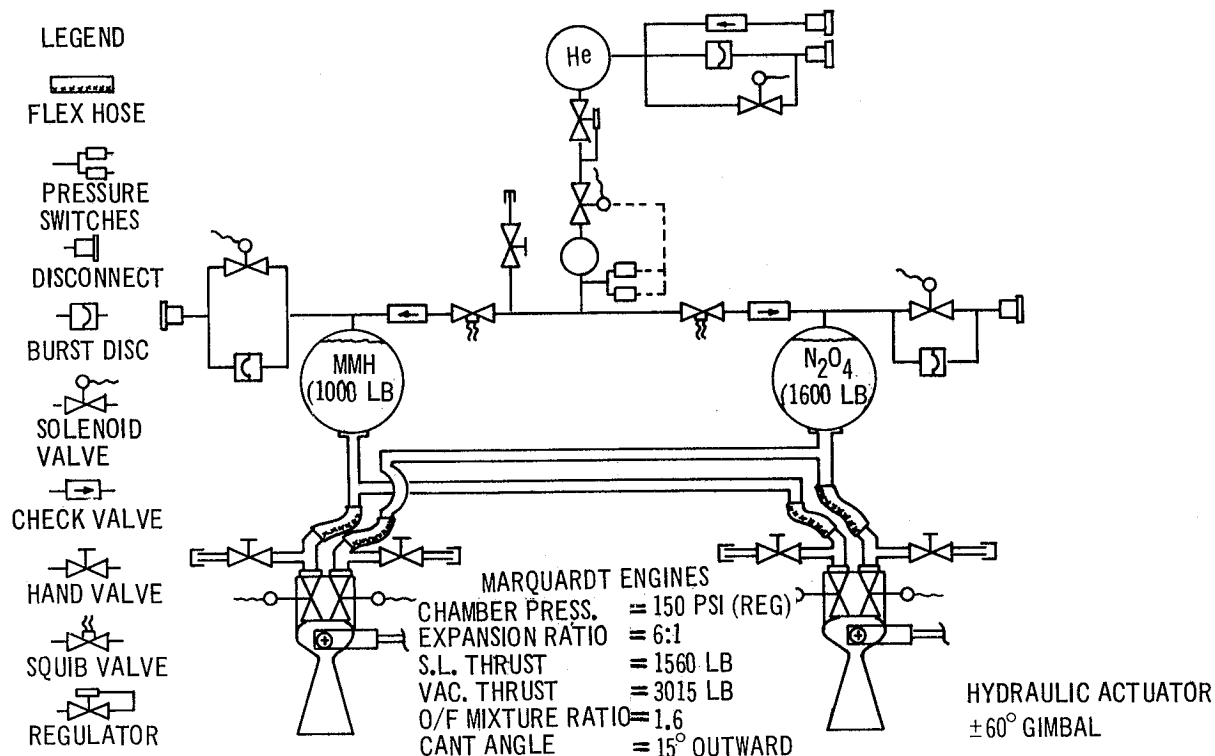


Figure 5-1. Roll Control System Schematic

which are fired open during the start sequence, and check valves, which prevent backflow once the squib valves are opened.

The second-stage RCS selected is basically the standard S-IVB/IB APS module with the outboard-facing pitch engines deleted. A tabulation of the design features of the first- and second-stage RCS's is shown on Table 5-1.

The S-IVB/IB APS is a completely self-contained modular propulsion subsystem. The modules are mounted on the interstage of the second stage 180° apart (shown in Figure 3-14); they require electrical power and command signals to provide the necessary stage functions. The configuration and dimensions of these units are shown in Figure 5-2. Each of the 2 modules, when used for RCS only, would contain two 150-lb-thrust, ablatively-cooled, liquid-bipropellant hypergolic engines; a positive expulsion propellant-feed system for zero operations; a helium pressurization system; and propellant tanks with 23.3 lb of MMH fuel and 37.7 lb of N₂O₄ oxidizer. The pitch engine is removed for this application. Pulse operation of up to 10 pulses/sec is possible. A mockup of the Saturn IB/S-IVB module is shown in Figure 5-3.

Table 5-1
DESIGN FEATURES OF ROLL CONTROL SYSTEMS

	260-in. -diam First Stage	156-in. -diam Second Stage
Engines		
Number required	2	4
Mounting configuration	Swivelled about CG	Fixed
Chamber pressure	150 psia	100 psia
Expansion ratio	6:1	---
Sea level thrust	1,560 lb	
Vacuum thrust	3,015 lb	150 lb
Vacuum impulse (minimum)	422,500 lb-sec	26,500 lb-sec
Axial impulse	50-90%	0
Operation	Continuous	Intermittent
Propulsion System		
Tank arrangement	Integrated	2 modules
	1 complete set	2 complete sets
	1 helium sphere	2 helium spheres
	1 N ₂ O ₄ tank	2 N ₂ O ₄ tanks
	1 MMH tank	2 MMH tanks
Tank design	Pressure-fed	Positive expulsion
Pressurization system	Simplified (continuous operation)	Similar to S-IVB APS
Propellant system	Simplified (continuous operation)	Similar to S-IVB APS

Propellants are fed from one set of tanks in each module to the two engines in each module through stainless steel tubing. Flexible metal hoses connect this tubing to the engine inlet hard-mount points.

The pressurization system is divided into a high-pressure storage system and a pressure control system. The high-pressure storage system is composed of a self-sealing fill disconnect fitting, a fill module (this houses a solenoid-operated dump valve and a relief valve) and a high-pressure

Figure 5-2. S-IVB Auxiliary Propulsion System

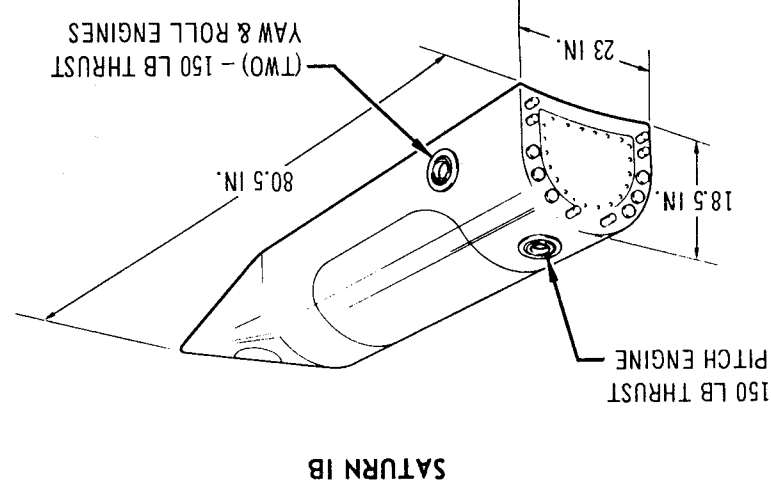
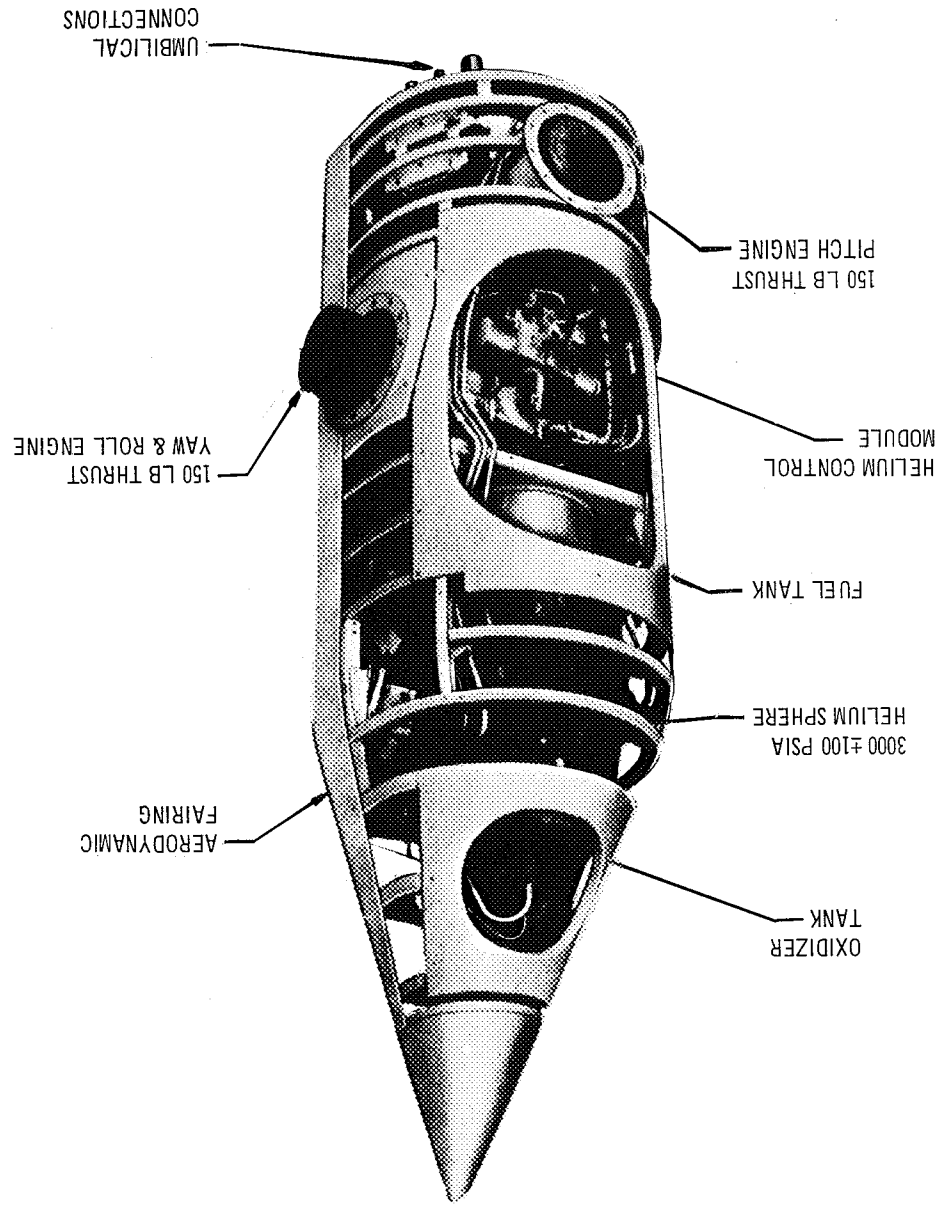


Figure 5-3. Saturn IB/S-IVB Auxiliary Propulsion System Module (Mockup)



storage bottle. This system initially stores gas at $3,100 \pm 100$ psia. The control pressure system is composed of a control pressure module (housing two series flowing pressure regulators and a filter), a plenum bottle (surge chamber), two quad check valves (one supplying the fuel tank ullage and one supplying the oxidizer tank ullage) and two ullage vent modules (one for fuel and one for oxidizer; each housing a solenoid operated dump valve, and a relief valve). The fuel and oxidizer tank ullages are formed between the tank wall and the positive expulsion bellows. The control pressure module maintains system pressure at $200 \pm$ psia.

The weight breakdown for both systems is shown in Tables 5-2 and 5-3.

5.2 DEPENDENT ROLL CONTROL SYSTEM

It is possible to integrate roll control with warm gas and hot gas TVC systems. Sketches of possible concepts are shown in Figures 5-4 and 5-5.

Table 5-2
FIRST-STAGE ROLL CONTROL SYSTEM WEIGHT BREAKDOWN

RCS Dry Weight (lb)	
Engines and Mounts	134
Vent Modules (2)	10
Propellant Tanks and Mounts	176
Pressurization Tank	125
Line and Fittings	54
Fill Valves	8
Control Module	12
Contingencies	52
Subtotal	571
Control Propellant	2,600
Pressurization Gas	9
RCS Wet Weight Total	3,180

Table 5-3

SECOND-STAGE ROLL CONTROL SYSTEM WEIGHT BREAKDOWN

RCS Dry Weight (lb)	
Engines (4)	115
Fairings	162
Fuel System	94
Oxidizer System	94
Pressurization System	112
Leak Check System	16
Mounting Hardware	53
Subtotal	646
Control Propellant	128
Pressurization Gas	3
RCS Wet Weight Total	777

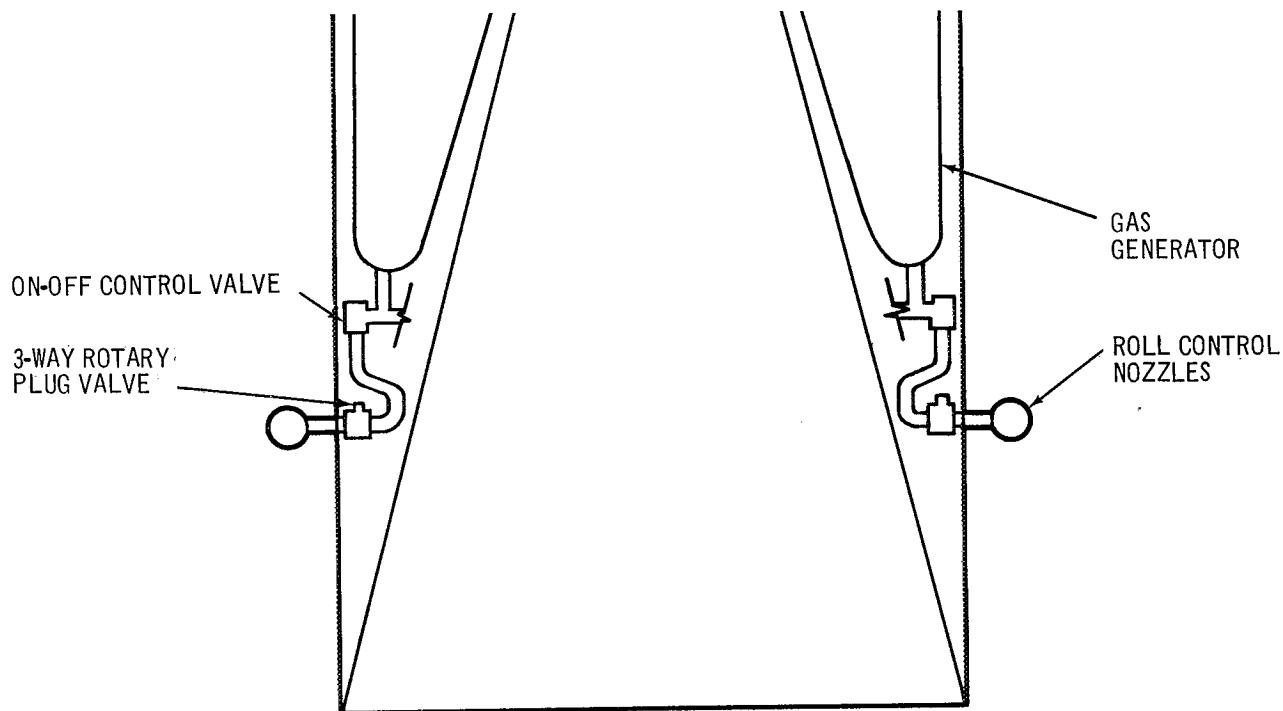


Figure 5-4. Roll Control System Using Warm Gas TVC Bypass

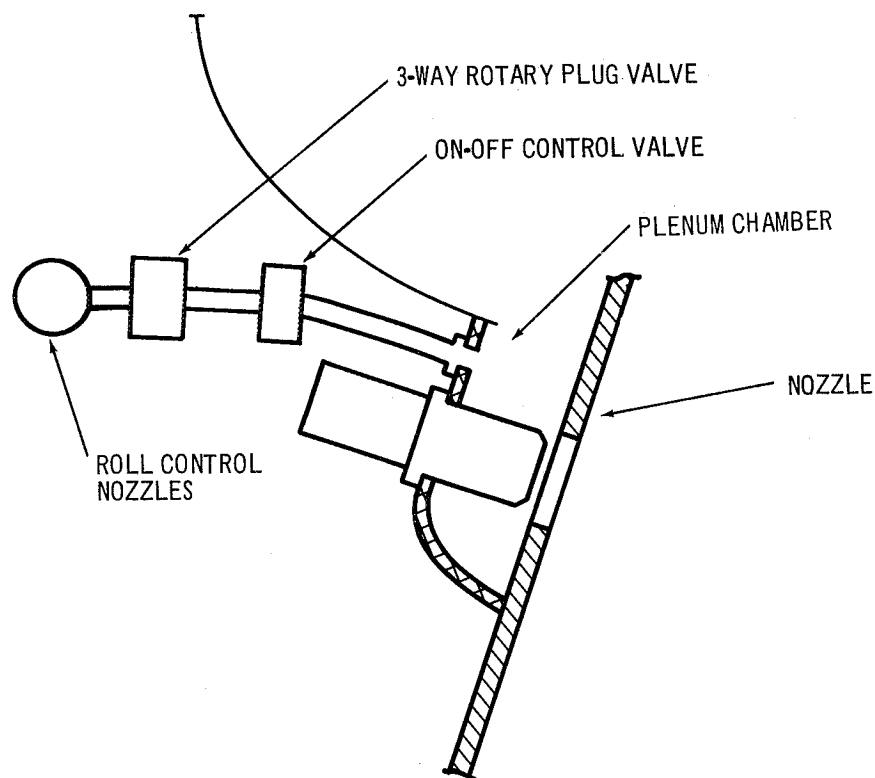


Figure 5-5. Roll Control System Using Hot Gas TVC Bypass

The warm gas RCS uses gas from two of the eight first stage and four second-stage gas generators to provide roll control. Demand for gas is controlled by an on-off valve then routed to a three-way rotary plug valve to direct the flow to the appropriate nozzle. Flow rates required to use this system are an order of magnitude smaller than those required for TVC. Therefore, the gas generators should be able to provide the flow required with no effect on TVC.

A hot gas RCS can draw gas from the plenum chamber using a system of valves similar to that described for warm gas roll control. The higher operating temperature, however, would require valves designed to operate at approximately 5,800°F.

Nozzle and propellant requirements for both of these concepts are shown in Table 5-4. The calculations are shown in Appendix A. 4.

Table 5-4
DEPENDENT ROLL CONTROL SYSTEM DATA

	260-in. -diam First Stage		156-in. -diam Second Stage	
	Hot Gas	Warm Gas	Hot Gas	Warm Gas
Nozzle				
Number Required	4	4	4	4
Thrust	3,015 lb	3,015 lb	150 lb	150 lb
Throat Area	2.70 sq in.	2.70 sq in.	0.131 sq in.	0.131 sq in.
Flow	15.08 lb/sec	17.2 lb/sec	0.75 lb/sec	0.86 lb/sec
Propellant Requirements	2,710 lb	3,100 lb	98 lb	112 lb

5.3 ROLL CONTROL RELIABILITY ANALYSIS

Independent and integral RCS's have been considered and evaluated. The independent systems are essentially APS's utilizing hypergolic-propellant thrusters to achieve roll control. The integral system, which is only applicable with the hot gas and warm gas TVC systems, uses the injectant gases to achieve roll control.

5.3.1 Independent Systems

The first stage uses a gimballed, continuous-firing hypergolic RCS identical to that proposed for the 260-in. -diam SRM first stage evaluated by Douglas for NASA and reported in Douglas Report SM-51896, Volume II, Saturn IB Improvement Study, Phase II. The advantages of this system, as detailed in the referenced report, are that (1) a gimballed system requires only two engine modules rather than four for the fixed-engine system and (2) continuous firing significantly improves reliability by eliminating valve cycling. In addition, engine gimbaling is accomplished by triple-redundant servo-actuators to assure high reliability. Based on the reliability analysis reported in the referenced study, this system has an estimated reliability of 0.997.

The second stage uses a fixed-engine RCS similar to the Saturn S-IVB/IB APS. This system employs two identical, completely self-contained modules. Each module contains two 150-lb-thrust engines that selectively pulse fire on command from the IU to achieve roll control. Based on a detailed failure mode, effects, and criticality analysis accomplished by Douglas for NASA under Contract No. NAS7-101, the predicted reliability of this system is 0.999.

5.3.2 Integral Systems

The integral RCS's for either the first or second stage are only applicable in conjunction with the Thiokol hot gas or Vickers warm gas TVC systems. These systems are essentially the same regardless of which TVC system is used. Injectant gases are bled off the plenum chamber for the hot gas system through shutoff valves to the control valves on the opposite sides of the vehicle which are selectively pulsed to achieve the required roll-control thrust. For the warm gas system, the injectant gases are bled off two of the gas generators and distributed in the same manner. The estimated reliabilities of these systems are 0.992 and 0.993 for the first- and second-stage hot gas system and 0.991 and 0.992 for the first- and second-stage warm gas system. As expected, the reliabilities are about the same since the systems are essentially the same. The warm gas system is slightly lower because of additional unreliability of the gas generators.

Figures-of-merit for each of the systems is shown in Table 5-5.

Table 5-5
RELIABILITY COMPARISON OF ROLL CONTROL SYSTEMS

	Independent RCS Auxiliary Propulsion Roll Control	Dependent RCS Hot Gas Roll Control	Warm Gas Roll Control
First-Stage	0.997	0.992	0.991
Second-Stage	0.999	0.993	0.992

Section 6

LAUNCH OPERATIONS

The four TVC system concepts were individually evaluated from a launch operations viewpoint to identify major advantages or disadvantages inherent in the system design. These evaluations considered such characteristics as complexity of ground support equipment and system checkout operations; ease of on-pad handling, system repair, or component replacement; capability of assuring a flight-ready vehicle on schedule; and capability for malfunction detection and post-flight analysis. The significant operational traits of each system are discussed in the following paragraphs.

6.1 GIMBAL NOZZLE SYSTEM

The gimbal nozzle system, for either first- or second-stage application, presents no major operational problems. Techniques and equipment for system checkout, instrumentation, and monitoring for the prelaunch, launch, and post-launch periods are well established as a result of experience with liquid-engine control systems and may be considered conventional. Since the system uses considerable off-the-shelf components, such as the Zeus power packs, adaptable operating and calibration procedures should be readily available.

All elements of the system are relatively small and compactly arranged within the nozzle compartments to provide ease of access for removal and replacement. Handling of the individual components should present no major problem, although the heavier components (actuator at 330 lb, 260-in. -diam stage; hydraulic power unit at 185 lb, 260-in. -diam stage) will require special equipment for on-pad removal and replacement, as well as normal handling. However, existing equipment performing similar functions may well be capable of adaptation.

Since the number of functional components in the system is low, logistics support requirements are also low even if critical components are stocked at the 100% spares level. This characteristic also contributes to a low demand on launch site calibration, laboratory time, and, when coupled with the ease of component replacement and relative ease of fault isolation (since there are only two major subsystems - pitch and yaw - with minimum functioning components), it contributes directly to a high capability for achieving vehicle flight readiness at a given time with reasonable checkout periods.

This system lends itself to direct measurement of the critical response characteristics which correct for flight path deviations. These are nozzle gimbal angle (actuator travel) and motor thrust (chamber pressure). Both parameters may be easily monitored and recorded in real time, and both may be readily displayed as malfunction detection parameters. Since there are few functional elements in the system, both malfunction detection and post-flight reconstruction analyses are enhanced. Additional malfunction detection parameters indicating impending system trouble may be monitored, if desired, such as, hydraulic power unit output, auxiliary pump outlet pressure, or battery power levels (current output).

An important consideration from the operational viewpoint is the relative ease of continuous monitoring and record keeping for an individual component, actuator, pump, and so forth, from run to run, from factory acceptance up to and through flight. The small number of components in this system simplifies the task of monitoring personnel to fully observe degradation trends in individual serialized components because of the relatively small number of records to be kept, organized, scrutinized, and evaluated.

The significant operational disadvantage for this system is the inability to properly inspect and/or repair or replace the flexible seal while on the launch pad. Installation of the seal is a carefully controlled manufacturing process, as is the nozzle stub for the fixed nozzles (press fit). Inaccessibility and major disassembly requirements preclude any field repair in this area. It is expected, however, that the motor transportation and handling environment will cause no concern for seal integrity, and checkout cycling and test limits will not subject the seal to potential failure modes.

6.2 WARM GAS SYSTEM

From the operations viewpoint, the warm gas system has two major drawbacks. First, the number of functional components required by the system complicates all of the significant operational characteristics, as follows:

1. Procedures checkout.
2. Number of parameters requiring instrumentation, monitoring, and record keeping.
3. Logistics support (spares and records) requirements.
4. Time for performing subsystem and system checkout (unless highly automated).
5. Number of personnel involved in subsystem and system checkout and monitoring.
6. Calibration requirements for components.
7. Ground support equipment (control, checkout, and instrumentation) complexity and cost.
8. Malfunction detection capability (significantly more parameters to be monitored and complexity of meaningful display for rapid recognition of impending malfunction).
9. Post-flight analysis capability. To reconstruct post-flight performance of this system, it is necessary to scrutinize and evaluate the real-time records for eight pneumatic control valves (actuator positions), relate these to a vector summed record, and also examine eight gas generator output traces, as a function of command inputs. Fault isolation to an individual control valve is at a relatively low confidence factor. Further, since the valves are extremely contaminant sensitive, actual flow from the gas generator, which is the predominant measure of thrust deflection, is somewhat questionable.

Second, the large size and weight of the solid-propellant gas generators (12, 339-lb each on the first stage and 1, 908-lb each on the second) presents a difficult operational problem for on-pad removal or replacement. In addition, on the first stage the limited access afforded by the packaging arrangement and shape of the required eight generators precludes ease of gas generator inspection and virtually dictates complete removal of the aft skirt for generator removal, or two sections of the main nozzle in addition to all plumbing to the TVC system injectant nozzles. Since the first-stage on-pad support utilizes the aft skirt for structural load distribution, the latter alternative seems likely. The consequent complexity of operations and equipment to achieve

the disassembly and lowering of the nozzle sections through the launch pad support pedestal should be quite obvious. No significant operational advantages are apparent for this system design, in either first-stage or second-stage application.

6.3 HOT GAS SYSTEMS

The major operational drawback of the hot gas systems is the number of valve assemblies required (16 on the first stage, 8 on the second). The resultant impact on GSE requirements, logistics support, procedures, and checkout unreliability is significant when compared with the dual-actuator system of the gimballed nozzle configurations. Accessibility to the system components is better than that afforded by the warm gas systems; however, the valve assemblies are excessively heavy for easy manual handling and will undoubtedly require special handling equipment and procedures.

Although valve-assembly design provides redundancy, the total number of assemblies is not conducive to ease of checkout with high degree of confidence for flight readiness of the launch vehicle. Any anomaly in system performance is difficult to assess and isolate to a specific valve or valve subassembly, and since it is doubtful that the launch vehicle will be committed to launch with a known flight control system degradation, redundancy does not, in this case, aid the situation; it tends to hinder. Redundancy for flight operation is, of course, significantly important.

An important aspect of these systems using a gas injected into the main exhaust chamber is that the measurement of thrust deflection is indirect: it is a function of gas flow (which can be affected by contaminant buildup in the valve orifices), main thrust, and position of the valve pintle. Monitoring of the valve pintle position is no more difficult than monitoring actuator position for the gimballed nozzle (except for number of measurements); however, no ready means of monitoring contaminant build-up is apparent. Hence, application of malfunction detection techniques to these systems represent a difficult technical problem.

Section 7

GENERAL COMPARISONS

7.1 VEHICLE CONFIGURATIONS

Vehicle configurations which use each of the candidate TVC systems in both stages of the basic launch vehicle--Configuration V from the Phase II HES Study--are shown in Figure 7-1. Figure 7-2 shows Configurations IV, V, and VI developed in the Phase II HES Study. The approach used to develop the HES Study vehicles differs from that used to develop the launch vehicles in this study. Propellant loadings were sized for a specific payload weight in the HES Study, while the propellant loading in this study was held constant and payload penalties or gains were determined. The data shown reflect five steering techniques: warm gas injection, gimbal nozzle, hot gas injection, head-end steering, and liquid injection TVC; two payload shapes: a ballistic Ballo spacecraft and a lifting winged, modified HL-10 spacecraft; the effects of first-stage fins on TVC requirements; and the effect of nozzle submergence on vehicle geometry. The data for Configurations I through IIIA were developed in this study, and the data for Configurations IV, V, and VI were extracted from the Phase II HES Study Report No. SM-51872.

Reliability values are relative to Configuration VI, for this vehicle was used as a base for reliability comparison in the Phase II HES Study. Vehicles using the advanced TVC systems show higher reliability than those using head-end steering and liquid-injection thrust-vector control (LITVC). This can be explained in part by the differences in methodology used in the two studies; however, LITVC is a complex system with an inherently low reliability, and head-end steering must operate without failure for the full duration of the mission.

The effect on the control system of a winged payload is also shown in this figure. During first-stage flight the thrust-vector deflection angles are higher than those for a similar vehicle with a ballistic payload shape, but still well within the capabilities of all TVC systems. However, for second-stage flight, control requirements are established by stage separation

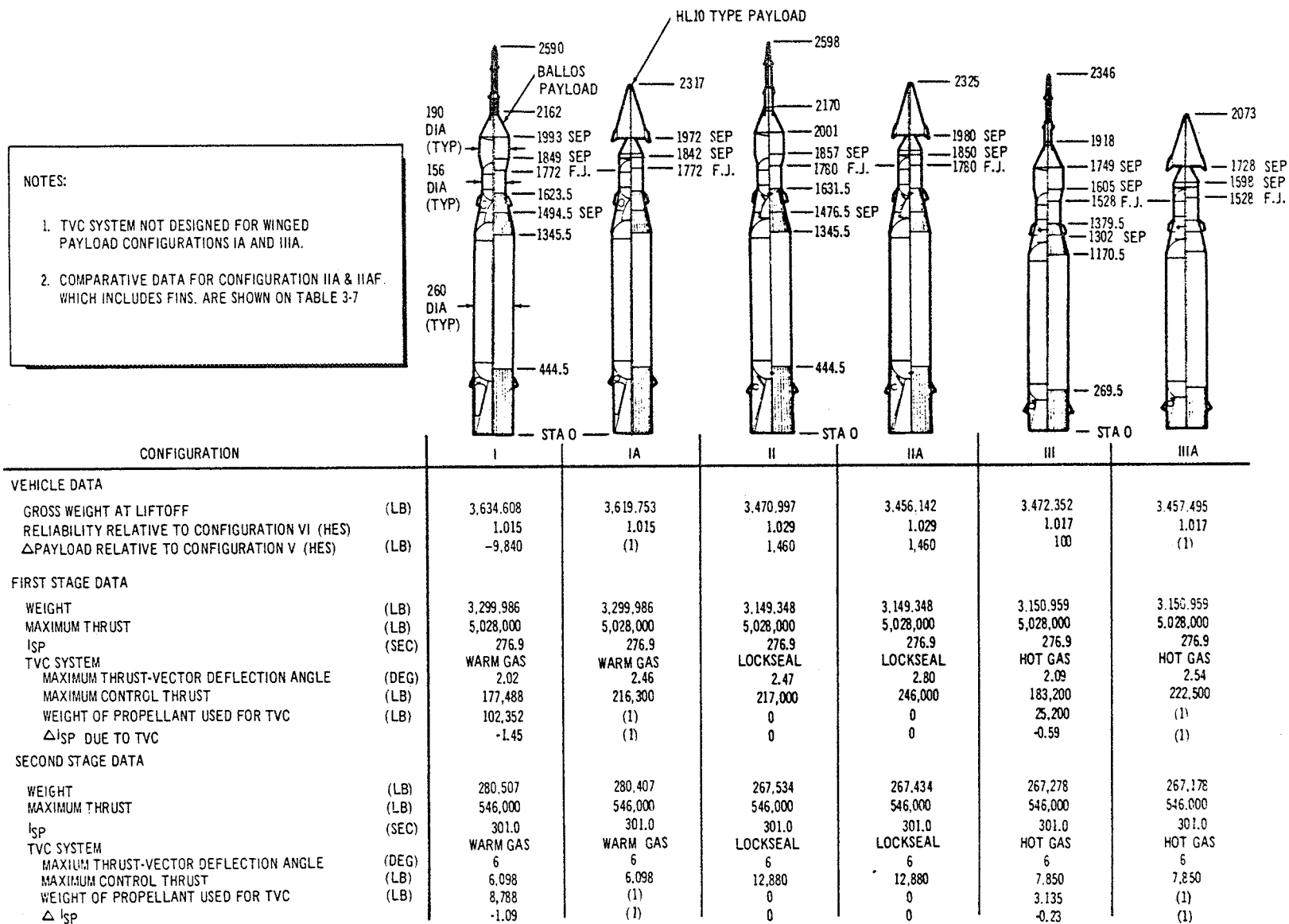
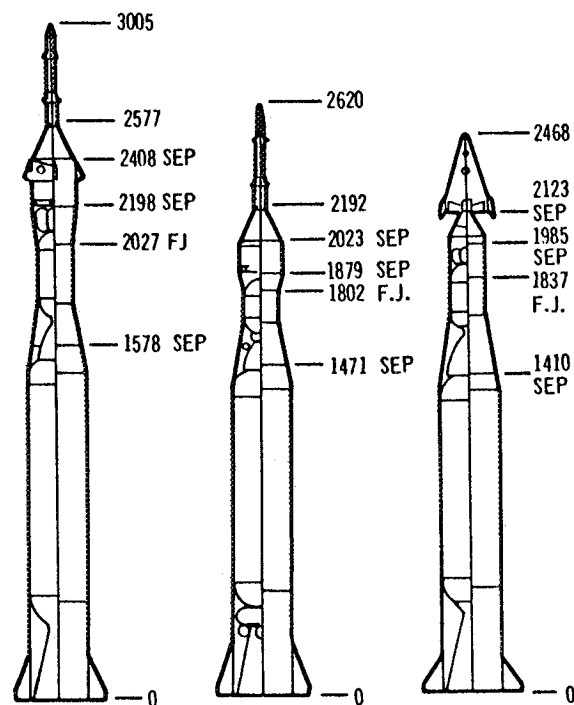


Figure 7-1. Study Launch Vehicle Comparisons

NOTES:

- DIFFERENCES BETWEEN PHASE II HES STUDY VEHICLE CONFIGURATIONS IV, V, & VI AND THE VEHICLES DEVELOPED FOR THE TVC SYSTEM STUDY ARE
 - CONFIGURATIONS IV, V, & VI HAVE FIRST STAGE FINS DESIGNED TO PRODUCE MINIMUM CONTROL MOMENT
 - FIRST AND SECOND STAGE NOZZLES ARE NOT SUBMERGED.
 - FIRST AND SECOND STAGE PROPELLANT LOADING FOR CONFIGURATION IV AND VI DIFFER FROM THE BASIC LAUNCH VEHICLE - CONFIGURATION V.
- DATA PERTAINING TO CONFIGURATIONS IV (HES), V (HES), & VI (HES) ARE OBTAINED FROM DOUGLAS REPORT NO. SM-51872, PHASE II STUDY OF HEAD-END STEERING FOR A SIMPLIFIED MANNED SPACE VEHICLE, MARCH 1966.
- N/A = NOT APPLICABLE.



CONFIGURATION		IV	V	VI
VEHICLE DATA				
GROSS WEIGHT AT LIFTOFF	(LB)	4,111,750	3,493,300	3,423,050
RELIABILITY RELATIVE TO CONFIGURATION VI (HES)		0.979	0.984	1.000
ΔPAYLOAD RELATIVE TO CONFIGURATION V (HES)	(LB)	(2)	(2)	(2)
FIRST STAGE DATA				
WEIGHT	(LB)	3,643,120	3,178,300	3,051,950
MAXIMUM THRUST	(LB)	5,729,055	5,028,000	4,902,153
I_{sp}	(SEC)	276.9	276.9	277.5
TVC SYSTEM		HES	LITVC	HES
MAXIMUM THRUST-VECTOR DEFLECTION ANGLE	(DEG)	± 30.0	0.27	± 30.0
MAXIMUM CONTROL THRUST	(LB)	18,100	23,500	21,500
WEIGHT OF PROPELLANT USED FOR TVC	(LB)	43,900	10,250	20,800
Δ I_{sp} DUE TO TVC		0	N/A	0
SECOND STAGE DATA				
WEIGHT	(LB)	353,430	267,610	299,560
MAXIMUM THRUST	(LB)	688,610	546,000	932,171
I_{sp}	(SEC)	302.6	301.0	302.6
TVC SYSTEM		HES	LITVC	HES
MAXIMUM THRUST-VECTOR DEFLECTION ANGLE	(DEG)	+ 30	3.5	± 30
MAXIMUM CONTROL THRUST	(LB)	4,000	33,400	6,000
WEIGHT OF PROPELLANT USED FOR TVC	(LB)	8,400	2,130	4,600
Δ I_{sp}		0	N/A	0

Figure 7-2. Phase II HES Study Launch Vehicle Data

transients. The second-stage vehicle diverges during the coast period after separation, and the control system is sized to meet this condition. It was found that payload shape had little influence on second stage control, for at separation inflight aerodynamic forces are low, while vehicle thrust misalignment and eccentricity, which are insensitive to payload shape, are the dominant factors. The effect of first-stage fins can be seen when comparing Configuration V with any of the vehicles developed from it. Configuration V has optimum fins to minimize the control moment and shows a maximum thrust-vector deflection requirement of 0.27° . Nominal valves may be below the sensitivity threshold limit of the most sophisticated control system. Vehicles without fins require deflection an order of magnitude greater and in the range of current launch vehicle requirements. It is for this reason that fins were not used in Configurations 1 through IIIA.

The results of the control-system sensitivity analysis presented in Section 3.5.5 have shown that the gas injection TVC systems offer no advantage over the gimbaled nozzle TVC system, and vice versa, from a control-system dynamic response standpoint. This conclusion holds as well for a LITVC system and for the head-end steering system considered in the Phase II HES Study.

The primary advantage of a gas or liquid-injection TVC system is the fast response characteristic relative to the response characteristics of a gimbaled nozzle TVC system. To take advantage of their fast response, the booster control-system response time must be increased beyond that presently used for large booster control systems. As was shown in Section 3.5.5, even decreasing control-system response time did not significantly improve the overall control system performance; therefore, a fast TVC system response time (beyond that available from a gimbaled nozzle TVC system) is not required.

The thrust-vector deflection angle requirement is directly proportional to the control moment needed to overcome the aerodynamic moment.

Since the control moment is a function of both the thrust-vector deflection angle and the location of the side force with respect to the CG, the TVC system located the maximum distance from the vehicle CG will give the minimum thrust-vector deflection angle requirement. The control-system dynamic response is insensitive to the location of the side force as long as the distance from the CG remains constant. Therefore, head-end steering, as studied thus far, offers no advantage over tail-end steering (and vice versa) from a control-system dynamic response standpoint, except a possible advantage in control-moment arm. Further studies are required to determine if structural load relief and improvements in cost effectiveness are possible through head-end control.

7.2 TVC COMPARISON CHART

Figure 7-3 shows the four TVC concepts evaluated in this study and salient parameters associated with each. Since the ABL concept was not continued in the design effort, data pertaining to it are incomplete.

7.3 PAYLOAD CAPABILITY

One measure of vehicle performance is the amount of cargo the vehicle can carry into the 260-nmi LORL orbit. Table 7-1 shows the change in weight that occurs for launch vehicles using each of the candidate TVC systems Configurations I, II, and III use common TVC systems for both stages, but the parameters that cause the change apply mainly to the stage. Therefore, the cargo variation resulting from any interchange of stages to form a launch vehicle could be obtained. There will be a slight error introduced because of differing vehicle geometry and resulting control requirements which affect the parameters, but this should be small making a comparison of this type valid.

Configuration V of the Phase II HES Study is used as the baseline for this evaluation. It has the capability of placing 15,455 lb of cargo and containers into the LORL orbit. The delta payload or cargo weights shown are obtained from the performance analysis described in Section 3.4 and from the vehicle and TVC system design tasks that generated the weight and ΔI_{sp} . The performance analysis considered payload as weight in a circular

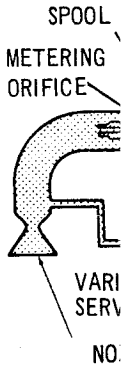
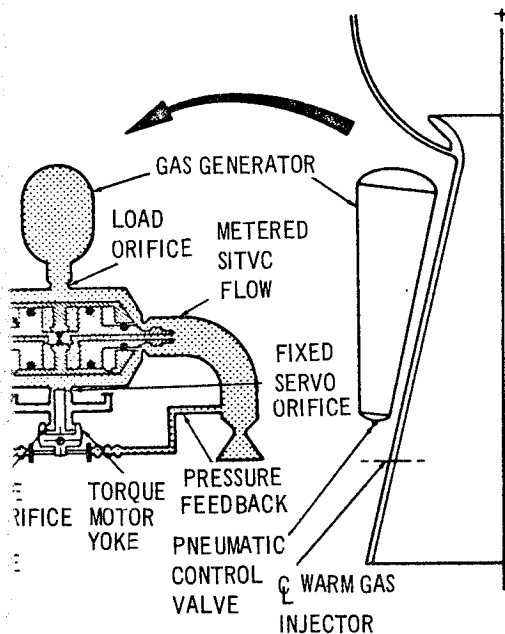
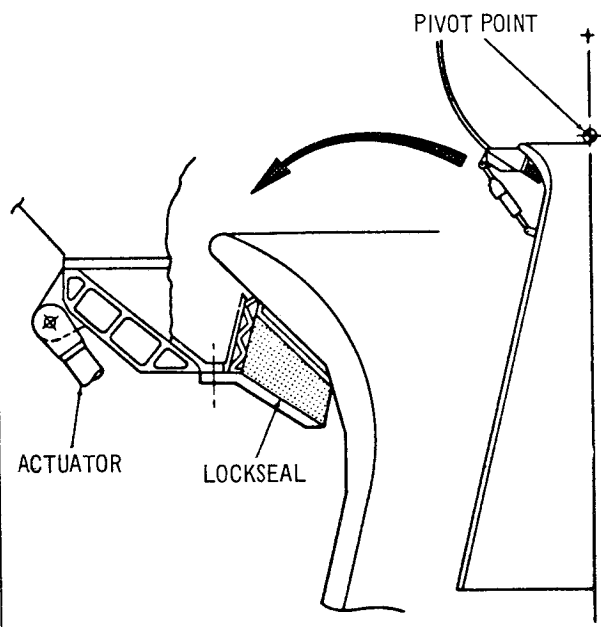
	 <p>SPOOL METERING ORIFICE VARI SERV NO</p>
	TWO-STAG
STAGE	
MAXIMUM THRUST VECTOR DEFLECTION (DEG)	
MAXIMUM THRST VECTOR DEFLECTION RATE (DEG/SEC)	
MAXIMUM THRUST VECTOR DEFLECTION ACCELERATION (DEG/SEC ²)	
FLOW RATE PER QUADRANT (LB/SEC)	
NUMBER OF VALVES	
THRUST VECTOR CONTROL METHOD	
TOTAL WEIGHT, TVC SYSTEM (LB)	156,
RELIABILITY (PROBABILITY OF SUCCESS)	

Figure 7-3. TVC System Comparisons

WARM GAS TVC (VICKERS)



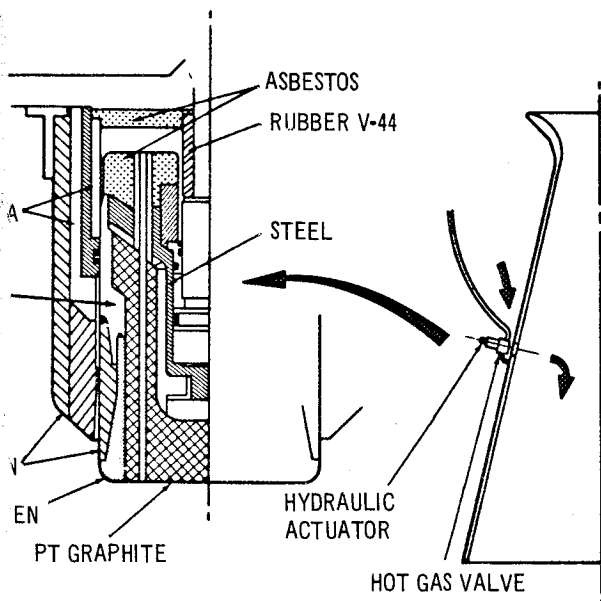
GIMBAL NOZZLE TVC (LOCKHEED)



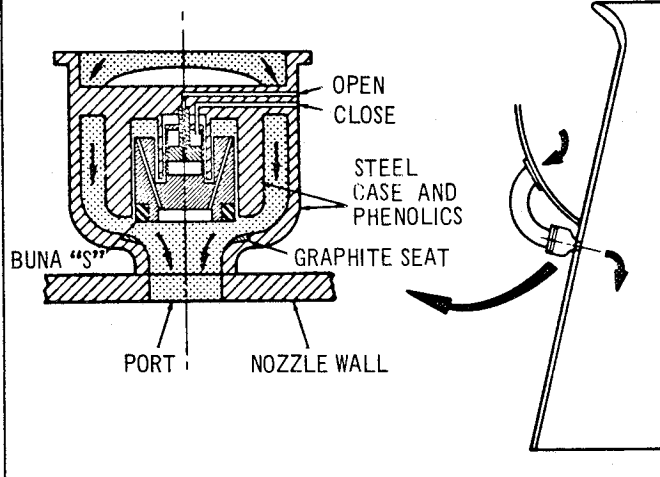
PNEUMATIC SERVO-VALVE SCHEMATIC

ST	SECOND	FIRST	SECOND	
2	6.00	2.47	6.00	
	15.0	7.5	15.0	
	200	30	200	
	180			
	4			
	GAS GENERATORS, T=2000° F		HYDRAULIC ACTUATORS	
	14,288	7,500	1,273	
88937	0.993959	0.998792	0.998840	

HOT GAS TVC (THIOKOL)
(MODULATED)



HOT GAS (ABL)
(BASIC ON-OFF DESIGN)



FIRST	SECOND	FIRST	SECOND
2.09	6.00	2.09	6.00
7.5	15.0	7.5	15.0
30	200	30	200
445	147	445	147
16	8	16	8
MAIN-MOTOR HOT GAS, T = 5,800°F			
.028	4,890	NA	NA
0.991409	0.995044	NA	NA

Table 7-1

VARIATION IN CARGO WEIGHT - 260-NMI ORBIT
COMPARED TO CONFIGURATION V (LITVC)

Items	Configuration (lb)		
	I	II	III
Baseline First-Stage Dry Weight	310,750	310,750	310,750
New First-Stage Dry Weight plus Retrorockets	337,725	289,439	291,050
Δ Weight	26,975	-21,311	-19,700
Δ Cargo Weight	-3,730	+2,560	2,360
First-Stage ΔI_{sp}	-1.45	---	-0.59
Δ Cargo Weight	-730	---	-300
Baseline First-Stage Propellant Weight	2,857,300	2,857,300	2,857,300
New First-Stage Propellant Weight	2,857,300	2,857,300	2,832,080
Δ Weight	---	---	-25,220
Δ Cargo Weight	---	---	-460
Baseline Second-Stage Dry Weight	40,030	40,030	40,030
New Second-Stage Dry Weight	45,393	41,208	40,952
Δ Weight	5,363	+1,178	+922
Δ Cargo Weight	-4,950	-1,100	-900
Second-Stage ΔI_{sp}	-1.09	---	-0.23
Δ Cargo Weight	-430	---	-100
Baseline Second-Stage Propellant Weight	225,450	225,450	225,450
New Second-Stage Propellant Weight	225,450	225,450	222,315
Δ Weight	---	---	-3,135
Δ Cargo Weight	---	---	-500
Total Change in Cargo Weight	-9,840	+1,460	+100

260-nmi orbit. Since the Ballos space craft and its maneuvering propellants are not changed in this study, the change in weight can only occur in cargo capacity.

7.4 LAUNCH VEHICLE WEIGHT MATRIX

The first and second stages developed in this study can, with the proper arrangement of each stage, represent nine launch vehicles which can accommodate the two payload shapes (Ballos and HL-10 type). A weight matrix has been developed for launch vehicles, exclusive of weight above the second stage. These weights are shown in Tables 7-2, 7-3 and 7-4. Weight above the second stage is shown in Table 7-5.

7.5 VEHICLE RELIABILITY VERSUS CONFIGURATION

Table 7-6 presents a reliability comparison of all potential vehicle configurations. This matrix is the result of considering all applicable combinations of TVC and roll-control systems with the launch vehicle. Roll-control systems designated APS are the baseline systems; hot gas refers to the dependent system using main-motor gas; and warm gas uses gases from the warm gas generators for roll-control.

The launch vehicle consists of the 260-in. -diam SRM first stage and 156-in. -diam SRM second stage as defined in the Phase II HES Study (Douglas Report No. SM-51872). On the basis of results of that study, the first- and second-stage SRM reliabilities were determined to be 0.971 and 0.978, respectively. With the use of these SRM reliabilities in conjunction with the various combinations of TVC and roll-control systems reliabilities determined in this study, the reliabilities of the vehicle configurations were computed. These results allow the vehicle reliability parameter to be easily and quickly extracted for use, in conjunction with other performance data, in conducting a comparative analysis of any selected configuration.

7.6 LAUNCH OPERATIONS - TOTAL VEHICLE SYSTEM

In the consideration of the operational aspects for the total launch vehicle (first and second stage), it is readily observed that the gimbal nozzle system on both stages represents the most conventional approach. The fewer number

Table 7-2
LAUNCH VEHICLE WEIGHT MATRIX--
HOT GAS FIRST STAGE (LB)

Items	Hot Gas	Warm Gas	Gimbal
Second Stage			
Aft Skirt	803	1,318	1,532
Nozzle	5,488	4,988	4,988
Motorcase	26,756	27,270	27,270
TVC System	1,755	5,500	1,273
TVC Control/System	100	100	100
Equipment and			
Instrumentation	4,558	4,552	4,558
Tunnels	47	47	47
Contingencies	1,445	1,612	1,440
Stage at Second-Stage Burnout	40,952	45,393	41,208
Igniter Propellant	240	240	240
Main Propellant	222,315	225,450	225,450
TVC Propellant	3,135	8,788	---
Roll Control Propellant	131	131	131
Stage at Second-Stage Ignition	266,773	280,002	267,029
First Stage			
	Hot Gas		
Aft Skirt	5,541	5,541	5,541
Nozzle	40,188	40,188	40,188
Motorcase	222,512	222,512	222,512
TVC System	5,208	5,808	5,808
TVC Control System	100	100	100
Forward Skirt	1,932	2,075	1,944
Equipment and			
Instrumentation	6,271	6,271	6,271
Tunnels	248	248	248
Contingencies	6,300	6,300	6,300
Stage at First-Stage Burnout	555,673	569,045	555,941
Main Propellant	2,832,080	2,832,080	2,832,080
TVC Propellant	25,220	25,220	25,220
Roll Control Propellant	2,609	2,609	2,609
Retrorocket Propellant	2,150	2,150	2,150
Stage at First-Stage Ignition	3,417,732	3,431,104	3,418,000

Table 7-3
LAUNCH VEHICLE WEIGHT MATRIX--
WARM GAS FIRST STAGE (LB)

Items	Hot Gas	Warm Gas	Gimbal
Second Stage			
Aft Skirt	803	1,318	1,532
Nozzle	5,488	4,988	4,988
Motorcase	26,756	27,270	27,270
TVC System	1,755	5,500	1,273
TVC Control System	100	100	100
Equipment and Instrumentation	4,558	4,558	4,558
Tunnels	47	47	47
Contingencies	1,445	1,612	1,440
Stage at Second-Stage Burnout	40,952	45,393	41,208
Main Propellant	222,315	225,450	225,450
TVC Propellant	3,135	8,788	---
Roll Control Propellant	131	131	131
Igniter Propellant	240	240	240
Stage at Second-Stage Ignition	266,773	280,002	267,029
First Stage			
	Warm Gas		
Aft Skirt	7,959	7,959	7,959
Nozzle	30,188	30,188	30,188
Motorcase	226,460	226,460	226,460
TVC System	54,279	54,279	54,279
TVC Control System	100	100	100
Forward Skirt	1,932	2,075	1,944
Equipment and Instrumentation	6,271	6,271	6,271
Tunnels	248	248	248
Contingencies	7,995	7,995	7,995
Stage at First-Stage Burnout	602,205	615,577	602,473
Main Propellant	2,857,300	2,857,300	2,857,300
TVC Propellant	102,352	102,352	102,352
Retrorocket Propellant	2,150	2,150	2,150
Roll Control Propellant	2,609	2,609	2,609
Stage at First-Stage Ignition	3,566,616	3,579,988	3,566,884

Table 7-5
WEIGHT ABOVE THE SECOND STAGE (LB)

Item	HL-10	Ballo
Spacecraft	15,470	21,895
Cargo and Adapter	23,890	23,470
Adapter Skirt	405	505
Total Weight	39,765	45,870
Launch Escape System	---	8,750

of system components, the similarity of checkout--potentially utilizing common equipment with conventional procedures--and the relative ease of repair and replacement of critical components make such a flight-control-system network attractive. There would appear to be no need to perform a simultaneous ground checkout of both stages since flight performance of the stages is sequential and since sequential checkout would also have to be performed. Relatively simple, sequenced switching techniques can be applied, using the same control and instrumentation loop.

Either the warm gas or hot gas system could be applied to either stage, but each system has its operational drawbacks. To marry two stages having these systems only complicates and magnifies the scope of the problem. Further, to intermix the types of systems provides no distinct off-setting advantages and could further complicate the system since two types of operation procedures and possibly personnel would be required, as well as two sets of GSE. If a technical advantage in vehicle performance dictated two different stage systems, however, one of the hot gas systems (preferably second stage with only eight valves required) could be coupled with a movable nozzle system. Application of the warm gas system would still be less desirable since the handling and access problems associated with the gas generators are not conducive to simple on-pad operating procedures and reasonable checkout time with assurance of flight readiness.

Table 7-4
LAUNCH VEHICLE WEIGHT MATRIX--
GIMBAL NOZZLE FIRST STAGE (LB)

Items	Hot Gas	Warm Gas	Gimbal
Second Stage			
Aft Skirt	803	1,318	1,532
Nozzle	5,488	4,988	4,988
Motorcase	26,756	27,270	27,270
TVC System	1,755	5,500	1,273
TVC Control System	100	100	100
Equipment and Instrumentation	4,558	4,558	4,558
Tunnels	47	47	47
Contingencies	1,445	1,612	1,440
Stage at Second-Stage Burnout	40,952	45,393	41,208
Igniter Propellant	240	240	240
Main Propellant	222,315	222,450	225,450
TVC Propellant	3,135	8,788	---
Roll Control Propellant	131	131	131
Stage at Second-Stage Ignition	266,773	280,002	267,029
Gimbal Nozzle			
First Stage			
Aft Skirt	8,353	8,353	8,353
Nozzle	30,188	30,188	30,188
Motorcase	226,460	226,460	226,460
TVC System	7,500	7,500	7,500
TVC Control System	100	100	100
Forward Skirt	1,932	2,075	1,944
Equipment and Instrumentation	6,271	6,271	6,271
Tunnels	248	248	248
Contingencies	6,225	6,225	6,225
Stage at First-Stage Burnout	554,050	567,422	554,318
Main Propellant	2,857,300	2,857,300	2,857,300
Roll Control Propellant	2,609	2,609	2,609
Retrorocket Propellant	2,150	2,150	2,150
Stage at First-Stage Ignition	3,416,109	3,429,481	3,416,377

Table 7-6 (Page 1 of 2)

RELIABILITY COMPARISON OF POTENTIAL LAUNCH VEHICLE CONFIGURATIONS

Motor		TVC System		Roll Control		Vehicle	Ranking
260-in. -diam	156-in. -diam	First Stage	Second Stage	First Stage	Second Stage		
0.971	0.978	Lockseal 0.998792	Lockseal 0.998840	APS 0.997	APS 0.999	0.944	1
0.971	0.978	Lockseal 0.998792	Hot Gas 0.995044	APS 0.997	APS 0.999	0.940	2
0.971	0.978	Lockseal 0.998792	Hot Gas 0.995044	APS 0.997	Hot Gas 0.993	0.934	5
0.971	0.978	Lockseal 0.998792	Warm Gas 0.993959	APS 0.997	APS 0.999	0.939	3
0.971	0.978	Lockseal 0.998792	Warm Gas 0.993959	APS 0.997	Warm Gas 0.992	0.932	7
0.971	0.978	Hot Gas 0.991409	Hot Gas 0.995044	APS 0.997	APS 0.999	0.933	6
0.971	0.978	Hot Gas 0.991409	Hot Gas 0.995044	APS 0.997	Hot Gas 0.993	0.927	11
0.971	0.978	Hot Gas 0.991409	Hot Gas 0.995044	Hot Gas 0.992	APS 0.999	0.928	10
0.971	0.978	Hot Gas 0.991409	Hot Gas 0.995044	Hot Gas 0.992	Hot Gas 0.993	0.923	15
0.971	0.978	Hot Gas 0.991409	Lockseal 0.998840	APS 0.997	APS 0.999	0.938	4
0.971	0.978	Hot Gas 0.991409	Lockseal 0.998840	Hot Gas 0.992	APS 0.999	0.933	6
0.971	0.978	Hot Gas 0.991409	Warm Gas 0.993959	APS 0.997	APS 0.999	0.933	6

Table 7-6 (Page 2 of 2)

Motor		TVC System		Roll Control		Vehicle	Ranking
260-in. -diam	156-in. -diam	First Stage	Second Stage	First Stage	Second Stage		
0.971	0.978	Hot Gas 0.991409	Warm Gas 0.993959	APS 0.997	Warm Gas 0.992	0.926	12
0.971	0.978	Hot Gas 0.991409	Warm Gas 0.993959	Hot Gas 0.992	APS 0.999	0.927	11
0.971	0.978	Hot Gas 0.991409	Warm Gas 0.993959	Hot Gas 0.992	Warm Gas 0.992	0.921	16
0.971	0.978	Warm Gas 0.988937	Warm Gas 0.993959	APS 0.997	APS 0.999	0.931	8
0.971	0.978	Warm Gas 0.988937	Warm Gas 0.993959	APS 0.997	Warm Gas 0.992	0.924	14
0.971	0.978	Warm Gas 0.988937	Warm Gas 0.993959	Warm Gas 0.991	APS 0.999	0.924	14
0.971	0.978	Warm Gas 0.988937	Warm Gas 0.993959	Warm Gas 0.991	Warm Gas 0.992	0.918	18
0.971	0.978	Warm Gas 0.988937	Lockseal 0.998840	APS 0.997	APS 0.999	0.934	5
0.971	0.978	Warm Gas 0.988937	Lockseal 0.998840	Warm Gas 0.991	APS 0.999	0.929	9
0.971	0.978	Warm Gas 0.988937	Hot Gas 0.995044	APS 0.997	APS 0.999	0.931	8
0.971	0.978	Warm Gas 0.988937	Hot Gas 0.995044	APS 0.997	Hot Gas 0.993	0.925	13
0.971	0.978	Warm Gas 0.988937	Hot Gas 0.995044	Warm Gas 0.991	APS 0.999	0.925	13
0.971	0.978	Warm Gas 0.988937	Hot Gas 0.995044	Warm Gas 0.991	Hot Gas 0.993	0.920	17

Section 8
BIBLIOGRAPHY

1. Phase I, A feasibility Study of Head End Steering for a Simplified Manned Space Vehicle. Douglas Report No. SM-48152, December 1964.
2. Phase II, Study of Head End Steering for a Simplified Manned Space Vehicle. Douglas Report No. SM-51872, March 1966.
3. The Douglas Saturn I-B Improvement Study-Solid First Stage. Douglas Report No. SM-47043, 24 February 1965.
4. Launch Vehicles for Spacecraft or Near-Term Vehicle Concepts (Expendable Rocket) (U), Vol I, Summary Report, April 1967, (C), Vol II, Technical Report, Douglas Report No. DAC-57990, April 1967 (C).
5. E. L. Pollack. Evaluation of Hot-Gas Injection Thrust Vector Control Performance Parameters with Defensive Missile System Boosters. Douglas Report No. DAC-59152, December 1966.
6. MLV Saturn I-B Improvement Studies Saturn I-B-16 Vehicle. Douglas Report Nos. DAC-56460 and, DAC-56457P, October 1966.
7. Saturn I-B Improvement Study (Solid First Stage) Phase II. Douglas Report Nos. SM-51897 and, SM-51896, March 1966.
8. Use of Large Solid Motors in Booster Applications, Final Report. Douglas Report Nos. DAC-58036, DAC-58037, and DAC-58038, August 1967.
9. Air Augmented Thrust Propulsion Nozzle Study (U). TRW Structures Division Final Report ER 6959, 12 October 1966 (C).
10. Project 3044: Submerged Hot-Gas Valve Development Program. Thiokol Chemical Corporation (Brigham City, Utah), June 1965.
11. Large Motor Technical Direction Meeting (U). Thiokol Chemical Corporation, Report No. TMC-231-9-6, 30 September 1966 (C).
12. D. M. Cos, Submerged Hot-Gas Valve TVC (U). ICRPG/AIAA Solid Propulsion Conference, Vol I, July 1966 (C).
13. J. W. Wilson. TU-562 Motor Design Report on Flexible Bearing Seal Assembly. Thiokol Chemical Corporation Report No. TWR-2356, 16 March 1967.

14. Manuel Fuentest and John Thirkill. Evaluation of TVC Systems for Solid Propellant Motor Application. Thiokol Chemical Corporation, 16 December 1963. Prepared for the AIAA Solid Propellant Conference, Palo Alto, California, 29 to 31 January 1964.
15. T. J. Dahn. Data Analysis, and Performance Prediction for the Thiokol Chemical Corporation TU-121 Motor Hot-Gas Secondary Injection TVC Tests (U). Vidya Corp., Technical Note 9166-TN-6, August 1964.
16. AF 156-9 Flexible Seal Nozzle Demonstration (U). Thiokol Chemical Corporation, Report No. TE 2-183-6-7, 27 June 1967.
17. Design Study and Cost Estimates for Application of Lockseal to 260-in. Solid Rocket Motor (U), Lockheed Propulsion Company, Report No. LPC 759-F.
18. Development of an Elastomeric Seal for Omniaxial Moveable Nozzles (Lockseal) (U). Lockheed Propulsion Company, Report No. AFRPL-TR-66-112, April 1966 (U).
19. Development of an Elastomeric Seal for Omniaxial Moveable Nozzles (Lockseal). LPC Progress Report No. 2, AFRPL-TR-65-173, August 1965 (C).
20. Cold Flow Gas Injection Performance Studies Allegheny Ballistics Laboratory (Cumberland, Maryland) ABL-TR-66-1, June 1963 to February 1966.
21. M. G. Haydin, Jr., et al. NASA Propellant Gas Valve Scale-Up Program (U), Final Report. Allegheny Ballistics Laboratory, Report No. ABL/R-62, March 1966 (C).
22. Valve and System Design for 6500^oF Chamber-Bled TVC. Allegheny Ballistics Laboratory Report No. ABL/Z-64, November 1963.
23. Application of Propellant Gas Valves for TVC of High-Pressure, High-Acceleration, Solid Propellant Rocket Motors. Allegheny Ballistics Laboratory, Report, No. ABL/Z-72, May 1964.
24. The Vickers Warm-Gas TVC System Study. Prepared for Langley Research Center, NASA under Contract Nos. NAS 1-2962 and NAS 1-4102, Vickers Incorporated (Troy, Michigan).
25. Proportional Solid Propellant Secondary Injection Thrust Vector Control Study. Prepared for NASA under Contract No. NAS 1-2962, September 1965.
26. Phase I, Study of Proportional Solid Propellant, S.I.T.V.C. Under Simulated Altitude Conditions. Prepared for NASA under Contract No. NAS 1-4102, June 1966.

27. Phase III, Development of a Proportional Two Stage Pressure Feedback Pneumatic Valve for 2,000°F Solid Propellant Systems. Prepared for NASA under Contract No. NAS 1-4102, July 1966.
28. G. E. Daniels, J. R. Scoggins, and O. E. Smith, Terrestrial Environment (Climatic) Criteria Guidelines for Use in Space Vehicle Development, 1966 Revision. NASA Technical Memorandum No. X-53328, 1 May 1966.
29. Failure Rate Data Handbook (FARADA). Bureau of Naval Weapons.
30. D. R. Earles and M. F. Eddins. Reliability Engineering Data Series - Failure Rates. Avco Corporation.

